

**C-C Bond Forming Reactions Catalyzed by Artificial
Metalloenzymes Based on the Biotin-Streptavidin
Technology**

Inauguraldissertation

zur

Erlangung der Würde eines Doktors der Philosophie

vorgelegt der

Philosophisch-Naturwissenschaftlichen Fakultät

der Universität Basel

von

Anamitra Chatterjee

Aus Indien

Basel, 2015

Originaldokument gespeichert auf dem Dokumentenserver der Universität Basel

edoc.unibas.ch

Genehmigt von der Philosophisch-Naturwissenschaftlichen Fakultät auf Antrag von:

Prof. Dr Thomas R. Ward

Prof. Dr Olivier Baudoin

Basel, den 13.10.2015

Prof. Dr. Jörg Schibler

Dekan

ACKNOWLEDGMENTS

Firstly, I would like to express my sincere gratitude to my advisor Prof. Thomas R. Ward for the continuous support of my Ph.D study and related research, for his patience, motivation, and immense knowledge. His guidance helped me in all the time of research and writing of this thesis. I could not have imagined having a better advisor and mentor for my Ph.D study.

Besides my advisor, I would like to thank the rest of my thesis committee: Prof. Olivier Baudoin for agreeing to co-referee this thesis and Prof. Dennis Gillingham, for agreeing to be faculty representative.

My sincere thank also goes to Dr. Raphael Reuter, Dr. Valentin Köhler, Dr. Anna Kajetanowicz, Dr. Mark Ringenberg and Dr. Hendrik Mallin, who taught me various laboratory and research skills. Without their precious support it would not be possible to conduct this research. Special thanks to Maxime Barnet for his generous help and support in docking and Bernhard Jung to solve all computer related problems, Mrs. Isa Worni and Mrs. Beatrice Erismann for all administrative help.

I thank my past and present fellow labmates: Jingming Zhao, Dr. Vincent Lebrun, Jaicy, Dr. Gaetano Angelici, Dr. Tillmann Heinisch, Martina Hesticova, Juliane Klehr, Sascha Keller, Yasunori Okamoto, Michela Maria Pellizzoni, Fabian Schwizer, Christian Trindler, Ewa Milopolska, Dr. Praneeth Vijayendran, Livia Knörr, Dr. Yvonne Wilson, Dr. Maurus Schmid, Dr. Christian Tagwerker, Julian Ruoss, Dr. Nobutaka Fujieda, Dr. Tommaso Quinto, Dr. Todd Hyster, Dr. Marc Duerrenberger, Dr. Marc Creus, Aping Niu, Narasimha Rao Uda and Dr. Zhe Liu for the stimulating discussions and for all the fun we have had in the last four years.

The most important, I would like to thank my family, especially my mother Parul Chatterjee and my father Debasish Chatterjee for the support they provided me through my entire life and in particular during my thesis. I don't forget my sister Sanghyamitra and brother-in-law Ritabrata. Finally, it is impossible to finish without addressing my deep love and gratitude to Somdutta. Her love, encouragement and help during my thesis make my life beautiful and the best days of my life.

TABLE OF CONTENTS

	Page
ABSTRACT	VI
PUBLICATION	VII
CHAPTER 1 INTRODUCTION	1
1.1 C-C Bond Formation.....	2
1.2 Artificial Metalloenzymes	3
1.3 Catalytic Scope of ArMs.....	6
1.4 Aim of the Thesis	6
1.5 References	7
CHAPTER 2 RECENT ADVANCES IN THE PALLADIUM CATALYZED SUZUKI-MIYaura CROSS-COUPling REACTION IN WATER	10
2.1 Introduction.....	11
2.2 Homogeneous SMC in Water	11
2.2.1 P-donors Ligands	11
2.2.2 N-donor Ligands	15
2.2.3 N-heterocyclic Carbene (NHC) Ligands	26
2.2.4 SMCs for Chemical Biology Applications	33
2.3 Heterogeneous SMC in water	35
2.3.1 Supported catalysts	35
2.3.2 Unsupported catalysts	45
2.3.3 SMCs for Chemical Biology Applications	49
2.4 Conclusion	50
2.5 References.....	50
CHAPTER 3 ENANTIOSELECTIVE ARTIFICIAL SUZUKIASE FOR THE SYNTHESIS OF AXIALLY CHIRAL BIARYL COMPOUNDS RELYING ON STREPTAVIDIN-BIOTIN TECHNOLOGY	57
3.1 Introduction.....	58
3.2 Aim of the Project.....	59
3.3 Outline of the Project	59
3.4 Results and Discussion	60
3.4.1 Chemical Optimizations.....	60
3.4.2 Genetic Optimizations	61
3.4.3 Substrate Scopes	65
3.4.4 X-ray Structure.....	68

3.5 Conclusions.....	70
3.6 References.....	70
CHAPTER 4 DEVELOPMENT OF ARTIFICIAL METATHESASE FOR RING CLOSING METATHESIS	73
4.1 Introduction.....	74
4.1.2 Mechanism of the Olefin Metathesis	76
4.2 Aim of the Project.....	76
4.3 Outline of the Project.....	77
4.4 Results and Discussion	78
4.4.1 Synthesis of Biotinylated Metathesis Catalysts	78
4.4.2 Activity Test in Organic and Aqueous Organic Solvent	82
4.4.3 Comparison of Artificial Metalloenzymes	87
4.4.4 Screening of Different Mutants with Biot-3 Catalyst.....	88
4.4.5 HPLC measurements	90
4.4.6 Catalysis in the Periplasm of E. coli with Biot-3.....	92
4.5 Conclusion	94
4.6 References.....	95
CHAPTER 5 ASYMMETRIC C–H ACTIVATION REACTION CATALYZED BY AN ARTIFICIAL BENZANNULASE USING UNPURIFIED PROTEIN SAMPLES	97
5.1 Introduction.....	98
5.1.1 Biocatalysts for C–H Activation.....	98
5.1.2 Biotin-(strept)avidin Artificial Metalloenzyme Technology	100
5.1.3 Prior Works.....	101
5.2 Aim of the Project.....	103
5.3 Outline of the Project.....	103
5.4 Results and Discussion	104
5.5 Conclusion	115
5.6 References.....	115
CHAPTER 6 CONCLUSION AND OUTLOOK	118
APPENDICES	
Appendix 1.....	120
Appendix 2.....	164
Appendix 3.....	205

ABSTRACT

The research in Ward group is merging organometallic chemistry with Biotechnology. With the aim of exploiting most attractive and complementary features of catalysts, it is proposed to merge homogeneous and enzymatic catalysis to yield artificial metalloenzymes. In the past, the incorporation of an active metal moiety within a protein environment afforded hybrid catalysts with very promising properties, including high activities and selectivity, reminiscent of both homogeneous and enzymatic catalysts.

Herein we discovered an artificial metalloenzymes for enantioselective Suzuki-Miyaura cross-coupling reaction. For this purpose, we synthesized a variety of biotinylated N-heterocycliccarbene- (NHC) and bulky phosphine ligands and tested these in the presence of a Pd-source combined with various streptavidin isoforms. We were able to achieve 90% ee with artificial suzukiase for the synthesis of a variety of axially chiral biaryl compounds.

We discovered an artificial metathesase which, in the presence of streptavidin displayed remarkable ring-closing metathesis activity either in the periplasm or on untreated cell-free extracts. The olefin functionality is underrepresented functional group in cellular media and displays only modest reactivity towards the various reactants present in complex media. This property makes it ideal for biorthogonal chemistry. Different biotinylated “Hoveyda-Grubbs” type catalysts were synthesized, characterized and screened for ring-closing metathesis. In order to speed up screening efforts, ring-closing metathesis leading to umbelliferone was used.

Efforts to implement the asymmetric C-H activation relying on rhodium (III) complexes bearing Cp* ligand in streptavidin in the presence of cellular extracts were also described herein.

PUBLICATIONS

1. Chatterjee A., Mallin H., Klehr J., Vallapurackal J., Finke A. D., Vera L., Marsh M. and Ward T.R., “An Enantioselective Artificial Suzukiase Based on the Biotin-Streptavidin Technology”, *Chem. Sci.* **2015**, just accepted.
2. Chatterjee A.*, Kajetanowicz A.*, Reuter R., and Ward T.R. (*equal contribution), “Biotinylated Metathesis Catalysts: Synthesis and Performance in Ring Closing Metathesis”, *Catalysis Letters* **2014**, *144*, 373.
3. Chatterjee A., Ward T.R., “Recent Advances of Palladium Catalyzed Suzuki cross-coupling in water” Review Article, Under preparation

Chapter 1

Introduction

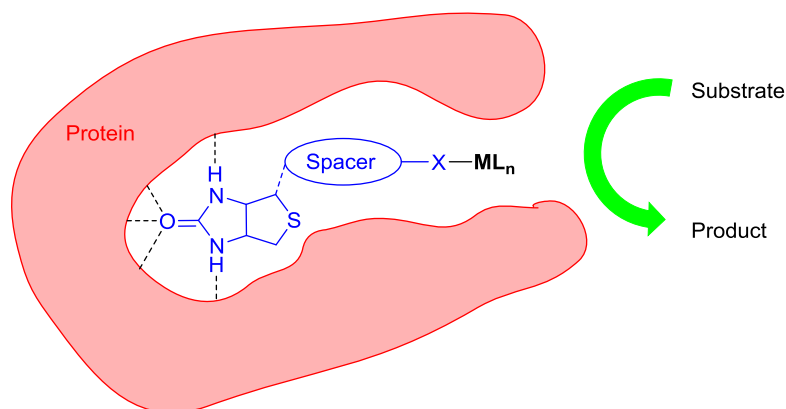
1.1 C-C Bond Formation

The formation of carbon–carbon bonds is of fundamental importance in organic synthesis. Such reactions are important in the production of many valuable chemicals in various fields such as pharmaceuticals, crop-protection, chemical industry, energy supply, materials science, nutrition, fragrances and flavors.¹ As a result, there are an ever-growing number of methods available for the carbon–carbon bond formation. Some examples of reactions which yield carbon–carbon bonds include: the Aldol reaction, the Diels–Alder reaction, the addition of a Grignard reagent to a carbonyl group, the Heck reaction, the Michael addition and the Wittig reaction. There are many existing strategies for catalytic C-C bond formation reactions. These have been classified as i) homogeneous ii) heterogeneous and iii) bio catalysis.

- i) Transition metal catalyzed homogeneous C-C bond formation reactions have been developed over five decades. There are more than hundred types of reactions which have been developed by homogeneous catalysis. For example, the olefin metathesis, the cross-coupling, the Wittig reaction, the Diels-Alder, the Grignard reaction etc.²⁻⁴
- ii) Tethering an organometallic complex to a silica particle or to the internal surface of a mesoporous host can be used to design heterogeneous catalysts for a variety of C-C bond forming reactions.⁵
- iii) Only a limited number of enzymatic C–C bond forming reactions have been applied in biocatalytic organic synthesis.⁶ For instance the Stetter and the Pictet–Spengler reaction or the oxidative C–C bond formation, the benzylation of aromatics, the intermolecular Diels-Alder or the reductive coupling of carbon monoxide. These reactions are catalyzed by aldolases, transketolases, lyases, oxidoreductases, transferases etc.⁷⁻⁹

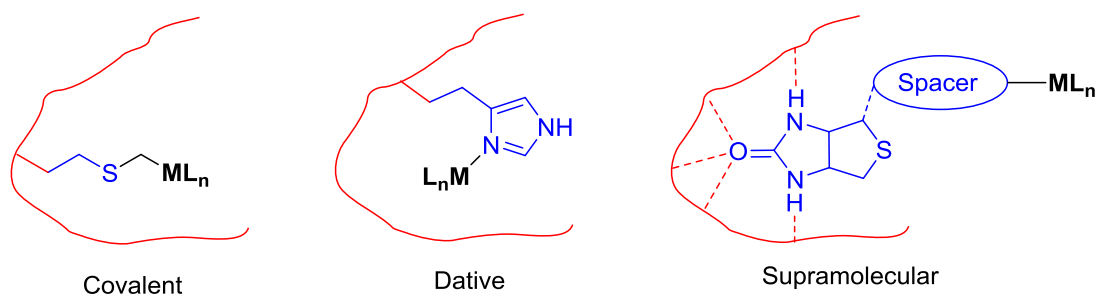
1.2 Artificial Metalloenzymes

In the past century, homogeneous-, enzymatic- and heterogeneous catalysis have evolved independently. Each catalytic system offer distinct advantages and disadvantages. In the context of high-added value chemicals, homogeneous and enzymatic catalysts are preferred.¹⁰ In many cases, homogeneous catalysts and enzymes display complementary features. In the past decade, artificial metalloenzymes (hereafter ArMs) have attracted increasing attention as they have been shown to combine attractive features of both homogeneous- and enzymatic catalysts.^{11–13} Such systems aim at bridging the gap between the transition metal catalysis and biocatalysis. Such hybrid catalysts result from anchoring a catalytically competent cofactor within a macromolecular scaffold (oligonucleotide or protein), Scheme 1.1.



Scheme 1.1 Construction of an artificial metalloenzyme based on the biotin-streptavidin technology. An achiral metal complex linked to biotin via a spacer is incorporated within a biotin-binding protein by supramolecular anchoring. Chemogenetic optimization of the hybrid system affords versatile enantioselective hybrid catalysts for a variety of organic transformations. M = metal, L = ligand, X = donor atom or ligand.

Various anchoring strategies have been pursued to ensure the localization of the abiotic cofactor within the macromolecular scaffold. These can be classified as: i) covalent, ii) dative and iii) supramolecular, Scheme 1.2.



Scheme 1.2 Various anchoring strategies used in the generation of artificial metalloenzymes: covalent, dative and supramolecular

- i) The covalent anchoring strategy relies on the creation of a covalent bond between nucleophilic amino acids (mostly cysteine, lysine or serine) and cofactors bearing an electrophilic moiety (or a thiol)^{14,15} (Scheme 1.2). Recently, Lewis and coworkers have engineered an azide containing unnatural amino acid that undergoes spontaneous 1,3-dipolar cycloaddition with abiotic cofactors bearing an cyclooctyne moiety.¹⁶
- ii) In the dative anchoring strategy, one Lewis-basic amino acid (histidine, cysteine, methionine, aspartate and glutamate etc.) of the biomolecule acts as a ligand for the coordinatively unsaturated metal cofactor. In this context, zinc-substitution within human carbonic anhydrase has proved propitious.¹⁷ Recently, Song and Tezcan reported the design and evolution of a metalloprotein assembly with *in vivo* hydrolytic activity (ampicillin hydrolysis in *E. coli*'s periplasm).¹⁸
- iii) The supramolecular anchoring strategy relies on weak interactions between small molecules and the biomolecular scaffold. The critical parameter in this strategy is the affinity of the guest molecule for the host biomolecular scaffold. Wilson and Whitesides outlined in 1978 the use of avidin as host for the supramolecular anchoring of biotinylated cofactors.¹⁹ They were the first to exploit the nearly irreversible binding of biotin (vitamin H) with

avidin ($K_d = \text{ca. } 10^{-14} \text{ M}$) to generate an artificial metalloenzyme for enantioselective hydrogenation.²⁰ Since then, several groups have picked up on this technology to engineer ArMs.^{21,22}

Chemical Optimization of the ArMs:

The chemical catalyst is generally optimized by screening different active metal complexes. Compared to the traditional transition metal catalysis, the advantage is that the ligand in most instances is not chiral, which reduces the synthetic complexity. Introduction of various spacers between the biotin anchor and the organometallic moiety allows probing the protein cavity in search of beneficial second coordination sphere interactions.

Genetic Optimization of ArMs:

Optimization of the protein scaffold can be achieved by design in combination with evolutionary approaches, such as designed and directed evolution.²¹ The different approaches to rationally (re)design a metal binding site in a protein have been recently summarized by Lu *et al.*²³

- 1) The empirical approach that includes the design by inspection, homology, and by replacement of modular units;
- 2) The theoretical approach that uses computer search algorithms that make predictions and help designing a new active site into a native scaffold by finding the optimal locations for ligands;
- 3) The semi theoretical approach that combines visual inspection of proteins to identify optimal locations for ligands to create a new metal binding site and computer program evaluation for the energetics of positioning appropriate amino acid residues.

1.3 Catalytic Scope of ArMs

The combination of a well-defined second coordination sphere (biomolecule) and the first coordination sphere (water compatible transition metal complex) opens fascinating perspectives towards the generation of ArMs for a wide range of organic transformations. Example of C-C bond formation reactions catalyzed by artificial metalloenzyme implemented to date include: allylic substitution,²⁴ cross-coupling,²⁵ benzannulation,²⁶ metathesis,²⁷ polymerisation,²⁸ Diels-Alder reaction,²⁹ Friedel-Crafts alkylation,³⁰ cyclopropanation,¹⁶ hydroformylation,¹⁷ etc.^{11,13}

1.4 Aim of the Thesis

The high stability of (strept)avidin combined with its high affinity towards biotinylated compounds offer a large number of promising and challenging applications. In this thesis, we focused our efforts on developing bio-orthogonal C–C bond forming reactions exploiting the potential of artificial metalloenzymes based on the biotin (strept)avidin technology. In this context, i) the Suzuki-Miyaura cross-coupling, ii) the olefin metathesis and iii) C-H activation reactions were investigated.

- i) In the past few years, the Suzuki cross-coupling reaction has attracted significant attention as a versatile, water compatible cross-coupling reaction.^{31,32} Importantly, several groups have demonstrated the biocompatibility and bio-orthogonality of the Suzuki cross-coupling, thus revealing interesting avenues for chemical biology applications.^{33–36} In this context, they have performed cross-coupling reactions on proteins and even *in vivo*.³³ To the best of our knowledge, however, these reactions are not catalytic as they require very high loadings of palladium.³⁷ In Chapter 2, we summarize recent developments of Suzuki-Miyaura cross-coupling reaction in water.
- ii) In Chapter 3, we present our efforts to develop an artificial enantioselective Suzukiase based on the biotin-streptavidin technology and test its biocompatibility in cellular extracts.

- iii) The olefin functionality is an underrepresented functional group in cellular media. In addition, this functionality displays only modest reactivity towards the various reactants present in this complex media. In Chapters 4 and 5, we present our efforts to develop bio-orthogonal reactions using olefins as partner. In Chapter 4, we present our efforts to develop the ring closing olefin metathesis *in vivo* by developing biotinylated *N*-heterocyclic ligands to anchor a Hoveyda-Grubbs type catalyst within streptavidin.
- iv) Rhodium (III) complexes bearing Cp* ligands proved to be highly versatile catalysts for the directed carbon-hydrogen (C–H) bond functionalizations of hydroxamic acid derivatives.²⁶ Previous work in the group demonstrated that high levels of both selectivity and reactivity could be achieved by an artificial metalloenzyme by engineering a basic carboxylate aminoacid residue in the proximity of the biotinylated Rh(III) center. In Chapter 5, we summarize our efforts to perform this asymmetric C–H activation in cellular extracts.

Finally, Chapter 6 presents an overview of the progress towards cell-compatible, catalytic C–C bond forming reactions.

1.5 References

- (1) Jacobsen, E. N.; Pfaltz, A.; Yamamoto, H. *Comprehensive Asymmetric Catalysis*, Springer, Berlin, **1999**.
- (2) Zultanski, S. L.; Fu, G. C. *J. Am. Chem. Soc.* **2013**, *135*, 624.
- (3) Watson, I. D. G.; Toste, F. D. *Chem. Sci.* **2012**, *3*, 2899.
- (4) Roscales, S.; Csákÿ, A. G. *Chem. Soc. Rev.* **2014**, *43*, 8215.
- (5) Thomas, J. M. *Angew. Chem. Int. Ed.* **1999**, *38*, 3588.
- (6) Resch, V.; Schrittwieser, J. H.; Siirola, E.; Kroutil, W. *Curr. Opin. Biotechnol.* **2011**, *22*, 793.

- (7) Müller, M.; Gocke, D.; Pohl, M. *FEBS J.* **2009**, *276*, 2894.
- (8) Clapés, P.; Fessner, W.-D.; Sprenger, G. A.; Samland, A. K. *Curr. Opin. Chem. Biol.* **2010**, *14*, 154.
- (9) Schneider, S.; Gutiérrez, M.; Sandalova, T.; Schneider, G.; Clapés, P.; Sprenger, G. A.; Samland, A. K. *Chembiochem* **2010**, *11*, 681.
- (10) Ward, T. R. *Acc. Chem. Res.* **2011**, *44*, 47.
- (11) Yu, F.; Cangelosi, V. M.; Zastrow, M. L.; Tegoni, M.; Plegaria, J. S.; Tebo, A. G.; Mocny, C. S.; Ruckthong, L.; Qayyum, H.; Pecoraro, V. L. *Chem. Rev.* **2014**, *114*, 3495.
- (12) Heinisch, T.; Ward, T. R. *Eur. J. Inorg. Chem.* **2015**, *21*, 3406.
- (13) Lewis, J. C. *ACS Catal.* **2013**, *3*, 2954.
- (14) Qi, D.; Tann, C.-M.; Haring, D.; Distefano, M. D. *Chem. Rev.* **2001**, *101*, 3081.
- (15) Basauri-Molina, M.; Riemersma, C. F.; Würdemann, M. A.; Kleijn, H.; Klein Gebbink, R. J. M. *Chem. Commun.* **2015**, *51*, 6792.
- (16) Yang, H.; Srivastava, P.; Zhang, C.; Lewis, J. C. *Chembiochem* **2014**, *15*, 223.
- (17) Jing, Q.; Kazlauskas, R. J. *ChemCatChem* **2010**, *2*, 953.
- (18) Song, W. J.; Tezcan, F. A. *Science* **2014**, *346*, 1525.
- (19) Wilson, M. E.; Whitesides, G. M. *J. Am. Chem. Soc.* **1978**, *100*, 306.
- (20) Davies, R. R.; Kuang, H.; Qi, D.; Mazhary, A.; Mayaan, E.; Distefano, M. D. *Bioorg. Med. Chem. Lett.* **1999**, *9*, 79.
- (21) Reetz, M. T.; Peyralans, J. J.-P.; Maichele, A.; Fu, Y.; Maywald, M. *Chem. Commun.* **2006**, *41*, 4318.
- (22) Ilie, A.; Reetz, M. T. *Isr. J. Chem.* **2015**, *55*, 51.
- (23) Lu, Y.; Yeung, N.; Sieracki, N.; Marshall, N. M. *Nature* **2009**, *460*, 855.
- (24) Pierron, J.; Malan, C.; Creus, M.; Gradinaru, J.; Hafner, I.; Ivanova, A.; Sardo, A.; Ward, T. R. *Angew. Chem.* **2008**, *120*, 713.

- (25) Abe, S.; Niemeyer, J.; Abe, M.; Takezawa, Y.; Ueno, T.; Hikage, T.; Erker, G.; Watanabe, Y. *J. Am. Chem. Soc.* **2008**, *130*, 10512.
- (26) Hyster, T. K.; Knörr, L.; Ward, T. R.; Rovis, T. *Science* **2012**, *338*, 500.
- (27) Lo, C.; Ringenberg, M. R.; Gnanndt, D.; Wilson, Y.; Ward, T. R. *Chem. Commun.* **2011**, *47*, 12065.
- (28) Abe, S.; Hirata, K.; Ueno, T.; Morino, K.; Shimizu, N.; Yamamoto, M.; Takata, M.; Yashima, E.; Watanabe, Y. *J. Am. Chem. Soc.* **2009**, *131*, 6958.
- (29) Podtetenieff, J.; Taglieber, A.; Bill, E.; Reijerse, E. J.; Reetz, M. T. *Angew. Chem. Int. Ed.* **2010**, *49*, 5151.
- (30) Boersma, A. J.; Megens, R. P.; Feringa, B. L.; Roelfes, G. *Chem. Soc. Rev.* **2010**, *39*, 2083.
- (31) Lipshutz, B. H.; Taft, B. R.; Abela, A. R.; Ghorai, S.; Krasovskiy, A.; Duplais, C. *Platinum Metals Review.* 2012, 62.
- (32) Suzuki, A. *Angew. Chem. Int. Ed.* **2011**, *50*, 6722.
- (33) Chankeshwara, S. V.; Indrigo, E.; Bradley, M. *Curr. Opin. Chem. Biol.* **2014**, *21*, 128.
- (34) Yang, M.; Li, J.; Chen, P. R. *Chem. Soc. Rev.* **2014**, *43*, 6511.
- (35) Prescher, J. A.; Bertozzi, C. R. *Nat. Chem. Biol.* **2005**, *1*, 13.
- (36) Chalker, J. M.; Wood, C. S. C.; Davis, B. G. *J. Am. Chem. Soc.* **2009**, *131*, 16346.
- (37) Völker, T.; Meggers, E. *Curr. Opin. Chem. Biol.* **2015**, *25*, 48.

CHAPTER 2

*Recent Advances in the Palladium Catalyzed
Suzuki-Miyaura Cross-Coupling Reaction in
Water*

2.1 Introduction

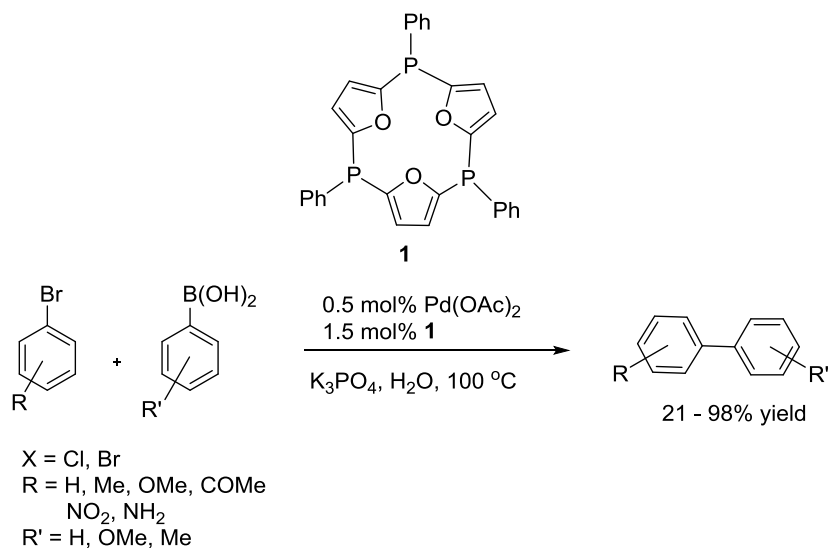
The Suzuki-Miyaura cross-coupling reaction (SMC hereafter) is one of the most important synthetic transformations developed in the 20th century.^{1,2} This is the most versatile methods for the synthesis of biaryls and alkene derivatives. These are structural constituents of numerous agrochemicals, natural products, pharmaceuticals, and polymers.²⁻⁵ Several reviews on the SMC have been published in the literature.⁶⁻¹¹ Recently, green chemistry awareness attempts to address the environmental impact of both chemical products and the processes by which these are produced.^{12,13} Around 80% of the chemical waste from a reaction mixture corresponds to the solvent. From environmental, economic and safety points of view, the use of water as solvent in organic reactions is a clear goal, although challenging and in most cases requires high reaction temperatures.¹⁴ In the case of the SMC, the stability of boronic acids in aqueous solvent are viewed as advantageous compared to other cross-coupling reactions to be performed in water. The literature on the SMC in water up to 2010 has been reviewed by Polshettiwar *et al.*¹⁵ Herein we focus on the use of water as a medium for SMC in homogeneous and heterogeneous systems. This review covers the period from 2011 up to August 2015. Current challenges of palladium catalysed SMC in water include a) the reactivity with low-cost aryl chlorides, b) low catalyst loading, c) the functional group tolerance and d) mild reaction conditions. To address these challenges, several groups developed the palladium catalysed SMC in water with either the homogenous or the heterogeneous system.

2.2 Homogeneous SMC in Water

2.2.1 *P*-donors Ligands

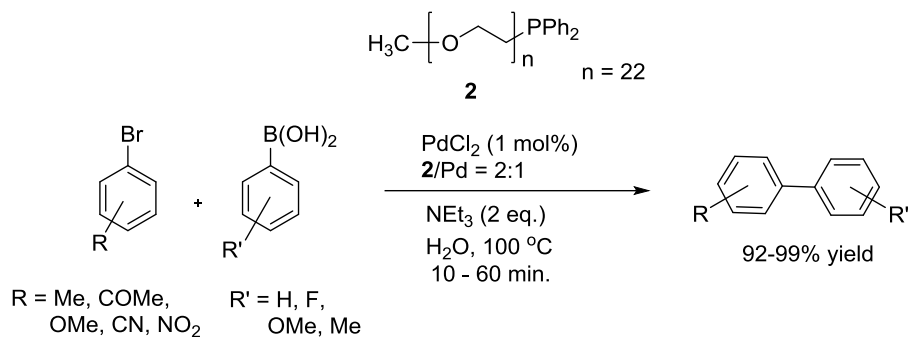
Because of the undesired decomposition of *P*-donors ligands, its use for aqueous SMC has remained limited compared to *N*-donor and NHC ligands. A handful example was found in recent literatures.

For example, Yu and co-workers reported SMC in water catalyzed by a supramolecular assembly held together with noncovalent interactions in the presence of palladium (Scheme 2.1).¹⁶ For this purpose, they designed the tridentate ligand Phenylphosphinacalix[3]trifuran **1**. In the presence of palladium acetate, the resulting catalyst proved extremely active with turnover numbers as high as 3.05×10^7 with 2×10^{-8} mol% Pd loading. The author suggested that these high TONs are not due to a facilitated oxidative addition step but longevity of the catalyst can be a key to reach high TONs.



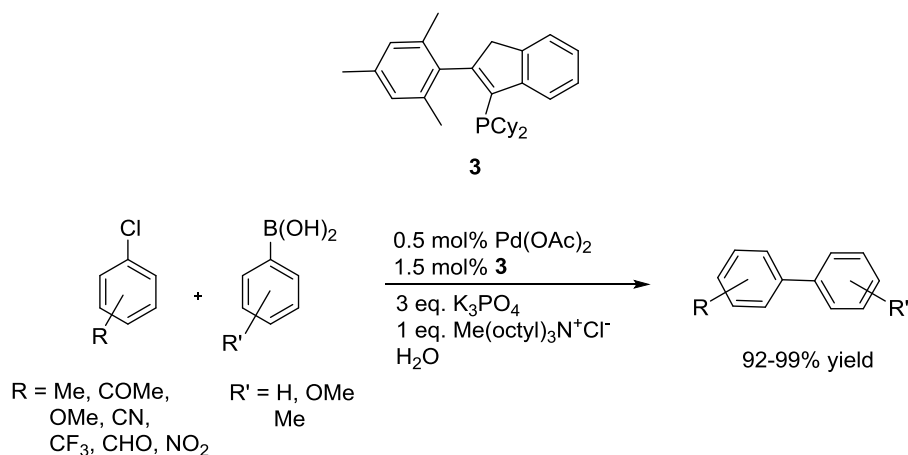
Scheme 2.1 Phenylphosphinacalix[3]trifuran as an efficient ligand for for the SMC in water.¹⁶

An efficient and recyclable protocol for the SMC in water was reported by Liu *et al.* based on the cloud point (Cp) of the thermoregulated ligand **2** (Scheme 2.2).¹⁷ The palladium catalyst remains in the aqueous phase at lower temperature ($< C_p$, 93°C) but transfers into the substrate phase at higher temperature ($> C_p$, 93°C). This method allowed the preparation of a variety of biaryls in high yields (up to 99%) with 0.05 mol% Pd loading. The catalytic system can be recycled four times with high efficiency.



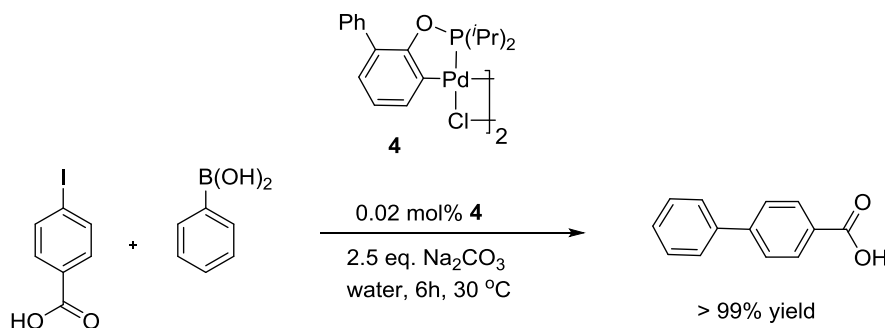
Scheme 2.2 A thermoregulated catalytic system for the SMC in water.¹⁷

Recently, Liu and co-workers¹⁸ reported a catalytic system consisting of the (2-mesitylindenyl)dicyclohexylphosphine ligand **3** in combination with $[\text{Pd}(\text{OAc})_2]$ and $[\text{Me}(\text{octyl})_3\text{N}]^+\text{Cl}^-$ as the phase transfer reagent. The resulting systems displayed high catalytic activity in the SMC of various aryl- and heteroaryl chlorides in water (Scheme 2.3).



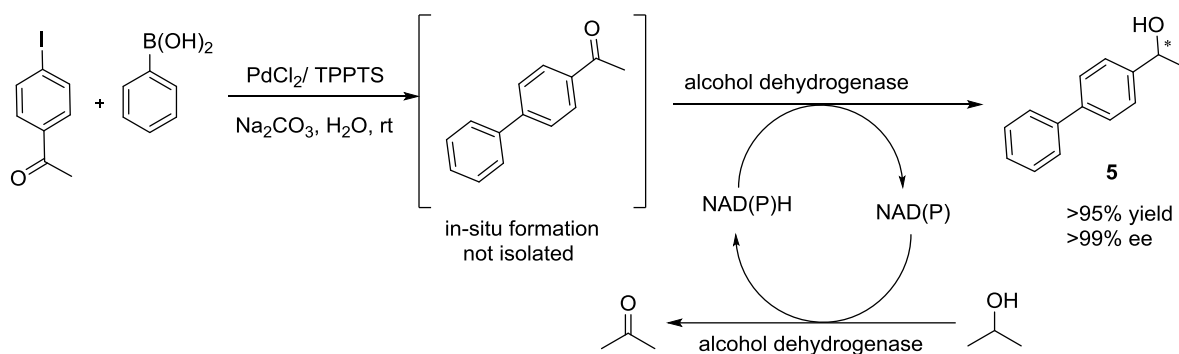
Scheme 2.3 Bulky monophosphine ligand for the SMC in water developed by Liu and co-workers.¹⁸

More recently, Eppinger and co-workers used palladacycle **4**, under air and at room temperature, for the coupling of aryl iodides and bromides with a variety of boronic acids.¹⁹ The biaryl products were obtained in excellent yields (up to 99%) with 0.02 mol% catalyst loading (Scheme 2.4). Poisoning experiments support the hypothesis of the homogenous nature of the catalytically active species, although the pre-catalyst **4** is insoluble in water.



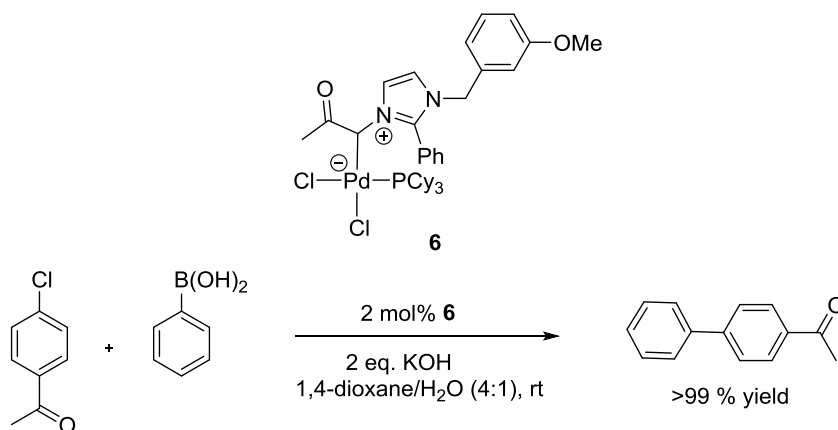
Scheme 2.4 Palladacycle **4** for SMC in water developed by Eppinger and co-workers.¹⁹

Later Gröger and co-workers reported the combination of a palladium-catalyzed SMC in aqueous medium with an enzymatic reduction in a one-pot process at room temperature.^{20,21} For the SMC, a water-soluble palladium catalyst was prepared from palladium chloride and TPPTS (TPPTS = tris(3-sulfonatophenyl)phosphine hydrate, sodium salt). After completion of the reaction and adjustment of the pH to 7.0, the biaryl ketone product was reduced *in situ* via alcohol dehydrogenase (ADH). The desired biaryl alcohol **5** was produced in up to >95% conversion (over the two steps) and excellent enantioselectivities (>99% ee) (Scheme 2.5).



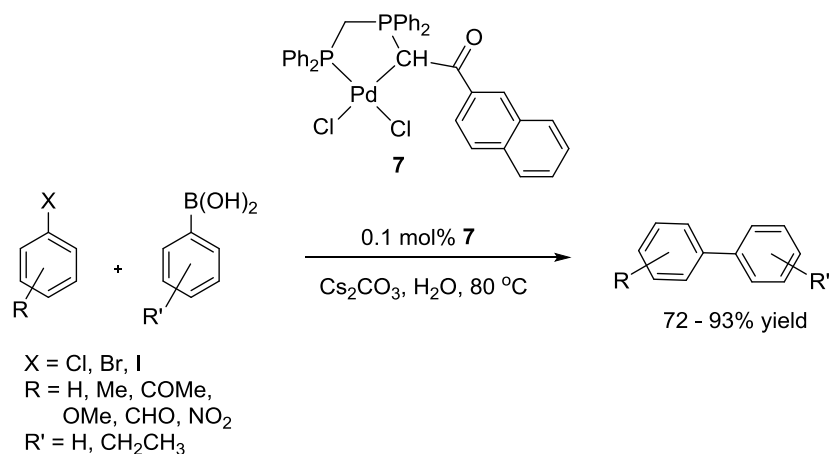
Scheme 2.5 SMC and subsequent enzymatic reduction for the synthesis of chiral biaryl alcohols in water.²⁰

In an independent study, zwitterionic palladium complexes were reported by Lee and co-workers for the SMC in water.²² The zwitterionic phosphine complex **6** was efficient in catalyzing the SMC of sterically hindered aryl chlorides and arylboronic acids in dioxane/water (4:1) or neat water at room temperature (Scheme 2.6).



Scheme 2.6 Zwitterionic palladium complexes for the SMC in water.²²

In a very recent study, Khazalpour and co-workers reported the palladium–phosphine system **7** as an active and recyclable pre-catalyst for SMC in water.²³ A five-membered chelate ring is formed upon coordination of the ligand through the phosphine and the ylidic carbon atom. The catalytic system could be reused four times without significant loss of activity (Scheme 2.7).



Scheme 2.7 A palladium–phosphine catalytic system for SMC in water developed by Khazalpour and co-workers.²³

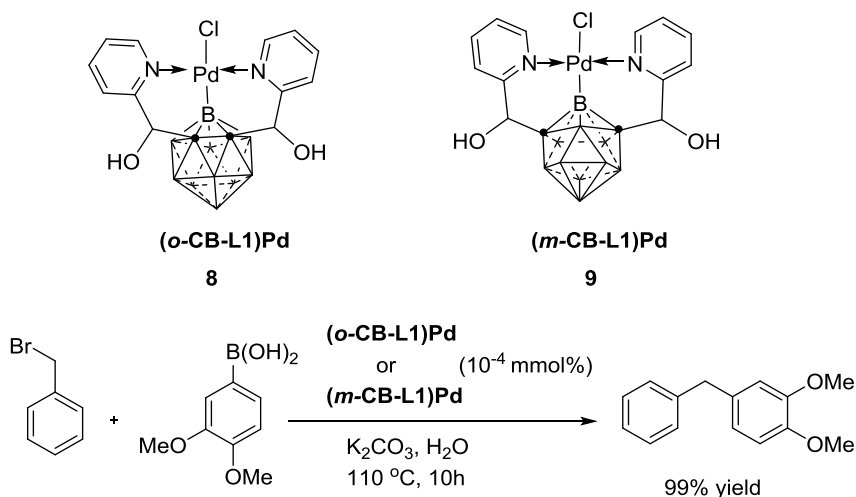
2.2.2 *N*-donor Ligands

Although *N*-donor ligands have been widely neglected in homogeneous organometallic catalysis,²⁴ there has been a resurgence of interest for *N*-donor ligands in SMC. Various types of *N*-donor ligands are presented below: i) pyridines/imines, ii)

imidates iii) pyrimidines iv) amines v) orthometallated palladacycles vi) amides and vii) hydrazones.

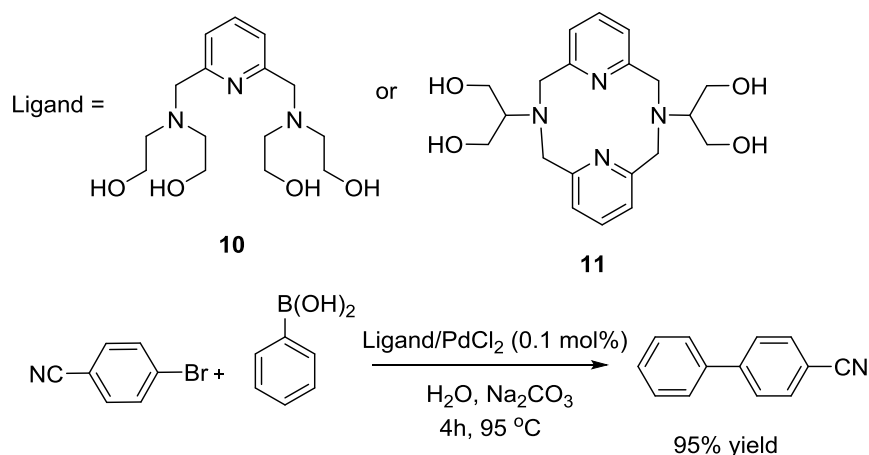
i) Pyridines/imines:

Planas and co-workers developed *o*- and *m*-carborane-based NBN pincer palladium complexes for SMC in water. These catalyst require remarkably low catalyst loadings (10^{-4} mmol%) and display good functional group tolerance.²⁵ They used NBN pincer complex instead of NCN pincer complex because of the stronger electron donating ability of the boron moiety which exhibited stronger *trans*-influence. Complex (***o*-CB-L1**)Pd **8** displayed a better catalytic profile than (***m*-CB-L1**)Pd **9** and with excellent conversions and TON values ranging from 770'000 to 990'000 (Scheme 2.8). Although potentially chiral, no mention is made on whether the ligands were used as a racemate, in their *meso*-form or in enantiopure form.



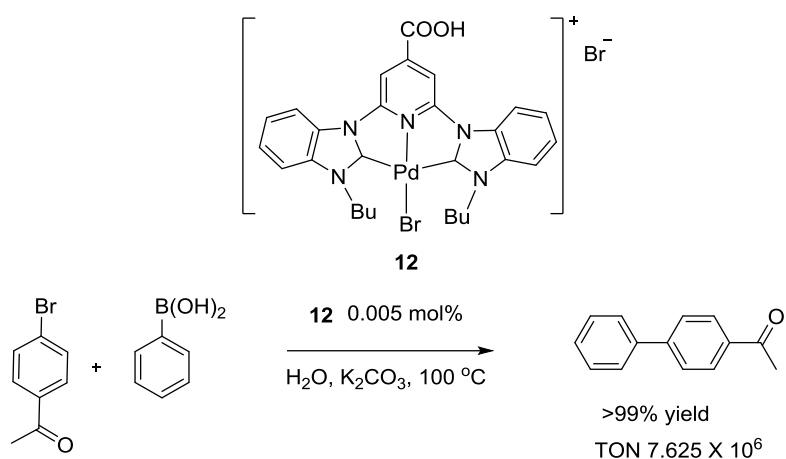
Scheme 2.8 SMC in water with *o*- and *m*-carborane-based NBN pincer palladium complexes.²⁵

A set of water soluble pincer pyridine-diamine ligands **10**, **11** was developed by the Morales group for the SMC (Scheme 2.9). The presence of hydroxy-groups on the ligand ensures water solubility. Excellent yields were achieved (950 TON) for the formation of biphenyls at 95°C in pure water.²⁶ Purification is readily achieved by decantation as the product is insoluble in water. The easy synthesis of the ligand from commercial starting materials, combined with the high catalytic activity of the corresponding complex deserves particular mention.



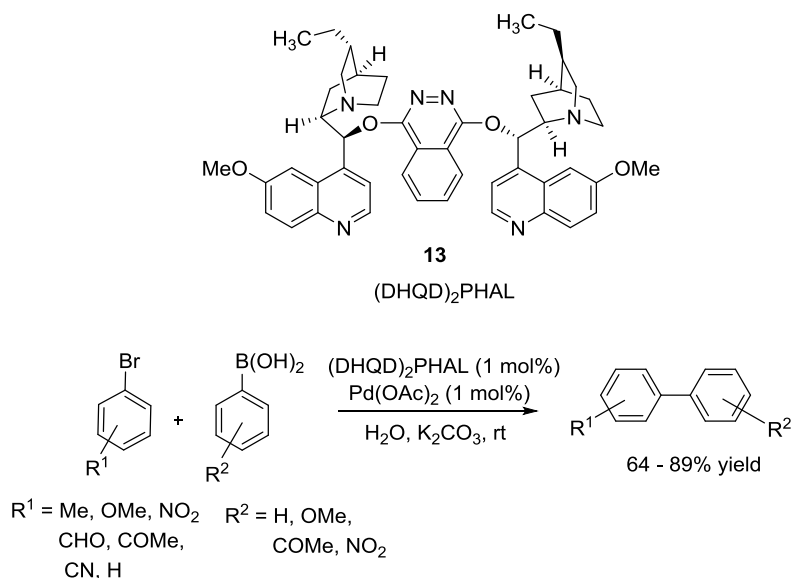
Scheme 2.9 SMC in water with water soluble pincer palladium complexes.²⁶

Recently, Tu and co-workers reported a hydrophilic pyridine-bridged bis-benzimidazolylidene palladium pincer complex **12** which is a highly efficient catalyst towards the SMC in water (Scheme 2.10).²⁷



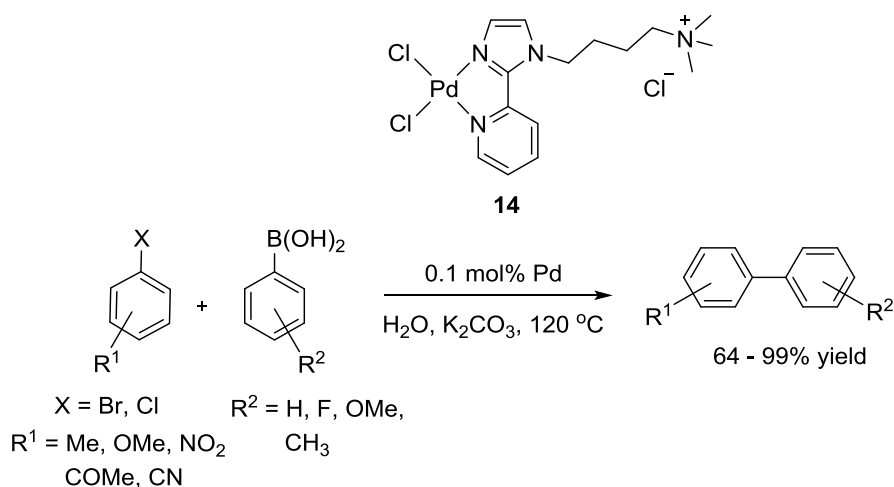
Scheme 2.10 Palladium-pincer complex for the SMC in water.²⁷

The Pd(OAc)₂-(DHQD)₂PHAL **13** catalyzed SMC was reported by Saikia and co-workers (Scheme 2.11). This is a very simple, mild and efficient protocol for the synthesis of biaryls/heterobiaryls in neat H₂O at room temperature. Furthermore, the catalyst system is recyclable and can be employed in several consecutive runs without significant loss in catalytic activity.²⁸ No mention was made concerning the enantioselective SMC with this system.



Scheme 2.11 Pd(OAc)₂–(DHQD)₂PHAL catalyzed SMC in water.²⁸ (DHQD)₂PHAL = Hydroquinidine 1,4-phthalazinediyl diether.

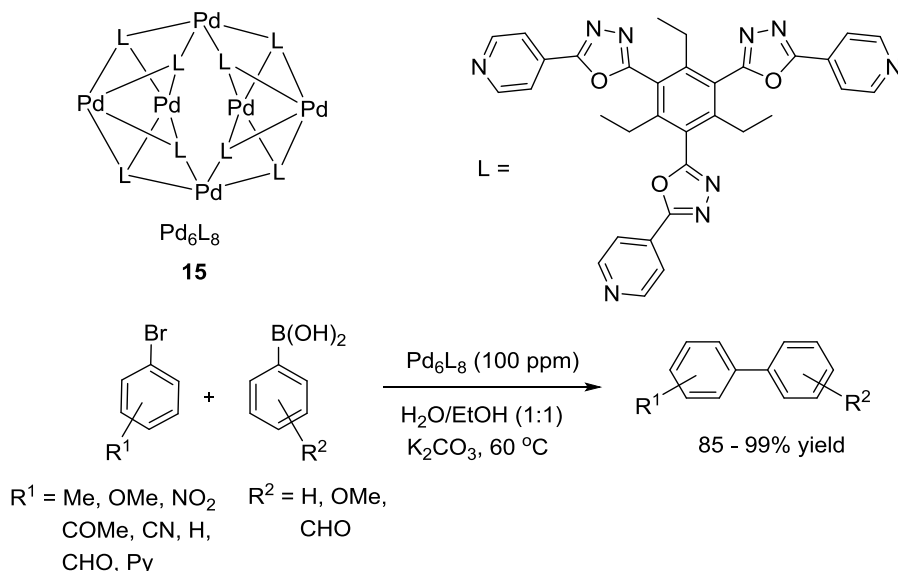
Wang and coworkers reported the synthesis of the palladium chelating complex **14** and its application for the SMC in air and water (Scheme 2.12).²⁹ The biaryl products were obtained in good to excellent yields with 0.1 mol% catalyst loading.



Scheme 2.12 Palladium chelating complex for SMC in water developed by Wang and coworkers.²⁹

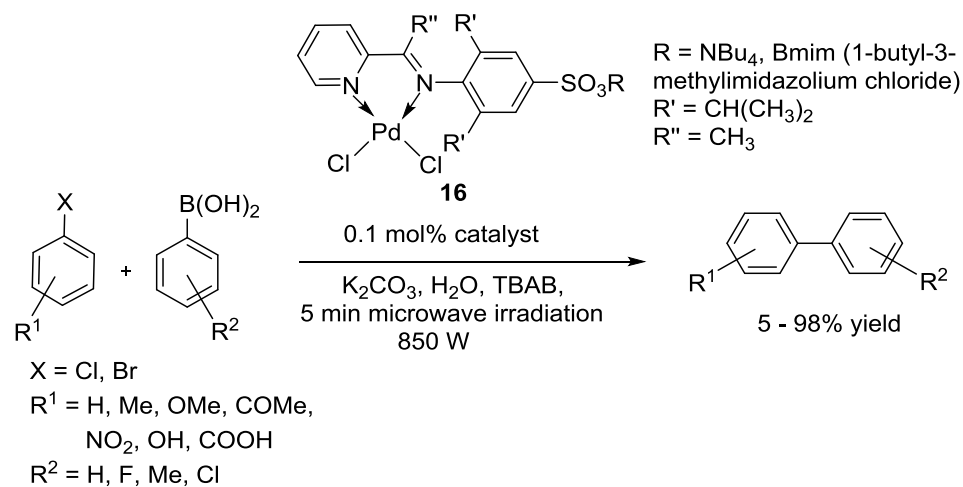
A self-assembled hexanuclear cluster Pd₆L₈ (L = 1,3,5-tris(4'-pyridyloxadiazo)-2,4,6-triethylbenzene) ball **15** was reported by Dong for the SMC at very low catalyst loadings (i.e.100 ppm) (Scheme 2.13).³⁰ Depending on the solvent used for the SMC,

the system was either homogeneous or heterogeneous: the reaction was homogeneous in water-ethanol whereas it was heterogeneous in xylene.



Scheme 2.13 A self-assembled Pd_6L_8 cluster for the SMC in water developed by Dong.³⁰

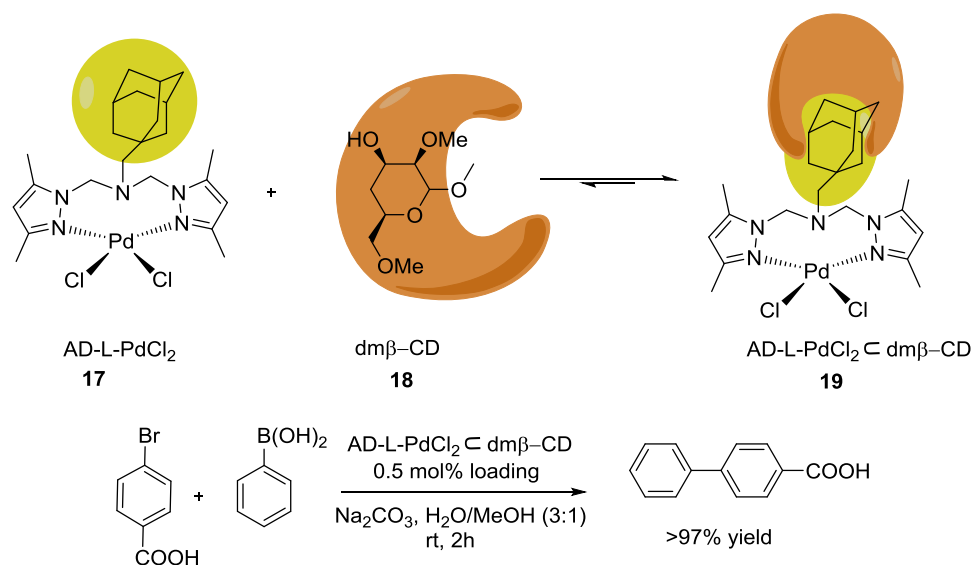
Senemoglu reported a microwave-assisted aqueous SMC catalyzed by unsymmetrical sulfonated water-soluble Pd(II)-pyridyl imine complexes **16** (Scheme 2.14).³¹ The compounds proved to be effective catalysts with up to 980 TON.



Scheme 2.14 Unsymmetrical sulfonated water-soluble Pd(II)-pyridyl imine complexes for SMC in water.³¹

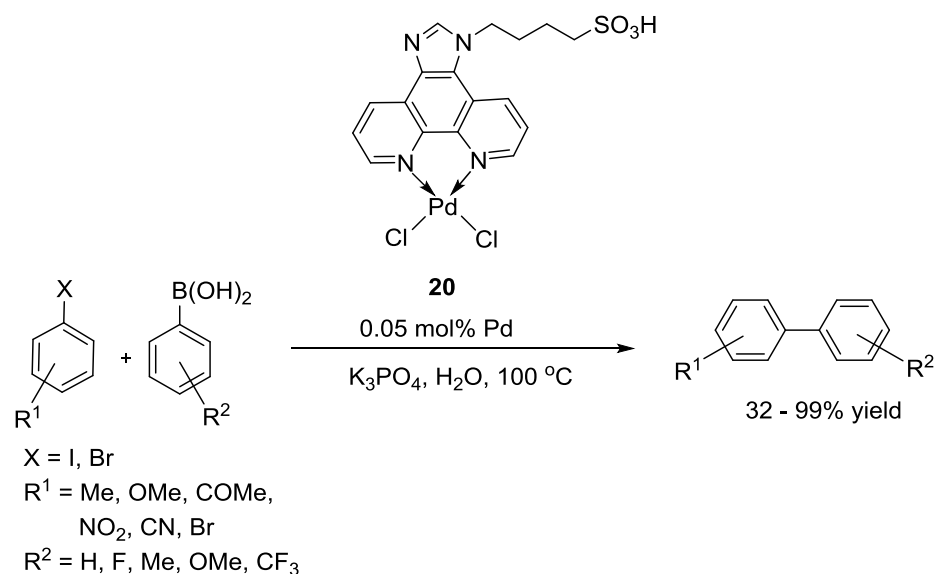
Recently, Hor and Young reported a supramolecular recyclable catalyst for the aqueous SMC (Scheme 2.15).³² Upon host-guest incorporation of **17** within

heptakis(2,6-di-*O*-methyl)- β -CD **18** in aqueous media, a water soluble supramolecular assembly **19** was generated. This catalyst **19** (0.5 mol%) efficiently catalyzed the SMC (>97% yield) between hydrophilic aryl bromides with aryl boronic acid at room temperature.



Scheme 2.15 Supramolecular catalyst for aqueous SMC developed by Hor and Young.³²

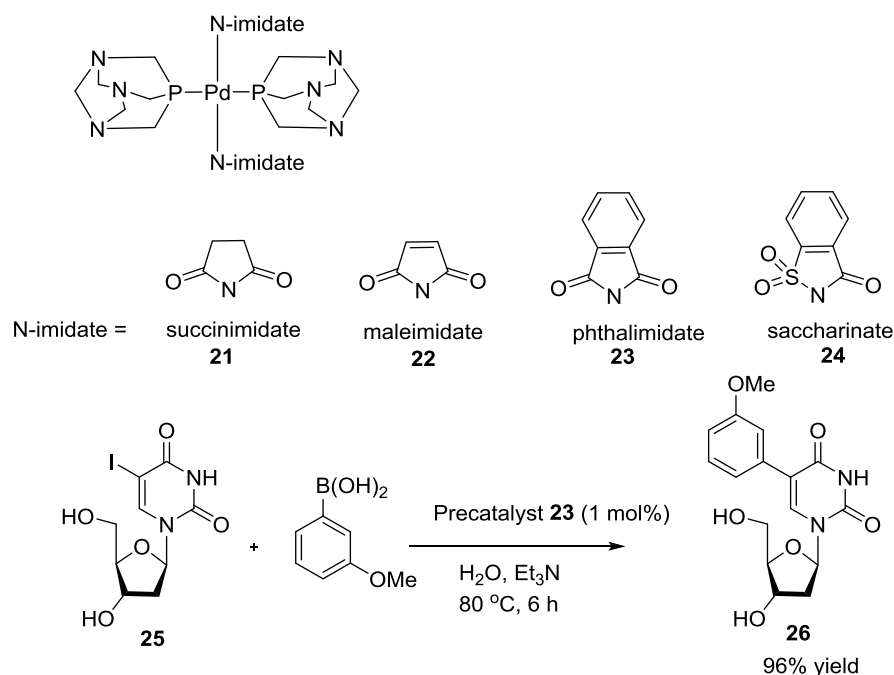
Lang and Li reported a PdCl_2 /sulfonate-tagged phenanthroline precatalyst **20** for the SMC at 100°C in water (Scheme 2.16).³³ The cross-coupling products were obtained in good to excellent yields (TON upto 1980).



Scheme 2.16 Sulfonate-tagged phenanthroline palladium precatalyst for SMC in water.³³

ii) Imidates:

Water-soluble palladium(II) complexes *trans*-[Pd(imidate)₂(PTA)₂] (imidate = succinimidate (suc) **21**, maleimidate (mal) **22**, phthalimidate (phthal) **23** or saccharinate (sacc) **24**) have shown to efficiently catalyze SMC of synthetically challenging substrates. The antiviral nucleoside analogue 5-iodo-2'-deoxyuridine **25** was used as substrate for the formation of the corresponding biaryl **26** in water under mild conditions (TON = 96).³⁴ Upon increasing the reaction time (48 hours), lower catalyst loadings (0.1 mol %) could also be used, without any appreciable erosion of the yield (Scheme 2.17).



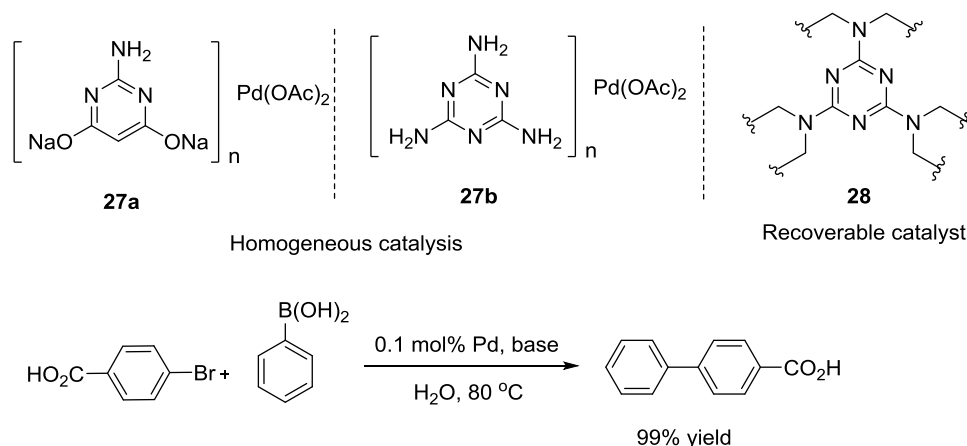
Scheme 2.17 Imidate as ligands for the SMC of 5-iodo-2'-deoxycytidine developed by Serrano and co-workers.³⁴

iii) Pyrimidines:

Ben Davis reported an active pyrimidine ligand **27a** in 2009 for the aqueous SMC.³⁵ Inspired by this work, Chalker and coworkers³⁶ developed a melamine-palladium

catalyst **27b** for the SMC in water (Scheme 2.18). The advantages of the melamine ligand over pyrimidine ligands are as follows:

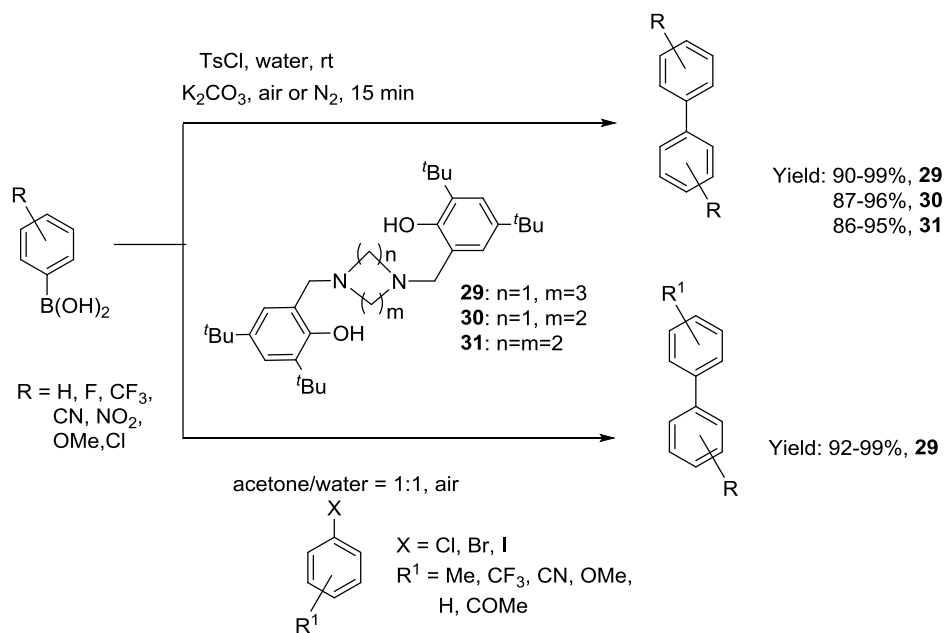
- i) It is less expensive than the pyrimidine.
- ii) It is soluble in both water and organic solvents.
- iii) The melamine-palladium catalyst can be cross-linked by reaction with formaldehyde to generate an insoluble polymeric catalyst **28** that can be recovered after the cross-coupling.



Scheme 2.18 Davis' ligand **27a** for aqueous SMC. Crosslinked and related insoluble melamine-palladium catalysts for the SMC in water developed by Chalker and coworkers.³⁶

iv) Amines:

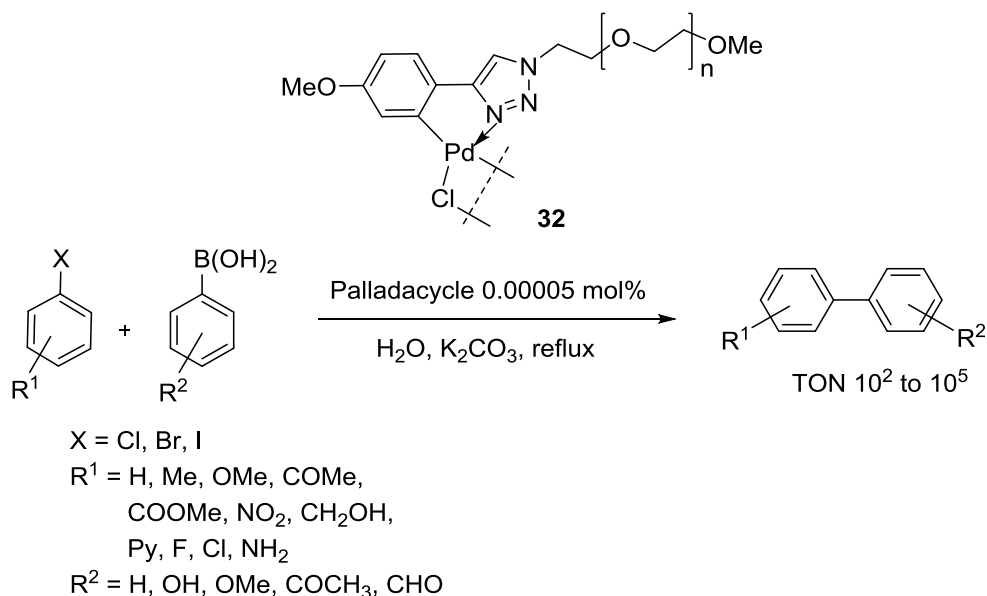
Zhou and coworkers³⁷ investigated the influence of the chelate ring size (i.e. 5 or 6), and the relative position of both *N*-donors and bulkiness of *N*-aryl substituents in amine-bridged bis(phenol) ligands (**29**, **30** and **31**) on the palladium-catalyzed SMC (Scheme 2.19). The homocoupling of arylboronic acid could be completed in neat water with the aid of a catalytic amount of *p*-toluenesulfonyl chloride (TsCl) in a very short time under anaerobic or aerobic conditions. Interestingly, the same catalytic system was efficient for the SMC in aqueous acetone under aerobic conditions in the absence of TsCl.



Scheme 2.19 Amine-bridged bis(phenol) ligands for the aqueous C-C coupling reaction.³⁷

v) Orthometallated palladacycles:

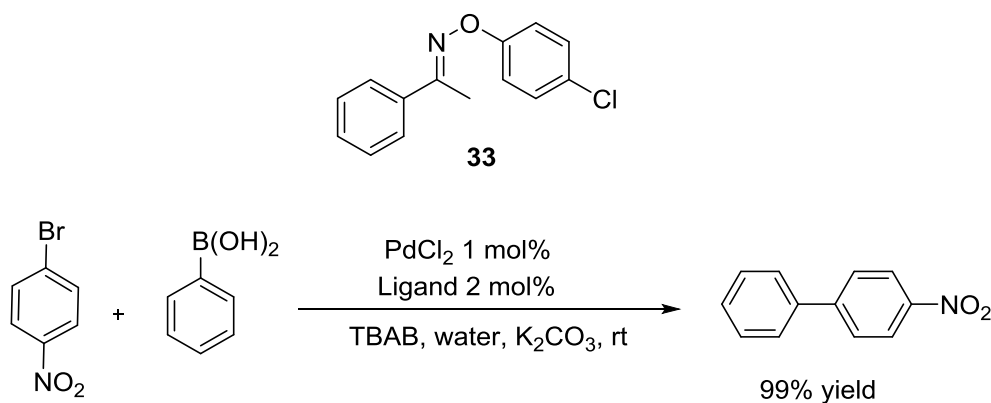
Palladacycles are interesting because they are believed to release highly active Pd(0) species at a very slow rate, which prevents the deactivation of Pd(0) such as nanoparticle formation, thus achieving high turnover numbers. Palladacycles are



Scheme 2.20 SMC in water with an orthometallated aryltriazole palladium complex bearing a PEG solubilizing unit.³⁸

formed by C-H activation of aromatic moiety near a coordination site in the ligand. A novel water-soluble palladacycle **32** has been reported by Ding³⁸ (Scheme 2.20). The catalyst exhibited superior catalytic activity towards the SMC in neat water with TONs of up to 9.8×10^5 . In addition, the catalyst could be reused at least 3 times without significant loss of activity.

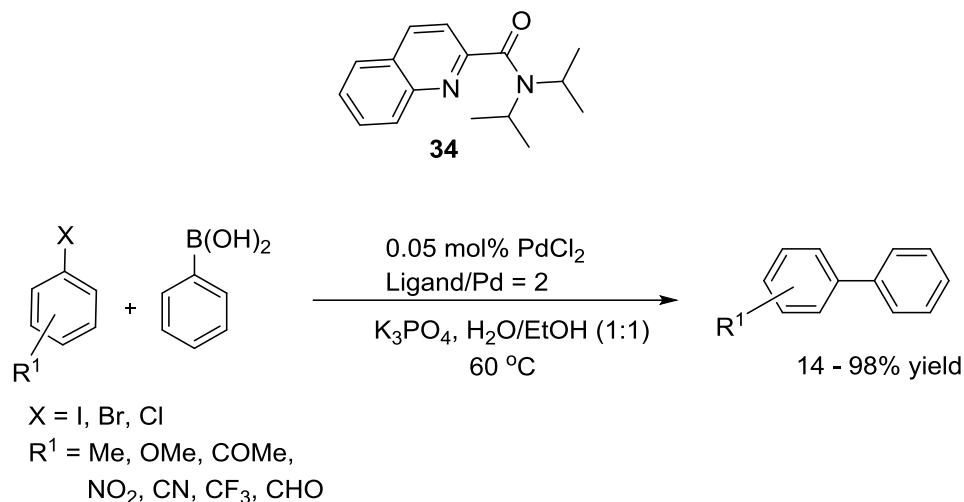
Bora and coworkers studied *O*-Aryloxime ether analog **33** as ligands in the palladium-catalyzed SMC of aryl bromides and aryl boronic acids in water at room temperature.³⁹ Reaction conditions for the cross-coupling were optimized using PdCl₂ and Pd(OAc)₂ under aerobic conditions (Scheme 2.21). To the best of our knowledge, this is the only example of oxime ether used as a ligand. The aryl ring of the aryloxime ether is expected to undergo orthometalation through C-H activation to form highly active palladacycle.



Scheme 2.21 *O*-Aryloxime ether as ligand in palladium-catalyzed SMC in water.³⁹

vi) Amides:

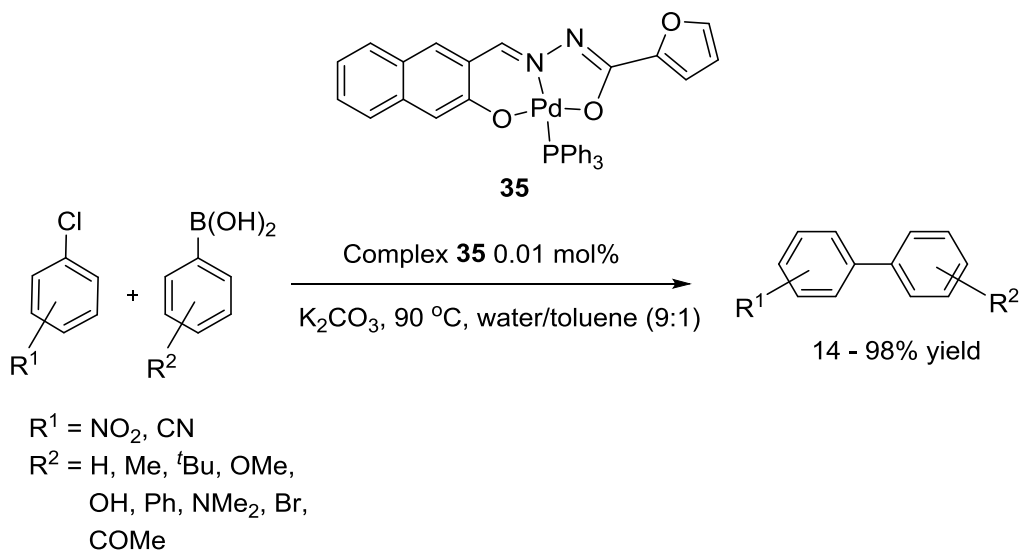
Jiang and Tan recently reported a SMC in water relying on the amide-bearing quinoline derivative **34** as a ligand.⁴⁰ With 0.05 mol% Pd loading, they obtained up to 98% yield at 60–90 °C under air (Scheme 2.22).



Scheme 2.22 Bidentate amide ligand based on a quinoline derivative used for the SMC in water.⁴⁰

vii) Hydrazones:

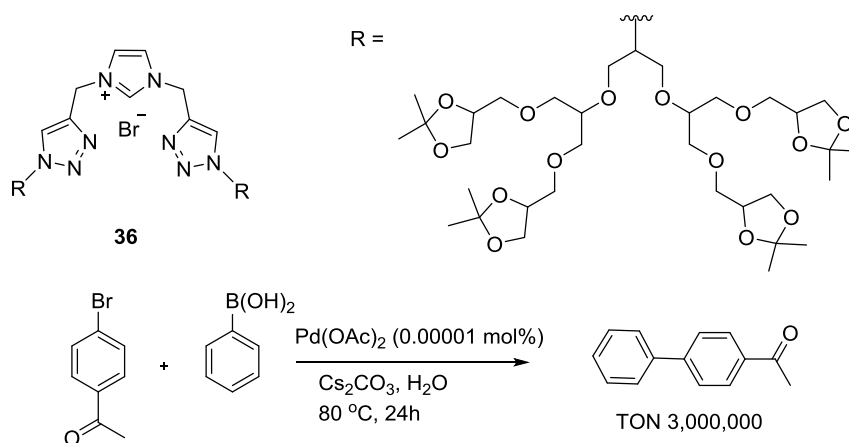
Nallasamy and co-workers reported a palladium(II) complex **35** bearing a series of ONO tridentate heterocyclic hydrazone ligands for SMC of substituted aryl boronic acids with aryl chlorides in a water–toluene system (9 : 1).⁴¹ The catalyst was highly active with 0.01 mol% loading to afford 99% yield of the coupled product (Scheme 2.23).



Scheme 2.23 Tridentate heterocyclic hydrazone ligand for SMC in water.⁴¹

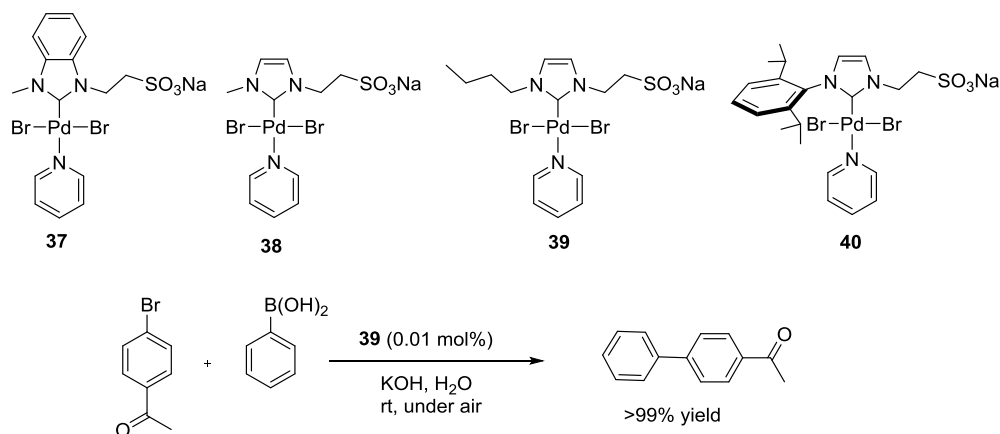
2.2.3 *N*-heterocyclic Carbene (NHC) Ligands

NHC ligands are strong electron donors and can be sterically demanding. Recently, their use in aqueous media has received attention. The carbene carbon of an NHC is strongly basic (pK_a about 20), which generally precludes their use as free ligands in aqueous media. Because of the strong metal-NHC bond, metal complexes of water-soluble NHCs are often water soluble. The Haag group reported a highly active glycerol-dendron-supported *N*-heterocyclic carbene ligand **36** with $Pd(OAc)_2$ as a catalyst (Scheme 2.24). A symmetrical ligand structure was designed to provide a larger micro-environment with the catalytic site at the core position. Deprotection of the dendritic-supported catalysts allowed to perform the catalytic reaction in neat water.⁴²



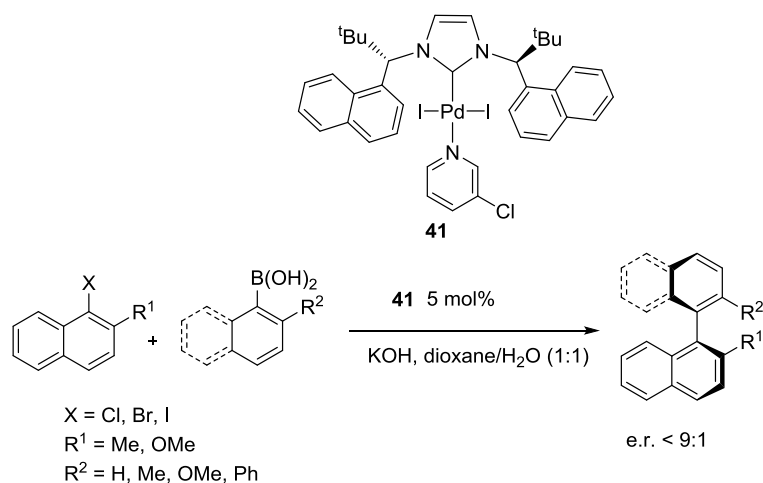
Scheme 2.24 Dendritic supported NHC-palladium catalysts for SMC with a L/Pd Ratio of 1.1:1.

Four water-soluble PEPPSI-type (pyridine, enhanced, precatalyst, preparation, stabilization and initiation) Pd-NHC complexes (**37–40**) were developed by Kühn and Pöthig for the SMC in water under air (Scheme 2.25).⁴³ Complex **37**, bearing a 2,6-diisopropylphenyl substituent, displayed the best catalytic activity for a variety of aryl bromides with a catalyst loading of 0.1 mol% even at room temperature. The catalyst can be used in at least four consecutive runs without significant loss of activity.



Scheme 2.25 Water-soluble PEPPSI-type -Pd-NHC complexes for aqueous SMC.⁴³ (PEPPSI = pyridine, enhanced, precatalyst, preparation, stabilization and initiation)

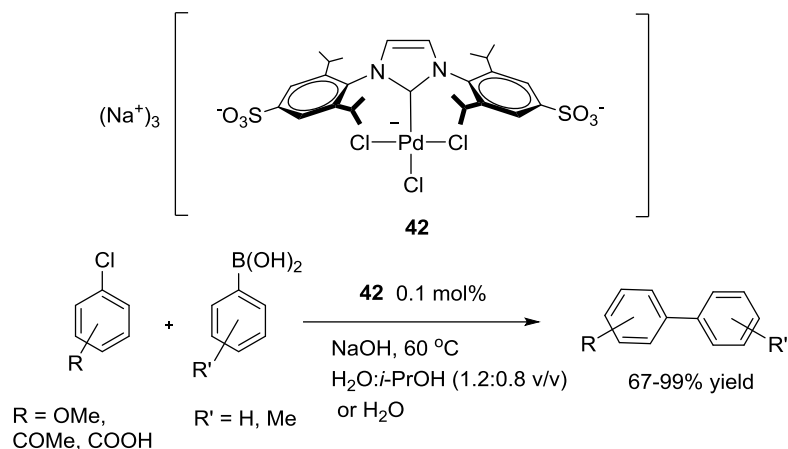
An asymmetric SMC using chiral PEPPSI complex **41** incorporating bulky enantiopure *N*-heterocyclic carbenes was developed by Kündig and coworkers.⁴⁴ They obtained up to 85% yield and 80% ee for coupling of 1-halo-2-methylnaphthalene with naphthylboronic acid. Unfortunately, the product was contaminated with an inseparable homocoupling product (Scheme 2.26).



Scheme 2.26 Asymmetric SMC with chiral PEPPSI complexes incorporating bulky *N*-heterocyclic carbene ligands.⁴⁴

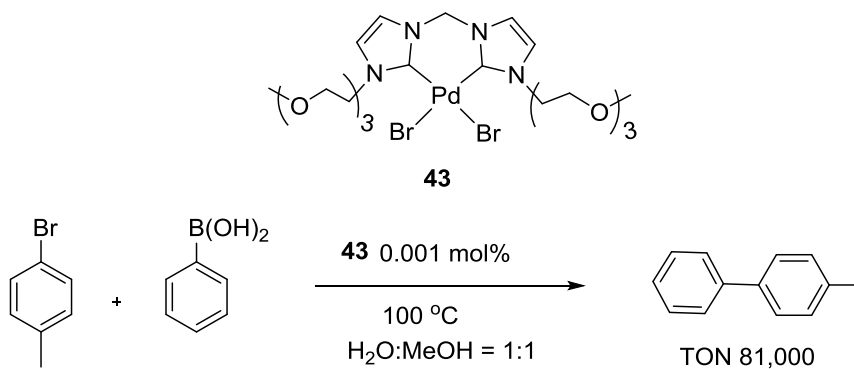
Water-soluble Pd(II)(NHC) complexes **42** containing two sterically-hindered sulfonated groups have been prepared by Jesus.⁴⁵ These complexes are active catalysts for the SMC of aryl chlorides and boronic acids in mixtures of isopropyl alcohol/water

or, in the case of water-soluble aryl chlorides, in pure water (Scheme 2.27). For some of the most hindered aryl chlorides, small amounts of monoarenes are formed via a competitive hydro dehalogenation process.



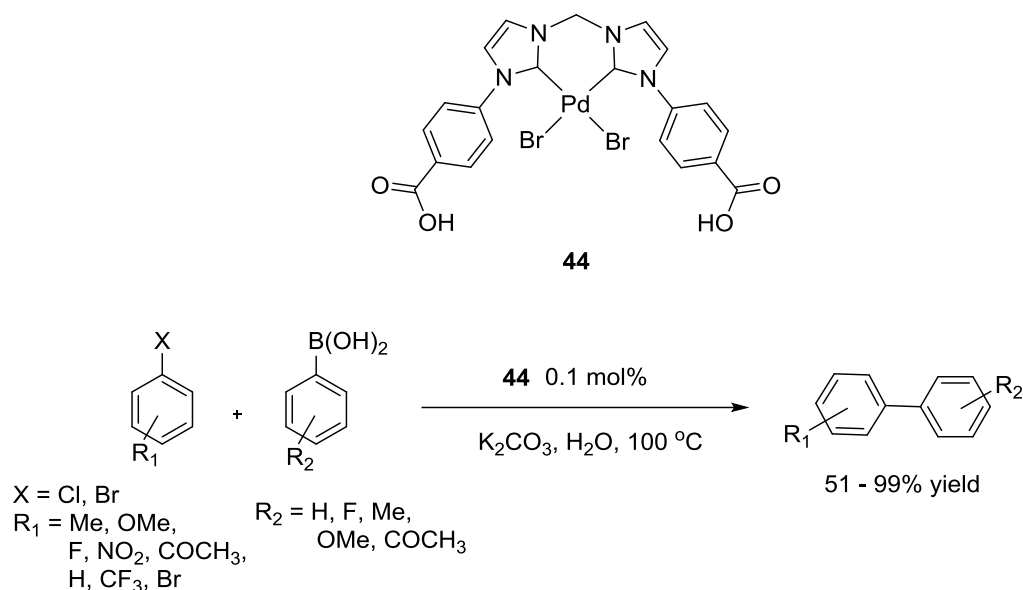
Scheme 2.27 Synthesis of biphenyls by SMC catalyzed by palladium(II) complexes bearing sulfonated N-Heterocyclic Carbenes.⁴⁵

Palladium complexes with chelating, oligo ethylene glycol-substituted bis-NHC ligands have been prepared by Strassner.⁴⁶ The resulting Pd-complex **43** displays excellent water solubility and very high catalytic activity. Up to 80'000 TONs could be achieved in a 1 : 1 water methanol mixture at 100 °C (Scheme 2.28). The palladium complexes showed excellent solubility in water. Very high catalytic activity was achieved even at ppm catalyst loadings.



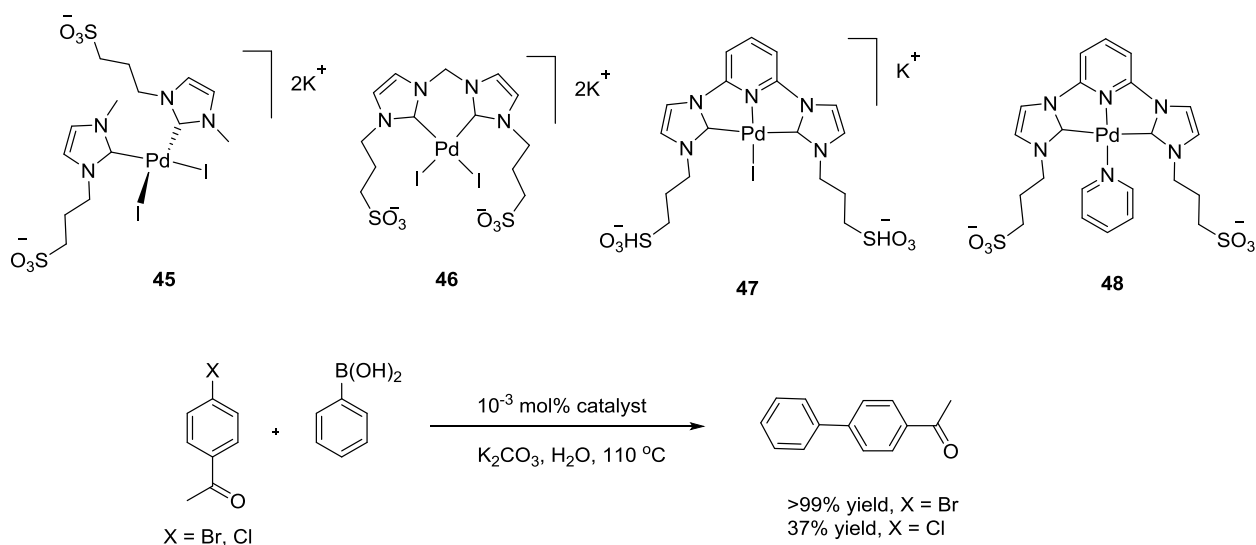
Scheme 2.28 Oligo ethylene glycol substituted bis-NHC ligands for SMC in a water-methanol mixture.⁴⁶

A very similar complex **44** was also prepared by Wang and coworkers.⁴⁷ Deprotonation of carboxylic acid group rendered it water-soluble (Scheme 2.29).



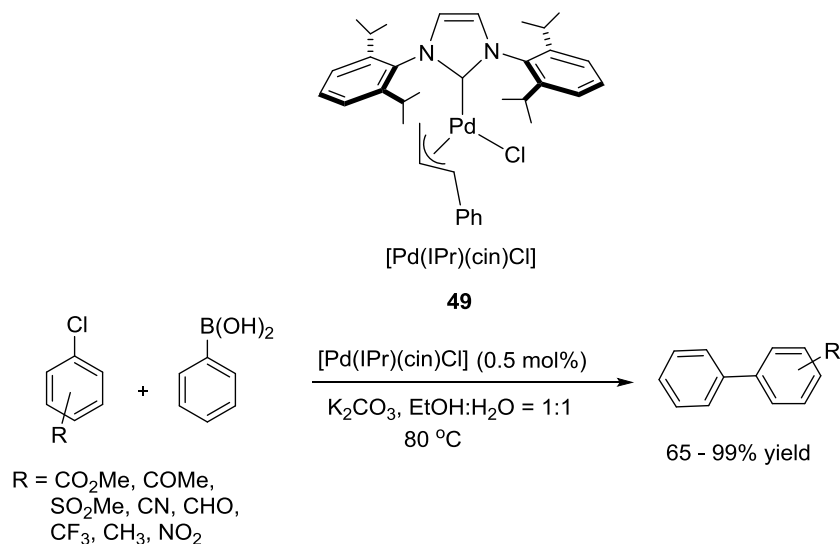
Scheme 2.29 Chelating-NHC-palladium complex for the SMC in water.⁴⁷

In a study, Peris and Godoy compared four bis-NHC-palladium complexes **45** – **48** for the SMC in water.⁴⁸ The bis-NHC-palladium complex **45**, in which the two NHC ligands are in a relative cis configuration, afforded the best catalytic system, with TONs $> 10^5$ for 4-bromoacetophenone and 3.7×10^4 for 4-chloroacetophenone (Scheme 2.30).



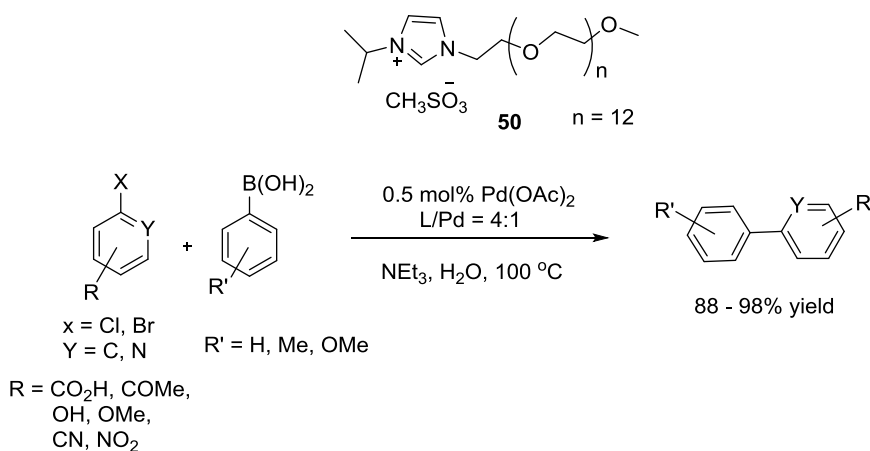
Scheme 2.30 Palladium catalysts with sulfonate-functionalized-NHC ligands for the SMC in water.⁴⁸

Nolan and coworkers recently reported the SMC using a Pd-NHC catalyst at low catalyst loading.⁴⁹ The commercially available and air-stable $[\text{Pd}(\text{IPr})(\text{cin})\text{Cl}]$ pre-catalyst **49** led to the formation of various functionalized biaryls from aryl chlorides and boronic acids under very mild conditions using a mixture of ethanol/water as solvent and an inorganic base (Scheme 2.31).



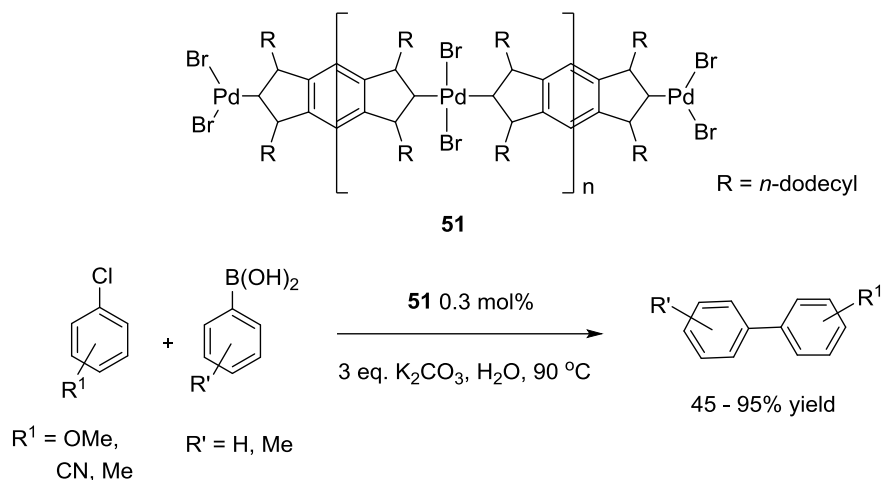
Scheme 2.31 Commercially available precatalyst for SMC in water.⁴⁹

Liu and coworkers⁵⁰ reported the synthesis of water-soluble imidazolium salts **50** bearing poly(ethyleneglycol) moieties directly attached to an *N*-atom of imidazole. The catalytic system generated in situ from a source of $[\text{Pd}(\text{OAc})_2]$, a precursor of imidazolium salt, and triethylamine catalyzes the SMC in water (Scheme 2.32).



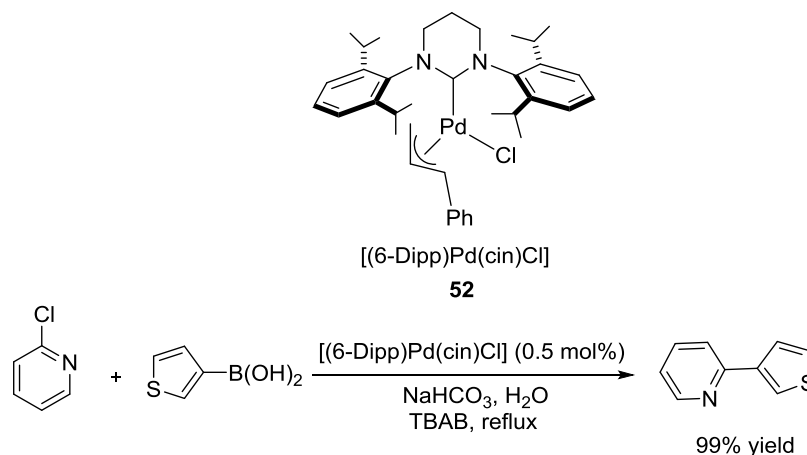
Scheme 2.32 Poly(ethylene glycol)-functionalized imidazolium salts–palladium-catalyzed SMC in water.⁵⁰

Karimi and coworkers showed that Pd-NHC polymers **51** can be used as catalyst for SMC in water (Scheme 2.33).^{51,52} Although the mechanism is not clear, this polymer showed very high activity for the coupling of aryl chlorides, together with excellent recyclability.



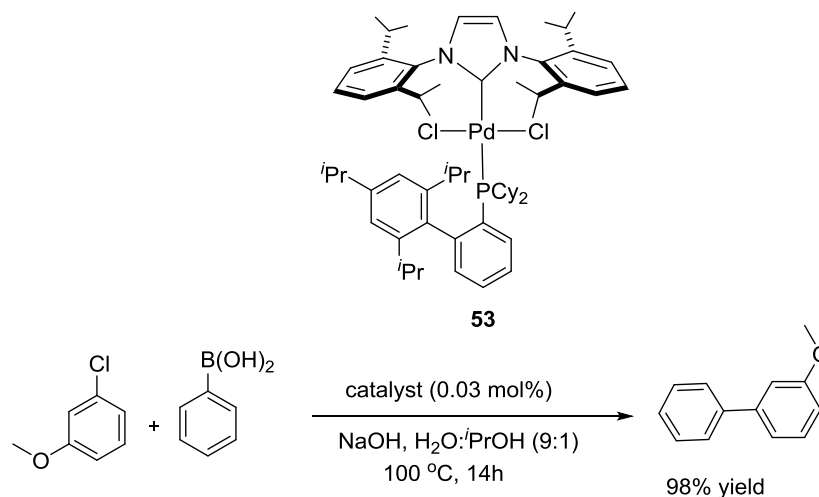
Scheme 2.33 Pd-NHC oligomers for aqueous SMC developed by Karimi.⁵¹

Recently, Nechaev and co-workers synthesized the six-membered ring NHC containing complex **52**, which was used for the cross-coupling of heteroaryl bromides and chlorides with heterocyclic boronic acids in water (Scheme 2.34).⁵³ The cross-coupled products were obtained in very good yield with 0.5 mol% catalyst loading (TON up to 200).



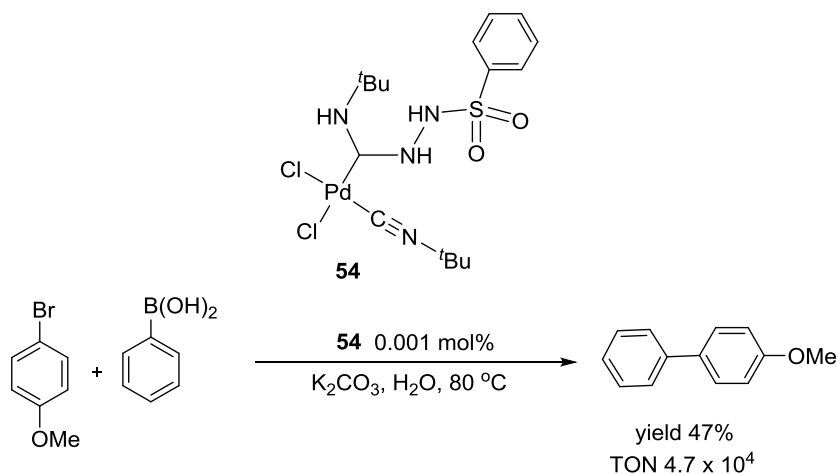
Scheme 2.34 Expanded ring NHC palladium complexes for the SMC in water.⁵³

The same year Cazin and co-workers reported on the synthesis of a mixed $\text{PR}_2\text{Ar}/\text{NHC}$ Pd complex **53** that were used in SMC of aryl chlorides using very low catalysts loadings in aqueous solutions (water/isopropanol 9:1) (Scheme 2.35).⁵⁴



Scheme 2.35 Mixed phosphine/N-heterocyclic carbene palladium complexes for SMC in water.⁵⁴

In an alternative strategy relying on acyclic carbene ligands, Boyarskiy and Luzyanin⁵⁵ reported palladium complexes with acyclic diaminocarbenes [Pd-(ADCs)] (Scheme 2.36). The catalyst **54** efficiently catalyzed the SMC of organohalides with a range of aryl boronic acids at 80°C within 2h (100°C and 3 h for the chlorides). Biaryls were obtained in yields up to 99% and with maximum TONs of 9.9×10^3 (for aryl iodides), 4.7×10^4 (for aryl bromides), and 9.2×10^3 (for aryl chlorides).

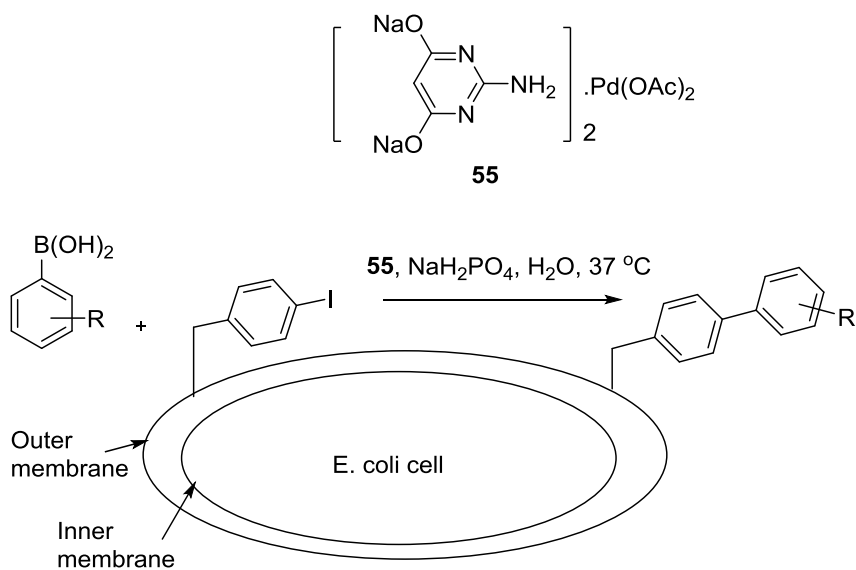


Scheme 2.36 Acyclic diaminocarbene (ADC) based palladium complexes for SMC in water.⁵⁵

2.2.4 Homogeneous SMC for Chemical Biology Applications

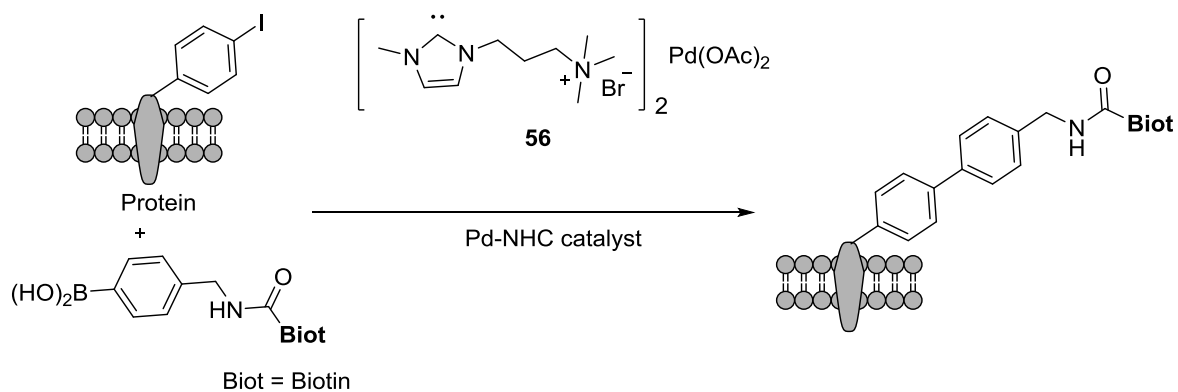
More recently, the SMC has found applications in the context of chemical biology. Indeed, both reactants (i.e. arylhalides and boronic acids) and products (i.e. biaryls) can be regarded as bio-orthogonal.^{35,56-61} In this context however, high catalyst loadings are routinely required for reactions performed in a biological environment.^{35,56,57,60,62-70} Ueno and coworkers anchored a palladium moiety within a ferritin container to yield an artificial metalloenzyme. The resulting artificial metalloenzyme however did not outperform the free cofactor (no enantioselectivity, turnover frequency: 3500 h⁻¹).⁵⁷

The Davis group reported a convenient catalyst for the SMC using a modified protein as substrate.^{35,59,71,72} An effective ADHP (2-amino-4,6-dihydropyrimidine)-based catalyst system [Pd(OAc)₂(ADHP)₂] **55** was given full conversion (>95% yield, 95 TON) between a protein bearing aryl iodide moiety and a broad range of aryl-/vinyl-boronic acids.⁶³ Recently, in a continuous effort to apply transition-metal-mediated reactions in living systems, the Davis' group demonstrated the first application of the SMC on the outer-membrane protein OmpC of *Escherichia coli* cells.⁶⁰ Here, a bacterial surface protein, OmpC was engineered by incorporation of 4-iodo-phenylalanine (Scheme 2.37). A reaction in the presence of a fluorescent boronic acid as coupling partner, catalyzed by [Pd(OAc)₂(ADHP)₂] (200 mol%), afforded the fluorescent cross-coupled product, anchored on the bacterial surface. The ADHP-based catalysts showed excellent labelling efficiency and low cytotoxicity in bacteria cells, although the reaction was not catalytic..⁷³



Scheme 2.37 (2-amino-4,6-dihydroxypyrimidine)-based catalyst system for SMC on the outer-membrane protein OmpC of *E. coli* developed by Davis group.⁶⁰

Wang and Chen reported on a water-soluble *N*-heterocyclic carbene (NHC)-stabilized-palladium complex for the SMC of biomolecules under mild conditions in water (Scheme 2.38).⁶⁷ The Pd–NHC complex **56** bearing hydrophilic groups was an efficient catalyst for the SMC of various unnatural arylhalide-bearing amino acids (TON up to 95). The authors further exploited this catalytic system for the rapid bioorthogonal labeling of proteins on the surface of mammalian cells. In this case, they used a stoichiometric amount of catalyst but there is no mention of yield or TON.



Scheme 2.38 Pd-NHC catalyzed SMC on a cellular system developed by Wang and Chen.⁶⁷

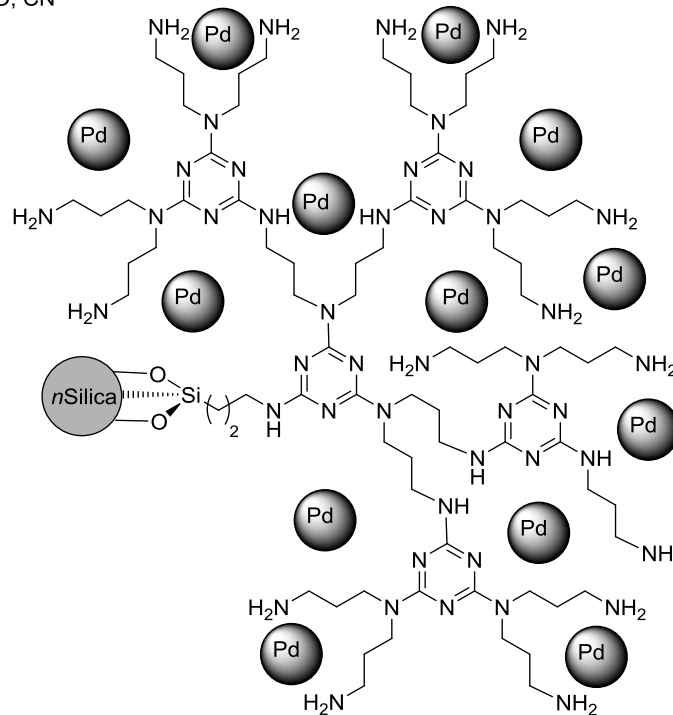
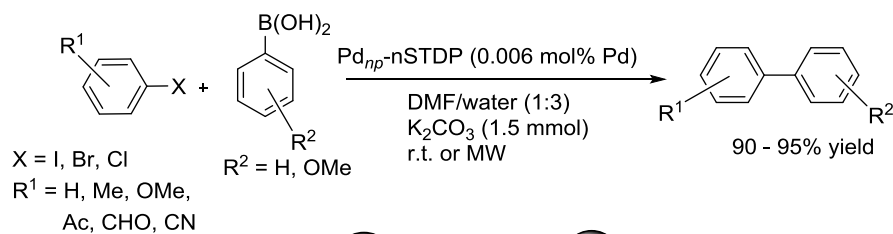
2.3 Heterogeneous SMC in water

In view of the high cost and the shortage of palladium, its recovery and recycling is an important issue for any large scale application. Therefore, a variety of inorganic and organic solid-supported catalytic systems have been developed to address these challenges. In this context, heterogeneous Pd-catalysts are more attractive than the homogeneous Pd-catalysts as their recovery is facilitated. Residual palladium is a particular concern in the synthesis of pharmacophores, where very stringent precious metal restrictions apply. Unfortunately, compared to their homogeneous counterparts, solid-supported catalysts often suffer from lower activity and selectivity. It is thus highly desirable to develop highly efficient supported SMC catalysts.

2.3.1 Supported catalysts

Polymer-modified nanoparticle-supported catalysts have generated a lot of interest due to their unique properties. Polymer supports can be chemically modified easily with functional groups to coordinate with transition metals, potentially improving the long-term stability of the catalyst. Moreover, the nanoparticles may enhance the catalytic performance thanks to their large surface-to-volume ratios and high densities of active sites relative to the bulk metals. Polymer-modified nanoparticles are expected to combine the advantages of both the homogeneous and heterogeneous catalysts.

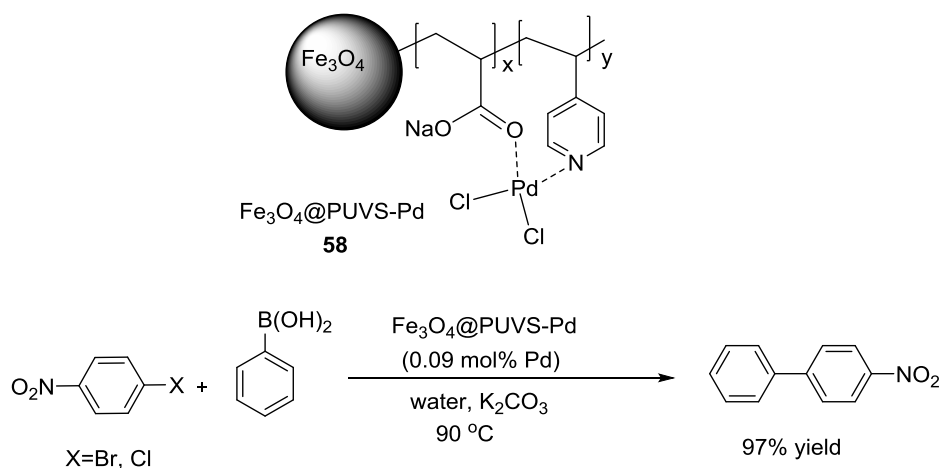
Isfahani and colleagues⁷⁴ recently prepared a catalyst **57** by immobilizing palladium nanoparticles on a nano-silica triazine dendritic polymer. This catalyst exhibited high activity for the SMC even with 0.006 mol% palladium loading (Scheme 2.39). In addition, it could be reused six times with no apparent decrease in yield. The catalyst was recovered by centrifugation, which might be a limitation for large scale applications.

Pd_{np}-nSTDP catalyst

57

Scheme 2.39 Palladium nanoparticles on the nano-silica triazine dendritic polymer as catalyst for aqueous SMC.⁷⁴

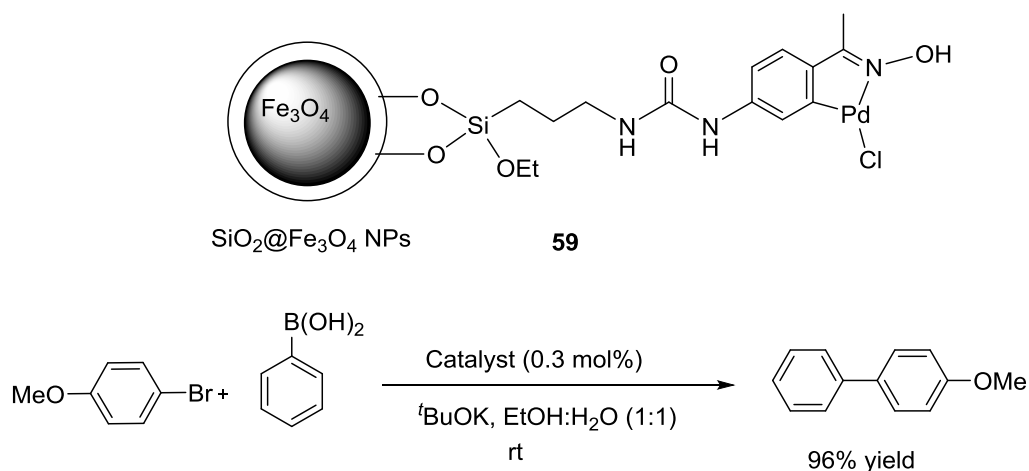
To circumvent the challenge associated with separation of catalyst from reaction medium by filtration or centrifugation, magnetically-separable catalysts have attracted much attention recently. A magnetically responsive polymer nanocomposite Fe₃O₄@poly(undecylenic acid-*co*-4-vinyl pyridine-*co*-sodium acrylate) (PUVS) **58** was introduced by Bian.⁷⁵ This catalyst exhibited excellent catalytic activity for both Heck and SMC in water, and could be conveniently separated and recovered by applying a permanent magnet (Scheme 2.40). The supported catalyst could be used consecutively for six runs without significant loss of catalytic activity.



Scheme 2.40 Magnetic polymer-nanocomposites as catalyst for SMC in water developed by Bian.⁷⁵

PUVS = poly(undecylenic acid-co-4-vinyl pyridine-co-sodium acrylate)

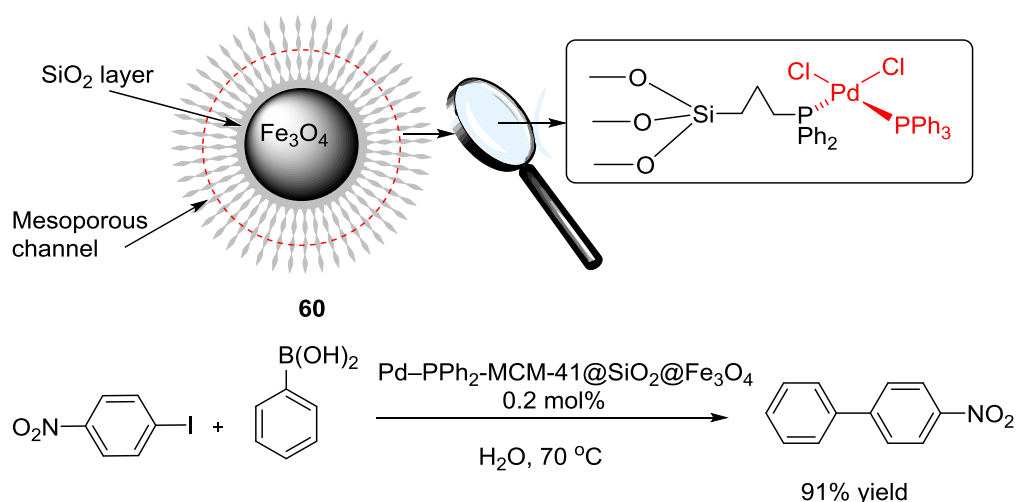
A novel magnetic nanoparticle-supported oxime palladacycle catalyst **59** was prepared and characterized by Gholinejad.⁷⁶ The magnetically recoverable catalyst was employed at room temperature for the SMC of aryl iodides and bromides in aqueous media. The catalyst was shown to be highly active under low Pd loading (0.3 mol%) (Scheme 2.41). The catalyst could be easily recovered from the reaction mixture using an external magnet and reused for six consecutive runs without significant loss of



Scheme 2.41 Magnetic nanoparticle-supported oxime palladacycle catalyst for the SMC in water.⁷⁶ activity. A similar kind magnetically-separable palladium catalyst was also developed by Karimi and co-workers relying on imidazolium ionic liquid bearing triethylene glycol moieties on the surface of silica-coated iron oxide nanoparticles.⁷⁷ The biaryl

products were obtained upto 95% yield with 0.25 - 0.50 mol% Pd loading under argon atmosphere.

Li and co-workers recently reported on a recyclable ordered mesoporous magnetic organometallic catalyst **60** for SMC in water (Scheme 2.42).⁷⁸ They immobilized the catalyst precursor onto undoped and functionalized ordered mesoporous silicas (MCM-41) coated on Fe₃O₄ magnetic microspheres. The catalytic efficiencies were comparable with those of the homogeneous catalysts, and they could be easily recycled (eight times) for reuse by applying an external magnet.



Scheme 2.42 Palladium complexes anchored to an MCM-41 thin layer coated on Fe₃O₄ microspheres as catalyst for the SMC in water.⁷⁸

Trzeciak and co-workers reported palladium supported on triazolyl-functionalized polysiloxane **61**, **62** as a recyclable catalyst for the SMC of aryl bromides with phenylboronic acid at 60 °C in a 2-propanol-water mixture (Figure 2.1).⁷⁹ In recycling experiments, very good results were obtained in eight consecutive runs.

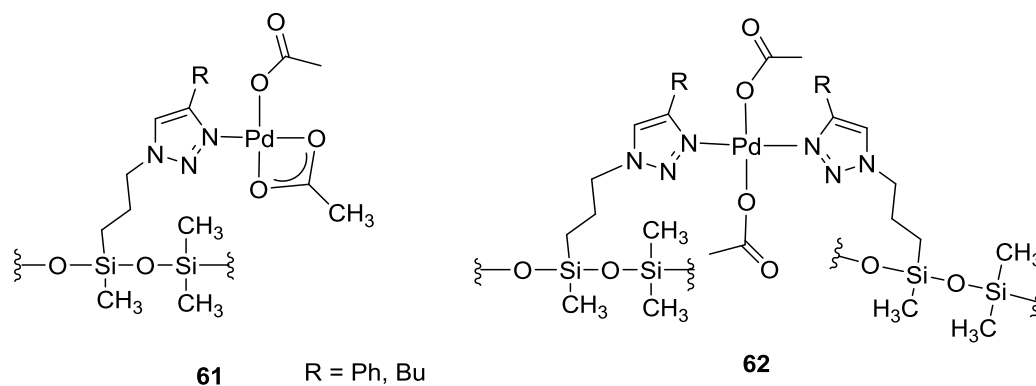
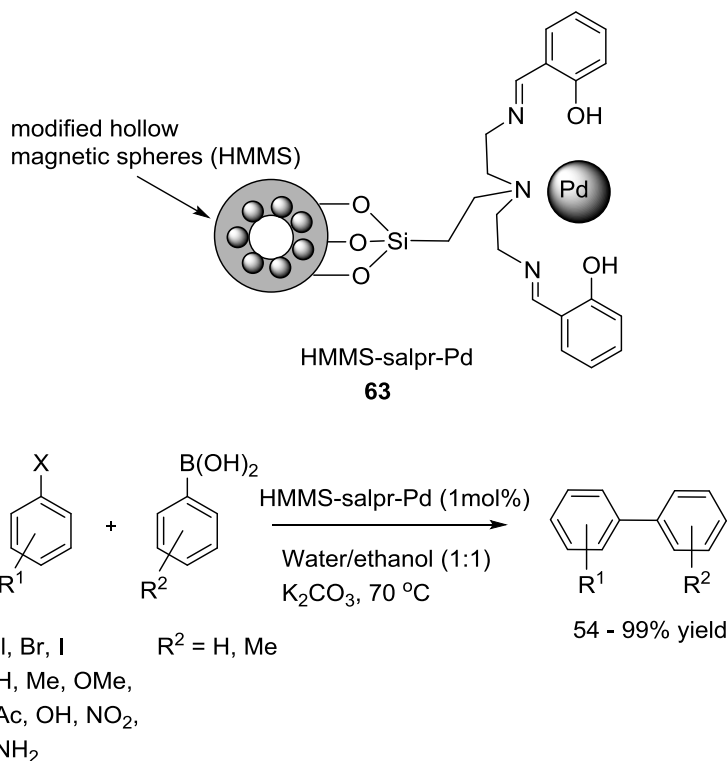


Figure 2.1 Triazole-functionalized siloxane co-polymers as supports for palladium-catalyzed SMC.⁷⁹

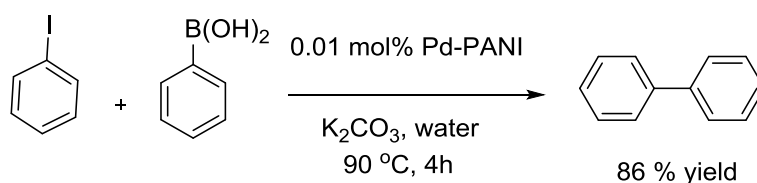
To overcome less accessible active sites for immobilized or supported palladium catalysts, Ma and co-workers recently developed a self-supported hollow material with tunable cavities. This material is potentially interesting thanks to its inherent features including: i) high surface area, ii) low density iii) easy recovery, iv) low cost, and v) surface permeability. Relying on tetrabutylphosphonium bromide (Bu_4PBr) as template, Ma prepared a mesoporous Pd–Fe alloy magnetic spheres catalyst with a



Scheme 2.43 Pd nanoparticles immobilized on modified hollow magnetic spheres (HMMS) for SMC in water developed by Ma.⁸¹

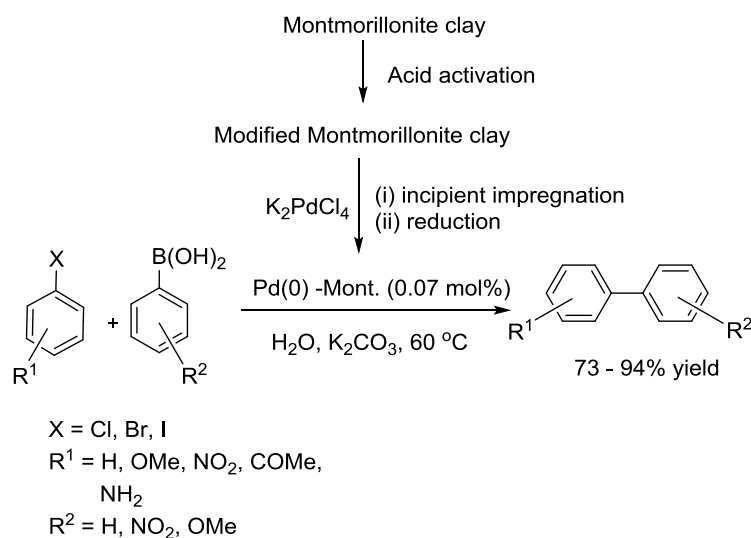
hollow chamber.⁸⁰ This catalyst displays high activity in the SMC. In a subsequent study, Ma reported a high-performance palladium catalyst **63** resulting from the covalent anchoring of a Schiff-base ligand, *N,N'*-bis(3-salicylidenaminopropyl)amine (salpr), on the surface of hollow magnetic mesoporous spheres (HMMS) followed by immobilization of Pd(0) (Scheme 2.43).⁸¹ The heterogeneous catalyst could readily be recovered from the reaction mixture and recycled six times without any loss of activity.

Recently, Siril and co-workers reported a palladium–polyaniline (Pd–PANI) nanocomposite for the SMC in aqueous media (Scheme 2.44).⁸² PANI is a conducting polymer which was used as a catalyst support. With this system, they showed that the SMC proceeds much faster in water than in toluene.



Scheme 2.44 Palladium-polyaniline nanocomposite for SMC in water.⁸²

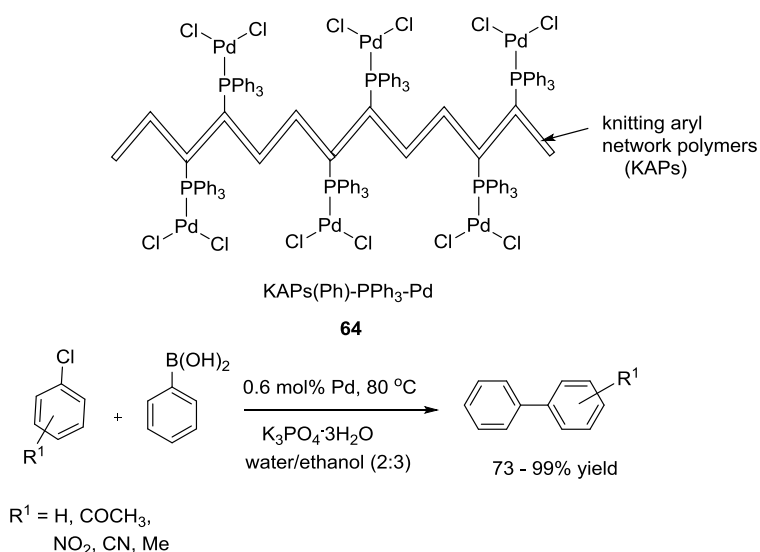
Dipak and co-workers reported on the application of the modified Montmorillonite clay supported Pd(0)-nanoparticles as an efficient catalyst for the SMC (Scheme 2.45).⁸³ This naturally occurring clay requires no surface functionalization and its pore



Scheme 2.45 Pd(0)-Montmorillonite clay composites catalyzed SMC in water.⁸³

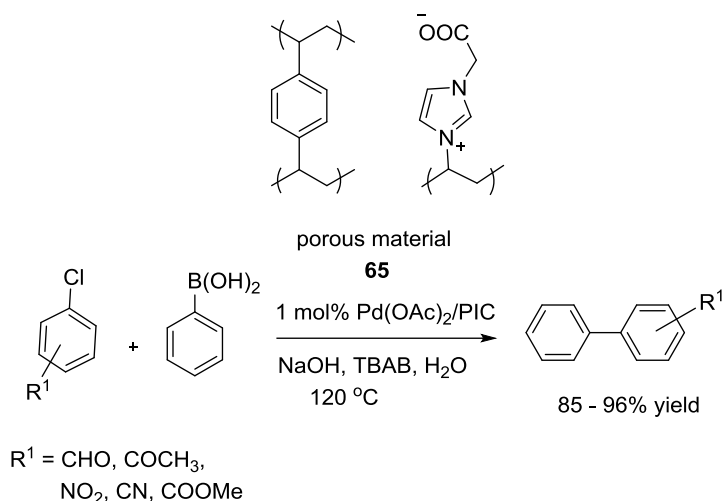
sizes can be tuned by an acid activation. The modification of Montmorillonite clay was carried out by activating with H_2SO_4 under controlled conditions to generate nanopores on the surface, thus serving as a ‘Host’ for the Pd(0)-nanoparticles. The supported Pd(0)-nanoparticles were efficient catalysts for the SMC (up to 94% yield) in water under ligand free conditions. The nano-catalyst could be recycled at least three consecutive runs with a little loss of catalytic activity.

Recently, Li⁸⁴ reported on a highly dispersed palladium chloride catalyst anchored in triphenylphosphine-functionalized knitting aryl network polymers (KAPs) **64**. These exhibited excellent activity for the SMC of aryl chlorides in aqueous media (Scheme 2.46). A potential reason for high catalyst activity was that the microporous polymers not only played the role of support, but also protected the Pd(0) species from aggregation and precipitation.



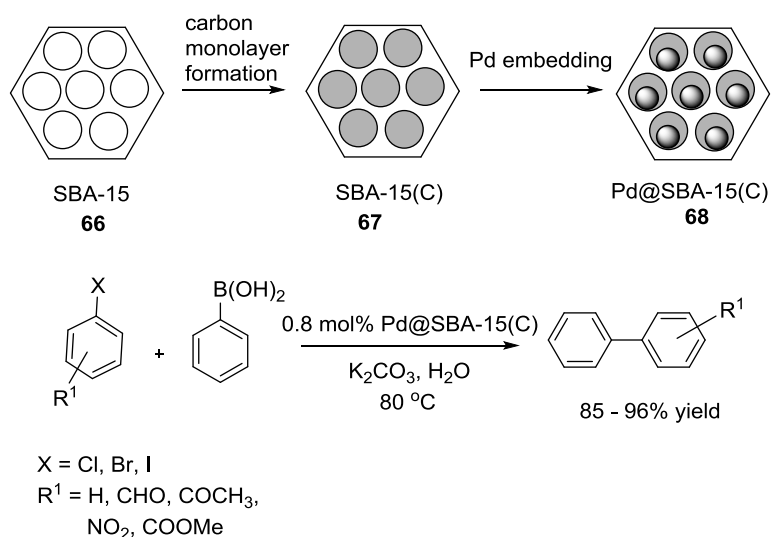
Scheme 2.46 Aqueous SMC catalyzed by KAPs(Ph-PPh₃)-Pd.⁸⁴

Huang and co-workers reported on the use of Pd nanoparticles on a porous ionic copolymer **65** of an ionic liquid and divinylbenzene for the coupling of aryl bromides and chlorides under air and in water, using Pd loadings as low as 10 ppm (Scheme 2.47).⁸⁵



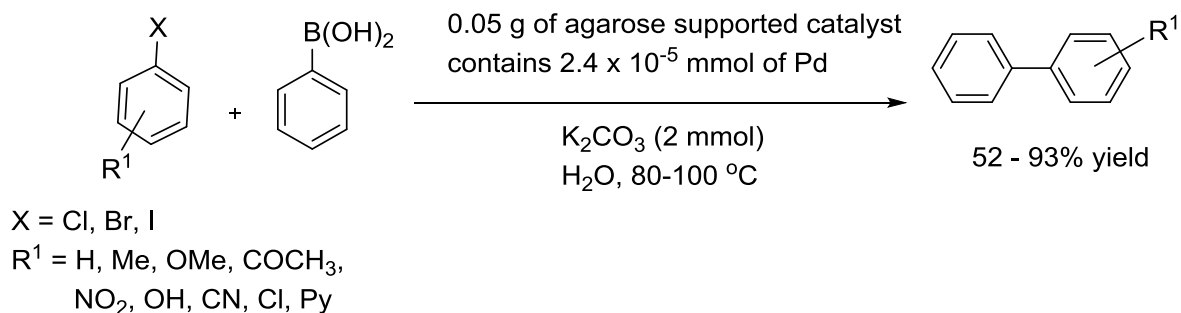
Scheme 2.47 A Pd(OAc)₂/porous ionic copolymer (PIC) catalyzes the SMC in water.⁸⁵

Hu and co-workers embedded Pd nanoparticles in carbon thin film-lined nanoreactors **67**. The resulting embedded nanoparticles **68** catalyzed the SMC yielding good results, allowing the recycling of the heterogeneous catalyst (Scheme 2.48).⁸⁶ Thanks to their controllable size, composition and morphology, mesoporous silica (e.g. SBA-15 **66**) are highly attractive supports for immobilizing Pd nanoparticles.



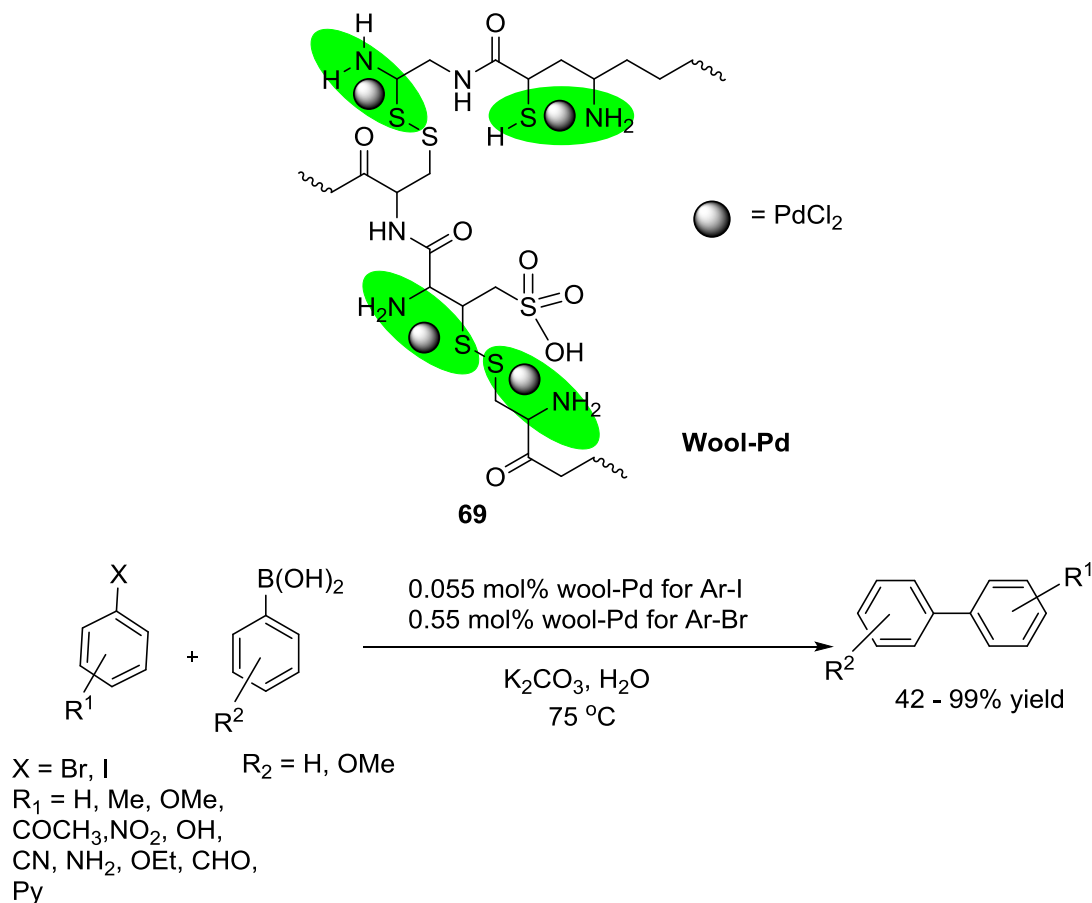
Scheme 2.48 Pd nanoparticles-embedded nanoreactor catalyzed SMC in water.⁸⁶

Firouzabadi and Iranpoor used an agarose hydrogel to contain the Pd for the SMC in water (Scheme 2.49).⁸⁷ The catalyst was efficiently recycled five times.



Scheme 2.49 Agarose hydrogel supported Pd nano catalyst for the SMC in water.⁸⁷

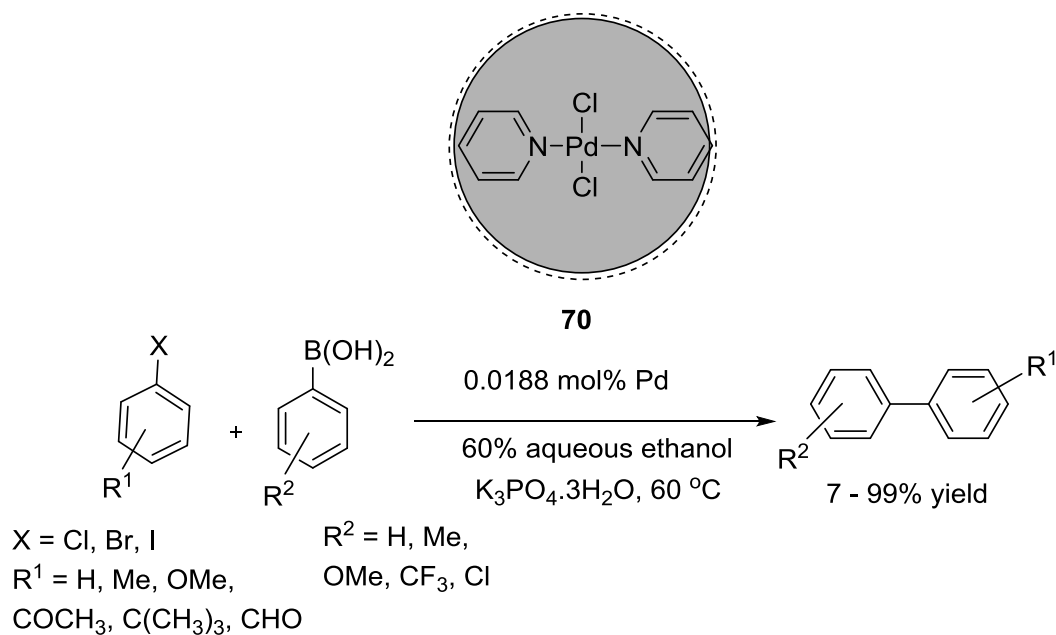
Ma and Lei prepared a heterogenous biopolymer complex consisting of wool-PdCl₂ **69** that performed the SMC of aryl chlorides in water (Scheme 2.50).



Scheme 2.50 A wool-Pd complex the the SMC in water.⁸⁷

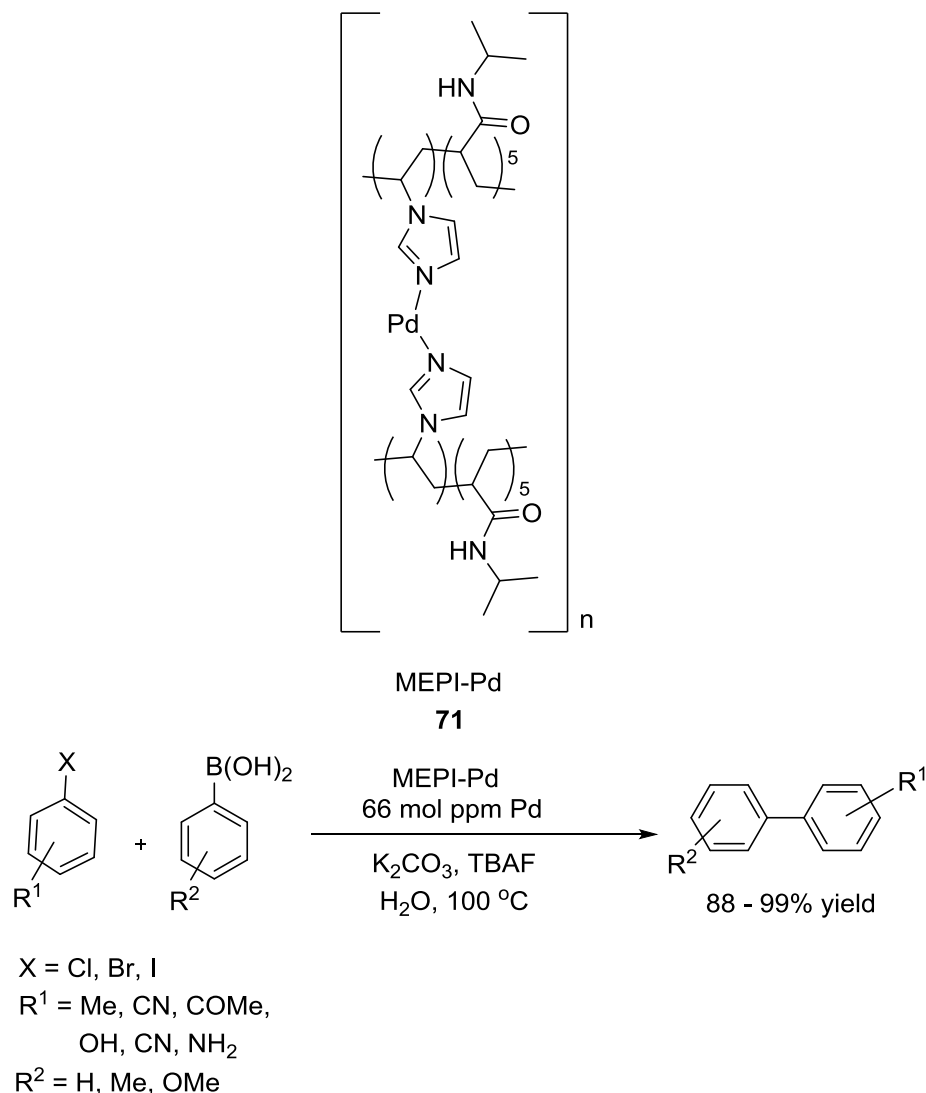
Li and co-workers used recyclable monodispersed zeolitic hollow spheres **70** containing [PdCl₂(pyridine)₂] to couple aryl bromides and iodides in a 60% aqueous ethanol solution (Scheme 2.51).⁸⁸ This catalyst afforded fast conversions for the SMC

of various aryl halides and arylboronic acids even at Pd loadings of 0.0188 mol%. Under mild and aerobic conditions, a TOF 63210 h⁻¹ is reported. This catalyst could be recycled at least 10 times without any loss of activity.



Scheme 2.51 Monodisperse zeolitic hollow spheres containing [PdCl₂(pyridine)₂] catalyze the SMC in water.⁸⁸

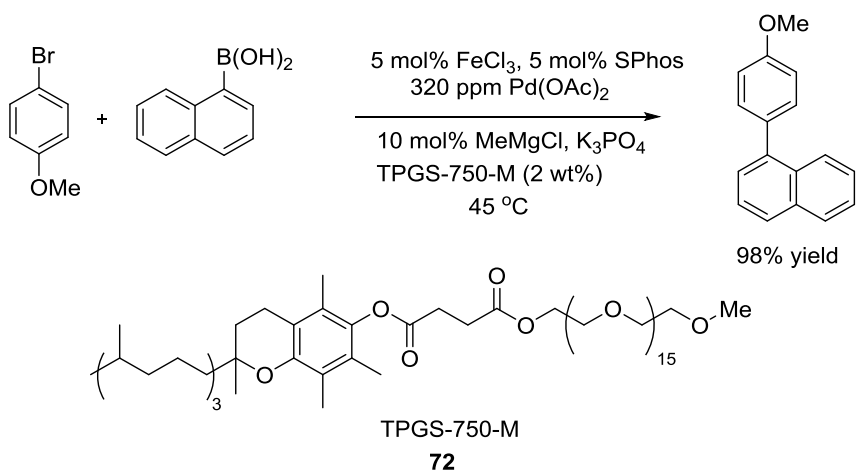
Yamada and Uozumi⁸⁹ developed a metalloenzyme-inspired polymer catalyst **71**: a self-assembled catalyst consisting of poly(imidazole-acrylamide) and [(NH₄)₂PdCl₄] that promoted the allylic arylation, alkenylation, and vinylation of allylic esters with aryl/alkenylboronic acids in water with TON varying between 20,000–1,250,000 (Scheme 2.52).



Scheme 2.52 A Metalloenzyme-inspired polymeric imidazole Pd catalyst (MEPI-Pd) for the SMC in water.⁸⁹

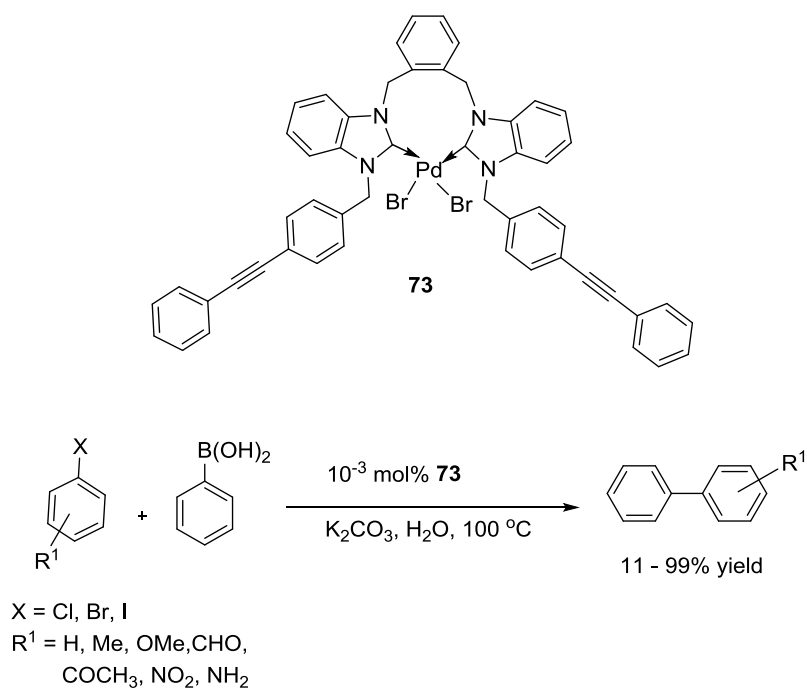
2.3.2 Unsupported catalyst

In a very recent study, Lipshutz and co-workers reported that nanoparticles formed from inexpensive FeCl₃ that contains parts-per-million (ppm) levels of Pd catalyze the SMC in water (Scheme 2.53).⁹⁰ This system however requires the use of designer surfactant TPGS-750-M **72**. This surfactant is composed of a lipophilic α -tocopherol moiety and a hydrophilic PEG-750-M chain, joined by an inexpensive succinic acid linker, spontaneously forms micelles upon dissolution in water.



Scheme 2.53 Fe-ppm Pd nanoparticle catalyzed SMC in water.⁹⁰

NHC-ligand is very common in homogeneous catalysis (*vide supra*), although it is rarely used in the heterogeneous catalysis to stabilize Pd(0). Recently, Schmitzer used an unsupported Pd-NHC complex **73** for SMC (Scheme 2.54).⁹¹ The catalyst is insoluble in water and the mercury drop test suggested the heterogeneity of the system. This heterogeneous catalyst was used in low loadings (10⁻³ mol%) for the SMC in pure water with very good recyclability (10 times) and high yield (TON = 10⁵).



Scheme 2.54 Support-free palladium-NHC catalyst for SMC in water.⁹¹

The first ligand-free SMC of aryl halides with potassium aryl-trifluoroborates in water was reported by Molander *et al.* in 2003.⁹² Following this report, many groups developed ligand free strategies for SMC in water. In this context, Bora⁹³ and Liu^{94,95} have recently shown that the only use of PdCl₂ and Pd(OAc)₂, respectively, in the presence of an adequate base can couple a variety of aryl bromides in water. Boruah and co-workers reported Pd(OAc)₂-catalyzed SMC of aryl bromides with arylboronic acids in aqueous tea extract at room temperature.⁹⁶ Recently, Corma and co-workers developed palladium clusters with three- or four palladium atoms (characterized by UV-visible spectroscopy) which were found to be the catalytically active species (3-300 ppm Pd, TOF up to 10⁵ h⁻¹) for the SMC.⁹⁷ These palladium cluster could be stabilized in water and stored for long periods of time for use on demand with no loss of activity. Qiu and Xu reported Pd-Pt nanodendrites for a ligand free SMC in an ethanol-aqueous solution.⁹⁸ Liu and co-workers reported an aerobic, ligand-free SMC catalyzed by Pd/C (3 mol%) in aqueous media.⁹⁹ Control experiments demonstrated that the Pd/C-catalyzed the SMC was much quicker when performed in air or oxygen (98% yield in 30 minutes) than under nitrogen (62% yield in 40 minutes). Deveau and coworkers¹⁰⁰ reported synthesis of Ethyl(4-phenylphenyl)acetate, a biaryl with anti-arthritis potential using Pd(OAc)₂ with no additional ligand in aqueous acetone (0.5 mol% catalyst loading, 90% yield). Liu and co-workers reported the SMC of potassium aryl-trifluoroborates with aryl bromides in water using Pd(OAc)₂ as a catalyst (1-3 mol%) with [bmim]PF₆ ionic liquid as an additive and Na₂CO₃ as a base under air.¹⁰¹ They obtained biaryl products upto 99% yield in 2-3 hours. Sarma and Saikia reported recently a recyclable Pd(OAc)₂ catalyzed SMC in neat “Water Extract of Rice Straw Ash” (WERSA) at room temperature.¹⁰² They obtained 45 – 90% yield for the synthesis of biaryl product with 1 mol% Pd loading.

Palladium nanoparticles (Pd-NPs) are nowadays widely used in catalysis and have become a strategic tool for organic transformations, thanks to their high catalytic activity. Pd-NPs are valuable alternatives to molecular catalysts as they do not require costly ligands. Astruc and co-workers showed that the SMC of aryl chloride proceeds

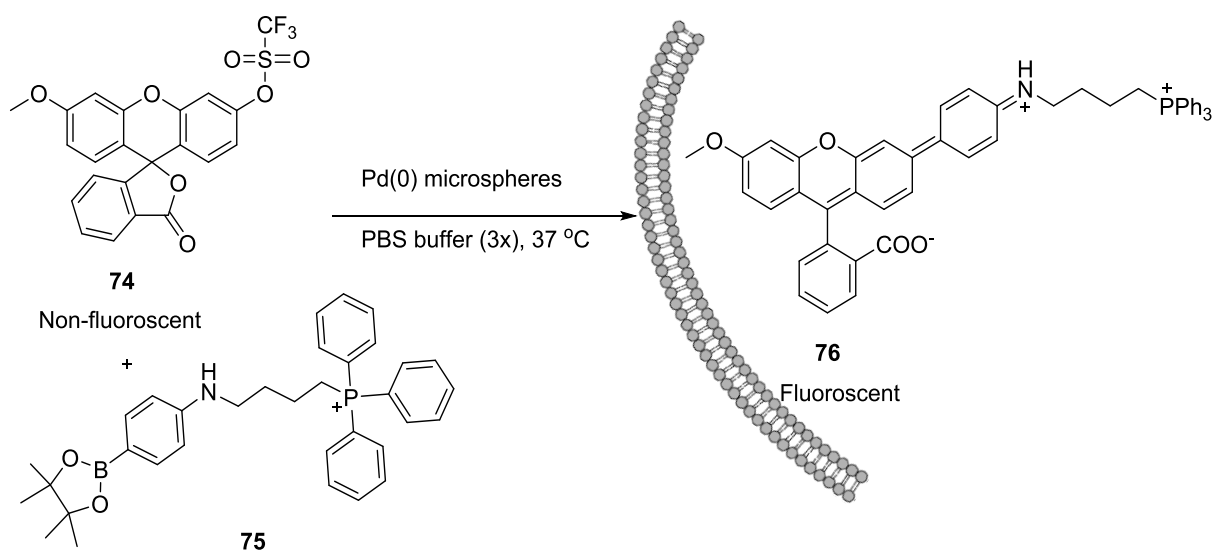
efficiently in water (or in organic-water mixtures) at high temperatures with ppm amounts of Pd-NPs.¹⁰³

Veisi and coworkers reported palladium nanoparticles (Pd-NPs) stabilised by *Pistacia atlantica kurdica* (*P. a. kurdica*) gum as catalyst for the SMC in water.¹⁰⁴ The Pd-NPs were employed as a heterogeneous catalyst in the SMC at low palladium loading (0.1 mol%) under aerobic and ligand-free conditions in water. The system was characterized by high TONs (up to 980). The catalyst could be recycled at least eight times without loss of activity.

The group of Martin reported the synthesis of stable Pd-NPs generated by electrochemical methods at room temperature via the electroreduction of an aqueous solution of H_2PdCl_4 in the presence of PVP.¹⁰⁵ These Pd-NPs exhibited high catalytic activity in the SMC in aqueous medium. Particularly high turnover numbers (TON 10^4 - 10^5) were achieved with aryl iodides and bromides. Recently, Pore and co-workers reported ionic liquid promoted in situ generation of palladium nanoparticles (particle size between 3-9 nm) which efficiently catalyzed SMC in water.¹⁰⁶ With 2 mol% $\text{Pd}(\text{OAc})_2$ and 20 mol% ionic liquid, they achieved upto 98% yield at 80 °C. The aqueous system containing ionic liquid along with Pd-NPs could be recycled seven times with any loss of activity. Maitra and co-workers reported hydrogel-stabilized palladium nanoparticles for SMC in water.¹⁰⁷ They obtained upto 90% yield for biaryl synthesis with 0.15 mol% Pd loading. Recently Tang and co-workers reported Pd-NPs supported and stabilized by mesoporous graphitic carbon nitride ($\text{g-C}_3\text{N}_4$).¹⁰⁸ The SMC proceeded smoothly with 97 % isolated yield (0.83 mol% Pd loading) in less than 30 minutes in water with PEG600 as the additive. Gholinejad and co-workers¹⁰⁹ reported a polymer containing phosphorus–nitrogen ligands for stabilization of palladium nanoparticles which was an efficient and recyclable catalyst for SMC in neat water. The biaryls products were obtained upto 99% yield with 0.08 mol% Pd loading in presence of $t\text{BuOK}$ as a base. Liu and coworkers¹¹⁰ developed a palladium-catalyzed ligand-free SMC of heteroaryl halides with *N*-methyliminodiacetic acid (MIDA) boronates in excellent yields (up to 96%) with 2 mol% Pd loading.

2.3.3 Heterogeneous SMC for Chemical Biology Applications

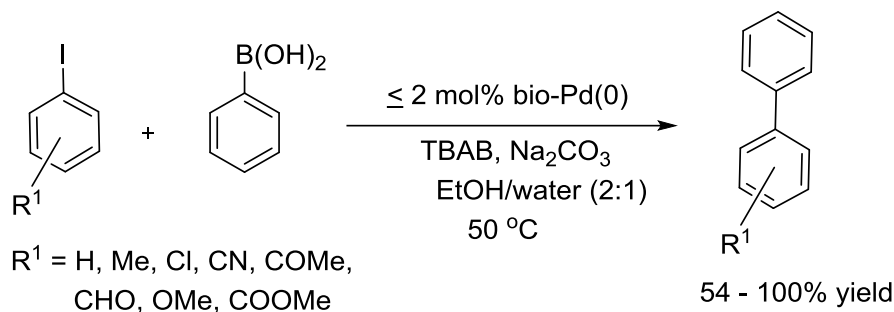
The first use of the SMC in mammalian cells was reported by Bradley and co-workers.⁵⁶ They trapped palladium nanoparticles within inert polymeric microspheres, with the catalysts derived from a recyclable, ligand-free heterogeneous palladium precursor. The resulting polystyrene microspheres were employed as ‘Trojan-horses’ to deliver the palladium nanoparticles into a cell, allowing to perform a SMC of **74** and **75** to afford the fluorescent product **76** *in cellulo* (Scheme 2.55).^{64,65} They used almost stoichiometric amount of catalyst and there is no mention of yield or TON in corresponding paper.



Scheme 2.55 Palladium nanoparticles encapsulated within inert polymeric microspheres as catalyst for the SMC *in cellulo*.⁵⁶

The research group of Parker demonstrated that Pd(0)-nanoparticles produced by living plants displayed excellent catalytic activity in the SMC.⁶⁶ Certain strains of bacteria (e.g. *Desulfovibrio desulfuricans*, *E. coli* and *Shewanella oneidensis*) can reduce soluble Pd(II) from stock solutions or acid extracts of spent catalysts, forming metallic palladium nanoparticles. This protocol involves biosorption of Pd(II) cations on the surface of bacteria and a subsequent reduction to Pd(0) using an electron donor. The formed nanoparticles are supported either on the bacterial outer-membrane or in the periplasmic space and remain attached to the cells (“bio-Pd(0)”). Skrydstrup and

coworkers⁶⁹ reported that the SMC can be catalysed by bio-generated palladium nanoparticles formed on the surface of Gram-negative bacteria (Scheme 2.56).



Scheme 2.56 “bio-Pd(0)” catalyzed SMC developed by Skrydstrup and coworkers.⁶⁹

Biological macromolecules have gained significant attention as alternative template materials for the generation of well-dispersed metal nanoparticle via electroless deposition. Yi and coworkers⁶⁸ demonstrated that the tobacco mosaic virus (TMV) is a suitable support for the generation of immobilized palladium (Pd) nanocatalysts which are active for the SMC in water.

2.4 Conclusion

In a green chemistry spirit, aqueous SMC has enjoyed an exponential growth in the past four years. In many cases however, the aqueous SMC require either high temperatures or the use of a co-solvent for chloride substrates. Future research will certainly be aimed to design more economical and high-performance catalysts.

2.5 References

- (1) Miyaura, N.; Suzuki, A. *Chem. Rev.* **1995**, *95*, 2457.
- (2) Suzuki, A. *Angew. Chem. Int. Ed.* **2011**, *50*, 6722.
- (3) Hassan, J.; Sévignon, M.; Gozzi, C.; Schulz, E.; Lemaire, M. *Chem. Rev.* **2002**, *102*, 1359.
- (4) Littke, A. F.; Fu, G. C. *Angew. Chem. Int. ed.* **2002**, *41*, 4176.
- (5) Kotha, S.; Lahiri, K.; Kashinath, D. *Tetrahedron* **2002**, *58*, 9633.
- (6) Han, F.-S. *Chem. Soc. Rev.* **2013**, *42*, 5270.

- (7) Fihri, A.; Bouhrara, M.; Nekoueishahraki, B.; Basset, J.-M.; Polshettiwar, V. *Chem. Soc. Rev.* **2011**, *40*, 5181.
- (8) Maluenda, I.; Navarro, O. *Molecules* **2015**, *20*, 7528.
- (9) Li, H.; Johansson Seechurn, C. C. C.; Colacot, T. J. *ACS Catal.* **2012**, *2*, 1147.
- (10) Kumar, A.; Rao, G. K.; Kumar, S.; Singh, A. K. *Dalton Trans.* **2013**, *42*, 5200.
- (11) Rossi, R.; Bellina, F.; Lessi, M. *Adv. Synth. Catal.* **2012**, *354*, 1181.
- (12) Sheldon, R. A. *Chem. Soc. Rev.* **2012**, *41*, 1437.
- (13) Simon, M.-O.; Li, C.-J. *Chem. Soc. Rev.* **2012**, *41*, 1415.
- (14) Shaughnessy, K. H.; DeVasher, R. B. *Current Organic Chemistry.* **2005**, *7*, 585.
- (15) Polshettiwar, V.; Decottignies, A.; Len, C.; Fihri, A. *ChemSusChem* **2010**, *3*, 502.
- (16) Sun, Y.; Yan, M.-Q.; Liu, Y.; Lian, Z.-Y.; Meng, T.; Liu, S.-H.; Chen, J.; Yu, G.-A. *RSC Adv.* **2015**, *5*, 71437.
- (17) Liu, N.; Liu, C.; Yan, B.; Jin, Z. *Appl. Organomet. Chem.* **2011**, *25*, 168.
- (18) Mao, S.-L.; Sun, Y.; Yu, G.-A.; Zhao, C.; Han, Z.-J.; Yuan, J.; Zhu, X.; Yang, Q.; Liu, S.-H. *Org. Biomol. Chem.* **2012**, *10*, 9410.
- (19) Marziale, A. N.; Jantke, D.; Faul, S. H.; Reiner, T.; Herdtweck, E.; Eppinger, J. *Green Chem.* **2011**, *13*, 169.
- (20) Burda, E.; Hummel, W.; Gröger, H. *Angew. Chem. Int. Ed. Engl.* **2008**, *47*, 9551.
- (21) Borchert, S.; Burda, E.; Schatz, J.; Hummel, W.; Gröger, H. *J. Mol. Catal. B Enzym.* **2012**, *84*, 89.
- (22) Lee, J.-Y.; Ghosh, D.; Lee, J.-Y.; Wu, S.-S.; Hu, C.-H.; Liu, S.-D.; Lee, H. M. *Organometallics* **2014**, *33*, 6481.
- (23) Sabounchei, S. J.; Hosseinzadeh, M.; Panahimehr, M.; Nematollahi, D.; Khavasi, H. R.; Khazalpour, S. *Transit. Met. Chem.* **2015**, *40*, 657.
- (24) Togni, A.; Venanzi, L. M. *Angew. Chem. Int. Ed.* **1994**, *33*, 517.

- (25) Tsang, M. Y.; Viñas, C.; Teixidor, F.; Planas, J. G.; Conde, N.; SanMartin, R.; Herrero, M. T.; Domínguez, E.; Lledós, A.; Vidossich, P.; Choquesillo-Lazarte, D. *Inorg. Chem.* **2014**, *53*, 9284.
- (26) Crisóstomo-Lucas, C.; Toscano, R. A.; Morales-Morales, D. *Tetrahedron Lett.* **2013**, *54*, 3116.
- (27) Tu, T.; Feng, X.; Wang, Z.; Liu, X. *Dalton Trans.* **2010**, *39*, 10598.
- (28) Saikia, B.; Ali, A. A.; Boruah, P. R.; Sarma, D.; Barua, N. C. *New J. Chem.* **2015**, *39*, 2440.
- (29) Zhou, C.; Wang, J.; Li, L.; Wang, R.; Hong, M. *Green Chem.* **2011**, *13*, 2100.
- (30) Zhao, C.-W.; Ma, J.-P.; Liu, Q.-K.; Yu, Y.; Wang, P.; Li, Y.-A.; Wang, K.; Dong, Y.-B. *Green Chem.* **2013**, *15*, 3150.
- (31) Hanhan, M. E.; Senemoglu, Y. *Transit. Met. Chem.* **2011**, *37*, 109.
- (32) Qi, M.; Tan, P. Z.; Xue, F.; Malhi, H. S.; Zhang, Z.-X.; Young, D. J.; Hor, T. S. A. *RSC Adv.* **2015**, *5*, 3590.
- (33) Li, Q.; Zhang, L.-M.; Bao, J.-J.; Li, H.-X.; Xie, J.-B.; Lang, J.-P. *Appl. Organomet. Chem.* **2014**, *28*, 861.
- (34) Kapdi, A.; Gayakhe, V.; Sanghvi, Y. S.; Garcia, J.; Lozano, P.; da Silva, I.; Perez, J.; Serrano, J. L. *RSC Adv.* **2014**, *4*, 17567.
- (35) Chalker, J. M.; Wood, C. S. C.; Davis, B. G. *J. Am. Chem. Soc.* **2009**, *131*, 16346.
- (36) Edwards, G. A.; Trafford, M. A.; Hamilton, A. E.; Buxton, A. M.; Bardeaux, M. C.; Chalker, J. M. *J. Org. Chem.* **2014**, *79*, 2094.
- (37) Zhou, Z.; Liu, M.; Wu, X.; Yu, H.; Xu, G.; Xie, Y. *Appl. Organomet. Chem.* **2013**, *10*, 562.
- (38) Zhang, G.; Zhang, W.; Luan, Y.; Han, X.; Ding, C. *Chinese J. Chem.* **2015**, *7*, 705.
- (39) Mondal, M.; Bora, U. *Tetrahedron Lett.* **2014**, *55*, 3038.
- (40) Liu, H.; Li, X.; Liu, F.; Tan, Y.; Jiang, Y. *J. Organomet. Chem.* **2015**, *794*, 27.

- (41) Arumugam, V.; Kaminsky, W.; Bhuvanesh, N. S. P.; Nallasamy, D. *RSC Adv.* **2015**, *5*, 59428.
- (42) Lukowiak, M.; Meise, M.; Haag, R. *Synlett* **2014**, *25*, 2161.
- (43) Zhong, R.; Pöthig, A.; Feng, Y.; Riener, K.; Herrmann, W. A.; Kühn, F. E. *Green Chem.* **2014**, *16*, 4955.
- (44) Benhamou, L.; Besnard, C.; Kündig, E. P. *Organometallics* **2014**, *33*, 260.
- (45) Garrido, R.; Hernández-Montes, P. S.; Gordillo, Á.; Gómez-Sal, P.; López-Mardomingo, C.; de Jesús, E. *Organometallics* **2015**, *34*, 1855.
- (46) Munz, D.; Allolio, C.; Meyer, D.; Micksch, M.; Roessner, L.; Strassner, T. *J. Organomet. Chem.* **2015**, *794*, 330.
- (47) Li, L.; Wang, J.; Zhou, C.; Wang, R.; Hong, M. *Green Chem.* **2011**, *13*, 2071.
- (48) Godoy, F.; Segarra, C.; Poyatos, M.; Peris, E. *Organometallics* **2011**, *30*, 684.
- (49) Izquierdo, F.; Corpet, M.; Nolan, S. P. *European J. Org. Chem.* **2015**, *9*, 1920.
- (50) Liu, N.; Liu, C.; Jin, Z. *Green Chem.* **2012**, *14*, 592.
- (51) Karimi, B.; Akhavan, P. F. *Inorg. Chem.* **2011**, *50*, 6063.
- (52) Karimi, B.; Fadavi Akhavan, P. *Chem. Commun.* **2011**, *47*, 7686.
- (53) Kolychev, E. L.; Asachenko, A. F.; Dzhevakov, P. B.; Bush, A. A.; Shuntikov, V. V.; Khrustalev, V. N.; Nechaev, M. S. *Dalton Trans.* **2013**, *42*, 6859.
- (54) Schmid, T. E.; Jones, D. C.; Songis, O.; Diebolt, O.; Furst, M. R. L.; Slawin, A. M. Z.; Cazin, C. S. J. *Dalton Trans.* **2013**, *42*, 7345.
- (55) Kinzhalov, M. A.; Luzyanin, K. V.; Boyarskiy, V. P.; Haukka, M.; Kukushkin, V. Y. *Organometallics* **2013**, *32*, 5212.
- (56) Yusop, R. M.; Unciti-Broceta, A.; Johansson, E. M. V; Sánchez-Martín, R. M.; Bradley, M. *Nat. Chem.* **2011**, *3*, 239.
- (57) Abe, S.; Niemeyer, J.; Abe, M.; Takezawa, Y.; Ueno, T.; Hikage, T.; Erker, G.; Watanabe, Y. *J. Am. Chem. Soc.* **2008**, *130*, 10512.
- (58) Li, J.; Chen, P. R. *Chembiochem* **2012**, *13*, 1728.

- (59) Gao, Z.; Gouverneur, V.; Davis, B. G. *J. Am. Chem. Soc.* **2013**, *135*, 13612.
- (60) Spicer, C. D.; Triemer, T.; Davis, B. G. *J. Am. Chem. Soc.* **2012**, *134*, 800.
- (61) Li, N.; Lim, R. K. V.; Edwardraja, S.; Lin, Q. *J. Am. Chem. Soc.* **2011**, *133*, 15316.
- (62) Gao, Z.; Gouverneur, V.; Davis, B. G. *J. Am. Chem. Soc.* **2013**, *135*, 13612.
- (63) Spicer, C. D.; Davis, B. G. *Chem. Commun.* **2011**, *47*, 1698.
- (64) Chankeshwara, S. V.; Indrigo, E.; Bradley, M. *Curr. Opin. Chem. Biol.* **2014**, *21*, 128.
- (65) Unciti-Broceta, A.; Johansson, E. M. V.; Yusop, R. M.; Sánchez-Martín, R. M.; Bradley, M. *Nat. Protoc.* **2012**, *7*, 1207.
- (66) Parker, H. L.; Rylott, E. L.; Hunt, A. J.; Dodson, J. R.; Taylor, A. F.; Bruce, N. C.; Clark, J. H. *PLoS One* **2014**, *9*, e87192.
- (67) Ma, X.; Wang, H.; Chen, W. *J. Org. Chem.* **2014**, *79*, 8652.
- (68) Yang, C.; Manocchi, A. K.; Lee, B.; Yi, H. *J. Mater. Chem.* **2011**, *21*, 187.
- (69) Søjberg, L. S.; Gauthier, D.; Lindhardt, A. T.; Bunge, M.; Finster, K.; Meyer, R. L.; Skrydstrup, T. *Green Chem.* **2009**, *11*, 2041.
- (70) Yang, M.; Li, J.; Chen, P. R. *Chem. Soc. Rev.* **2014**, *43*, 6511.
- (71) Cobo, I.; Matheu, M. I.; Castellón, S.; Boutureira, O.; Davis, B. G. *Org. Lett.* **2012**, *14*, 1728.
- (72) Dumas, A.; Spicer, C. D.; Gao, Z.; Takehana, T.; Lin, Y. A.; Yasukohchi, T.; Davis, B. G. *Angew. Chem. Int. Ed.* **2013**, *52*, 3916.
- (73) Spicer, C. D.; Davis, B. G. *Chem. Commun.* **2013**, *49*, 2747.
- (74) Isfahani, A. L.; Mohammadpoor-Baltork, I.; Mirkhani, V.; Khosropour, A. R.; Moghadam, M.; Tangestaninejad, S.; Kia, R. *Adv. Synth. Catal.* **2013**, *355*, 957.
- (75) Wang, D.; Liu, W.; Bian, F.; Yu, W. *New J. Chem.* **2015**, *39*, 2052.
- (76) Gholinejad, M.; Razeghi, M.; Najera, C. *RSC Adv.* **2015**, *5*, 49568.
- (77) Karimi, B.; Mansouri, F.; Vali, H. *Green Chem.* **2014**, *16*, 2587.

- (78) Zhang, F.; Chen, M.; Wu, X.; Wang, W.; Li, H. *J. Mater. Chem. A* **2014**, *2*, 484.
- (79) Mieczyska, E.; Borkowski, T.; Cypriak, M.; Pospiech, P.; Trzeciak, A. M. *Appl. Catal. A Gen.* **2014**, *470*, 24.
- (80) Liu, M.; Zhu, X.; Wu, L.; Zhou, X.; Li, J.; Ma, J. *RSC Adv.* **2015**, *5*, 38264.
- (81) Liu, H.; Wang, P.; Yang, H.; Niu, J.; Ma, J. *New J. Chem.* **2015**, *39*, 4343.
- (82) Dutt, S.; Kumar, R.; Siril, P. F. *RSC Adv.* **2015**, *5*, 33786.
- (83) Borah, B. J.; Borah, S. J.; Saikia, K.; Dutta, D. K. *Appl. Catal. A Gen.* **2014**, *469*, 350.
- (84) Li, B.; Guan, Z.; Wang, W.; Yang, X.; Hu, J.; Tan, B.; Li, T. *Adv. Mater.* **2012**, *24*, 3390.
- (85) Yu, Y.; Hu, T.; Chen, X.; Xu, K.; Zhang, J.; Huang, J. *Chem. Commun.* **2011**, *47*, 3592.
- (86) Zhi, J.; Song, D.; Li, Z.; Lei, X.; Hu, A. *Chem. Commun.* **2011**, *47*, 10707.
- (87) Firouzabadi, H.; Iranpoor, N.; Gholinejad, M.; Kazemi, F. *RSC Adv.* **2011**, *1*, 1013.
- (88) Guan, Z.; Hu, J.; Gu, Y.; Zhang, H.; Li, G.; Li, T. *Green Chem.* **2012**, *14*, 1964.
- (89) Yamada, Y. M. A.; Sarkar, S. M.; Uozumi, Y. *J. Am. Chem. Soc.* **2012**, *134*, 3190.
- (90) Handa, S.; Wang, Y.; Gallou, F.; Lipshutz, B. H. *Science* **2015**, *349*, 1087.
- (91) Charbonneau, M.; Addoumeh, G.; Oguadinma, P.; Schmitzer, A. R. *Organometallics* **2014**, *33*, 6544.
- (92) Molander, G. A.; Biolatto, B. *J. Org. Chem.* **2003**, *68*, 4302.
- (93) Mondal, M.; Bora, U. *Green Chemistry.* **2012**, 1873.
- (94) Liu, C.; Zhang, Y.; Liu, N.; Qiu, J. *Green Chem.* **2012**, *14*, 2999.
- (95) Liu, C.; Rao, X.; Song, X.; Qiu, J.; Jin, Z. *RSC Adv.* **2013**, *3*, 526.

- (96) Goswami, L.; Gogoi, P.; Gogoi, J.; Borah, A.; Das, M. R.; Boruah, R. C. *Tetrahedron Lett.* **2014**, *55*, 5539.
- (97) Leyva-Pérez, A.; Oliver-Meseguer, J.; Rubio-Marqués, P.; Corma, A. *Angew. Chem. Int. Ed.* **2013**, *52*, 11554.
- (98) Wang, Z.-J.; Lv, J.-J.; Feng, J.-J.; Li, N.; Xu, X.; Wang, A.-J.; Qiu, R. *RSC Adv.* **2015**, *5*, 28467.
- (99) Liu, C.; Rao, X.; Zhang, Y.; Li, X.; Qiu, J.; Jin, Z. *Eur. J. Org. Chem.* **2013**, *20*, 4345.
- (100) Costa, N. E.; Pelotte, A. L.; Simard, J. M.; Syvinski, C. A.; Deveau, A. M. *J. Chem. Edu.* **2012**, *89*, 1064.
- (101) Liu, L.; Dong, Y.; Pang, B.; Ma, J. *J. Org. Chem.* **2014**, *79*, 7193.
- (102) Boruah, P. R.; Ali, A. A.; Chetia, M.; Saikia, B.; Sarma, D. *Chem. Commun.* **2015**, *51*, 11489.
- (103) Deraedt, C.; Astruc, D. *Acc. Chem. Res.* **2014**, *47*, 494.
- (104) Veisi, H.; Faraji, A. R.; Hemmati, S.; Gil, A. *Appl. Organomet. Chem.* **2015**, *29*, 517.
- (105) Uberman, P. M.; Pérez, L. A.; Martín, S. E.; Lacconi, G. I. *RSC Adv.* **2014**, *4*, 12330.
- (106) Patil, J. D.; Korade, S. N.; Patil, S. A.; Gaikawad, D. S.; Pore, D. M. *RSC Adv.* **2015**, *5*, 54129.
- (107) Maity, M.; Maitra, U. *J. Mater. Chem. A* **2014**, *2*, 18952.
- (108) Zhao, Y.; Tang, R.; Huang, R. *Catal. Letters* **2015**, *145*, 1900.
- (109) Gholinejad, M.; Hamed, F.; Biji, P. *Dalton Trans.* **2015**, *44*, 14293.
- (110) Liu, C.; Li, X.; Liu, C.; Wang, X.; Qiu, J. *RSC Adv.* **2015**, *5*, 54312.

CHAPTER 3

*Enantioselective Artificial Suzukiase for the
Synthesis of Axially Chiral Biaryl Compounds
Relying on the Streptavidin-Biotin Technology*

3.1 Introduction

The palladium-catalyzed Suzuki–Miyaura cross-coupling reaction (SMC hereafter) of organic halides with boronic acids is one of the most versatile methods for the synthesis of biaryls.^{1–3} Such structural motifs are present in numerous agrochemicals, natural products, pharmaceuticals, and polymers.^{4,5} For this purpose, the SMC has been widely studied.^{6–11} More recently, the SMC has found applications in the context of chemical biology. Indeed, both reactants and products can be regarded as bio-orthogonal.^{12–18} In this promising context however, high catalyst loadings are routinely required with reactions performed in a biological environment.^{12,13,15,17,19–27}

In stark contrast to the SMC, Nature relies on very different mechanisms to install (atropisomeric) C_{aryl}–C_{aryl} bonds.²⁸ Despite numerous reports on asymmetric SMC in organic media,^{6–8,29} only two reports describe enantioselective SMC in water.^{30,31} Uozumi reported on an heterogeneous SMC in water requiring a high catalyst loading (TON < 10, 94% ee at 80 °C).³⁰ More recently, Kündig *et al.* reported an asymmetric SMC in an water-organic solvent mixture (TON = 17, up to 80 % ee) at room temperature.³¹ To complement these efforts, we speculated that, thanks to their well-defined second coordination sphere, artificial metalloenzymes (ArMs hereafter) may offer a propitious environment to engineer an asymmetric “Suzukiase”- that is, an enzyme that catalyzes the SMC reaction. ArMs result from the incorporation of an abiotic cofactor within a macromolecule (protein or oligonucleotide).^{13,14,32–35} In this context, Ueno and coworkers anchored a palladium moiety within a ferritin container to yield an artificial Suzukiase. The resulting artificial Suzukiase however did not outperform the free cofactor (no enantioselectivity, turnover frequency: 3500 h⁻¹).¹³ Inspired by a seminal contribution by Whitesides in 1978,³² we report herein our effort to engineer an asymmetric artificial Suzukiase based on the biotin-streptavidin technology.

3.2 Aim of the Project

Within this project a Pd-dependent artificial Suzukiase based on the biotin-streptavidin technology was to be developed. Within this context a set of milestones had to be accomplished:

1. Diversify biotinylated ligands (phosphines and NHC-carbenes)
2. Chemical optimization of the biotinylated cofactor (Pd-complexes) for the respective reaction
3. Diversify of the genetic library to optimize the activity as well as the selectivity of the resulting constructs
4. Perform catalysis at low catalyst loadings under near physiological conditions to approach *in vivo* implementation.
5. Develop methods for performing catalysis with unpurified protein systems to accelerate the screening strategy.

3.3 Outline of the Project

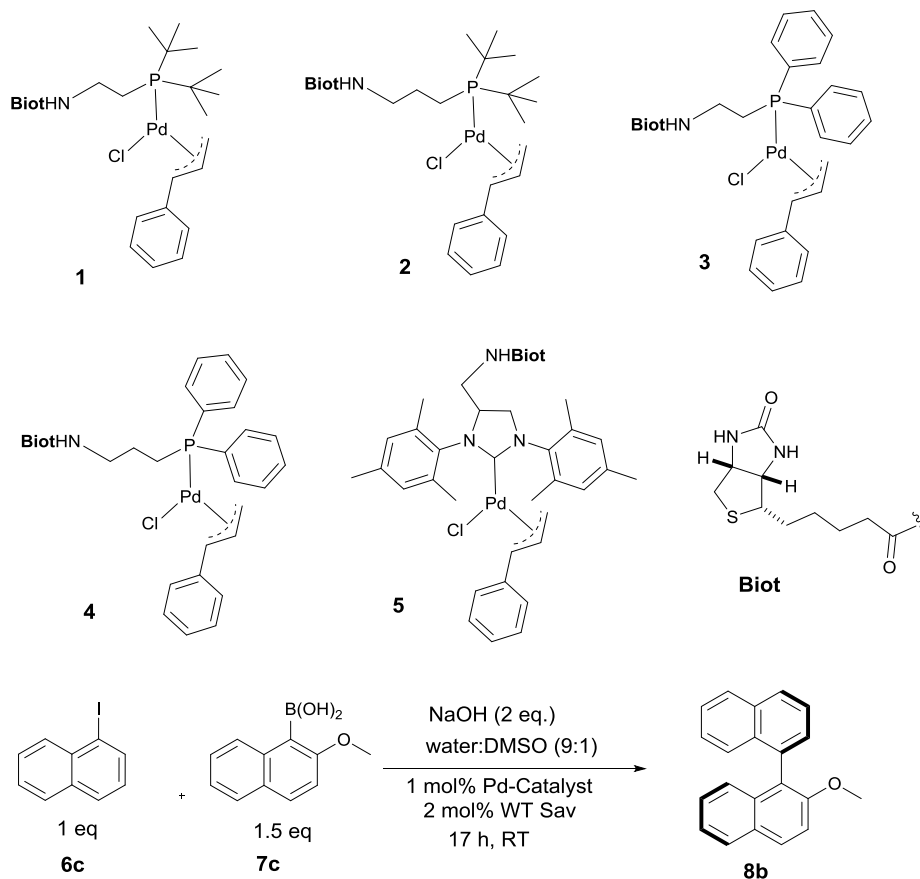
As demonstrated in several chemical-biology applications, the SMC is a promising bio-orthogonal reaction. However, the systems reported to date require multiple equivalents of palladium to proceed in biological environments. Here we anticipate that screening more diverse Sav libraries will allow rapidly improving the performance of the artificial Suzukiase. With the aim of identifying the most suitable catalyst precursor, it is proposed to synthesize and screen biotinylated N-Heterocyclic Carbenes and phosphines.

In order to ensure that the cross-coupling reaction is indeed catalyzed by the ArM (and not adventitious Pd-nanoparticles), we will focus on asymmetric C–C bond formation, while varying the nature of the activating groups (iodide, bromide, chloride as well as boronic acid, boronic ester and trifluoroborate). Both inter- and intramolecular reactions will be tested. We anticipate that an intramolecular version may allow to significantly decrease the concentration of the substrate, to ultimately allow the

catalytic reaction to be performed *in vivo* at low catalyst loading and substrate concentration. With this goal in mind, we will also screen substrates which lead to the formation of a fluorescent product. Ultimately, we believe that the artificial Suzukiases will allow to perform cross-coupling reactions on cellular extracts and ultimately *in vivo* with low catalyst loadings.

3.4 Results and Discussion

3.4.1 Chemical Optimizations



Scheme 3.1 Biotinylated cofactors **1-5** tested in the presence of (strept)avidin as artificial Suzukiase for the synthesis of enantioenriched 2-methoxy-1,1'-binaphthyl **8b**.

With the aim of identifying suitable cross-coupling reaction conditions, we evaluated five different biotinylated catalyst precursors **1-5** in the presence of either avidin or streptavidin (Avi and Sav hereafter). For this purpose, the reaction of 1-iodonaphthalene **6c** with 2-methoxy-1-naphthaleneboronic acid **7c** was selected as a model system (Scheme 3.1). Initial experiments revealed that protonolysis of the boronic acid led to modest cross-coupling yields. Systematic variation of the base, pH, and organic co-solvent led to the identification of suitable reaction conditions: sodium hydroxide in DMSO : water (1 : 9) proved to be particularly effective in preventing protonolysis. However, competing deboronation required the use of excess boronic acid (1.5 equivalents vs. aryl halide) to achieve full conversion. Gel electrophoresis of the reaction mixture revealed that Sav remained largely tetrameric and active toward biotin binding even after an SMC performed at 50 °C (see Appendix 1, Figure S3).

3.4.2 Genetic Optimizations

Having identified suitable reaction conditions, we screened biotinylated phosphine- and NHC ligands **1-5** combined with WT (strept)avidin (Table 3.1). This screening led to the identification of complexes **1**, **2**, and **3** as the most promising catalysts in combination with WT Sav. Complexes **1-3** were thus screened with a small library of Sav mutants. The results of the chemogenetic optimization for the synthesis of 2-methoxy-1,1'-binaphthyl **8b** are displayed as a fingerprint in Figure 3.1, and selected results are collected in Table 3.2.

From these data, the following features emerge:

- a) Compared to the free cofactor, higher conversions are observed with the artificial Suzukiase. This demonstrates that the Sav host protein exerts a beneficial influence on both the activity (i.e. protein accelerated catalysis) and the selectivity.

Table 3.1 Identification of the most suitable ligand for the synthesis of 2-methoxy-1,1'-binaphthyl **8b** ^[a]

Entry	Complex	Protein	ee [%] ^[b]	TON
1	1	WT Sav	58 (<i>R</i>)	78
2	2	WT Sav	10 (<i>S</i>)	73
3	3	WT Sav	42 (<i>R</i>)	45
4	4	WT Sav	6 (<i>R</i>)	8
5	5	WT Sav	rac.	<5
6	1	WT Avi	3 (<i>R</i>)	10

[a] Reactions were carried out with 50 mM substrate in a total reaction volume 0.2 mL using 1 mol% complex **1-5** (see Appendix 1 for experimental details). [b] ee value determined by HPLC on a chiral stationary phase; absolute configuration assigned by comparison with literature data. WT = wild-type, Sav = streptavidin, Avi = avidin.

- b) The electron-donating properties and bulkiness of the phosphine play a key role in determining the activity of the corresponding artificial Suzukiase. Accordingly, the (*t*-Bu)₂P-bearing catalysts outperform the (Ph)₂P-systems. Strikingly, both ligands **1** and **3** (Table 3.2, entries 10-13) show similar activity in case of S112M and S112A mutants
- c) The enantioenriched nature of the cross-coupled product **8b** strongly supports the hypothesis that the SMC is indeed catalysed by a homogeneous protein-embedded Pd-cofactor rather than Pd-nanoparticles.^{12,25,26,36}
- d) Varying the spacer between the biotin anchor and the P(*t*-Bu)₂ from ethyl to propyl affords opposite enantiomers of biaryl **8b** for a given Sav mutant. The best ees in favour of (*S*)-**8b** were obtained with **2** · Sav K121A and **2** · Sav S112M Table 3.2, entries 8 and 9).

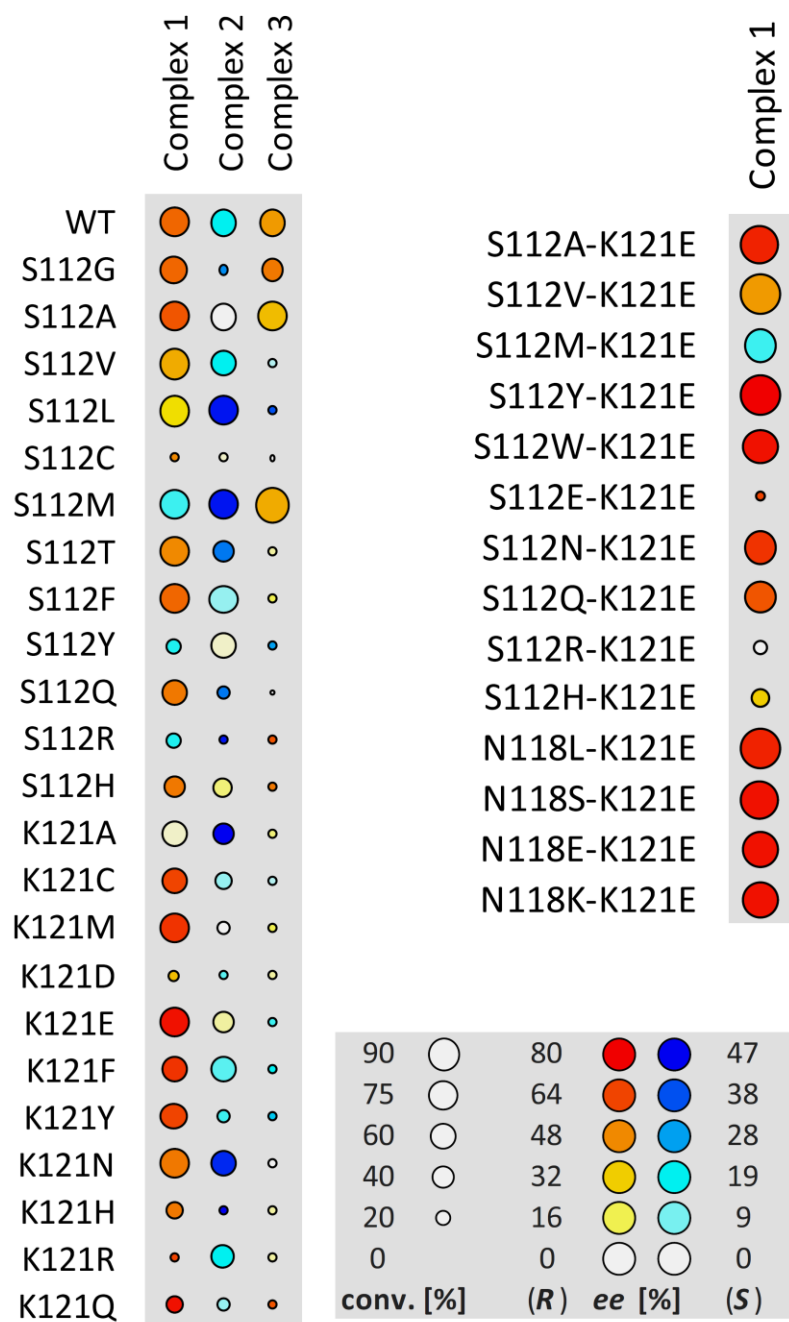


Figure 3.1. Fingerprint display of the results of the chemogenetic optimization for the synthesis of 2-methoxy-1,1'-binaphthyl **8b**. The size of the circles is proportional to the conversion, and the color codes the enantiomeric excess. Numerical results are collected Table 3.2 and in Table S1 (Appendix 1).

Table 3.2 Selected results for genetic optimization of the artificial Suzukiase for the synthesis of 2-methoxy-1,1'-binaphthyl **8b**

Entry	Temp [°C]	Complex	Protein	ee [%]	TON
1	RT	1	-	rac.	20
2	RT	1	WT	58 (<i>R</i>)	78
3	RT	1	K121E	76 (<i>R</i>)	50
4	RT	1	K121D	34 (<i>R</i>)	7
5	RT	1	K121Q	74 (<i>R</i>)	20
6	RT	1	K121M	67 (<i>R</i>)	59
7	RT	1	K121F	67 (<i>R</i>)	38
8	RT	2	K121A	47 (<i>S</i>)	32
9	RT	2	S112M	44 (<i>S</i>)	53
10	RT	3	S112M	38 (<i>R</i>)	78
11	RT	3	S112A	36 (<i>R</i>)	52
12	RT	1	S112M	14 (<i>S</i>)	58
13	RT	1	S112A	60 (<i>R</i>)	58
14	RT	1	N118K-K121E	74 (<i>R</i>)	73
15	RT	1	N118S-K121E	76 (<i>R</i>)	79
16	RT	1	N118E-K121E	76 (<i>R</i>)	75
17	RT	1	N118L-K121E	72 (<i>R</i>)	86
18	RT	1	S112W-K121E	76 (<i>R</i>)	64
19	RT	1	S112N-K121E	69 (<i>R</i>)	61
20	RT	1	S112A-K121E	70 (<i>R</i>)	80
21	RT	1	S112Y-K121E	80 (<i>R</i>)	90
22	RT	1	S112Y-K121E	80 (<i>R</i>)	160 ^[a]
23	16	1	S112Y-K121E	84 (<i>R</i>)	50
24	4	1	S112Y-K121E	86 (<i>R</i>)	50 ^[b]
25	4	1	S112Y-K121E	90 (<i>R</i>)	50 ^[c]

[a] 0.50 mol % catalyst loading, 0.25 mol % Sav (tetramer) loading [b] 0.50 mol % catalyst loading, 0.25 mol % Sav (tetramer) loading, after 7 days. [c] preparative scale (100 μmol)

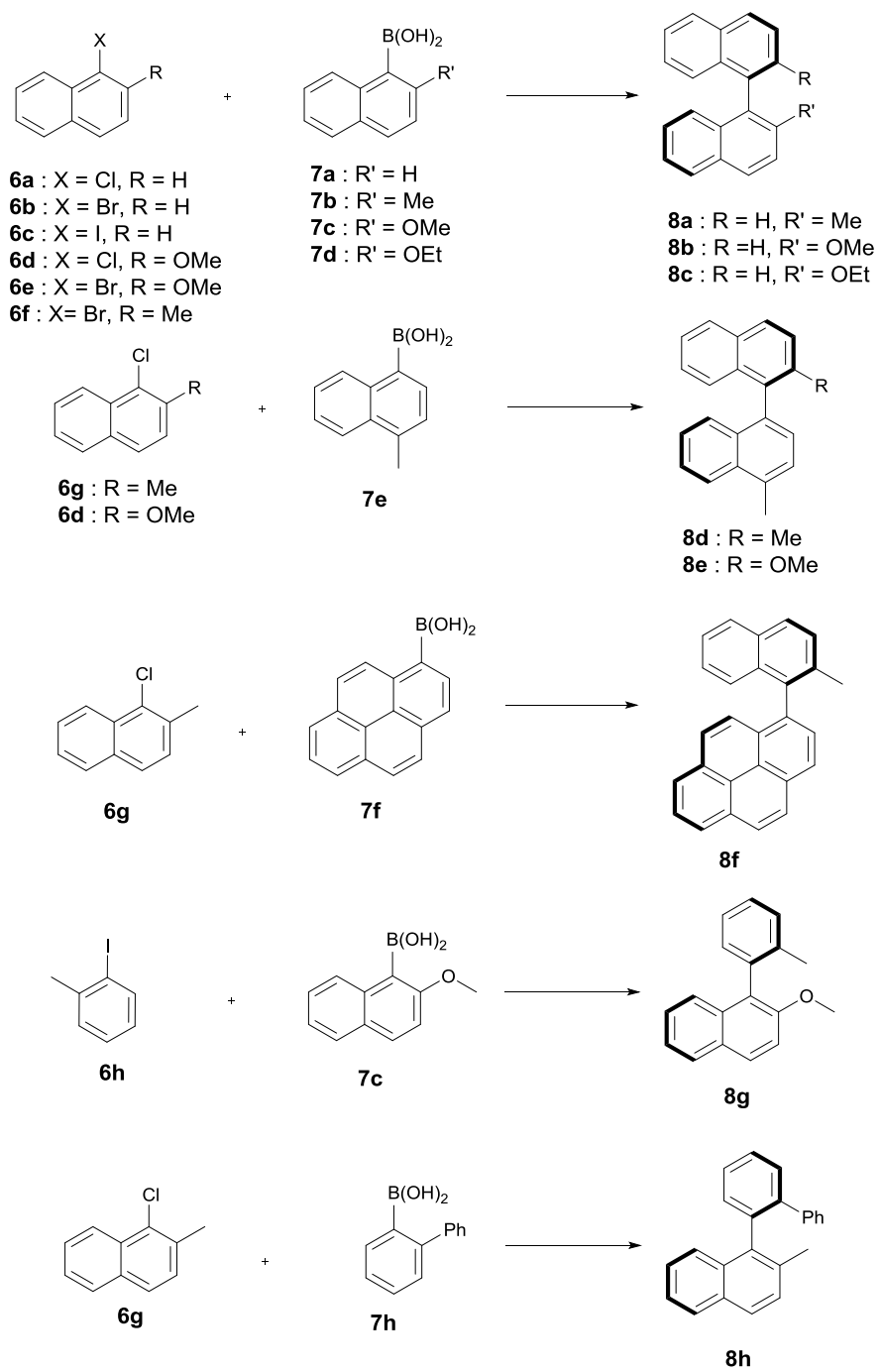
Having identified **1** · Sav K121E as a promising first generation Suzukiase (Table 3.2, entry 3), we screened double mutants bearing a glutamate at position 121 (Figure 3.1 and Table 3.2, entries 14-21):

- a) The double mutant **1** · Sav S112A-K121E (Table 3.2, entry 20) gives better ee and TON than the single mutant Sav S112A (Table 3.2, Entry 13). Likewise, **1** · Sav S112Y-K121E gave the highest turnover with good ee (Table 3.2, entry 22). This finding highlights the non-additive nature of multiple mutations.^{37,38} Decreasing the temperature to 4°C leads to an improvement in enantioselectivity (86 % ee, Table 3.2, entry 24) albeit at the cost of a slower rate.
- b) Increasing the ratio of complex **1** vs. Sav tetramer (S112Y-K121E mutant) from one to four leads to a gradual erosion of enantioselectivity (from 80 to 69% ee, see Table S4, Appendix 1). This suggests that an empty biotin binding site adjacent to a complex **1** within Sav is favorable for selectivity.
- c) On a preparative scale, up to 90% ee (*R*)-**8b**, were obtained using 0.50 mol % catalyst loading and 0.25 mol % Sav (tetramer) loading at 4 °C (Table 3.2, entry 25).

3.4.3 Substrate Scope

The artificial Suzukiase performed well on a range of hydrophobic substrates, leading to the following observations (Table 3.3):

- a) The nature of the aryl halide does not influence the enantioselectivity but to lower conversions on going from iodide to bromide to chloride **6c-6a** (Table 3.3, entries 6-8).



Scheme 3.2 Substrates tested for the asymmetric Suzuki-Miyaura cross-coupling reaction catalysed by **1** · S112Y-K121E.

- b) Substitution of the methoxy group by either a methyl and ethoxy group on the arylboronic acid (compare **7c** to **7b** and **7d**) leads lower enantioselectivities (Table 3.3, entries 7, 10 and 12).
- c) The system affords the highest enantioselectivity for binaphthyls or naphthyl-*o*-biphenyl products. In the presence of one smaller coupling partner, (e.g. **6h**), the enantioselectivity is significantly lower.

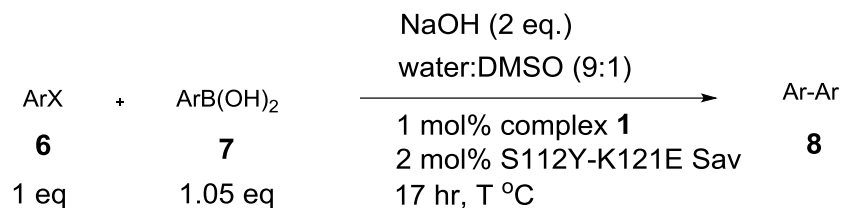


Table 3.3 Selected results for the SMC with **1** · S112Y-K121E Sav on a variety of substrates ^[a]

Entry	ArX	ArB(OH) ₂	Product	Temp [°C]	ee [%]	TON
1	6d	7a	8b	RT	80 (<i>R</i>)	32
2	6g	7e	8d	50	80 (<i>S</i>)	20
3	6d	7e	8e	50	74 (<i>R</i>)	61
4	6g	7f	8f	50	64 (<i>S</i>)	50
5	6g	7h	8h	RT	65 (<i>R</i>)	29
6	6a	7c	8b	RT	80 (<i>R</i>)	7
7	6b	7c	8b	RT	80 (<i>R</i>)	63
8	6c	7c	8b	RT	80 (<i>R</i>)	80
9	6f	7a	8a	RT	69 (<i>S</i>)	64
10	6b	7b	8a	50	76 (<i>S</i>)	81
11	6b	7b	8a	4	87 (<i>S</i>)	8 ^[b]
12	6c	7d	8c	RT	68 (<i>R</i>)	88
13	6e	7a	8b	RT	77 (<i>R</i>)	55
14	6h	7c	8g	RT	35 (<i>R</i>)	80

[a] Results are the average of two independent runs, see Supporting Information for experimental details. [b] after 7 days

3.4.4 X-ray Structure

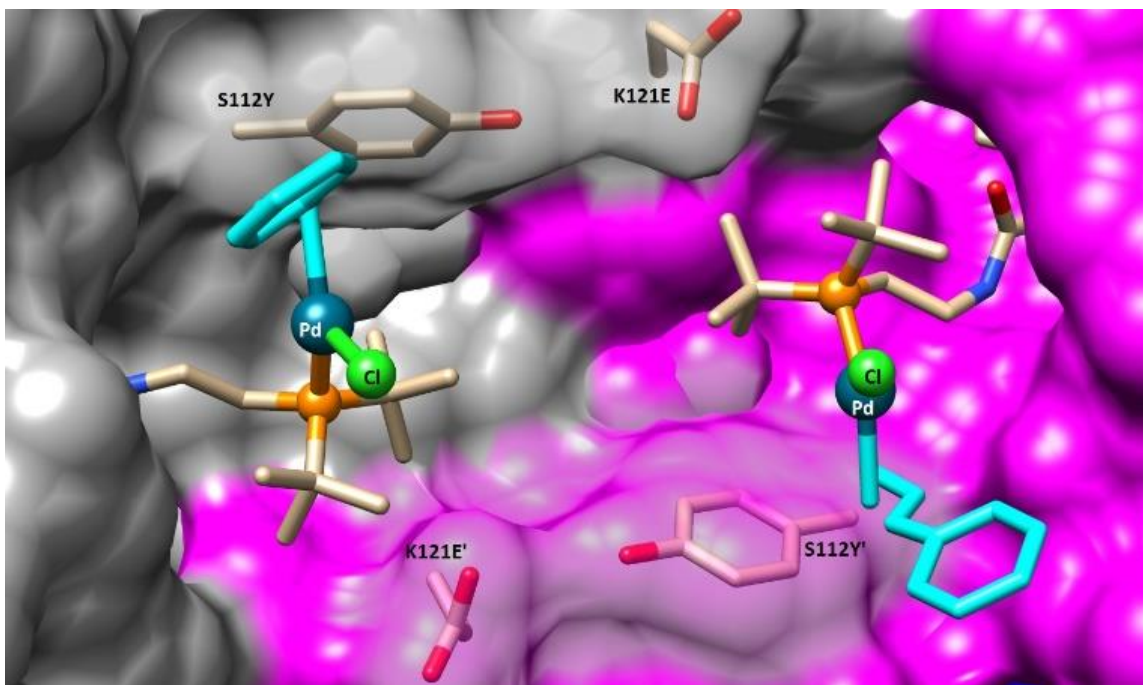


Figure 3.2. Close-up view of the structure of the artificial Suzukiase **1** · S112Y-K121E Sav. The solvent-excluded surface of two symmetry-related Sav monomers are highlighted in grey and magenta respectively. The biotinylated Pd-cofactor **1** and the mutated residues S112Y and K121E are displayed as stick. No electron density for the cinnamyl-moiety (turquoise) could be detected and was thus modelled, minimizing steric-clashes.

To gain structural insight on the second coordination sphere around the Pd moiety, crystals of Sav S112Y-K121E were grown and soaked with a solution of **1** in DMSO (For details, see Supporting Information). The resulting crystals were subjected to X-ray diffraction at the beamline X06DA at the Swiss Light Source. In the resulting structure of complex **1** · S112Y-K121E Sav, there is strong residual electron density in the 2Fo-Fc difference map in the biotin-binding vestibule. The Pd atom was unambiguously assigned as a strong peak in the difference map (12σ) with a corresponding peak in the anomalous difference map (8σ). The density map clearly highlights the presence of the phosphine ligand, the palladium, and the chloride (Figure 3.3). However, the cinnamyl ligand could not be resolved, likely due to

disorder caused by ligand fluxionality. The amide linker exhibits two H-bonding interactions with the protein backbone: the amide nitrogen exhibits an H-bonding interaction with the side-chain of S88, and the carbonyl oxygen exhibits an H-bonding interaction with the backbone nitrogen of N49. The palladium atoms of two symmetry related-cofactors (face-to-face) are separated by 11.7 Å. The palladium was found in the vicinity of the O atoms of S112Y and K121E (Pd····O distance 6.4 Å and 7.1 Å respectively). The average B-factor of Pd is 36.10, suggesting that the complex may be fluxional or located in a shallow energy minimum.

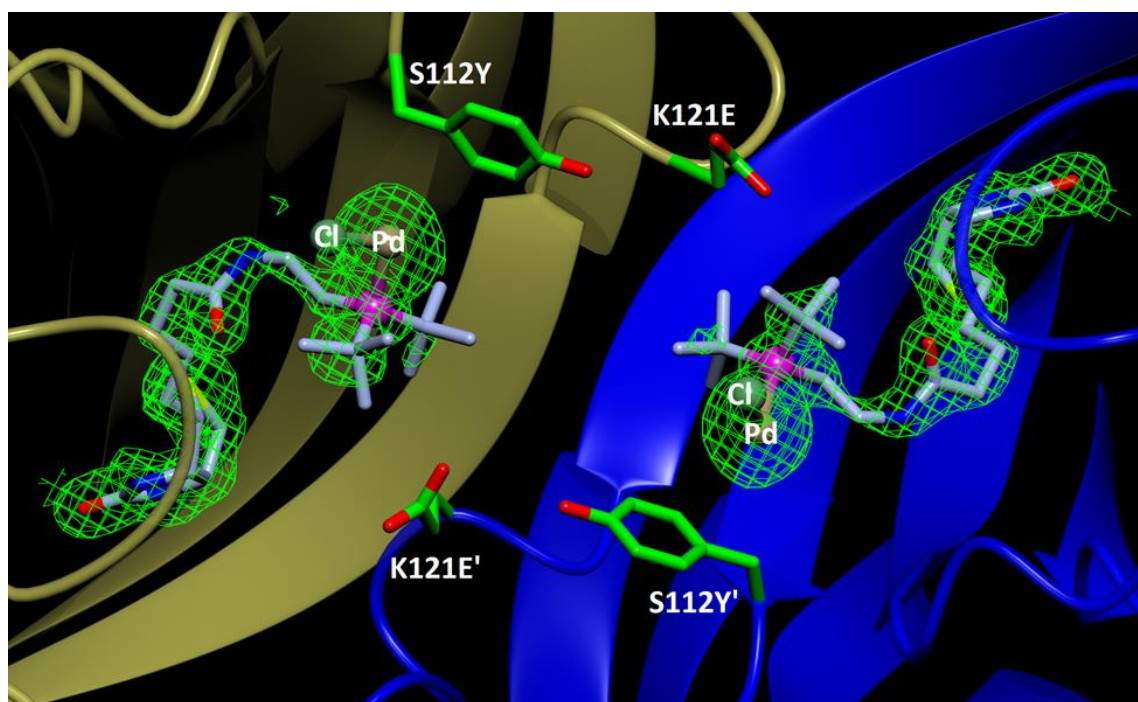


Figure 3.3 Close-up view of the X-ray structure of 1 · S112Y- K121E Sav. The two monomeric chains (blue and gold) and biotinylated complexes are related by a twofold symmetry axis. The electron density around 1 (green) was generated from a 2Fo-Fc map (0.5 electrons/Å³).

Based on this structural insight, we hypothesize that π - π interactions between the tyrosine (Y112) and the naphthyl moiety may enhance the enantioselectivity. Similar interactions between both coupling partners were shown by DFT calculations to critically influence the enantioselectivity of the SMC reaction.³⁹

3.5 Conclusions

In summary, incorporation of an electron-rich phosphino-palladium moiety within Sav affords an artificial Suzukiase for the synthesis of enantioenriched binaphthyls (up to 90 % ee and 50 TONs for 2-methoxy-binaphthyl **8b**). Importantly, it was shown that the hybrid catalyst offers vast opportunities for chemogenetic optimization of the catalytic performance: site-directed mutagenesis leads to a significant increase in enantioselectivity. Current efforts are aimed at performing catalytic asymmetric SMC with artificial Suzukiases *in vivo*.

3.6 References

- (1) Suzuki, A. *Angew. Chem. Int. Ed. Engl.* **2011**, *50*, 6722.
- (2) Miyaura, N.; Suzuki, A. *Chem. Eur. J.* **1995**, *95*, 2457.
- (3) Hassan, J.; Sévignon, M.; Gozzi, C.; Schulz, E.; Lemaire, M. *Chem. Rev.* **2002**, *102*, 1359.
- (4) Littke, A. F.; Fu, G. C. *Angew. Chem. Int. ed.* **2002**, *41*, 4176.
- (5) Kotha, S.; Lahiri, K.; Kashinath, D. *Tetrahedron* **2002**, *58*, 9633.
- (6) Shen, X.; Jones, G. O.; Watson, D. A.; Bhayana, B.; Buchwald, S. L. *J. Am. Chem. Soc.* **2010**, *132*, 11278.
- (7) Zhang, D.; Wang, Q. *Coord. Chem. Rev.* **2015**, *286*, 1.
- (8) Bermejo, A.; Ros, A.; Fernández, R.; Lassaletta, J. M. *J. Am. Chem. Soc.* **2008**, *130*, 15798.
- (9) Lipshutz, B. H.; Petersen, T. B.; Abela, A. R. *Org. Lett.* **2008**, *10*, 1333.
- (10) Lipshutz, B. H.; Ghorai, S. *Aldrichimica Acta.* **2008**, *59*.
- (11) Polshettiwar, V.; Decottignies, A.; Len, C.; Fihri, A. *ChemSusChem* **2010**, *3*, 502.
- (12) Yusop, R. M.; Unciti-Broceta, A.; Johansson, E. M. V; Sánchez-Martín, R. M.; Bradley, M. *Nat. Chem.* **2011**, *3*, 239.

- (13) Abe, S.; Niemeyer, J.; Abe, M.; Takezawa, Y.; Ueno, T.; Hikage, T.; Erker, G.; Watanabe, Y. *J. Am. Chem. Soc.* **2008**, *130*, 10512.
- (14) Li, J.; Chen, P. R. *Chembiochem* **2012**, *13*, 1728.
- (15) Chalker, J. M.; Wood, C. S. C.; Davis, B. G. *J. Am. Chem. Soc.* **2009**, *131*, 16346.
- (16) Gao, Z.; Gouverneur, V.; Davis, B. G. *J. Am. Chem. Soc.* **2013**, *135*, 13612.
- (17) Spicer, C. D.; Triemer, T.; Davis, B. G. *J. Am. Chem. Soc.* **2012**, *134*, 800.
- (18) Li, N.; Lim, R. K. V.; Edwardraja, S.; Lin, Q. *J. Am. Chem. Soc.* **2011**, *133*, 15316.
- (19) Gao, Z.; Gouverneur, V.; Davis, B. G. *J. Am. Chem. Soc.* **2013**, *135*, 13612.
- (20) Spicer, C. D.; Davis, B. G. *Chem. Commun.* **2011**, *47*, 1698.
- (21) Chankeshwara, S. V.; Indrigo, E.; Bradley, M. *Curr. Opin. Chem. Biol.* **2014**, *21*, 128.
- (22) Unciti-Broceta, A.; Johansson, E. M. V.; Yusop, R. M.; Sánchez-Martín, R. M.; Bradley, M. *Nat. Protoc.* **2012**, *7*, 1207.
- (23) Parker, H. L.; Rylott, E. L.; Hunt, A. J.; Dodson, J. R.; Taylor, A. F.; Bruce, N. C.; Clark, J. H. *PLoS One* **2014**, *9*, e87192.
- (24) Ma, X.; Wang, H.; Chen, W. *J. Org. Chem.* **2014**, *79*, 8652.
- (25) Yang, C.; Manocchi, A. K.; Lee, B.; Yi, H. *J. Mater. Chem.* **2011**, *21*, 187.
- (26) Søbberg, L. S.; Gauthier, D.; Lindhardt, A. T.; Bunge, M.; Finster, K.; Meyer, R. L.; Skrydstrup, T. *Green Chem.* **2009**, *11*, 2041.
- (27) Yang, M.; Li, J.; Chen, P. R. *Chem. Soc. Rev.* **2014**, *43*, 6511.
- (28) Aldemir, H.; Richarz, R.; Gulder, T. A. M. *Angew. Chem. Int. Ed.* **2014**, *53*, 8286.
- (29) Cammidge, A. N.; Crépy, K. V. L. *Chem. Commun.* **2000**, *18*, 1723.
- (30) Uozumi, Y.; Matsuura, Y.; Arakawa, T.; Yamada, Y. M. A. *Angew. Chem. Int. Ed.* **2009**, *48*, 2708.
- (31) Benhamou, L.; Besnard, C.; Kündig, E. P. *Organometallics* **2014**, *33*, 260.
- (32) Wilson, M. E.; Whitesides, G. M. *J. Am. Chem. Soc.* **1978**, *100*, 306.
- (33) Pierron, J.; Malan, C.; Creus, M.; Gradinaru, J.; Hafner, I.; Ivanova, A.; Sardo, A.; Ward, T. R. *Angew. Chemie* **2008**, *120*, 713.

- (34) Hyster, T. K.; Knörr, L.; Ward, T. R.; Rovis, T. *Science* **2012**, 338, 500.
- (35) Dürrenberger, M.; Ward, T. R. *Curr. Opin. Chem. Biol.* **2014**, 19, 99.
- (36) Deraedt, C.; Astruc, D. *Acc. Chem. Res.* **2014**, 47, 494.
- (37) Reetz, M. T.; Sanchis, J. *Chembiochem* **2008**, 9, 2260.
- (38) Weinreich, D. M.; Delaney, N. F.; Depristo, M. A.; Hartl, D. L. *Science* **2006**, 312, 111.
- (39) Tang, W.; Patel, N. D.; Xu, G.; Xu, X.; Savoie, J.; Ma, S.; Hao, M.-H.; Keshipeddy, S.; Capacci, A. G.; Wei, X.; Zhang, Y.; Gao, J. J.; Li, W.; Rodriguez, S.; Lu, B. Z.; Yee, N. K.; Senanayake, C. H. *Org. Lett.* **2012**, 14, 2258.

CHAPTER 4

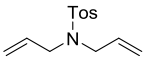
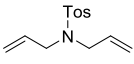
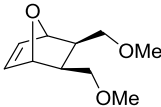
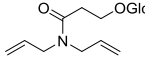
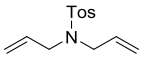
Development of Artificial Metathesase for Ring Closing Metathesis

4.1 Introduction

In the past forty years, the olefin metathesis reaction has emerged and matured as a very efficient and elegant method for formation of C=C double bonds.¹ It is widely used not only in small-scale laboratory research, but also in large-scale industrial production. Among the frontiers in olefin metathesis, one should mention: i) control of *E/Z* selectivity,^{2,3} ii) enantioselective ring-closing metathesis (enantioselective RCM hereafter),⁴ iii) the application of metathesis for the conversion of biomass into useful products,⁵⁻⁸ and iv) metathesis as a bioorthogonal ligation tool.^{9,10} In the latter context, aqueous-phase metathesis remains a challenge.¹¹⁻¹³

To address this challenge, we and others have relied on the creation of artificial metalloenzymes for olefin metathesis.¹⁴⁻¹⁷ There are a total of five artificial metathesases reported in the literature to date.¹⁸ Those are summarized in Table 4.1. The following features emerge from Table 4.1: i) the systems from the Hilvert group and Ward group do not require an inert atmosphere; ii) the substrate concentration in the metathesase based on hCA II is the lowest of all systems reported to date; iii) The highest turnover frequency was observed for the metathesase based on FhuA which however requires a surfactant iv) Hilvert reported highly acidic conditions whereas Schwaneberg, Ward and Matsuo group reported RCM at pH 7.0 and physiological conditions. v) Hilvert, Schwaneberg and Matsuo reported a covalent anchoring strategy of the Ru cofactor, whereas the Ward group relied on supramolecular and dative anchoring. Based on this comparison, we conclude that no general trend for the structure and reaction conditions for artificial metathesases can be identified.

Table 4.1 Summary of the catalytic performance of artificial metathesases reported to date

	Hilvert ¹⁵	Ward ¹⁴	Schwaneberg ^{16,19}	Matsuo ¹⁷	Ward ¹⁸
[Substrate]	 5 mM	 15.21 mM	 100 mM	 8 mM	 1 mM
Reaction type	RCM	RCM	ROMP	RCM	RCM
Anchoring of Ru-cofactor	Covalent	Supramolecular	Covalent	Covalent	Dative
Host protein	MjHSP ^a 4 mol%	Avidin 4.8 mol%	FhuA ΔDCVF ^{tev b} 0.08 mol%	α – chymotrypsin 0.63 mol%	hCA II 1 mol%
Temp.	45 °C	40 °C	25 °C	25 °C	37 °C
Time	12h	16h	68h	2h	4h
pH	2	4	7	7	7
Reaction conditions	10 mM HCl, Water/ <i>t</i> -BuOH(4/1) under air	0.1M acetate Water/ DMSO(5/1) 0.5 M MgCl ₂ , under air	Water/THF(9/1) SDS 1% under N ₂	Degassed 100 mM, KCl, under N ₂	0.1 M phosphate Water/ DMSO (9/1) under air
TON	25	20	955	20	28

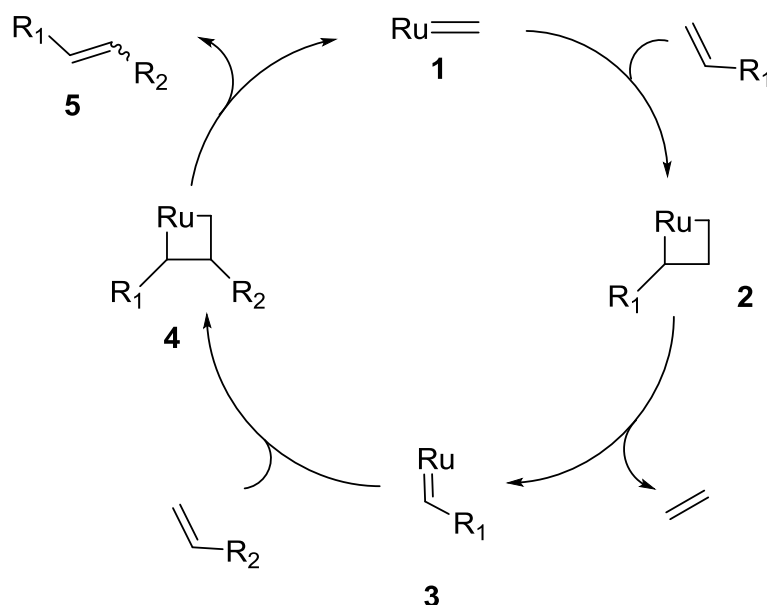
^a MjHSP: *M. jannaschii* small heat shock protein. ^b FhuA ΔDCVF^{tev}: engineered variants of the β-barrel ferric hydroxamate uptake protein component A. ROMP

The excellent stability of (strept)avidin combined with its high affinity towards biotinylated compounds offers a large number of promising applications (See Chapter 1). In this context, we have been exploiting the biotin-streptavidin technology to create artificial metalloenzymes for a variety of transformations,^{20,21} including hydrogenation,²² transfer hydrogenation,²³ allylic alkylation,²⁴ benzannulation,²⁵

sulfoxidation,²⁶ dihydroxylation²⁷ as well as olefin metathesis.^{14,18,28} Among these reactions, the olefin metathesis is a versatile means to create new C-C bonds. In view of the scarcity of olefins in metabolites, the olefin metathesis can be viewed as bio-orthogonal: both substrates and products of the olefin metathesis will most probably not react with any of the enzymes present in a cell.²⁹

4.1.2 Mechanism of the Olefin Metathesis

The first mechanistic hypothesis for the olefin metathesis was put forward by Chauvin.³⁰ It has since been confirmed and is now widely accepted (Scheme 4.1).^{31,32} The direct [2+2] cycloaddition of two alkenes is formally symmetry forbidden and thus has a high activation energy. The Chauvin mechanism involves the [2+2] cycloaddition of an alkene double bond to a transition metal alkylidene **1/3** to form a metallacyclobutane intermediate **2/4**. The metallacyclobutane produced can then cyclorevert to give either the original species or a new alkene **5** and alkylidene. Interaction with the d-orbitals on the metal catalyst lowers the activation energy enough so that the reaction can proceed rapidly at modest temperatures.



Scheme 4.1 Mechanism of the olefin metathesis

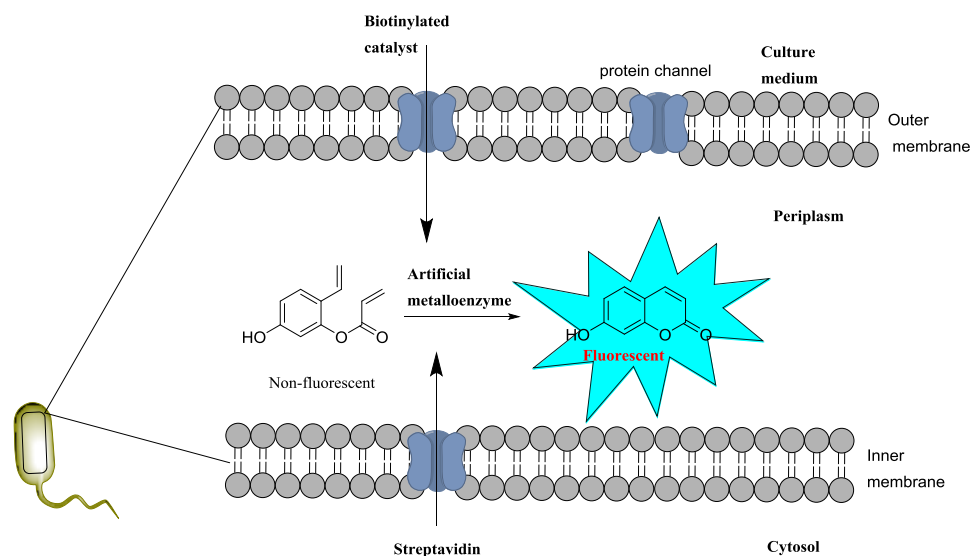
4.2 Aim of the Project

In this project, we focused on exploiting the potential of streptavidin as a biomolecular scaffold to broaden the scope of artificial metalloenzymes based on the biotin (strept)avidin technology. Traditionally, a chemogenetic optimization scheme is applied to improve catalytic performance of artificial metalloenzymes. Genetic diversity is created by introducing point mutations on the streptavidin gene. Chemical diversity is achieved by variation of the spacer between the anchor and the Ru-moiety. Previous experience clearly demonstrated that catalytic activity of artificial metalloenzymes is critically dependent on the first coordination sphere around the active metal and thus it is recommended to test a variety of different catalyst precursors. With this goal in mind, we focused on the synthesis and evaluation of the catalytic performance of nine biotinylated metathesis catalysts.

The milestones are summarized as follows.

- ❖ Create chemical diversity by preparing a library of biotinylated catalysts.
Synthesize suitable substrates for high-throughput screening.
- ❖ Identify a suitable expression system for *in vivo* screening.

4.3 Outline of the Project



Scheme 4.2 RCM reaction in the periplasm of *E. coli* to yield a fluorescent product

The olefin functionality is an underrepresented functional group in cellular media. In addition, this functionality displays only modest reactivity towards the various reactants present in this complex media. Our effort thus focused on developing biorthogonal reactions using olefins as partner.²⁰ Previously, we had shown that such ArM are complementary with natural enzymes, thus opening interesting perspectives towards the implementation of non-natural reaction cascades for *in vitro* and *in vivo* selection.³³ This approach could ultimately lead to the development of bacteria acting as molecular factories for the production of complex molecules resulting from non-natural reaction cascades. As a proof-of-principle, it is proposed to use a ring closing metathesis reaction. The main idea is to transport streptavidin from the cytoplasm into the periplasm of *E. coli* cells. Then, addition of biotinylated catalyst will lead to the formation of artificial metalloenzyme which can catalyze the RCM reaction releasing a fluorescent product (Scheme 4.2). By detecting the fluorescence, a large library of mutants can be screened within a short time. This strategy will ultimately lead towards high throughput screening and directed evolution of ArM's.

This project was highly collaborative and was part of an EU project entitled METACODE. Two additional coworkers actively contributed to the results presented herein: Dr. Raphael Reuter, and MSc Biol Markus Jeschek. Their contributions are clearly highlighted throughout this chapter.

Raphael Reuter synthesized the fluorescent substrate and screened single mutants. Markus Jeschek developed *E. coli* strain that express streptavidin inside the periplasm of *E. coli* and developed methods for high throughput screening of RCM activity in the periplasm of *E. coli*.

4.4 Results and Discussion

4.4.1 Synthesis of Biotinylated Metathesis Catalysts

The Ward group previously reported on an artificial metathesase relying on combining either avidin or streptavidin with either **Biot-1** or **Biot-*m*-ABA-1**.¹⁴ In this

study, we set out to vary the position of the biotin-anchor and to identify the most promising catalyst under various catalytic conditions. All complexes tested in this study are presented in Figure 4.1.

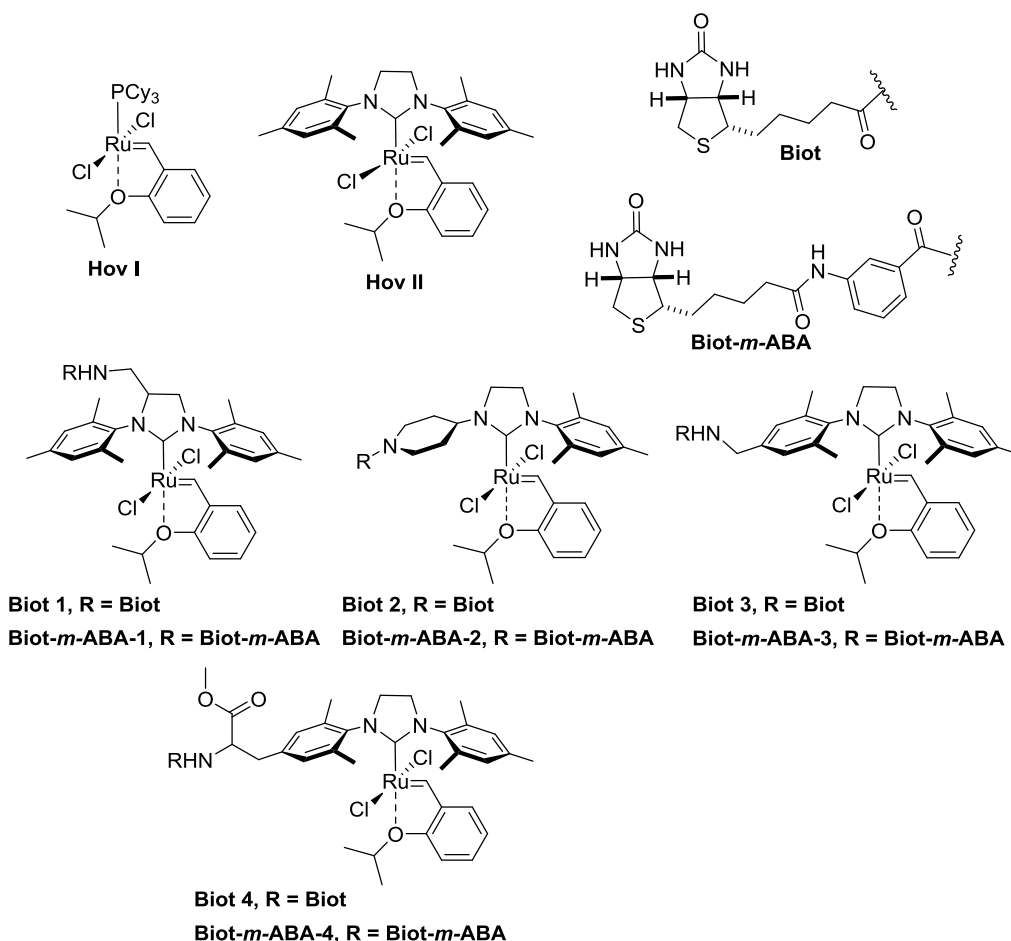
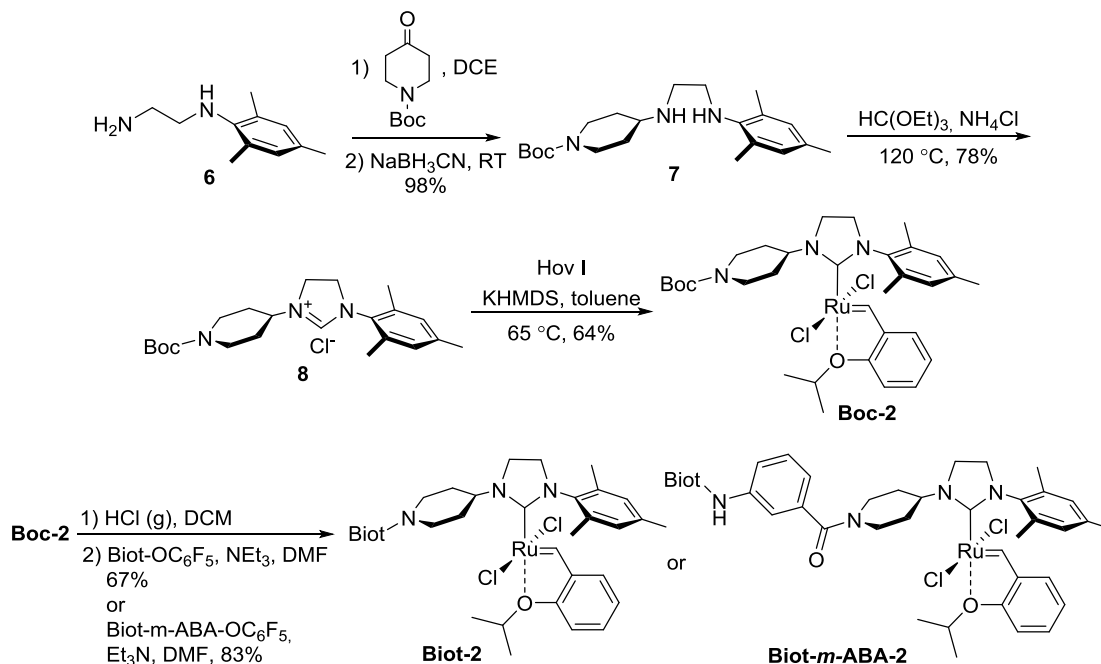


Figure 4.1 Biotinylated metathesis catalysts prepared and tested in this study.

While one *N*-mesityl substituent is critical for high RCM activity,³⁴ we set out to link the biotin anchor on the other *N*-substituent of the *N*-heterocyclic carbene moiety. We evaluated both aromatic (e.g. **Biot-3**, **Biot-*m*-ABA-3**, and **Biot-4**, **Biot-*m*-ABA-4**), as well as aliphatic substituents (e.g. **Biot-2** and **Biot-*m*-ABA-2**) at this position.

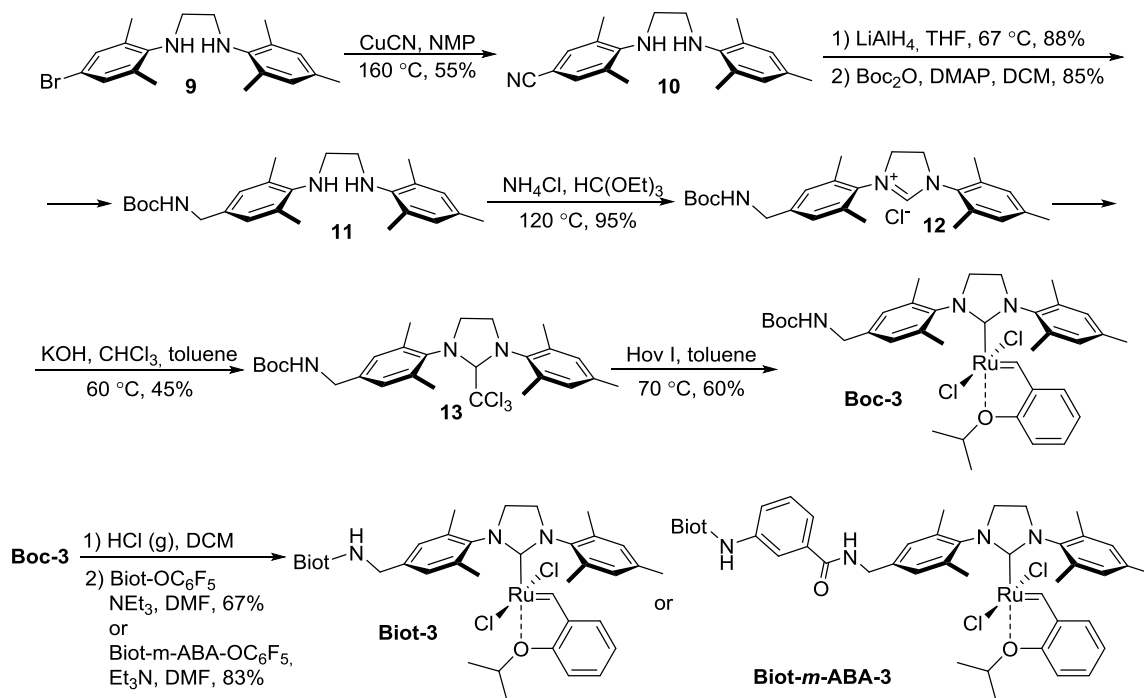
With this aim, we set out to prepare the key Boc-protected imidazolium intermediate **Boc-2**. Reductive amination of the alkylated aniline **6**³⁵ yielded the 1,2-diamine **7** (Scheme 4.3). Cyclisation with triethyl orthoformate provided the imidazolium salt **8**.

Ligand exchange with Hoveyda-Grubbs first generation catalyst **Hov I** afforded the Boc-protected ruthenium NHC complex **Boc-2**. Deprotection with gaseous hydrogen chloride and coupling with either activated biotin or activated biotin *m*-aminobenzoic acid afforded **Biot-2** and **Biot-*m*-ABA-2** respectively.



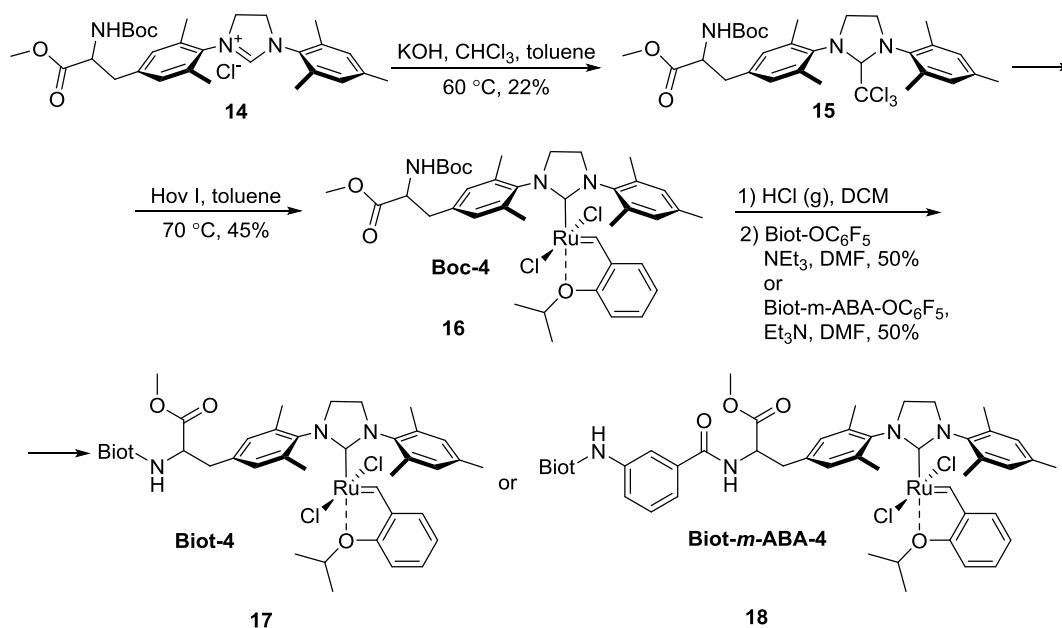
Scheme 4.3 Synthesis of the biotinylated complexes **Biot-2** and **Biot-*m*-ABA-2**.

The next biotinylated catalysts included two mesityl groups with a biotin linked to one of these. For this purpose, we used the procedure reported by Gilbertson *et al.* relying on the unsymmetrical diamine **9**.³⁶ Rosenmund-von Braun cyanation followed by reduction and Boc-protection yielded compound **11**. This latter was reacted with triethylorthoformate in the presence of ammonium chloride to provide the imidazolium salt **12**. Reaction of **12** with chloroform and KOH yielded the chloroform adduct **13**.³⁷ Ligand exchange with **Hov I** catalyst provided the ruthenium NHC complex **Boc-3** which after Boc-deprotection was reacted with activated biotin and biotin *m*-aminobenzoic acid to afford **Biot-3** and **Biot-*m*-ABA-3** respectively (Scheme 4.4).



Scheme 4.4 Synthesis of the biotinylated complexes **Biot-3** and **Biot-m-ABA-3**

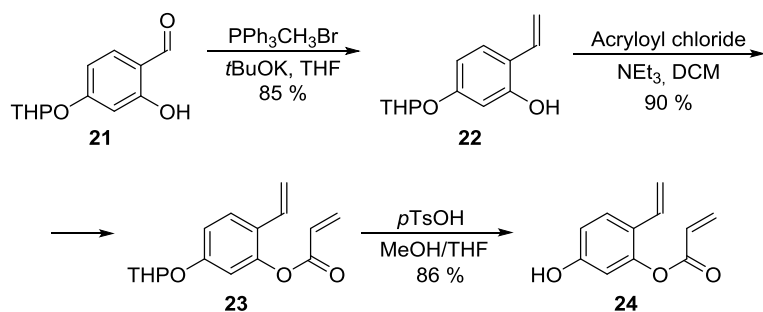
To evaluate the influence of the spacer length between the biotin-anchor and the NHC, we synthesized another type of catalysts (**Biot-4** and **Biot-m-ABA-4**) which bear an additional carbon when compared to **Biot-3** and **Biot-m-ABA-3**. The NHC ligand **14** was synthesized according to a published procedure.³⁶ Both **Biot-4** and **Biot-m-ABA-4** were synthesized as racemate. Preparation of the chloroform adduct followed by reaction with **Hov I** yielded the ruthenium NHC complex **Boc-4**. After Boc deprotection and reaction with activated biotin derivatives, **Biot-4** and **Biot-m-ABA-4** were obtained (Scheme 4.5).



Scheme 4.5 Synthesis of the biotinylated complexes **Biot-4** and **Biot-*m*-ABA-4**

4.4.2 Activity Test in Organic and Aqueous Organic Solvent

The performance of the biotinylated catalysts was evaluated in the ring closing metathesis of two model substrates: the diallyl tosylamide **19** and the coumarin precursor **24**. The second substrate was produced by Raphael Reuter from aldehyde **21**³⁸ via a Wittig reaction followed by esterification with acryloyl chloride and deprotection of the hydroxy group (Scheme 4.7).



Scheme 4.7 Synthesis of coumarin precursor **24**, substrate for RCM reaction.³⁹

The activity of the new biotinylated catalysts was compared with that of second-generation Grubbs-Hoveyda complex **Hov II**. The results for RCM reaction of diallyl tosylamide **19** are summarized in Table 4.1 and Chart 4.1 and results for RCM reaction of coumarin precursor **24** are presented in Table 4.2 and on Chart 4.2. All RCM reactions were analysed by reversed phase HPLC and revealed no product isomerization.

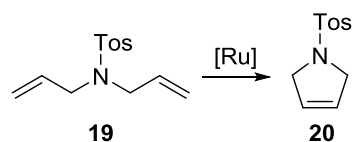


Table 4.1 Comparison of activity of catalysts in RCM of diallyl tosylamide **19**.

Entry	Catalyst ^[a]	Yield [%] ^[b]	Yield [%] ^[c]	Yield [%] ^[d]
1	Hov II	>99	>99	75
2	Biot-1	93	83	13
3	Biot-<i>m</i>-ABA-1	96	76	28
4	Biot-2	43	18	1
5	Biot-<i>m</i>-ABA-2	41	19	1
6	Biot-3	79	70	17
7	Biot-<i>m</i>-ABA-3	76	49	7
8	Biot-4	69	35	12
9	Biot-<i>m</i>-ABA-4	97	84	10

^[a] 1 mol% of **[Ru]**, 37 °C, 24h; ^[b] CH₂Cl₂, **[19]** = 0.1M; ^[c] CH₂Cl₂, **[19]** = 0.01M, ^[d] H₂O/DMSO 84:16, **[19]** = 0.1M. Experiments were performed in triplicate (yield +/- 2 %, in case of low yields <10% all results were almost the same). See Appendix 2 for experimental details.

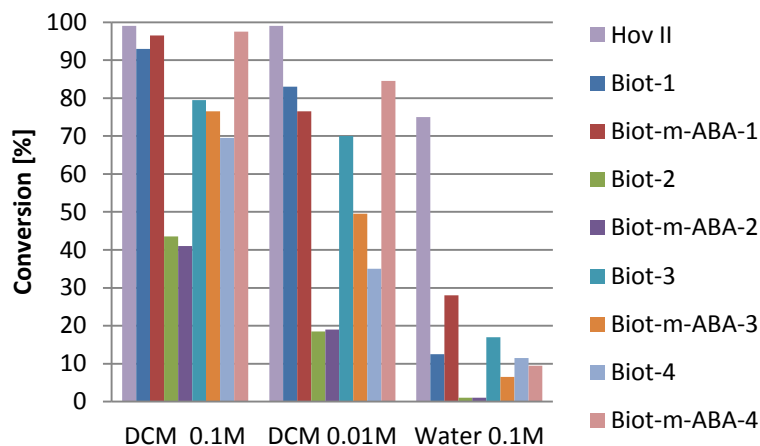


Chart 4.1 Comparison of catalysts activity in RCM reaction of diallyl tosylamide.

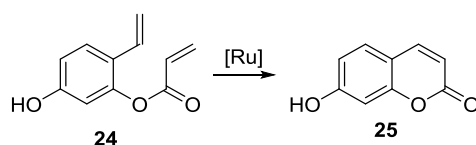
As a starting point, we performed the RCM of diallyl tosylamide **19** with 1 mol% of biotinylated catalysts with a 0.1M substrate concentration at 37 °C in dichloromethane. The results reveal that most of biotinylated catalysts with two mesityl moieties bound to imidazoline ring, viz. **Biot-1**, **Biot-*m*-ABA-1** and **Biot-*m*-ABA-4** exhibit the same activity as the parent **Hov II** catalyst and reached almost full conversion. Similar results were also observed for structurally related complexes, namely **Biot-3**, **Biot-*m*-ABA-3** and **Biot-4** with conversion around 70-80%. These results are consistent with previous observations suggesting that catalysts containing two bulky aromatic substituents in the NHC ligand have the highest activity and stability. Accordingly, **Biot-2** and **Biot-*m*-ABA-2**, are less active.

Upon decreasing the substrate concentration to 0.01 M, similar trends were observed. The presence of a biotin moiety led to marked decrease in conversion, especially with complexes bearing an alkyl substituent on the NHC (e.g. **Biot-2** and **Biot-*m*-ABA-2**).

Next, the reactions were performed in water: DMSO, 84:16 mixtures (DMSO was required to dissolve both substrate and catalyst while both substrates and all catalysts exhibit very low solubility in pure water). Except for **Hov II** (75 % yield), the yields were dramatically lower. The best biotinylated catalyst, **Biot-*m*-ABA-1**, reached only ca. 30% yield. In this case, the reason for such low yield of the RCM reactions may be low catalysts' stability in a mixture of water : DMSO. During the reactions, all

reaction mixtures changed colour from green (Hoveyda-type catalysts) or purple (Grubbs-type catalyst) to brownish. Catalysts also underwent a slow decay in DCM but it seems that the reactions in this solvent were faster which made it possible to obtain a high yield of the desired product.

Table 4.2 Comparison of activity of catalysts in RCM reaction of coumarin precursor **24**.



Entry	Catalyst ^[a]	Yield [%] ^[b]	Yield [%] ^[c]
1	Hov II	>99	4
2	Biot-1	97	1
3	Biot-<i>m</i>-ABA-1	70	3
4	Biot-2	99	1
5	Biot-<i>m</i>-ABA-2	88	1
6	Biot-3	50	4
7	Biot-<i>m</i>-ABA-3	48	1
8	Biot-4	52	1
9	Biot-<i>m</i>-ABA-4	50	1

^[a] 5 mol% of [Ru], 37 °C, 24h; ^[b] CH₂Cl₂, [24] = 0.025M; ^[c] H₂O/DMSO 84:16, [24] = 0.025M. Experiments were performed in triplicate (yield +/- 5 %; in reactions performed in H₂O/DMSO all results were the same). See Appendix 2 for experimental details.

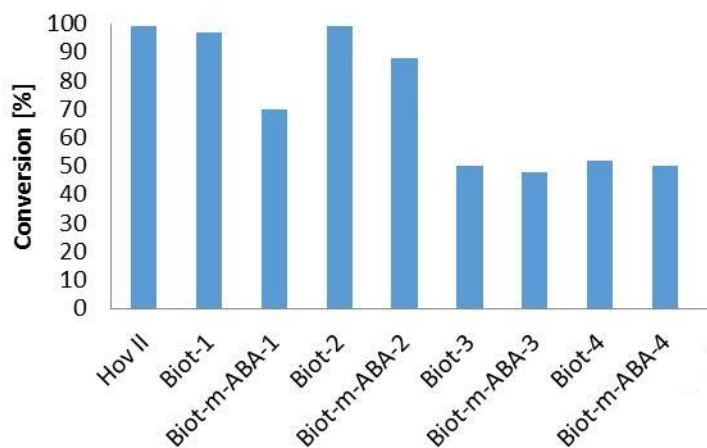


Chart 4.2 Comparison of catalysts activity in RCM reaction of 5-hydroxy-2-vinylphenyl acrylate in CH_2Cl_2 .

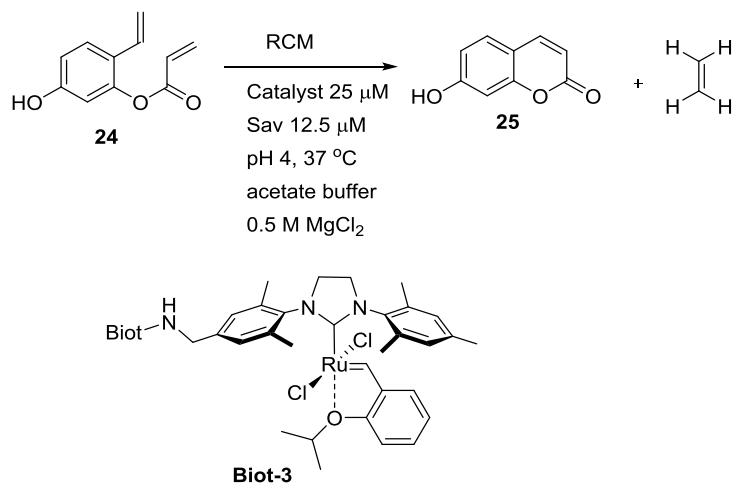
As the umbelliferone precursor **24** bears an electron withdrawing olefinic moiety which significantly decreases its reactivity, the corresponding RCM reactions were performed with 5 mol% biotinylated catalysts (Table 4.2) in 0.025M concentration at 37 °C in dichloromethane. Under these conditions, the two biotinylated catalysts, **Biot-1** and **Biot-2** reached near quantitative conversions. The other biotinylated Hoveyda-type catalysts gave moderate yields approaching 50%. When reactions were performed in a water : DMSO mixture, < 5% conversion was obtained for all catalysts, including **Hov II**.

In RCM reaction of diallyl tosylamide **19** **Biot-2** used in a 1 mol% loading gave relatively low yield, 43%, while in the reaction of a more demanding substrate, coumarin precursor **24**, when 5 mol% of catalyst was used, it reached almost quantitative yield. This is probably due to the balance between the activity and the stability of this catalyst in DCM. **Biot-2** can be very active and at the same time it may be subject to a rapid decomposition in an organic solvent. In such a situation, RCM reaction of even quite simple substrate like diallyl tosylamide **19** with a 1 mol% catalyst loading can produce low conversions. In the second reaction with the umbelliferone precursor **24**, 5 mol% catalyst loading was used and due to its high activity almost quantitative yield was obtained.

N,N-diallyl tosylamine **19** was used as model substrate for the RCM reaction and its cyclization was performed in homogeneous water–organic solvent mixtures by several research groups. In most cases, 5 mol% either of classic (e.g. **Gr II**, **Hov II**) or water soluble complexes were used mostly in the mixture of water and organic solvent (EtOH, DME, MeOH and DMSO). Among the catalysts tested, when a reaction was performed in the mixture of DME : water (2:1), the classical Grubbs-Hoveyda second generation complex turned out to be the most effective, providing a very good conversion (>95%) of the substrate with a relatively low catalyst loading (1 mol%). When the reaction was performed with 5 mol% of Raines'⁴⁰ or Blechert's⁴¹ catalysts, the results were very good, as well. A reaction in pure water was also performed mainly with 5 mol% of catalyst. In these case either classic **Gr I** and **Gr II** were used in the presence of surfactants,⁴² calix[*n*]arenes⁴³ or dendrimers⁴⁴ or catalysts that bear groups acting as a surfactant.⁴⁵

Biotinylated catalysts presented in this study often gave lower conversions than the examples above; however, it is difficult to attempt to have any meaningful comparison due to the fact that each reaction was carried out under distinct conditions (temperature, substrate concentration, catalyst loading, and solvent).

4.4.3 Comparison of Artificial Metalloenzymes



Scheme 4.8 RCM catalyzed by artificial metalloenzyme

After comparison of biotinylated catalysts without protein, we tested all the biotinylated catalysts in acetate buffer at pH 4 in presence of streptavidin (Scheme 4.8). As a starting point, we performed the RCM of the coumarin precursor **24** with 25 μ M of biotinylated catalysts with a 10 mM substrate concentration at 37 °C in acetate buffer. The reaction without biotinylated catalyst was set as a control. The results reveal that **Biot-3** outperformed all other catalysts (Chart 4.3). Moreover, this catalyst also showed protein acceleration, since the reaction showed a slightly better performance inside the protein scaffold than outside the protein. This result is important for screening purposes and suggests that the RCM reaction is indeed catalysed by the artificial metathesases rather than free catalyst.

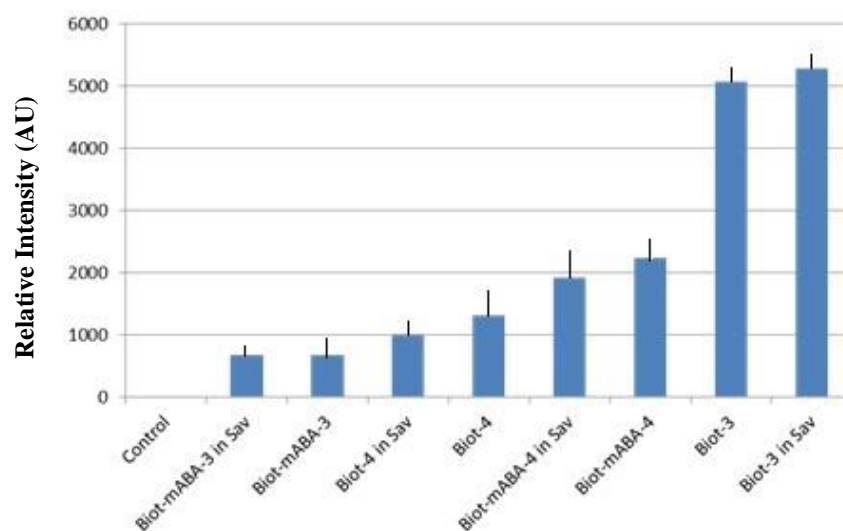


Chart 4.3 Comparison of catalyst activities in RCM reactions of 5-hydroxy-2-vinylphenyl acrylate **24** in acetate buffer (pH 4) in the presence of streptavidin. All reactions were performed in duplicate.

4.4.4 Screening of Different Mutants with Biot-3 Catalyst

Docking studies with **Biot-3** suggest that S112 and K121 residues lie in the immediate proximity of the metal centre upon incorporation within Sav.

We screened different single mutants to optimize the performance of **Biot-3** catalyst in the RCM of 5-hydroxy-2-vinylphenyl acrylate **24** in acetate buffer (pH 4) (Scheme 4.8). We found that neutral amino acids (glycine, alanine) are better than acidic (glutamic acid) or basic side aminoacid (arginine).

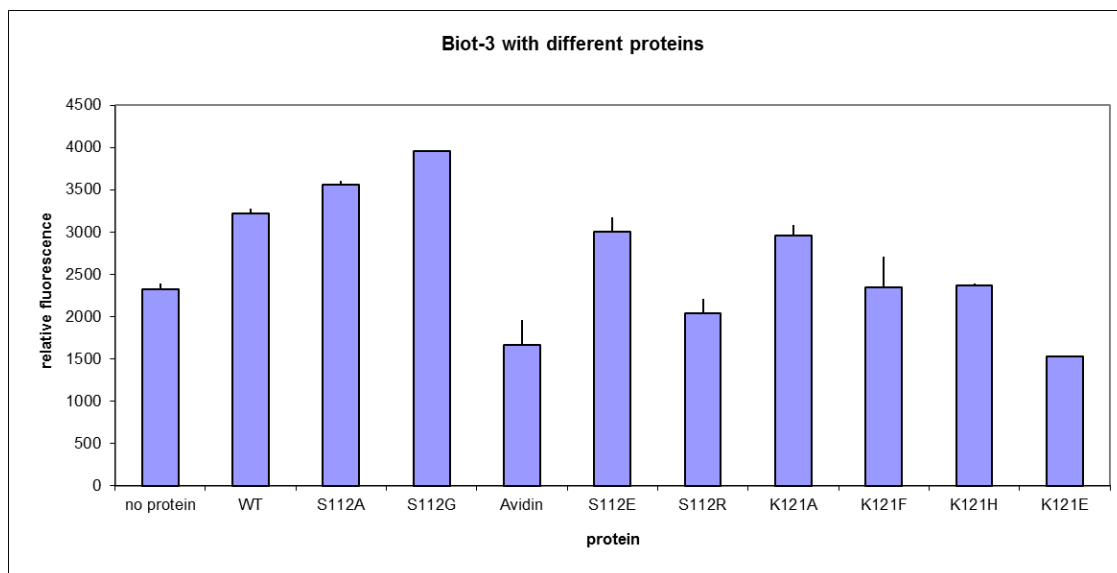


Chart 4.6 Comparison of streptavidin single mutants in RCM reaction of 5-hydroxy-2-vinylphenyl acrylate **24** in acetate buffer (pH 4) using **biot-3** as cofactor. RCM were performed in duplicate.

Having identified **Biot-3**:S112G and **Biot-3**:S112A as a promising first generation metathesase, we screened selected double mutants (Chart 4.7). Our findings reveal that S112A-K121N outperformed among all other mutants tested. The activity inside the protein is significantly higher than outside of the protein. However, the turnover number remains below 1 in all cases.

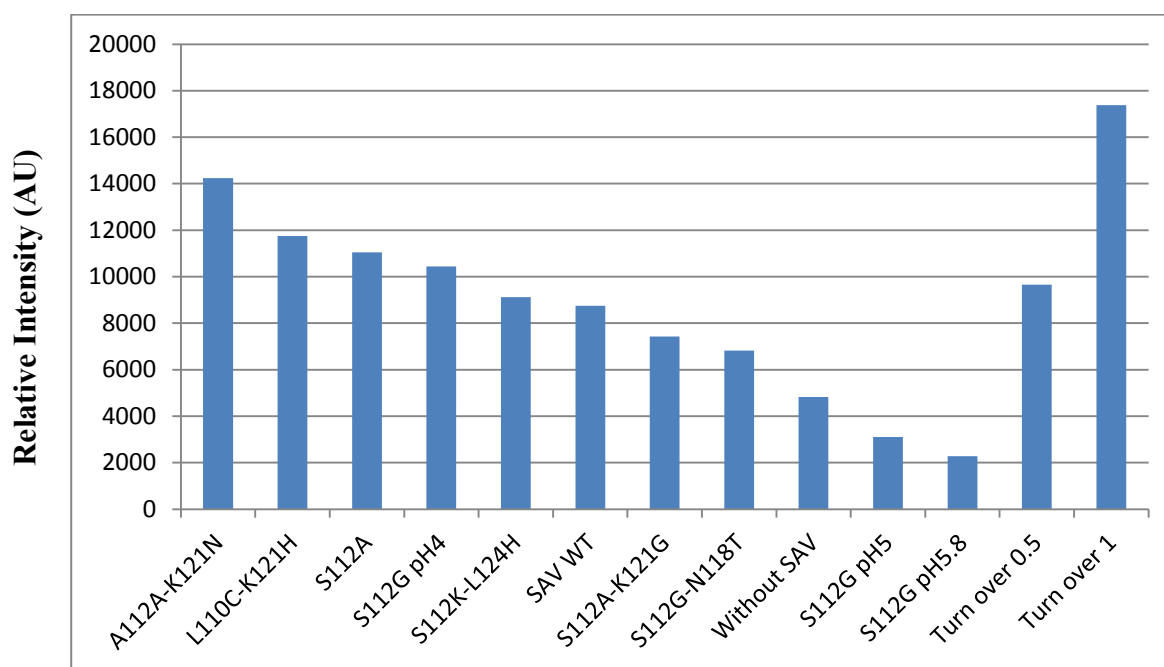
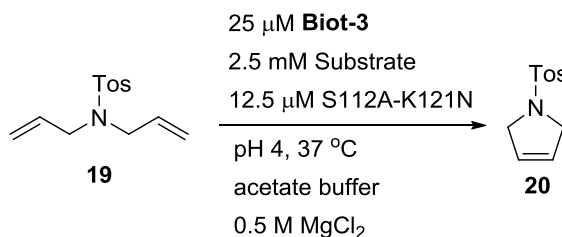


Chart 4.7 Comparison of streptavidin mutants in RCM reaction of 5-hydroxy-2-vinylphenyl acrylate **24** in acetate buffer (pH 4). The fluorescence obtained for 1 TON and 0.5 corresponds to 17,000 and 10,000 AU respectively.

4.4.5 HPLC measurements

For quantitative determination of the yield, we rely on HPLC. Having identified **Biot-3** as the most active catalyst, we screened $[\text{Ru}]/[\text{Sav}]_{\text{mon}}$ ratio for RCM reaction of diallyl *N*-tosylamide **19** (Scheme 4.9) keeping the substrate- (2.5 mM) and ruthenium concentration (25 μM) constant. The result suggests that upon increasing the $[\text{Ru}]/[\text{Sav}]_{\text{mon}}$ ratio, the TON per Ru increases.



Scheme 4.9 RCM reaction of diallyl tosylamide

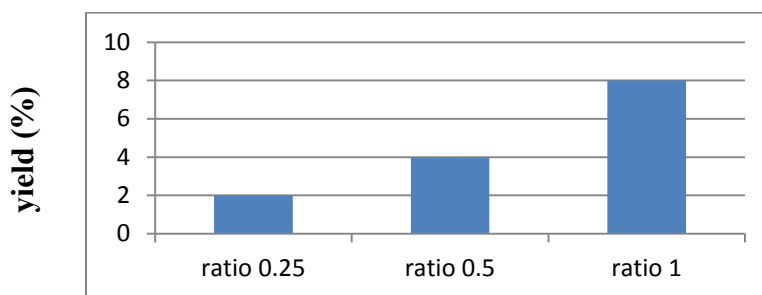


Chart 4.4 Comparison of [Ru]/[Sav]_{mon} ratio.

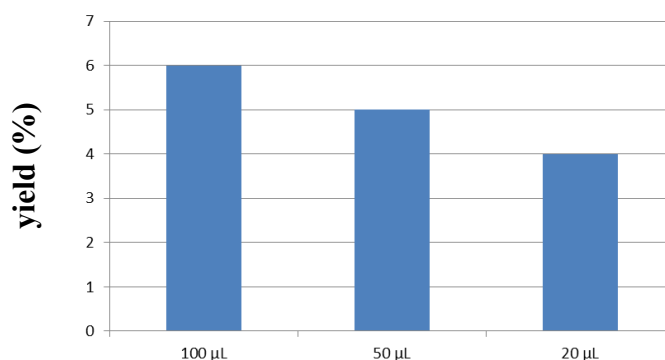


Chart 4.5 Comparison of the total reaction volume

With the aim of miniaturizing the screening, the reaction volume was decreased. For that purpose we screened different total reaction volumes with 25 µM catalyst (1 mol %) (Scheme 4.9, Chart 4.5). It was found, that volume modestly effects the total conversion. Importantly, the conversion remained unchanged when performing the reaction in the glass tubes instead of plastic tubes.

Typical Sav production protocols require 1 mM EDTA to prepare cell free extracts. EDTA is chelating ligand and it may inhibit the catalysis by coordinating to the metal. To test the effect of this adjuvant combining with different salts on the artificial metathesase, pure Sav (12.5 µM) samples were spiked with EDTA (1 mM) and different salts (0.5 M) (Table 4.3). Since chloride is necessary for catalyst stabilization, we varied only the metal ions. The result revealed that the presence of excess EDTA did not inhibit the catalysis. Varying metal ions did not effect on the conversion of RCM.

Table 4.3 The effect of EDTA and salts in RCM reaction of diallyl *N*-tosylamide **19**

Entry	Protein (12.5 μ M)	Salt (0.5 M)	Conversion (%)
1	S112A-K121N	MgCl ₂	6
2	S112A-K121N	CaCl ₂	6
3	S112A-K121N	NaCl	5
4	S112A-K121N	KCl	5
5	S112A-K121N	MgCl ₂ + EDTA	6
6	S112A-K121N	CaCl ₂ + EDTA	6
7	S112A-K121N	NaCl + EDTA	4
8	S112A-K121N	KCl + EDTA	5
9	S112A-K121N	-	0
10	-	MgCl ₂	30
11	-	CaCl ₂	35
12	-	NaCl	40
13	-	KCl	30
14	-	MgCl ₂ + EDTA	35
15	-	CaCl ₂ + EDTA	40
16	-	NaCl + EDTA	30
17	-	KCl + EDTA	40
18	-	-	6

Reaction conditions: 25 μ M catalyst, 12.5 μ M Sav, 2.5 mM Sub **19**, acetate buffer (pH 4), 37 °C.

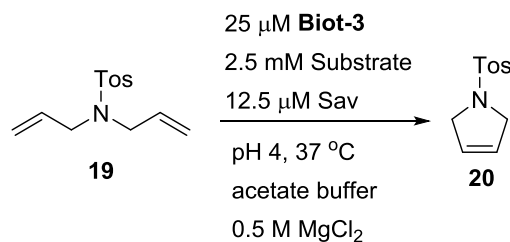
4.4.6 Catalysis in the Periplasm of *E. coli* with Biot-3

In a first attempt, catalysis was performed within *E. coli* with varying degrees of success. The reducing environment of the cytoplasm, where Sav is expressed and localized, is not ideal for catalysis. Indeed, we hypothesize that the presence of millimolar concentrations of glutathione irreversibly inhibits catalysis. Additionally,

the complexity of metabolites and proteins present in the cytoplasm further complicates catalysis. Consequently, the bacteria were genetically modified to secrete all Sav into the periplasmic space, found between the inner cell wall and the outer membrane in gram-negative bacteria. The periplasm contains far fewer molecules than the cytoplasm and the oxidising environment ensures that most thiols are present as disulphides. To test the activity of biotinylated catalysts in cellular media, Markus Jeschek from ETH Zurich engineered *E. coli* strains to secrete streptavidin into the periplasm after expression.

E. Coli cells (strain BL21(DE3)-pET30-T7sav-OmpA) were grown at 37°C, 200 rpm in TP media (137 mM NaCl, 1.5% yeast extract, 2% tryptone, 2% Na₂HPO₄ stock solution (457 mM) and 1% KH₂PO₄ stock solution (735 mM) in deionised water) with kanamycin (50 mg/mL stock, final concentration 50 µg/mL) overnight. A fresh batch of sterilised TP medium was inoculated with the preculture to OD₆₀₀ 0.05, kanamycin (50 mg/mL stock, final concentration 50 µg/mL) was added and the culture incubated at 37°C, 200 rpm for 2 hours. The temperature of the incubator was reduced to 23°C and the cells incubated for a further hour. Isopropyl β-D-thiogalactopyranoside (IPTG, 50 mM stock, final concentration 50 µM) was added and the cells incubated at 23°C, 200 rpm for 5 hours. The cells were harvested by centrifugation (4600g, 10 mins). The biotinylated catalyst (25 µM) was incubated with the cell pellets for 30 minutes at 37 °C. After that, cell pellets were washed with the washing buffer two times and then centrifuged (4600g, 10 mins). The cell pellets were resuspended in reaction buffer (acetate buffer, pH 4, 0.5M MgCl₂). The substrate was added and stirred for overnight under air at 37°C.

We tested diallyl *N*-tosylamide **19** (2.5 mM) for RCM in the periplasm of *E. coli* with 25 µM **Biot-3** catalyst (1 mol%) in acetate buffer at pH 4. With WT and S112A mutant, we were able to achieve 2% yield which corresponds to only 2 TON (Table 4.4), whereas S112A-K121N failed to give any product. The empty vector also gave 2% yield. Yield was measured in reverse phase HPLC. All reactions were performed in duplicate.

Table 4.4 RCM reactions of diallyl tosylamide **19** in cell

Entry	Cell	TON
1	Empty	2
2	WT	2
3	S112A	2
4	S112A-K121N	0
5	No cell, only medium	0

4.5 Conclusion

In this study, a series of biotinylated ruthenium-based catalysts were synthesized and their activity was evaluated for two model RCM reactions with either diallyl tosylamide **19** or the umbelliferone precursor **24**. While all biotinylated catalysts performed reasonably well in concentrated dichloromethane, their performance decreased significantly in aqueous solution. In our opinion, the decreased stability of the biotinylated catalysts in aqueous solutions can play a key role. In organic solvent, the high reaction rate and the slow catalyst decomposition make it possible to obtain the desired products with average to good yields. In aqueous solvents however, catalyst decomposition is faster¹¹ and **20** and **25** were only obtained in low yield. For umbelliferone precursor **24**, modest to good conversions were observed in dichloromethane. In stark contrast, RCM in water does not proceed. In the context of artificial metalloenzyme design, this substrate, which upon RCM yields the fluorescent umbelliferone **25**, lead to significant improvement in conversion by

generating a hydrophobic pocket which might shield the substrate-catalyst complex from water. After performing RCM inside the protein, we moved to the next development step and performed RCM inside the periplasm of *E.coli* to avoid the laborious protein purification process. In order to improve the activity, we rely on high throughput screening. Currently we are investigating the method for high throughput screening and directed evolution in close collaboration with Prof. Sven Panke, ETH Zurich.

4.6 References

- (1) Fürstner, A. *Science* **2013**, *341*, 1229713.
- (2) Occhipinti, G.; Hansen, F. R.; Törnroos, K. W.; Jensen, V. R. *J. Am. Chem. Soc.* **2013**, *135*, 3331.
- (3) Luján, C.; Nolan, S. P. *Catal. Sci. Technol.* **2012**, *2*, 1027.
- (4) Kress, S.; Blechert, S. *Chem. Soc. Rev.* **2012**, *41*, 4389.
- (5) Ohlmann, D. M.; Tschauder, N.; Stockis, J.-P.; Goossen, K.; Dierker, M.; Goossen, L. J. *J. Am. Chem. Soc.* **2012**, *134*, 13716.
- (6) Miao, X.; Fischmeister, C.; Dixneuf, P. H.; Bruneau, C.; Dubois, J.-L.; Couturier, J.-L. *Green Chem.* **2012**, *14*, 2179.
- (7) Miao, X.; Malacea, R.; Fischmeister, C.; Bruneau, C.; Dixneuf, P. H. *Green Chem.* **2011**, *13*, 2911.
- (8) Rybak, A.; Fokou, P. A.; Meier, M. A. R. *Eur. J. Lipid Sci. Technol.* **2008**, *110*, 797.
- (9) Lin, Y. A.; Chalker, J. M.; Davis, B. G. *J. Am. Chem. Soc.* **2010**, *132*, 16805.
- (10) Lin, Y. A.; Chalker, J. M.; Floyd, N.; Bernardes, G. J. L.; Davis, B. G. *J. Am. Chem. Soc.* **2008**, *130*, 9642.
- (11) Binder, J. B.; Blank, J. J.; Raines, R. T. *Org. Lett.* **2007**, *9*, 4885.
- (12) Skowerski, K.; Szczepaniak, G.; Wierzbička, C.; Gułajski, Ł.; Bieniek, M.; Grela, K. *Catal. Sci. Technol.* **2012**, *2*, 2424.

- (13) Lipshutz, B. H.; Ghorai, S.; Leong, W. W. Y.; Taft, B. R.; Krogstad, D. V. *J. Org. Chem.* **2011**, *76*, 5061.
- (14) Lo, C.; Ringenberg, M. R.; Gnanndt, D.; Wilson, Y.; Ward, T. R. *Chem. Commun.* **2011**, *47*, 12065.
- (15) Mayer, C.; Gillingham, D. G.; Ward, T. R.; Hilvert, D. *Chem. Commun.* **2011**, *47*, 12068.
- (16) Philippart, F.; Arlt, M.; Gotzen, S.; Tenne, S.-J.; Bocola, M.; Chen, H.-H.; Zhu, L.; Schwaneberg, U.; Okuda, J. *Chem. Eur. J.* **2013**, *19*, 13865.
- (17) Matsuo, T.; Imai, C.; Yoshida, T.; Saito, T.; Hayashi, T.; Hirota, S. *Chem. Commun.* **2012**, *48*, 1662.
- (18) Zhao, J.; Kajetanowicz, A.; Ward, T. R. *Org. Biomol. Chem.* **2015**, *13*, 5652.
- (19) Sauer, D. F.; Bocola, M.; Broglia, C.; Arlt, M.; Zhu, L.-L.; Brocker, M.; Schwaneberg, U.; Okuda, J. *Chem. Asian J.* **2015**, *10*, 177.
- (20) Ward, T. R. *Acc. Chem. Res.* **2011**, *44*, 47.
- (21) Reetz, M. T.; Peyralans, J. J.-P.; Maichele, A.; Fu, Y.; Maywald, M. *Chem. Commun.* **2006**, *41*, 4318.
- (22) Rusbandi, U. E.; Lo, C.; Skander, M.; Ivanova, A.; Creus, M.; Humbert, N.; Ward, T. R. *Adv. Synth. Catal.* **2007**, *349*, 1923.
- (23) Letondor, C.; Humbert, N.; Ward, T. R. *Proc. Natl. Acad. Sci. U. S. A.* **2005**, *102*, 4683.
- (24) Pierron, J.; Malan, C.; Creus, M.; Gradinaru, J.; Hafner, I.; Ivanova, A.; Sardo, A.; Ward, T. R. *Angew. Chem. Int. Ed.* **2008**, *47*, 701.
- (25) Hyster, T. K.; Knörr, L.; Ward, T. R.; Rovis, T. *Science* **2012**, *338*, 500.
- (26) Pordea, A.; Creus, M.; Panek, J.; Duboc, C.; Mathis, D.; Novic, M.; Ward, T. R. *J. Am. Chem. Soc.* **2008**, *130*, 8085.
- (27) Köhler, V.; Mao, J.; Heinisch, T.; Pordea, A.; Sardo, A.; Wilson, Y. M.; Knörr, L.; Creus, M.; Prost, J.-C.; Schirmer, T.; Ward, T. R. *Angew. Chem. Int. Ed.* **2011**, *50*, 10863.
- (28) Kajetanowicz, A.; Chatterjee, A.; Reuter, R.; Ward, T. R. *Catal. Lett.* **2013**, *144*, 373.

- (29) Binder, J. B.; Raines, R. T. *Curr. Opin. Chem. Biol.* **2008**, *12*, 767.
- (30) Jean-Louis Hérisson, P.; Chauvin, Y. *Die Makromol. Chemie* **1971**, *141*, 161.
- (31) Grubbs, R. H.; Burk, P. L.; Carr, D. D. *J. Am. Chem. Soc.* **1975**, *97*, 3265.
- (32) Sanford, M. S.; Love, J. A.; Grubbs, R. H. *J. Am. Chem. Soc.* **2001**, *123*, 6543.
- (33) Köhler, V.; Wilson, Y. M.; Dürrenberger, M.; Ghislieri, D.; Churakova, E.; Quinto, T.; Knörr, L.; Häussinger, D.; Hollmann, F.; Turner, N. J.; Ward, T. R. *Nat. Chem.* **2013**, *5*, 93.
- (34) Ledoux, N.; Allaert, B.; Pattyn, S.; Vander Mierde, H.; Vercaemst, C.; Verpoort, F. *Chem. Eur. J.* **2006**, *12*, 4654.
- (35) Roche, S. P.; Teyssot, M.-L.; Gautier, A. *Tetrahedron Lett.* **2010**, *51*, 1265.
- (36) Xu, G.; Gilbertson, S. R. *Org. Lett.* **2005**, *7*, 4605.
- (37) Trnka, T. M.; Morgan, J. P.; Sanford, M. S.; Wilhelm, T. E.; Scholl, M.; Choi, T.-L.; Ding, S.; Day, M. W.; Grubbs, R. H. *J. Am. Chem. Soc.* **2003**, *125*, 2546.
- (38) Nicolaou, K. C.; Pfefferkorn, J. A.; Roecker, A. J.; Cao, G.-Q.; Barluenga, S.; Mitchell, H. J. *J. Am. Chem. Soc.* **2000**, *122*, 9939.
- (39) Schmidt, B.; Krehl, S. *Chem. Commun.* **2011**, *47*, 5879.
- (40) Binder, J. B.; Guzei, I. A.; Raines, R. T. *Adv. Synth. Catal.* **2007**, *349*, 395.
- (41) Connon, S. J.; Rivard, M.; Zaja, M.; Blechert, S. *Adv. Synth. Catal.* **2003**, *345*, 572.
- (42) Lipshutz, B. H.; Ghorai, S.; Aguinaldo, G. T. *Adv. Synth. Catal.* **2008**, *350*, 953.
- (43) Brendgen, T.; Fahlbusch, T.; Frank, M.; Schühle, D. T.; Seßler, M.; Schatz, J. *Adv. Synth. Catal.* **2009**, *351*, 303.
- (44) Diallo, A. K.; Boisselier, E.; Liang, L.; Ruiz, J.; Astruc, D. *Chem. Eur. J.* **2010**, *16*, 11832.
- (45) Gawin, R.; Czarnecka, P.; Grela, K. *Tetrahedron* **2010**, *66*, 1051.

CHAPTER 5

*An Asymmetric C–H Activation Reaction
Catalyzed by an Artificial Benzannulase Using
Unpurified Protein Samples*

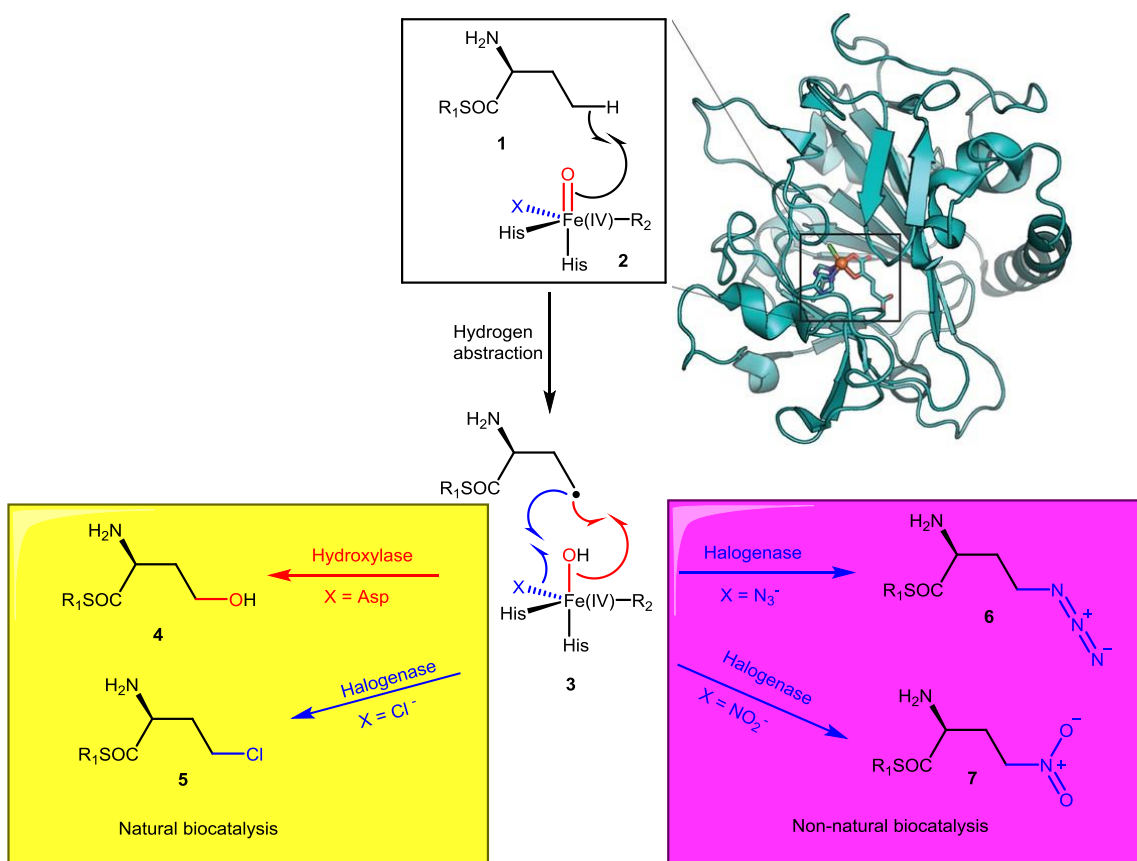
5.1 Introduction

During the past decade, catalyzed C–H bond activation reactions have emerged as attractive tools for atom- and step-economical C–C and C–heteroatom bond forming processes.^{1–5} Unactivated C–H bonds possess high bond dissociation energies (BDE), and their pK_a values range from 41 to 51, as estimated in aqueous solutions,⁶ or from 41 to 56, as measured in DMSO.⁷ Representative examples of typical unactivated hydrocarbons include benzene ($pK_a \sim 43$,⁶ BDE $\approx 474 \text{ kJmol}^{-1}$)⁸, methane ($pK_a \sim 48$,⁶ BDE $\approx 440 \text{ kJmol}^{-1}$)⁸ or ethane ($pK_a \sim 50$,⁶ BDE $\approx 465 \text{ kJmol}^{-1}$)⁸. C–H bonds are generally unreactive; however, there are several methods for activating and functionalizing C–H bonds. For over a century, it has also been known that transition metals can mediate or catalyze C–H functionalization reactions.^{9–15} For organic chemists, this is of particular interest because of the diverse reactivity of different transition metals and the coordination environment around the metal. The selectivity and reactivity can thus be finely tuned through ligand design.

5.1.1 Biocatalysts for C–H Activation

In nature, C–N bonds are typically formed through the transamination of carbonyl substrates. A compelling synthetic strategy, the direct catalytic amination of C–H bonds, is an example where biological variations are almost entirely absent. Matthews et al.¹⁶ took a step toward filling this gap by demonstrating that a bacterial aliphatic halogenase SyrB2 **2** can be coaxed to install nitrogenous anions in place of unactivated aliphatic C–H bonds **1**, generating C–N bonds **6–7** through chemistry not previously observed in nature (Scheme 5.1).

Arnold and coworkers^{17,18} showed that cytochrome P450s can access metallocarbenoid and nitrenoid insertion reactions when provided with non-natural diazoacetate and sulfonazide reagents. This is an example of bio-catalytic C–H bond functionalization which had not previously been observed in Nature.



Scheme 5.1 Repurposing an iron-dependent halogenase into a C–N bond forming enzyme. In the native enzyme, the carbon-based radical recombines with an iron-bound hydroxide (hydroxylase) or chloride (halogenase) to afford an hydroxylase (X = Asp) or an halogenase (X = Cl⁻) (yellow box). Substituting the chloride ligand in halogenase SyrB2 (structure shown; PDB code 2FCT) with the nitrogenous anions (i.e. N₃⁻ or NO₂⁻) results in C-N bond coupling reactions not previously observed in nature (purple box). R₁ = SyrB1 carrier protein; R₂ = carboxylate substrate.¹⁹

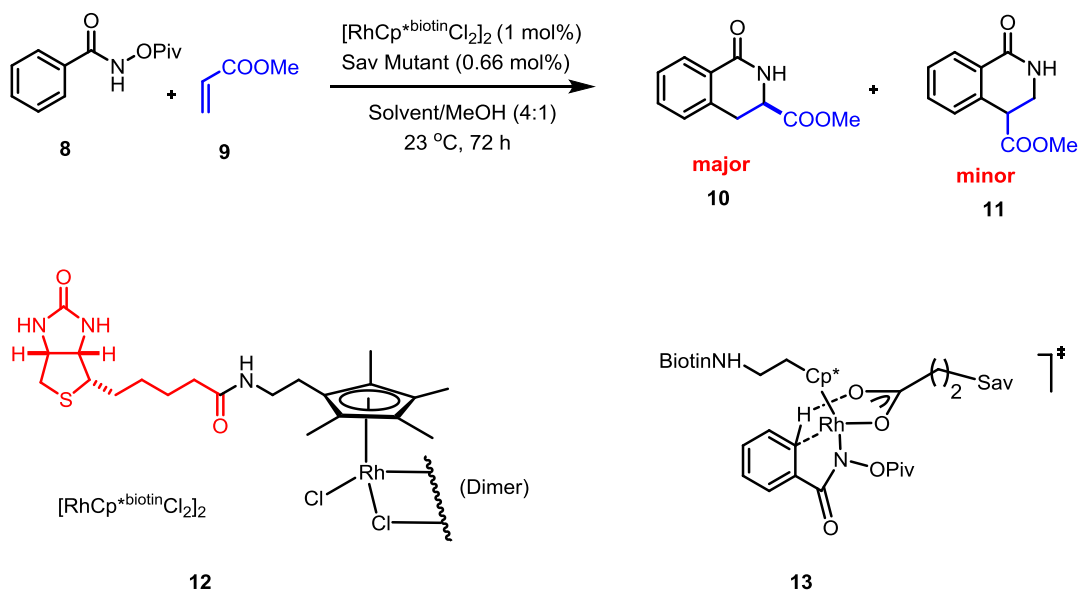
5.1.2 Biotin-(strept)avidin Artificial Metalloenzyme Technology

The cleavage of unactivated C–H bonds is one of the most challenging reactions chemistry. Metalloenzymes can efficiently perform these transformations with exquisite selectivity. Metalloenzymes based on the biotin-(strept)avidin artificial metalloenzyme have been developed in the Ward group to effect a C–H activation

ultimately leading to benzannulated products.²⁰ The biotin-(strept)avidin system was selected thanks to the affinity of biotin for streptavidin ($K_a = 10^{14}$ L/mol). Importantly, derivatization of the valeric acid side chain of biotin does not significantly decrease the affinity, thus allowing to exploit this anchoring strategy to ensure localization of a biotinylated metal cofactor within streptavidin. (Strept)avidin is a 16.1 kDa protein expressed by *Streptomyces Avidinii*. The secondary structure of the homotetrameric protein consists mainly of anti-parallel β -sheets assemble into β -barrels.²¹ Biotin binds inside the β -barrel with the carboxylate residue pointing towards the surface of the biotin-binding vestibule. The tetramer binds four equivalents of biotin, with two of the biotin moieties sitting within 18-19 Å (distance between two carboxylate oxygen atoms) of one another. This protein has been particularly popular in the field of biotechnology thanks to its high affinity for substrates bearing a biotin anchor.²² Furthermore, the protein has exceptional stability at high temperatures ($T_m = 112.2$ °C fully ligated in phosphate buffer or $T_m = 75.5$ °C unligated in phosphate buffer) and organic solvents.²³

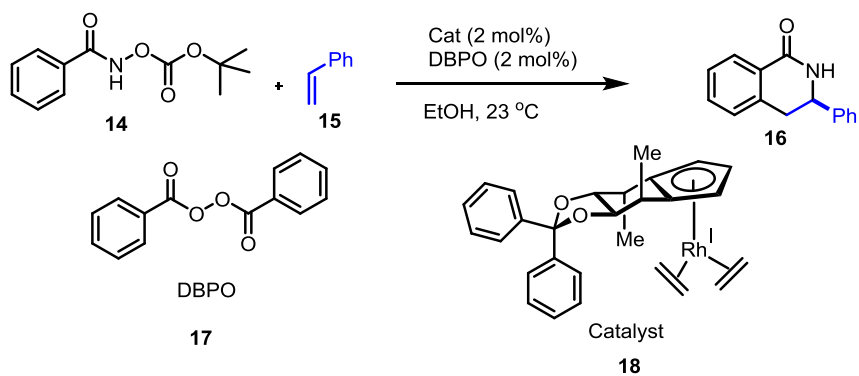
5.1.3 Prior Works

Hyster *et. al.* reported in 2012 the creation of a bifunctional artificial metalloenzyme in which a glutamic acid or aspartic acid residue engineered into streptavidin acts in concert with a docked biotinylated rhodium(III) complex **12** to enable catalytic asymmetric C–H activation (Scheme 5.2).²⁰ The coupling of benzamides **8** and alkenes **9** to access dihydroisoquinolones **10**, **11** proceeded with up to nearly a 100-fold rate acceleration compared with the activity of the isolated rhodium complex. Enantiomeric ratios (er hereafter) up to er 93:7 were obtained.



Scheme 5.2 Synthesis of dihydroisoquinolones **10**, **11** via C–H activation. Catalyst precursor **12** and postulated transition state **13** for the rate determining C–H activation step.

In a related report (using a traditional organometallic catalyst), Cramer and coworkers developed the use of chiral cyclopentadienyl ligands **18** for the Rh(III) catalyzed synthesis of isoquinolones **16** (Scheme 5.3).²⁴ Cramer used a tartrate-based ligand and obtained excellent levels of enantioselectivity with sterically bulky alkenes.



Scheme 5.3 Concurrent work by the Cramer group.

5.2 Aim of the Project

Rhodium (III) complexes bearing Cp-ligands proved highly enantioselective catalysts for directed C–H bond functionalization of hydroxamic acid derivatives.^{25–28} Previous work²⁰ proved that high levels of both selectivity and reactivity could be achieved by an artificial metalloenzyme by genetically engineering a basic carboxylate residue in proximity of the metal center. Our current efforts were centered on the asymmetric C–H activation in the presence of cellular extracts. The aims of the project were following.

- ❖ Neutralize detrimental Glutathione (GSH)
- ❖ Ensure access of both the substrate and the catalyst in the periplasm of *E. coli*
- ❖ Identify a buffer compatible with both cells and the reaction conditions
- ❖ Develop a suitable screening method

5.3 Outline of the Project

In a first attempt, we set out to adapt the artificial benzannulase for catalysis using unpurified Sav samples. Purification of Sav isoforms is the bottleneck of the entire optimization process: Screening unpurified protein samples would allow to significantly decrease the screening time from 21 days (for purified Sav samples) to 8 days (unpurified samples). To address this challenge, five different approaches were investigated.

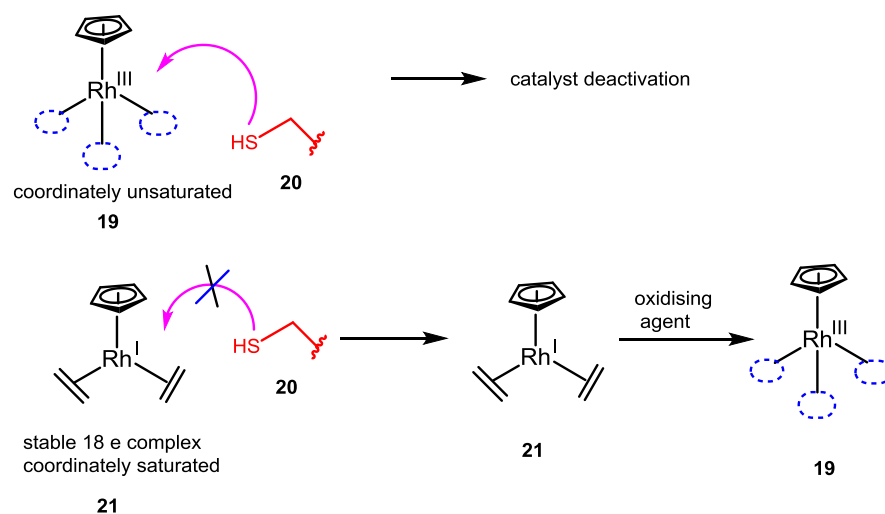
Firstly, since Rh(III) catalyst **19** is coordinately unsaturated, there is high probability to nucleophilic attack at the metal by GSH **20**, resulting in deactivation of the catalyst. To circumvent this challenge we set out to test a coordinately saturated Rh(I) precursor complex **21** eventually minimizing GSH attack (Scheme 5.4).

Secondly, Wilson *et al.* have shown that various Michael acceptors and oxidizing agents may neutralize the detrimental effect of GSH on precious metal catalyst.²⁹

Thirdly, we synthesized different precatalysts that may better tolerate the complex cellular extracts.

Fourthly, we considered testing catalysis with semipurified Sav.

Finally, we tested an imino-biotin bead batch purification to isolate Sav from cellular extracts at pH 9.

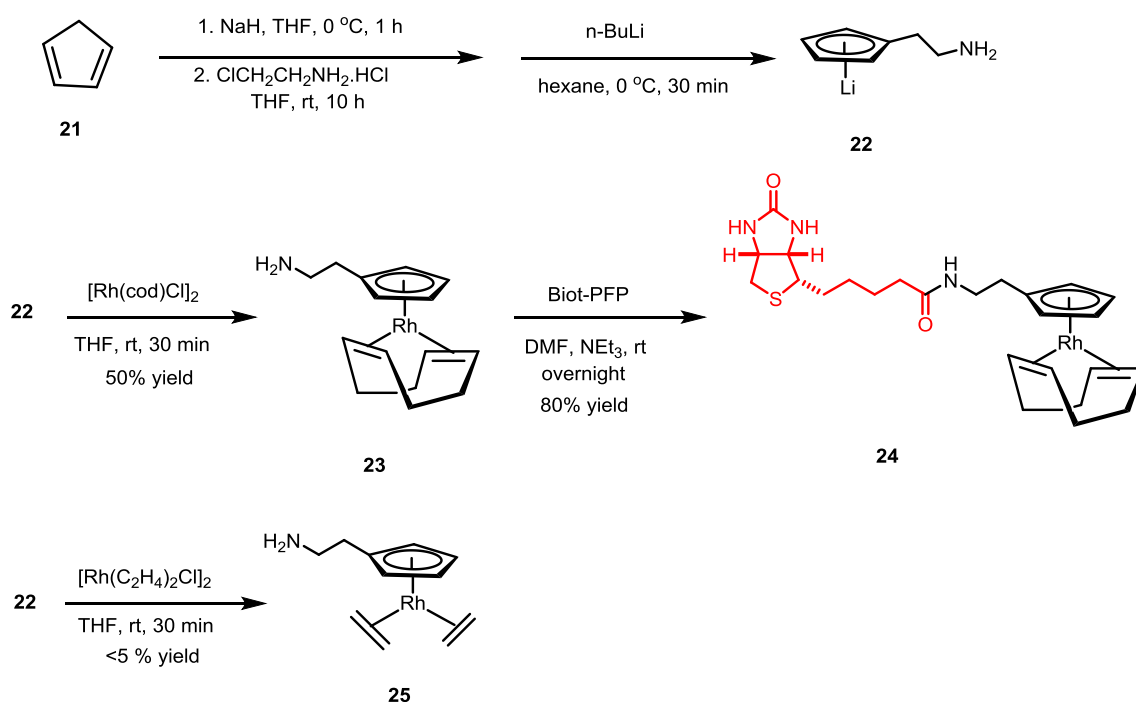


Scheme 5.4 Coordinately unsaturated{CpRh(III)} **19** vs. coordinately saturated{CpRh(I)} **21** catalyst precursors to avoid GSH attack

5.4 Results and Discussion

Inspired by Cramer's report, we synthesized a biotinylated Rh(I) complex **24** bearing a cyclopentadiene (Cp) and a cyclooctadiene (cod) ligand as an artificial cofactors with the objective of catalyzing C-H activation to form dihydroisoquinolones. The Cp and cod ligands bind to the Rh metal with η^5 - and η^4 -coordination modes respectively, Scheme 5.5. Cracking dicyclopentadiene led to its monomer **21**. Upon deprotonation by NaH and addition of [ClCH₂CH₂NH₂·HCl] in

THF led to $[C_5H_5CH_2CH_2NH_2]$ which was converted to $Li[C_5H_5CH_2CH_2NH_2]$ **22** via the dropwise addition of *n*-BuLi in hexane at 0 °C under argon. Addition of $[Rh(cod)Cl]_2$ in THF afforded the Rh(I) complex **23** which was isolated in 50 % overall yield. Biotin conjugation was achieved by addition of biotin-pentafluorophenyl ester (biot-PFP) in DMF in the presence of NEt_3 , Scheme 5.5. With the aim of introducing more labile ligands, the synthesis of the corresponding bis ethylene complex **25** was attempted. Unfortunately, all attempts were vain as only <5% could be isolated.



Scheme 5.5 Synthesis of Rh(I) complex.

Previous work in the group revealed that water-methanol (or acetate-methanol) mixtures were most efficient.²⁰ We thus selected these solvent mixtures for Rh(I) complex (0.5 mM) using *O*-pivaloyl benzhydroxamic acid **8** (50 mM) and methyl acrylate **9** (50 mM) as substrate. As reported by Cramer, we used dibenzoylperoxide **17** (0.5 mM) for the *in-situ* oxidation of the Rh(I) to Rh(III). The activity with or without Sav was found to be nearly identical: 4 TON (Table 5.1).

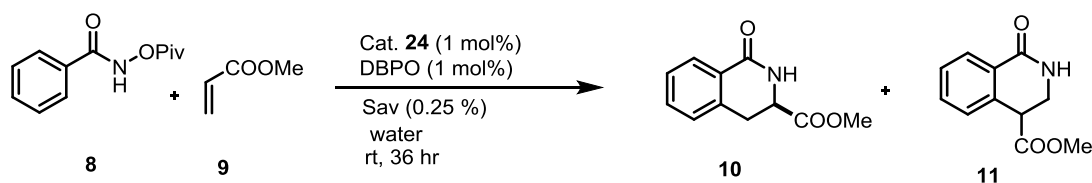
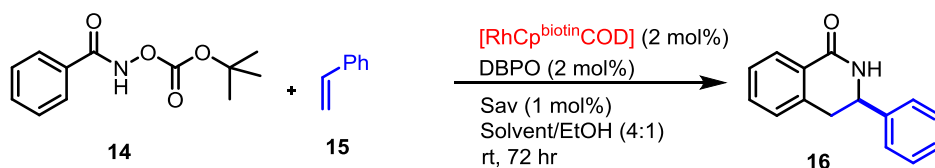


Table 5.1 Synthesis of the dihydroisoquinolones **10** (major) via C–H activation.^a

Entry	Protein	Solvent/MeOH (4:1)	Conversion (%)
1	-	Acetate buffer	4
2	-	water	4
3	Sav WT	Acetate buffer	4
4	Sav WT	water	4

^a [Sub] = 50 mM, [**24**] = 0.5 mM, [DBPO] = 0.5 mM, reaction volume = 200 μ L

We speculated that the system reported by Cramer may not be suitable for the substrates **8**, **9** that we had been testing. Indeed, Cramer focused on styrene **15** (rather than acrylic acid derivatives **9**) and benzamides containing carbonate **14** (rather than an ester **8**) as internal oxidant. We thus tested catalyst **24** (1 mM) with **14** and **15** (50 mM) as substrates. Under these conditions, we obtained 4 % conversion using 20 % MeOH in acetate buffer or water. Upon increasing the amount of organic solvent (from 20% to 50%), the conversion increased to 15%, but the product was formed as a racemate (Table 5.2).

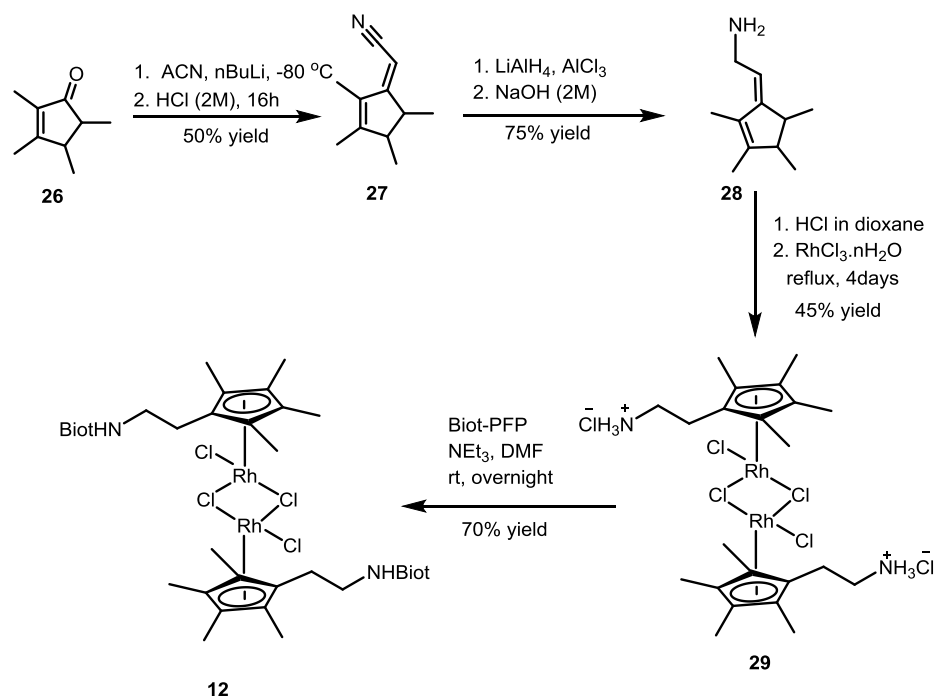
Table 5.2 Synthesis of the dihydroisoquinolones **16** via C–H activation.^a

Entry	Protein	Solvent/MeOH	Solvent/ MeOH	Conv.	er
		(4:1)	(1:1)		
1	-	Acetate buffer	-	4	ND
2	-	water	-	4	ND
3	Sav WT	Acetate buffer	-	4	ND
4	Sav WT	water	-	4	ND
5	Sav WT	-	Acetate buffer	15	50:50
6	Sav WT	-	water	15	54:46

^a [Sub] = 50 mM, [**24**] = 1 mM, [DBPO] = 1 mM, reaction volume = 200 μL . ND = not determined

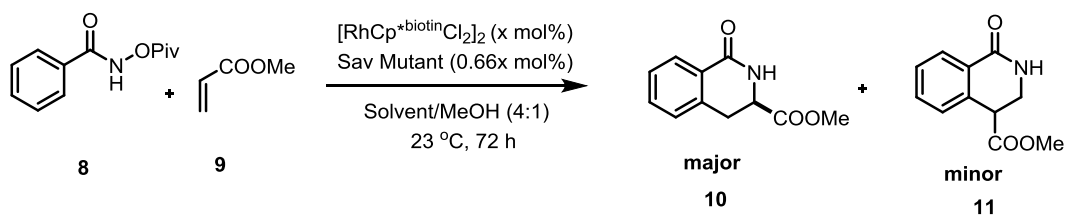
These exploratory results suggest that, under the reaction conditions required for the creation of artificial metalloenzymes, the biotinylated Rh(I) precursor **24** is not an efficient catalyst for the production of dihydroisoquinoline **10** or **16**. We thus selected the Rh(III) complex for further investigation of C–H activation in the presence of unpurified Sav samples.

For the synthesis of the $\{\text{Cp}^*\text{Rh(III)}\}$ complex, the procedure developed by Zimbron was used (Scheme 5.6).³⁰ Treatment of 2,3,4,5-tetramethylcyclopent-2-enone **26** with deprotonated acetonitrile in THF at -80°C afforded the hydroxy intermediate. Upon acidic treatment, dehydration yielded the corresponding exocyclic diene **27**. Reduction followed by complexation with RhCl_3 and coupling with biotin pentafluorophenyl ester yielded the final compound **12**.



Scheme 5.6 Synthesis of biotinylated dirhodium complex **12**.

To perform the C-H functionalization reaction in the cell free extract or in a cellular medium, it is necessary to perform the catalysis at very low catalyst concentration as the Sav concentrations are usually $< 50 \mu\text{M}$. Turning back to the system reported by Hyster (i.e. using the catalyst precursor **12**), we selected *O*-pivaloyl benzhydroxamic acid **8** and methyl acrylate **9** as substrates. While maintaining the same catalyst loading (1 mol%), we decreased the catalyst concentration as well as substrate concentration to identify the lowest concentration that yields detectable product. The result is summarized in Table 5.3. The activity with 0.5 mM and 0.25 mM (entries 1, 2) are same. Further decreasing the catalyst concentration resulted significantly lower TON (entries 3-6).

Table 5.3 Screening of catalyst concentration^a

Entry	Protein	Solvent	Cat. Conc. (μM)	Sub Conc. (mM)	er	TON
1	S112Y-K121E	water	500	50	88:12	90
2	S112Y-K121E	water	250	25	88:12	90
3	S112Y-K121E	water	125	12.5	88:12	54
4	S112Y-K121E	water	60	6	88:12	25
5	S112Y-K121E	water	30	3	88:12	7
6	S112Y-K121E	water	15	1.5	88:12	4

^a Catalyst loading = 1 mol%, reaction volume = 200 μL .

The reaction of *O*-pivaloyl benzhydroxamic acid **8** and methyl acrylate **9** with Rh(III) complex **12** was reported by Hyster to require long reaction time (72 hrs).²⁰ Our screening efforts led to the realization that the reaction is complete in 20 hrs with S112Y-K121E (instead of 72 hours) mutant and in 10 hrs with N118-K121E mutant (Table 5.4). Although good er were obtained, these were systematically lower than those reported by Hyster. Upon longer reaction time, conversion and ee did not change.

Table 5.4 Optimized reaction time for the Rh-catalyzed benzannulation^a

Entry	Protein	Solvent	Time	er	Conv.
1	S112Y-K121E	water	20 hrs	88:12	90
2	N118K-K121E	water	10 hrs	80:20	93

^a [Sub] = 50 mM, [12] = 0.5 mM, 20% MeOH in water, rt, reaction volume = 200 μ L.

Typical Sav production protocols in the group require the presence of MOPS or Tris buffer containing 20 % Sucrose. For cell lysis, 1 mM EDTA is added to prepare cell free extracts. To test the effect of these adjuvants on the artificial benzannulase, pure Sav samples were spiked with Tris (5 mM), sucrose (20%) and EDTA (1 mM) (Table 5.5). The presence of EDTA and Tris completely inhibited catalysis. The presence of sucrose did not inhibit the catalysis at all.

Table 5.5 Effect of cell free extract adjuvants on the performance of the artificial benzannulase.^a

Entry	Protein	Solvent	Adjuvant	er	Conv.
1	S112Y-K121E	water	-	88:12	90
2	S112Y-K121E	water	20 % Sucrose	88:12	90
3	S112Y-K121E	water	5 mM Tris	-	-
4	S112Y-K121E	water	1 mM EDTA	-	-

^a [Sub] = 50 mM, [12] = 0.5 mM, 20% MeOH in water, rt, reaction volume = 200 μ L.

In the context of an artificial metathesase, Markus Jeschek (in the group of Prof. Panke, dbse ethz@basel) developed a Sav production secreted to the periplasm. The key incentive for this effort was the realization that the periplasm is oxidizing,

resulting in the presence of oxidized glutathione (GS—SG). Furthermore, the periplasm contains significantly fewer proteins, thus reducing the potential inhibition of the Rh-catalyst by endogeneous proteins. Isolation and purification of both Sav samples from the cytoplasm and from the periplasm revealed no notable difference between both cytoplasmic and periplasmic Sav. This suggests that the periplasm may be a propitious environment to compartmentalize the artificial benzannulase for *in vivo* screening.

From our result (Table 5.6) it is very clear that there is no functional difference between periplasmic and cytoplasmic streptavidin.

Table 5.6 Cytoplasmic vs. periplasmic Sav.^a

Entry	Protein	Solvent	er	Conv.
1	WT	Acetate buffer	75:25	46
2	Periplasmic Sav	Acetate buffer	75:25	46

^a [Sub **8**] = 50 mM, [**12**] = 0.5 mM, rt, reaction volume = 200 μ L.

We selected Michael acceptors and oxidizing agents known to react with GSH to yield the corresponding thioether and disulfide, respectively. The following Michael acceptors were tested: methyl acrylate **32**, maleinimide **33**, 2-iodo-1-phenylethanone **31**, and 3-phenyl-2-propenenitrile **30**. The following oxidizing agents were selected: oxone **37**, 1,4-benzoquinone **34**, $K_3[Fe(CN)_6]$ **36** and diamide **35**, Figure 5.1. For this purpose, solutions with Sav were spiked with 1.5 mM GSH and incubated overnight in the presence of different concentrations of a particular GSH neutralizing agent before adding the Rh-catalyst **12**. The screening results were summarized in a bubble chart, Figure 5.2.

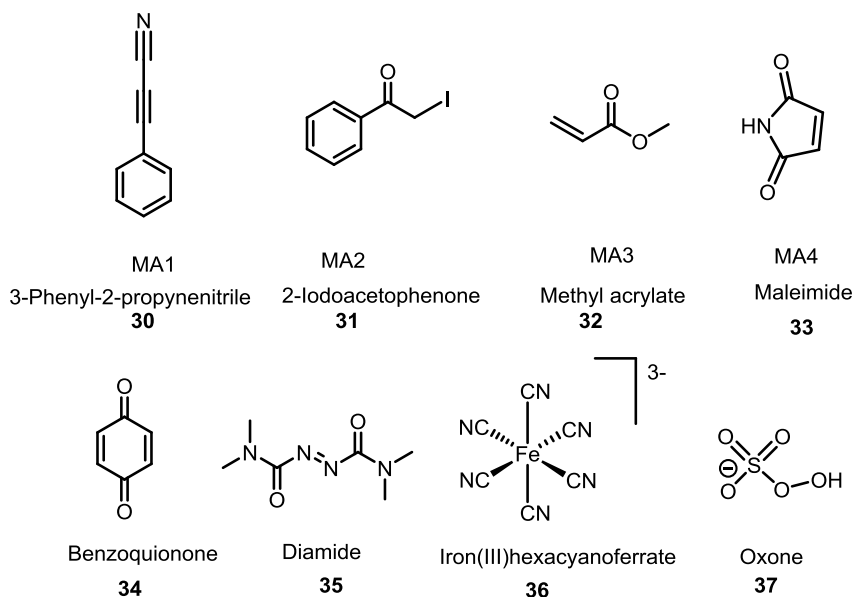


Figure 5.1 Michael acceptors and oxidizing agents used to neutralize the detrimental effect of GSH

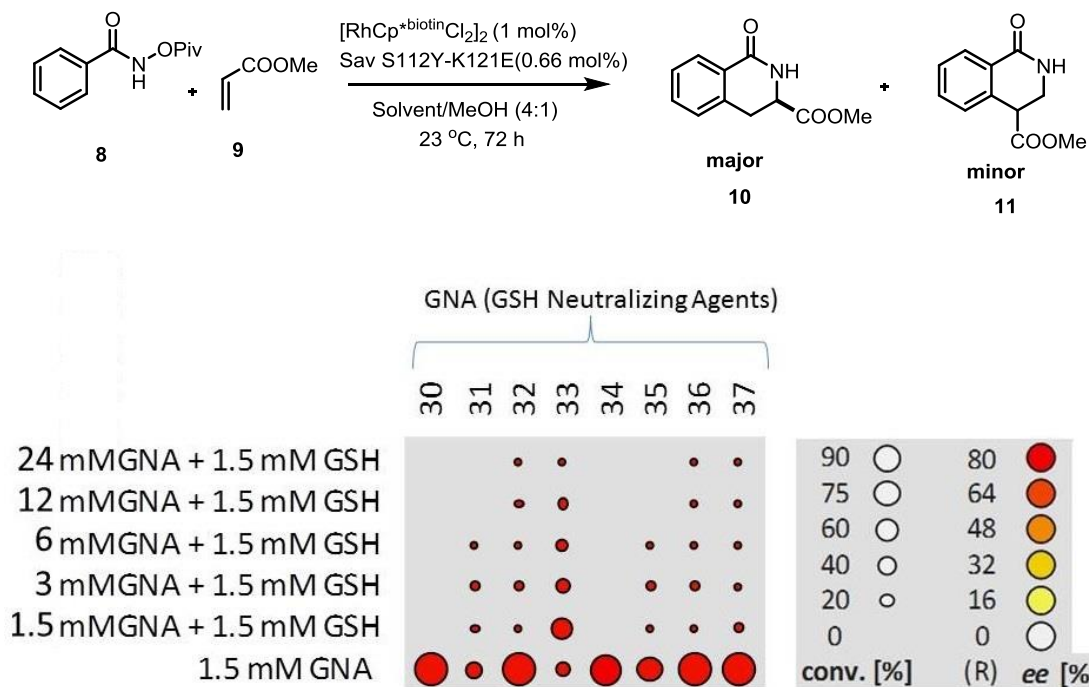
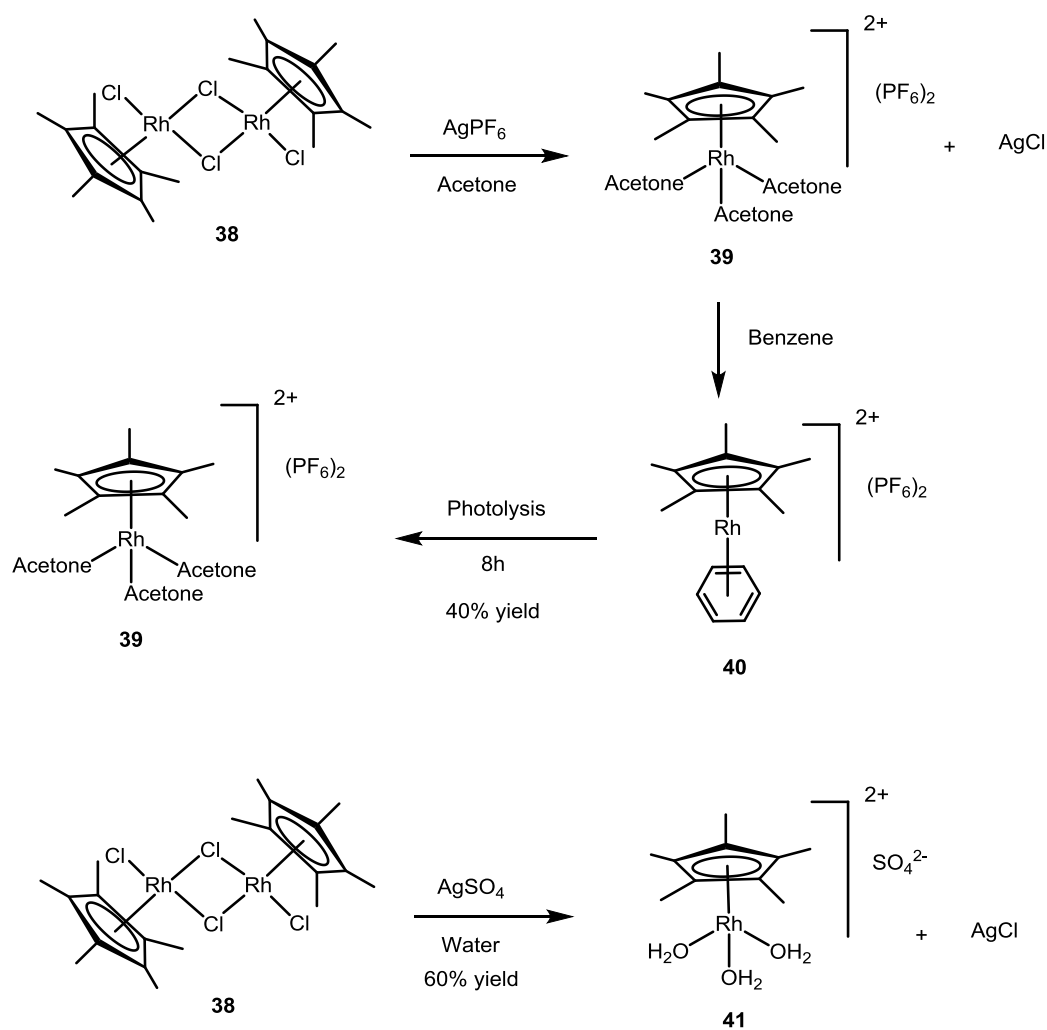


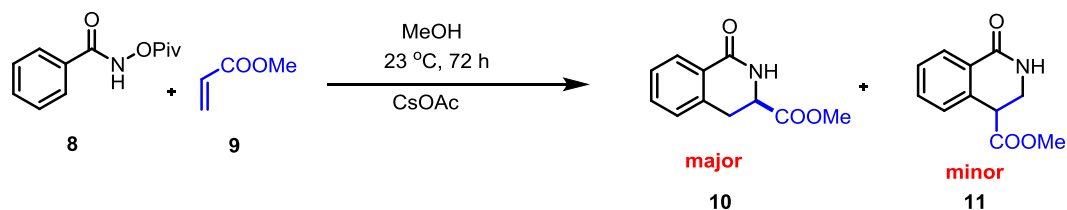
Figure 5.2 Bubble chart results summarizing the screening of Michael acceptors and oxidizing agents (GNA : glutathione neutralizing agent) used to neutralize the detrimental effect of spiked GSH (1.5 mM). The concentration of the neutralizing agent is given. Size of the bubble and intensity of the color correspond to conversion (%) and ee (%) respectively. Reaction conditions: [Sub] = 50 mM, [Cat] = 0.5 mM.

From the result obtained in Figure 5.2, we thus conclude that oxidizing GSH or deriving its thiol function could not prevent inhibition of Rh(III) catalyst.

Finally, new Rh(III) precatalysts were synthesized and tested for their performance as catalyst in the benzannulation. Three different water soluble catalysts **40**, **39** and **41** were prepared according to literature procedures^{31,32} with moderate yield (40 – 60%) (Scheme 5.7). Prior to preparing the biotinylated catalysts, catalysts **40**, **39** and **41** were evaluated for the benzannulation between *O*-pivaloyl benzhydroxamic acid **8** and methyl acrylate **9**, Scheme 5.8.



Scheme 5.7 Synthesis of the Rh(III) precatalysts.



Scheme 5.8 Synthesis of dihydroisoquinolones **10** via C–H activation.

Table 5.7 Precatalyst screening for the synthesis of dihydroisoquinolones **10**.^a

Entry	Catalyst (1 mol%)	Conversion (%)
1	Compound 40	4
2	Compound 39	6
3	Compound 41	6

^a [Sub] = 50 mM, [catalyst] = 0.5 mM, rt, reaction volume = 200 μ L.

From this result (Table 5.7), we conclude that catalysts **41**, **41** and **43** are not suitable precursors for C–H activation reactions.

Having failed in identifying suitable reaction conditions to screen crude cellular extracts containing Sav isoforms, we set out to test affinity purification of Sav using iminobiotin-sepharose beads. For this purpose, cell free extracts containing Sav (400 μ l in PBS buffer) were transferred into a 24 deep-well plates. Iminobiotin binding buffer (1 ml, IB hereafter) was added to each well to adjust the pH \sim 9. The iminobiotin-sepharose beads (100 μ l of a thoroughly shaken suspension prior to pipetting) were added and incubated with rapid shaking (800 rpm, RT, 1 h). The plate was centrifuged (5300 g, 15 min.) and the supernatant was discarded. The beads were resuspended in IB-buffer (1 ml), centrifuged (5300 g, 15 min.) and the supernatant was discarded. This washing step was repeated three times. Next, the thoroughly washed beads were used for catalysis. Those beads were resuspended in acetate buffer

(pH 5.6) and the catalyst and substrates were added. At acidic pH, Sav is released from the iminobiotin-sepharose beads as the guanine moiety is protonated,³³ resulting in an homogeneous ArM. Unfortunately, the conversions remained very modest (4-5 %, corresponding to <10 TON). We hypothesized that at pH 5.6, the Sav remains bound to the iminobiotin-matrix as the guanine moiety is not protonated.

To solve this problem, we performed catalysis in the presence of semi-purified Sav. For that purpose, cell free extracts were subjected to dialysis with guanidinium hydrochloride (6 M, pH 1.5) to remove biotin followed by dialysis in Tris/HCl (20mM, pH 7.4) to neutralize the pH. Dialysis against water to remove the salts yielded a semi-purified Sav. To our delight, good conversions (20 TON) were obtained with this purification protocol for the C-H activation catalyzed by Rh(III) catalyst in this semi purified system. Although TON is improved compared to previous approaches, this process remains time consuming for high-throughput screening purposes.

5.5 Conclusion

In this study we have applied different strategies aiming at performing a C-H activation reaction in cellular extracts. Unfortunately, none of them gave satisfactory result to address this problem. So we speculated that cellular extracts contains something that is coordinating to metal and inhibiting catalysis. The major problem is associated with the catalyst system, which did not allow performing catalysis at the low catalyst concentration (< 0.1 mM).

5.6 References

- (1) Engle, K. M.; Yu, J.-Q. *J. Org. Chem.* **2013**, 78, 8927.
- (2) Collins, K. D.; Glorius, F. *Nat. Chem.* **2013**, 5, 597.
- (3) Kozhushkov, S. I.; Potukuchi, H. K.; Ackermann, L. *Catal. Sci. Technol.* **2013**, 3, 562.

- (4) Mousseau, J. J.; Charette, A. B. *Acc. Chem. Res.* **2013**, *46*, 412.
- (5) Shang, X.; Liu, Z.-Q. *Chem. Soc. Rev.* **2013**, *42*, 3253.
- (6) Smith M.B. *March's Advanced Organic Chemistry, Willey, New York, 7th Edition* **2013**.
- (7) Bordwell, F. G. *Acc. Chem. Res.* **1988**, *21*, 456.
- (8) Blanksby, S. J.; Ellison, G. B. *Acc. Chem. Res.* **2003**, *36*, 255.
- (9) Parshall, G. W. *Acc. Chem. Res.* **1975**, *8*, 113.
- (10) Crabtree, R. H. *Chem. Rev.* **1985**, *85*, 245.
- (11) Arndtsen, B. A.; Bergman, R. G.; Mobley, T. A.; Peterson, T. H. *Acc. Chem. Res.* **1995**, *28*, 154.
- (12) Shilov, A. E.; Shul'pin, G. B. *Chem. Rev.* **1997**, *97*, 2879.
- (13) Dyker, G. *Angew. Chem. Int. Ed.* **1999**, *38*, 1698.
- (14) Labinger, J. A.; Bercaw, J. E. *Nature* **2002**, *417*, 507.
- (15) Jazzar, R.; Hitce, J.; Renaudat, A.; Sofack-Kreutzer, J.; Baudoin, O. *Chem. Eur. J.* **2010**, *16*, 2654.
- (16) Matthews, M. L.; Chang, W.; Layne, A. P.; Miles, L. A.; Krebs, C.; Bollinger, J. M. *Nat. Chem. Biol.* **2014**, *10*, 209.
- (17) Coelho, P. S.; Brustad, E. M.; Kannan, A.; Arnold, F. H. *Science* **2013**, *339*, 307.
- (18) McIntosh, J. A.; Coelho, P. S.; Farwell, C. C.; Wang, Z. J.; Lewis, J. C.; Brown, T. R.; Arnold, F. H. *Angew. Chem. Int. Ed.* **2013**, *52*, 9309.
- (19) Brustad, E. M. *Nat. Chem. Biol.* **2014**, *10*, 170.
- (20) Hyster, T. K.; Knörr, L.; Ward, T. R.; Rovis, T. *Science* **2012**, *338*, 500.
- (21) Hendrickson, W. A.; Pähler, A.; Smith, J. L.; Satow, Y.; Merritt, E. A.; Phizackerley, R. P. *Proc. Natl. Acad. Sci. U. S. A.* **1989**, *86*, 2190.
- (22) Holmberg, A.; Blomstergren, A.; Nord, O.; Lukacs, M.; Lundeberg, J.; Uhlén, M. *Electrophoresis* **2005**, *26*, 501.

- (23) González, M.; Argaraña, C. E.; Fidelio, G. D. *Biomol. Eng.* **1999**, *16*, 67.
- (24) Ye, B.; Cramer, N. *Science* **2012**, *338*, 504.
- (25) Kuhl, N.; Schröder, N.; Glorius, F. *Adv. Synth. Catal.* **2014**, *356*, 1443.
- (26) Lyons, T. W.; Sanford, M. S. *Chem. Rev.* **2010**, *110*, 1147.
- (27) Song, G.; Li, X. *Acc. Chem. Res.* **2015**, *48*, 1007.
- (28) Han, Y.-F.; Jin, G.-X. *Chem. Soc. Rev.* **2014**, *43*, 2799.
- (29) Wilson, Y. M.; Dürrenberger, M.; Nogueira, E. S.; Ward, T. R. *J. Am. Chem. Soc.* **2014**, *136*, 8928.
- (30) Zimbron, J. M.; Heinisch, T.; Schmid, M.; Hamels, D.; Nogueira, E. S.; Schirmer, T.; Ward, T. R. *J. Am. Chem. Soc.* **2013**, *135*, 5384.
- (31) Cayemittes, S.; Poth, T.; Fernandez, M. J.; Lye, P. G.; Becker, M.; Elias, H.; Merbach, A. E. *Inorg. Chem.* **1999**, *38*, 4309.
- (32) White, C.; Thompson, S. J.; Maitlis, P. M. *J. Organomet. Chem.* **1977**, *134*, 319.
- (33) Hofmann, K.; Wood, S. W.; Brinton, C. C.; Montibeller, J. A.; Finn, F. M. *Proc. Natl. Acad. Sci. U. S. A.* **1980**, *77*, 4666.

Chapter 6

Conclusion and Outlook

In this thesis, efforts at developing bio-orthogonal C–C bond forming reactions catalyzed by artificial metalloenzymes based on the biotin (strept)avidin technology are presented. In this study, we have tested three important C-C bond forming reactions – Suzuki cross-coupling, olefin metathesis and C-H activation reactions in the context of bio-orthogonal chemistry.

At the very beginning of the thesis, in Chapter 2, we reviewed recent developments in the palladium catalyzed Suzuki-Miyaura cross-coupling reaction in water. This review covers the period from 2011 to August 2015.

In Chapter 3, we have developed a new artificial Suzukiase incorporating of an electron-rich phosphino-palladium moiety within Sav for the synthesis of enantioenriched binaphthyls (up to 90 % ee and 180 TONs). Importantly, it was shown that the hybrid catalyst offers vast opportunities for chemogenetic optimization of the catalytic performance: site-directed mutagenesis leads to a significant increase in enantioselectivity. Future efforts can be aimed at performing catalytic asymmetric SMC with artificial Suzukiases *in vivo*. Our system may be useful for many synthetic biology and chemical biology applications (red biotechnology). For example vaccine and antibody production, bio-based chemicals, plastics and textiles production etc.

In Chapter 4, we have developed a new artificial metathesase incorporating Hoveyda-Grubbs type catalyst within streptavidin. We also present our efforts to develop the ring closing olefin metathesis *in vivo* using *E. coli* cells. Since our system showed protein acceleration, this may have a high potential for high-throughput screening and directed evolution of artificial metalloenzymes (white biotechnology).

In summary, the studies presented in this thesis provide the great potential of artificial metalloenzymes to complement both homogeneous and enzymatic catalysts.

APPENDIX 1

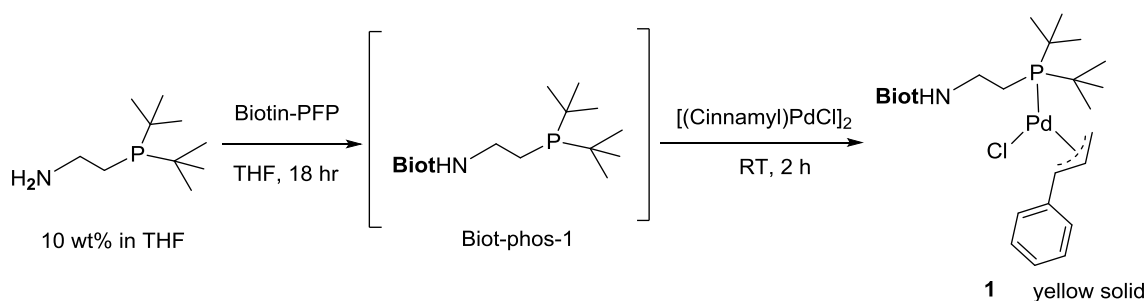
*Enantioselective Artificial Suzukiase for the
Synthesis of Axially Chiral Biaryl Compounds
Relying on the Straptavidin-Biotin Technology*

General: All Chemicals were of reagent grade and used as commercially purchased without further purification. ^1H and ^{13}C spectra were recorded on a Bruker 400 MHz. Chemical shifts are reported in ppm (parts per million). Signals are quoted as s (singlet), d (doublet), t (triplet), brs (broad) and m (multiplet). Analysis of the catalytic runs were performed on an Agilent 1100 normal phase HPLC with an analytical Chiracel OJ-H column ($5\mu\text{m}$, $250 \times 4.6 \text{ mm}$) of Daicel Chemical Ind.

Protein expression and purification:

Native, egg avidin was obtained from Belovo and used without further purification. Recombinant streptavidin isoforms were engineered, expressed, purified and quantified as previously described.¹

Synthesis of biotinylated catalysts:



Scheme 1 Synthesis of complex 1

Complex 1: The Biotin-PFP ester² (200 mg, 0.49 mmol) was set in a schlenk flask. The flask was evacuated and backfilled with nitrogen three times and dry THF was added. The 2-(Di-*t*-butylphosphino)ethylamine (10 wt. % in THF, 1 ml, 0.49 mmol) was added slowly to the suspension. The reaction mixture was stirred at room temperature overnight (18-20 h). Then $[\text{Pd}(\text{cinnamyl})(\mu\text{-Cl})_2]$ (130 mg, 0.25 mmol)

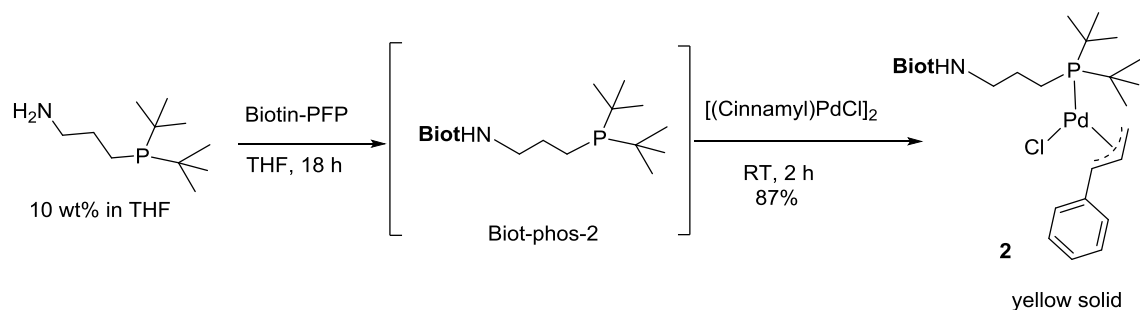
was added to the clear solution and stirred for 2 h at room temperature. After this time, THF was removed under reduced pressure and the crude product was purified by flash chromatography on silica gel (MeOH : CH₂Cl₂ 5:95) to afford the complex **1** as yellow solid (240 mg, 74%).

¹H NMR (400 MHz, CDCl₃): δ = 7.49 (d, J = 7.7 Hz, 2H), 7.42 – 7.29 (m, 3H), 5.88 – 5.72 (m, 1H), 5.23 (dd, J = 13.2, 9.2 Hz, 1H), 5.07 (s, 1H), 4.44 – 4.32 (m, 1H), 4.23 (dd, J = 14.6, 7.5 Hz, 1H), 3.97 (s, 1H), 3.59 (s, 2H), 3.13 (s, 1H), 2.81 – 2.62 (m, 1H), 2.22 – 2.05 (m, 2H), 1.76 – 1.53 (m, 6H), 1.54 – 1.15 (m, 24H).

¹³C NMR (100 MHz, CDCl₃): δ = 173.5, 164.1, 136.5, 128.7, 128.2, 127.9, 108.7, 101.8, 61.7, 60.0, 56.0, 48.1, 40.8, 37.1, 35.8, 30.0, 28.1, 27.8, 25.6, 21.5, 21.4.

³¹P NMR (162 MHz, CDCl₃): δ = 62.3.

HRMS [ESI(+)/TOF]: calculated for C₂₉H₄₇N₃O₂PPdS [M-Cl]⁺ 638.2156; found 638.2172.



Scheme 2 Synthesis of complex **2**

Complex 2: Complex **2** was synthesized following the same procedure used for the synthesis of Complex **1**, using Biotin-PFP ester (90 mg, 0.49 mmol), 3-(Di-*t*-butylphosphino)propylamine (10 wt. % in THF, 0.5 ml, 0.22 mmol) and

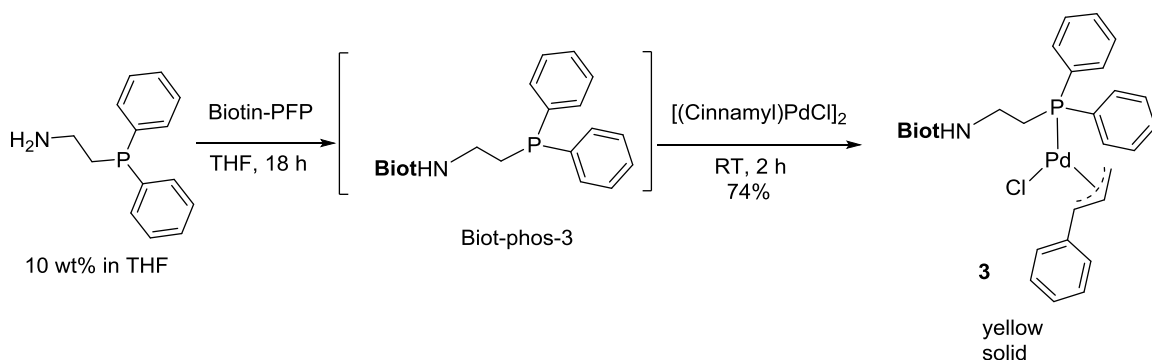
[Pd(cinnamyl)(μ -Cl)]₂ (67 mg, 0.12 mmol). The crude product was purified on silica gel by 5% MeOH/CH₂Cl₂ to yield the title product as yellow solid (140 mg, 87%).

¹H NMR (400 MHz, CDCl₃): δ = 7.58 – 7.30 (m, 5H), 5.89 – 5.67 (m, 1H), 5.38 – 5.24 (m, 1H), 4.88 (d, J = 20.4 Hz, 1H), 4.40 – 4.31 (m, 1H), 4.25 – 4.05 (m, 1H), 3.93 (dd, J = 6.9, 5.4 Hz, 1H), 3.28 (s, 2H), 3.15 (s, 1H), 2.92 (s, 1H), 2.77 – 2.57 (m, 2H), 2.17 (t, J = 7.3 Hz, 2H), 2.12 – 1.82 (m, 4H), 1.79 – 1.46 (m, 6H), 1.44 – 1.11 (m, 20H).

¹³C NMR (100 MHz, CDCl₃): δ = 174.3, 163.6, 136.5, 129.3, 128.8, 128.2, 127.9, 108.9, 103.2, 61.6, 59.9, 55.8, 40.6, 40.5, 35.8, 34.9, 34.8, 30.1, 30.0, 27.8, 25.7, 18.5.

³¹P NMR (162 MHz, CDCl₃): δ = 66.7.

HRMS [ESI(+)]TOF]: calculated for C₃₀H₄₉N₃O₂PPdS [M-Cl]⁺ 652.2312; found 652.2325.



Scheme 3 Synthesis of complex 3

Complex 3: Complex 3 was synthesized following the same procedure used for the synthesis of Complex 1, using Biotin-PFP ester (181 mg, 0.44 mmol), 3-(Di-*t*-butylphosphino)propylamine (10 wt. % in THF, 85 μ l, 0.22 mmol) and

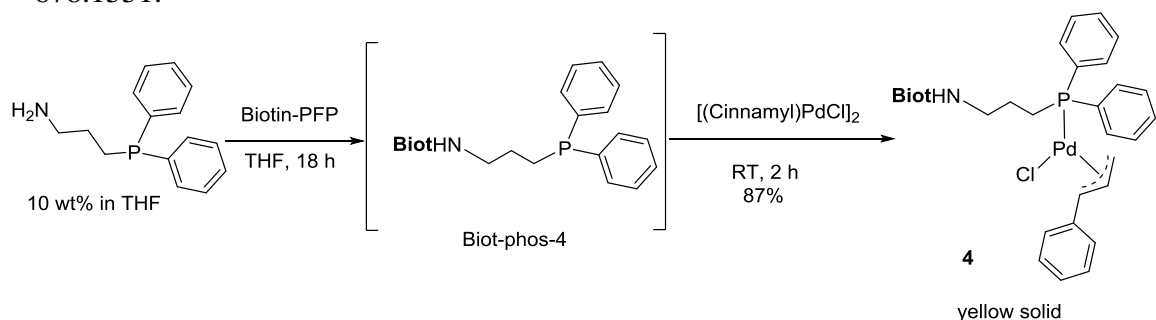
$[\text{Pd}(\text{cinnamyl})(\mu\text{-Cl})_2]$ (67 mg, 0.12 mmol). The crude product was purified on silica gel by 5% MeOH/ CH_2Cl_2 to yield the title product as yellow solid (140 mg, 87%).

^1H NMR (400 MHz, CDCl_3): δ = 7.63 – 7.28 (m, 18H), 6.18 (s, 1H), 5.99 (dt, J = 13.2, 9.4 Hz, 2H), 5.40 – 5.19 (m, 2H), 4.44 – 4.31 (m, 1H), 4.29 – 4.17 (m, 1H), 3.49 (dd, J = 16.3, 6.0 Hz, 2H), 3.31 – 2.94 (m, 1H), 2.76 (s, 2H), 1.93 (t, J = 7.3 Hz, 2H), 1.75 (s, 2H), 1.63 – 1.36 (m, 3H), 1.30 (d, J = 6.5 Hz, 2H).

^{13}C NMR (100 MHz, CDCl_3): δ = 173.6, 163.7, 136.2, 132.8, 132.7, 132.6, 130.6, 129.0, 128.9, 128.5, 127.9, 111.5, 100.7, 100.4, 61.4, 59.8, 56.5, 35.6, 28.1, 27.9, 27.8, 27.6, 25.4.

^{31}P NMR (162 MHz, CDCl_3): δ = 18.4.

HRMS [ESI(+)]TOF]: calculated for $\text{C}_{33}\text{H}_{39}\text{N}_3\text{O}_2\text{PPdS}$ $[\text{M}-\text{Cl}]^+$ 678.1530; found 678.1551.



Scheme 4 Synthesis of complex 4

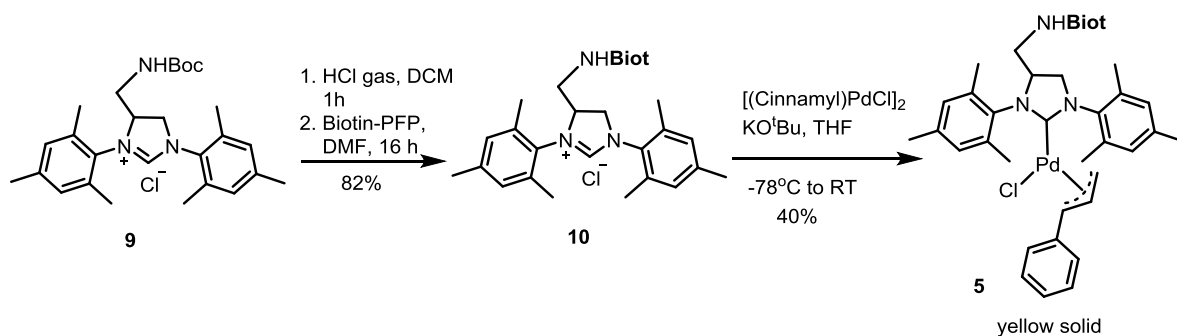
Complex 4: Complex 4 was synthesized following the same procedure used for the synthesis of Complex 1, using Biotin-PFP ester (123 mg, 0.3 mmol), 3-(Di-*t*-butylphosphino)propylamine (10 wt. % in THF, 97 mg, 0.4 mmol) and $[\text{Pd}(\text{cinnamyl})(\mu\text{-Cl})_2]$ (67 mg, 0.12 mmol). The crude product was purified on silica gel by 5% MeOH/ CH_2Cl_2 to yield the title product as yellow solid (140 mg, 87%).

^1H NMR (400 MHz, CDCl_3): δ = 7.63 – 7.29 (m, 15H), 6.19 – 5.83 (m, 3H), 5.43 – 5.26 (m, 1H), 5.16 (s, 1H), 4.34 – 4.19 (m, 1H), 4.20 – 4.06 (m, 1H), 3.26 (s, 4H), 2.76 – 2.36 (m, 3H), 2.18 (t, J = 7.0 Hz, 2H), 1.87 – 1.51 (m, 8H), 1.35 (br, 2H).

^{13}C NMR (100 MHz, CDCl_3): δ = 173.9, 163.5, 137.0, 136.4, 136.3, 132.7, 130.6, 129.2, 128.9, 128.8, 128.5, 128.3, 127.8, 127.7, 111.1, 111.0, 101.0, 100.0, 61.1, 59.6, 54.5, 39.7, 35.8, 27.7, 27.4, 25.5, 25.0, 24.8, 24.1.

^{31}P NMR (162 MHz, CDCl_3): δ = 24.6.

HRMS [ESI(+)-TOF]: calculated for $\text{C}_{34}\text{H}_{41}\text{N}_3\text{O}_2\text{PPdS}$ $[\text{M}-\text{Cl}]^+$ 692.1686; found 692.1703.



Scheme 5 Synthesis of complex 5

Biot-NHC (10): Complex 9 was synthesized according to literature procedure.³ Complex 9 (236 mg, 0.5 mmol) was dissolved in CH_2Cl_2 (2 ml) and HCl gas was bubbled through the solution for 1 hour at room temperature. The gaseous HCl was generated by the dropwise addition of concentrated H_2SO_4 to NH_4Cl . The solution was stirred for 2 hours at room temperature. The deprotection step was monitored by thin-layer chromatography (MeOH/ CH_2Cl_2 1:9). The solvent was evaporated and the

resulting solid was dissolved in DMF (2 ml). Biotin pentafluorophenol (164 mg, 0.4 mmol) and Et₃N (1.4 ml, 10 mmol) was added to the solution and stirred for 16 h at room temperature. The solvent was removed at reduced pressure. The crude product was purified on silica gel by 10% MeOH/CH₂Cl₂ to yield compound **10** as white solid (197 mg, 82%).

¹H NMR (400 MHz, CD₂Cl₂): δ = 9.38 (d, J = 5.3 Hz, 1H), 8.86 (br, 1H), 7.05 – 6.90 (m, 4H), 6.72 (s, 1H), 6.32 (s, 1H), 5.16 (br, 1H), 4.52 (s, 2H), 4.31 (s, 1H), 4.11 (s, 1H), 3.67 (d, J = 42.9 Hz, 1H), 3.32 (d, J = 9.9 Hz, 1H), 3.27 – 3.13 (m, 1H), 2.79 – 2.69 (m, 1H), 2.62 (dd, J = 19.7, 12.8 Hz, 1H), 2.50 – 2.21 (m, 20H), 2.12 (s, 2H), 1.71 – 1.38 (m, 4H).

¹³C NMR (100 MHz, CD₂Cl₂): δ = 174.7, 160.2, 140.9, 140.7, 135.9, 135.8, 135.7, 130.8, 130.7, 130.4, 130.2, 129.7, 129.6, 62.8, 62.2, 62.0, 60.5, 56.3, 56.2, 56.1, 46.2, 40.9, 35.8, 28.5, 28.4, 25.9, 25.6, 21.3, 21.2, 19.2, 18.7, 8.8.

HRMS [ESI(+)]TOF: calculated for C₃₂H₄₄N₅O₂S [M-Cl]⁺ 562.3215; found 562.3212.

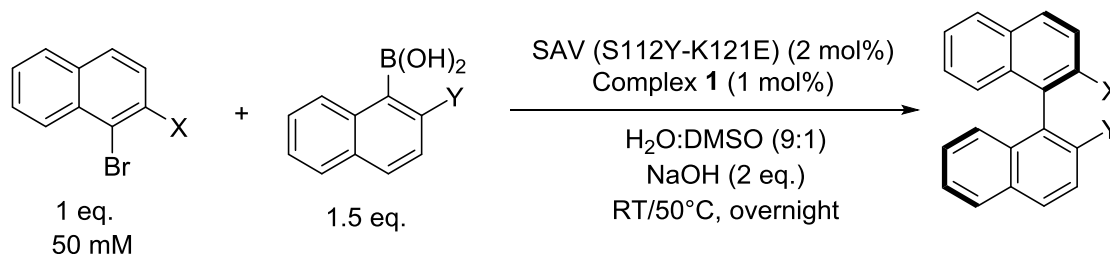
Complex 5: Compound **10** (201 mg, 0.34 mmol), [Pd(cinnamyl)(μ-Cl)]₂ (82 mg, 0.16 mmol) and KO^tBu (38 mg, 0.34 mmol) were set in a schlenk flask. The flask was evacuated and backfilled with nitrogen three times, then 9 ml dry THF was added. The flask was cooled at -78 °C for 1h and then warmed to RT and stirred for another 1h. The solvent was removed under reduced pressure. The crude product was purified on silica gel using 10% MeOH/CH₂Cl₂ to yield compound **5** as yellow solid (52 mg, 40%).

^1H NMR (400 MHz, CD_2Cl_2): δ = 7.36 – 6.90 (m, 9H), 6.49 (s, 1H), 5.83 (s, 1H), 4.94 – 4.68 (m, 1H), 4.54 – 4.31 (m, 2H), 4.17 (d, J = 11.8 Hz, 2H), 4.01 (t, J = 10.7 Hz, 1H), 3.91 – 3.76 (m, 1H), 3.50 (br, 1H), 3.36 – 3.07 (m, 3H), 2.88 (m, 2H), 2.65 (d, J = 8.4 Hz, 1H), 2.55 – 2.20 (m, 18H), 2.15 – 1.98 (m, 3H), 1.75 – 1.42 (m, 6H).

^{13}C NMR (100 MHz, CD_2Cl_2): δ = 209.8, 168.0, 162.1, 145.7, 136.4, 135.1, 127.7, 126.9, 125.9, 125.3, 122.9, 107.6, 89.8, 61.6, 60.3, 58.6, 54.3, 52.8, 45.0, 31.6, 27.1, 27.0, 26.8, 25.3, 24.2, 23.3, 22.5.

HRMS [ESI(+)]TOF]: calculated for $\text{C}_{41}\text{H}_{52}\text{N}_5\text{O}_2\text{PdS}$ [M-Cl] $^+$ 784.2876; found 784.2890.

General procedure for Catalysis on an analytical scale:



Apart from the extraction and the purification of the products everything was carried out in the glove-box using nitrogen-flushed solvents.

A stock solution of Sav (0.20 μmol , 0.02 eq.) in mQ water and the catalyst (0.10 μmol , 0.01 eq.) in DMSO were prepared, added together and stirred for ten minutes at room

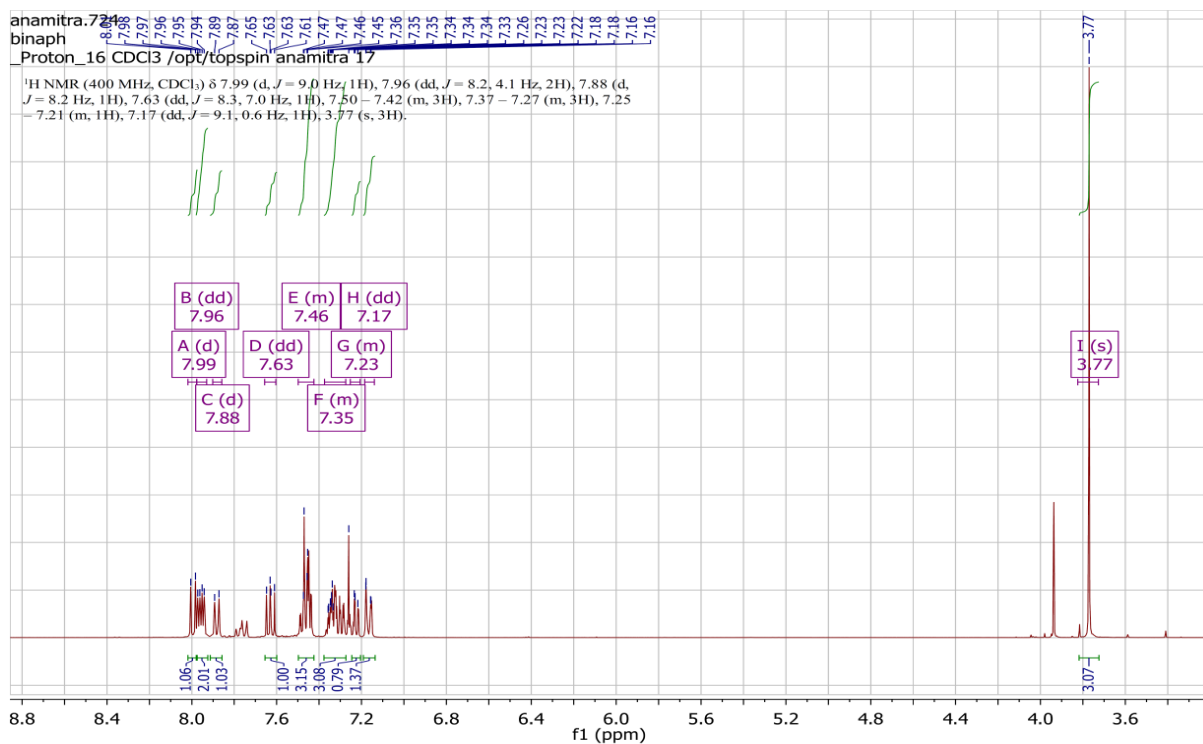
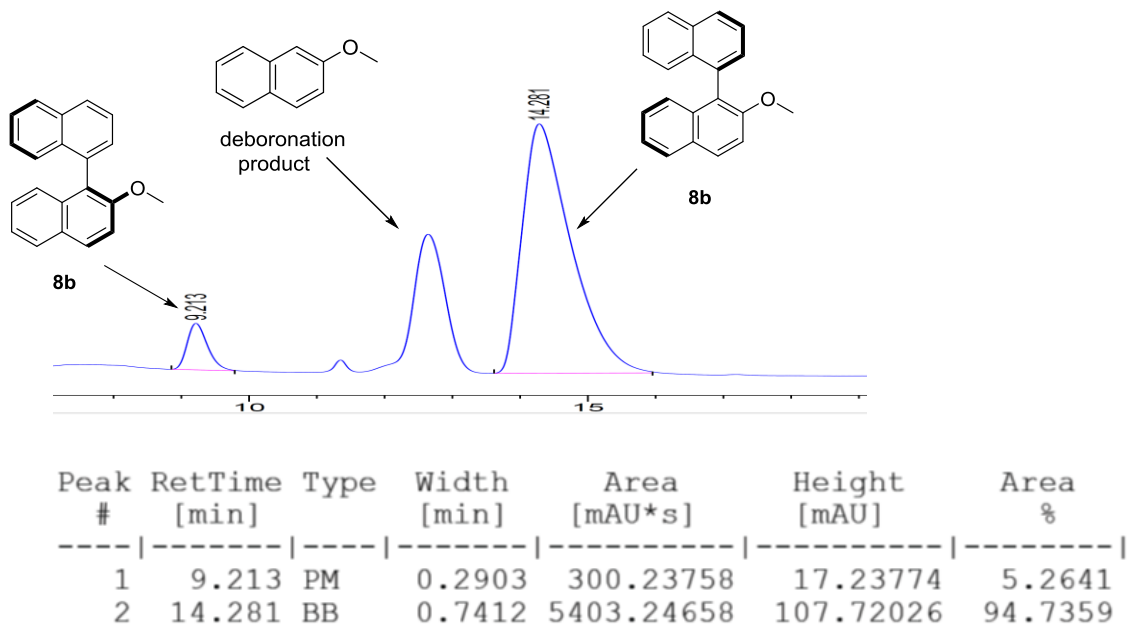
temperature. Stock solutions of NaOH (20 μmol , 2.00 eq.) in mQ water, aryl-halide (10 μmol , 1.00 eq.) and boronic acid (15 μmol , 1.50 eq.) in DMSO were prepared, added to the mixture and stirred overnight. The reactions were performed with iodonaphthalene, bromonaphthalene and chloronaphthalene derivatives at two different temperatures (RT and 50 $^{\circ}\text{C}$) in the scale of 50 mM in 200 μL total volume.

Upon completion of the reaction, the reaction vessel was removed from the glove box and 1,2,4-trimethylbenzene (100 μL , 10.0 mM in TBME, as internal standard) was added. It was then extracted with TBME (700 μL), dried over Na_2SO_4 . The conversion and enantiomeric excess were determined by chiral HPLC using an Analytical Chiracel OJ-H column (4.6 mm x 250 mmL, particle size 5 μm) and a hexane / isopropanol mixture as eluent.

Reactions on 100 μmol scale (preparative scale), general procedure:

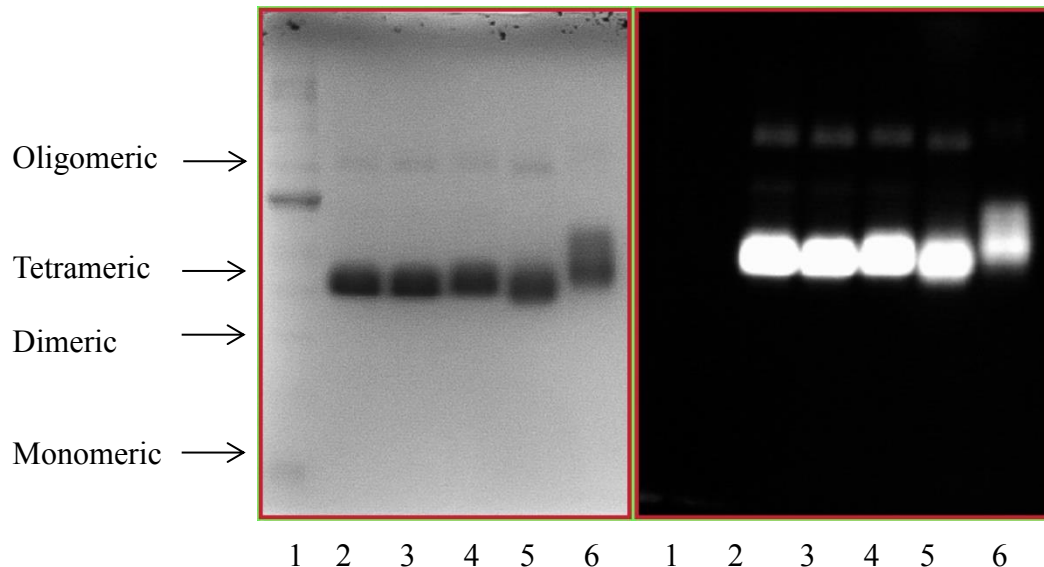
Following the above protocol 1-Iodonaphthalene (15 μl , 100 μmol) and 2-methoxy-1-naphthaleneboronic acid (30 mg, 150 μmol) were allowed to react for 7 days at 4 $^{\circ}\text{C}$ in a sealed vial under nitrogen. The reaction mixture was extracted with EtOAc (3 x 10 ml). After drying of the organic phases and removal of volatiles, the crude product was purified by column chromatography over silica gel with EtOAc/cyclohexane (1 : 10). The product was obtained as colourless oil (7 mg, 25 %, 90 % ee). See SI Figure 1 and 2 for ^1H NMR and chiral phase HPLC-analysis.

^1H NMR (400 MHz, CDCl_3) δ 7.99 (d, $J = 9.0$ Hz, 1H), 7.96 (dd, $J = 8.2, 4.1$ Hz, 2H), 7.88 (d, $J = 8.2$ Hz, 1H), 7.63 (dd, $J = 8.3, 7.0$ Hz, 1H), 7.50 – 7.42 (m, 3H), 7.37 – 7.27 (m, 3H), 7.25 – 7.21 (m, 1H), 7.17 (dd, $J = 9.1, 0.6$ Hz, 1H), 3.77 (s, 3H).

Supporting Figure 1 ¹H NMR of isolated product **8b**.

Supporting Figure 2 Chiral phase HPLC data of isolated product.

SDS-Page Analysis of reaction mixtures:



- 1 = protein ladder
- 2 = S112Y-K121E
- 3 = S112Y-K121E + Catalyst +DMSO
- 4 = S112Y-K121E + Catalyst +DMSO + NaOH
- 5 = S112Y-K121E + Catalyst +DMSO + NaOH + substrate
- 6 = S112Y-K121E + Catalyst +DMSO + NaOH + substrate + 24 hr

Supporting Figure 3 SDS-Page Gels. Right - B₄F Stain, Left - Comassie Stain.

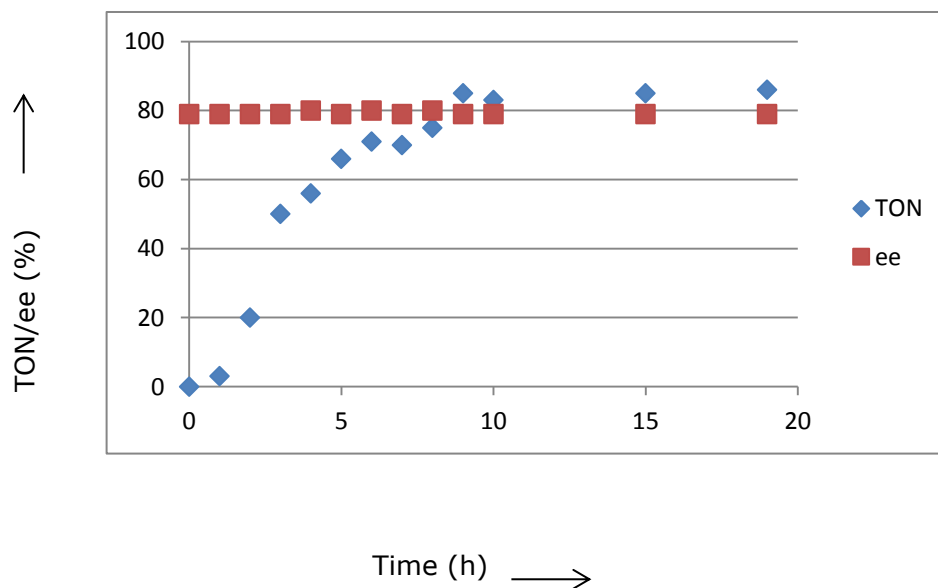
It is well established that non-denatured, active streptavidin can be detected by SDS-PAGE using biotinylated fluorescein as a specific marker (right side of SI Fig. 3).^{4,5} The same SDS-PAGE gels can also be stained with comassie-blue to visualize all proteins (left side of Fig. 4). Under non-denaturing conditions, streptavidin migrates primarily as an active tetramer, although the protein also has a tendency to aggregate to form oligomers (in some cases, dimers and monomers of streptavidin are also commonly detected as minor, active species). In the present study, under catalytic conditions (including 75 equivalents of boronic acid and 100 equivalents of NaOH),

the reaction mixture formed a suspension; upon microcentrifugation at 14'000 rpm, this suspension could be separated into a pellet and a clear supernatant. The supernatant contained active streptavidin (Non-denatured), which binds biotinylated fluorescein. The migrating properties of the protein in this supernatant were similar to a Sav control (Non-denatured S112Y-K121E), with the corresponding expected molecular weight (Protein Ladder).

These figures show that as each solvent and compound is added to the reaction, the Sav isoform remains largely as the active tetramer. The isolated precipitate reactions is largely starting material and product.

Ee and conversion over the time course of the reaction:

Following the general protocol for catalysis, 13 individual vials were prepared. The reactions were extracted at the indicated time points as described for the reactions on an analytical scale and analysed by HPLC.



Supporting Figure 4 Conversion over the time course of the reaction.

Supporting Table 1. Complete list of catalytic experiments carried out for the chemogenetic optimization (see fingerprint display, Figure 1) with complex **1**, **2** and **3**.

Enantiomeric excess > 0 corresponds to $[S] > [R]$; enantiomeric excess < 0 $[R] > [S]$

Complex	Mutant	TON	ee [%]
1	WT	55	-57
1	S112Y	14	+16
1	S112L	59	-26
1	S112V	60	-38
1	S112F	55	-54
1	S112M	58	+14
1	S112T	58	-49
1	S112Q	43	-50
1	S112C	<5	-48
1	S112R	14	+16
1	S112G	48	-56
1	S112H	26	-50
1	S112A	58	-60
1	WT	53	-57
1	K121R	6	-62

1	K121E	50	-76
1	K121D	7	-34
1	K121A	39	-4
1	K121Y	46	-64
1	K121F	38	-67
1	K121M	59	-67
1	K121N	52	-50
1	K121H	17	-53
1	K121C	37	-62
1	-	20	rac
2	WT	44	+19
2	S112Y	37	-3
2	S112L	51	+45
2	S112V	39	+18
2	S112F	49	+7
2	S112M	53	+44
2	S112T	26	+33
2	S112Q	8	+33
2	S112C	<5	-3
2	S112R	<5	+44
2	S112G	6	+31

2	S112H	22	-11
2	S112A	46	Rac
2	WT	42	+19
2	K121R	33	+19
2	K121E	30	-9
2	K121D	<5	+12
2	K121A	32	+47
2	K121Y	9	+14
2	K121F	35	+11
2	K121M	12	Rac
2	K121N	36	+43
2	K121H	<5	+47
2	K121C	17	+7
2	-	-	-
3	WT	45	-42
3	S112Y	<5	+28
3	S112L	<5	+37
3	S112V	<5	+5
3	S112F	<5	-15
3	S112M	78	-38

3	S112T	<5	-9
3	S112Q	-	-
3	S112C	-	-
3	S112R	<5	-60
3	S112G	32	-50
3	S112H	<5	-50
3	S112A	52	-36
3	K121R	<5	-9
3	K121E	<5	+13
3	K121A	5	-13
3	K121Y	<5	+23
3	K121F	<5	+19
3	K121M	5	-15
3	K121N	<5	<i>Rac.</i>
3	K121H	<5	-9
3	K121C	<5	+4
3	K121G	<5	-9
3	S112D	<5	-45
3	S112E	-	-
3	S112K	5	-56

Supporting Table 2. Complete list of control experiments carried out with complex **1** at RT for the synthesis of enantioenriched 2-methoxy-1,1'-binaphthyl **8b**

Entry	Catalyst (Complex 1) μmol	S112Y- K121E Sav μmol	Phosphine Ligand without biotin μmol	[Pd(cinnamyl)(μ - Cl)] ₂ μmol	Biotin μmol	TON	ee [%]
1	0.1	-	-	-	-	20	<i>Rac.</i>
2	-	0.2	-	-	-	-	-
3	-	0.2	-	0.1	-	-	-
4	0.1	0.2	-	-	0.2	5	-47
5	-	0.2	-	0.1	0.2	-	-
6	0.1	0.2	-	-	-	90	-80
7	-	-	0.1	-	-	-	-
8	-	-	0.1	0.1	-	-	-

Supporting Table 3. Complete list of optimization of co-solvent and overall conc. of aryl halide carried out with complex **1** and WT Sav at RT for the synthesis of enantioenriched 2-methoxy-1,1'-binaphthyl **8b**

Entry	Co-solvent	ArX (6c) Conc. (mM)	TON	ee [%]
-------	------------	---------------------------------	-----	--------

1	MeOH	50	72	-52
2	DMSO	50	80	-57
3	THF	50	62	-57
4	Dioxane	50	36	-56
5	DMSO	100	78	-57
5	DMSO	25	50	-55
6	DMSO	12	63	-54
7	DMSO	6	50	-50
8	DMSO	3	45	-49

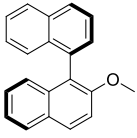
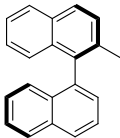
Supporting Table 4. Complete list of optimization of co-solvent amount, base amount and partial Sav loading carried out with complex **1** and S112Y-K121E Sav at RT for the synthesis of enantioenriched 2-methoxy-1,1'-binaphthyl **8b**

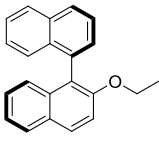
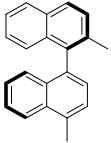
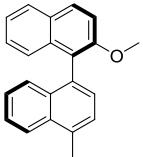
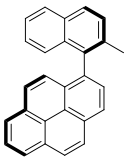
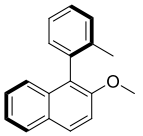
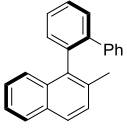
Entry	Pd : Sav tetramer ratio	Equivalents base added	DMSO in water (%)	TON (vs. Pd)	ee [%]
1	1/4	2	10	73	-78
2	2/4	2	10	77	-78
3	3/4	2	10	74	-76
4	4/4	2	10	89	-69
5	2/4	1	10	48	-79

5	2/4	1.5	10	57	-80
6	2/4	3	10	34	-79
7	2/4	5	10	5	-56
8	2/4	2	5	53	-81
9	2/4	2	15	65	-78
10	2/4	2	20	70	-77
11	2/4	2	25	37	-74
12	2/4	2	30	52	-70
13	2/4	2	35	-	-

Supporting Table 5. Retention times measured on an analytical Chiracel OJ-H

column (5 μ m, 250 x 4.6 mm) at 40 °C with a flow rate: 1.00 ml/min (λ = 254 nm):

Compound	Eluent (hexane/isopropanol)	(<i>R</i>) enantiomer	(<i>S</i>) enantiomer
 8b	95:5	14.28 min	9.21 min
 8a	95:5	6.58 min	9.49 min

 8c	95:5	11.12 min	7.66 min
 8d	90:10	4.75 min	13.27 min
 8e	90:10	13.68 min	4.79 min
 8f	90:10	7.62 min	23.38 min
 8g	95:5	7.48 min	10.46 min
 8h	95:5	7.60 min	5.02 min

Protein Crystallography

(This work entirely performed by Aaron D. Finke, Laura Vera, May Marsh at the PSI)

Crystallization. The crystallization screens were carried out by sitting drop vapor diffusion with 1 μ l equivolumetric drops of protein and reservoir solution using CrysChem plates that were equilibrated at 20°C. The reservoir solution consisted of 15-25% PEG 1500, 100mM SPG buffer (mixed succinic acid, sodium dihydrogen phosphate and glycine in the ratio 2:7:7; 75% at pH 4 and 25% at pH 10).⁶ Good

quality crystal could be obtained when drops were streak seeded⁷ in low PEG concentration immediately after setting up the drops with crystals growing from high PEG concentration.

The crystals were transferred and soaked for 20 minutes in a cryo-protecting solution containing the biotinylated complex **1**. The cryo-protecting solution consisted of the condition C7 from CryoProtX (Molecular Dimensions)⁸ mixed to 20% PEG 1500, 100mM SPG buffer (75% at pH 4 and 25% at pH 10). 0.5uL of ligand **5** at 20mM in 100% DMSO was added to 10μL of the cryo-protecting solution and crystals were flash-cooled in liquid nitrogen.

Data Processing and Refinement. X-ray diffraction data were collected at beam line X06DA at the Swiss Light Source. Data were processed with the XDS software package.⁹ The structures were solved by molecular replacement with the Phaser-MR routine of the Phenix¹⁰ software package, using the 1LUQ structure from the PDB with the waters and ligand removed as a model compound. Structure refinement was performed with the phenix.refine utility.¹⁰ Crystallographic details are given in Table 1.

The Sav S112Y-K121E protein contains two monomers in the asymmetric unit related by non-translational NCS, which form a tetramer by application of the twofold axis. The 12 residues at the N-terminus and the 26 residues at the C-terminus are not resolved. There is strong residual electron density in the 2Fo-Fc difference map in the biotin binding pocket and vestibule. There is a significant peak in the anomalous difference map (8σ) at the interface of the vestibule near Y112, correlating with a strong peak in the density map (12σ); this position was determined to be the Pd atom. Pd atoms display significant anomalous scattering at 1 Å ($2e$). No other significant peak was found in the anomalous difference map. The density map clearly shows the presence of the phosphine ligand, Pd, and chlorine, but the cinnamyl ligand could not be resolved, likely due to disorder caused by ligand fluxionality. Generation of the

initial model and restraints for ligand **1** (without cinnamyl ligand) was done with the eLBOW¹¹ routine in Phenix. The bond lengths and angles for the phosphine ligand, palladium, and chlorine were referenced from a related structure, [(*t*-Bu₂(4-dimethylanilino)P)PdCl(cinnamyl)],¹² and the biotin and amide linker geometries were optimized with the generalized Amber forcefield in Avogadro v1.1.1¹³ (the Pd metal center and ligands were fixed during this step). The amide linker exhibits two H-bonding interactions with the protein backbone: the amide nitrogen exhibits an H-bonding interaction with the sidechain of S88, and the carbonyl oxygen exhibits an H-bonding interaction with the backbone nitrogen of N49.

Wavelength (Å)	1.00
Resolution Range	48.62 - 1.792 (1.856 - 1.792)
Space Group	C 2 2 2 ₁
Unit Cell	$a = 81.368, b = 81.46, c = 90.811$ $\alpha = \beta = \gamma = 90^\circ$
Total Reflections	329716 (25103)
Unique Reflections	27986 (2541)
Multiplicity	11.8 (9.9)
Completeness (%)	97.60 (89.28)
Mean I/sigma(I)	18.18 (3.20)
Wilson B-factor	18.93
R-merge	0.09055 (0.7346)
R-meas	0.09459
CC1/2	0.999 (0.914)
CC*	1 (0.977)
R-work	0.2231 (0.3084)
R-free	0.2558 (0.3121)
Number of non-hydrogen atoms	1973
Macromolecules	1863
Ligands	60
Water	50
Protein residues	245
RMS(bonds)	0.007
RMS(angles)	1.11
Ramachandran favored	97
Ramachandran allowed	0
Ramachandran outliers	0
Clashscore	2.73
Average B-factor	24.20

Macromolecules	23.80
Ligands	36.10
Solvent	25.00

Statistics for the highest-resolution shell are shown in parenthesis.

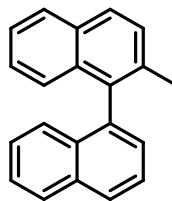
General procedure for racemic products synthesis:

A Schlenk-tube was charged with the boronic acid (1.05 eq.), Pd(OAc)₂ (0.05 eq.), K₃PO₄ (2.00 eq.) and solid aryl-halide (1.00 eq.) and set under the nitrogen atmosphere. Dry toluene (0.5 mL) and the aryl-halide (1.00 eq.), if present as a liquid, were added via syringe. The reaction mixture was stirred overnight at 100 °C and checked by TLC. It was extracted with ethyl acetate (3 x 10 mL), washed with brine (2 x 5 mL), dried over Na₂SO₄ and concentrated. The residue was further purified by column chromatography using hexane or hexane-ethyl acetate mixtures as eluents.

2-Methyl-1,1'-binaphthyl (8a): Following the general procedure from 1-iodonaphthalene (37.5 μL, 0.250 mmol, 1.00 eq.) and 2-methyl-1-naphthaleneboronic acid (76.6 mg, 0.375 mmol, 1.05 eq.) the product was isolated as a clear liquid (**8a**) (64.7 mg, **quant. yield**).

Retention times: Measured on an analytical Chiracel OJ-H column (5μm, 250 x 4.6 mm) with hexane/isopropanol (95:5) as the mobile phase at 40 °C and flow rate: 1.00 ml/min: enantiomer (*R*): 6.40 min; enantiomer (*S*): 9.50 min.

¹H-NMR: (400 MHz, CDCl₃): δ = 7.96 (d, 1H, ³J_{HH} = 8.40 Hz), 7.88 (dd, 2H, ³J_{HH} = 8.40 Hz, ⁴J_{HH} = 2.00 Hz), 7.62 (m, 1H), 7.51-7.14 (m, 9H), 2.11 (s, 3H).



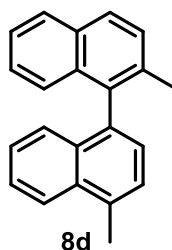
8a

2-Methyl-4'-methyl-1,1'-binaphthyl (8d): Following the general procedure from 1-bromo-2-methylnaphthalene (55.3 mg, 39.2 μL, 0.250 mmol, 1.00 eq.) and

4-methyl-1-naphthaleneboronic acid (48.8 mg, 0.263 mmol, 1.05 eq.) the product was isolated as a liquid (**8d**) (77.1 mg, **quant. yield**).

Retention times: Measured on an analytical Chiracel OJ-H column (5 μ m, 250 x 4.6 mm) with hexane/isopropanol (90:10) as the mobile phase at 40 °C and flow rate: 1.00 ml/min: enantiomer (*R*): 4.90 min; enantiomer (*S*): 14.9 min.

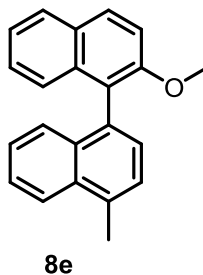
¹H-NMR: (400 MHz, CDCl₃): δ = 8.11 (d, 1H, ³*J*_{HH} = 8.40 Hz), 7.87 (dd, 3H, ³*J*_{HH} = 8.40 Hz, ⁴*J*_{HH} = 4.00 Hz), 7.53-7.16 (m, 8H), 2.82 (s, 3H), 2.12 (s, 3H).



2-Methoxy-4'-methyl-1,1'-binaphthyl (8e): Following the general procedure from 1-bromo-2-methoxynaphthalene (55.3 mg, 39.2 μ L, 0.250 mmol, 1.00 eq.) and 2-methyl-1-naphthaleneboronic acid (0.375 mmol, 76.6 mg, 1.50 eq.) 2-methoxy-1,1'-binaphthyl was isolated as a white solid (**8e**) (44 mg, **59% yield**).

Retention times: Measured on an analytical Chiracel OJ-H column (5 μ m, 250 x 4.6 mm) with hexane/isopropanol (90:10) as the mobile phase at 40 °C and flow rate: 1.00 ml/min: enantiomer (*R*): 4.90 min; enantiomer (*S*): 14.9 min.

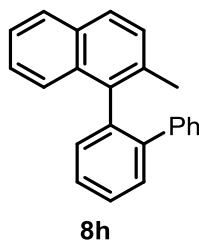
¹H-NMR: (400 MHz, CDCl₃): δ = 8.13-7.95 (m, 4H), 7.86 (d, 1H, ³*J*_{HH} = 8.00 Hz), 7.57-7.16 (m, 7H), 3.76 (s, 3H), 2.12 (s, 3H).



1-(2-Biphenyl)-2-methylnaphthalene (8h): Following the general procedure from 1-bromo-2-methylnaphthalene (0.250 mmol, 37.5 μ L, 1.00 eq.) and 2-methyl-1-naphthaleneboronic acid (0.375 mmol, 76.6 mg, 1.50 eq.) 2-Methyl-1,1'-binaphthyl was isolated as a clear liquid (**8h**) (106 mg, **144% yield**).

Retention times: Measured on an analytical Chiracel OJ-H column (5 μ m, 250 x 4.6 mm) with hexane/isopropanol (95:5) as the mobile phase at 40 °C and flow rate: 1.00 ml/min: enantiomer (*R*): 4.40 min; enantiomer (*S*): 7.80 min.

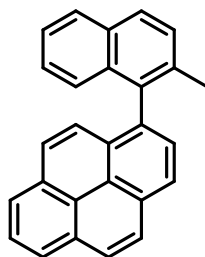
¹H-NMR: (400 MHz, CDCl₃): δ = 7.78 (m, 1H), 7.66 (d, 1H, ³*J*_{HH} = 8.40 Hz), 7.55-7.30 (m, 8H), 7.19 (d, 1H, ³*J*_{HH} = 8.40 Hz), 7.05-6.99 (m, 5H), 1.98 (s, 3H).



4-(2-Methylnaphthalen-1-yl)pyrene (8f): Following the general procedure from 1-bromo-2-methylnaphthalene (0.250 mmol, 37.5 μ L, 1.00 eq.) and 2-methyl-1-naphthaleneboronic acid (0.375 mmol, 76.6 mg, 1.50 eq.) 2-Methyl-1,1'-binaphthyl was isolated as a clear liquid (**8f**) (125 mg, **58% yield**).

Retention times: Measured on an analytical Chiracel OJ-H column (5 μ m, 250 x 4.6 mm) with hexane/isopropanol (90:10) as the mobile phase at 40 °C and flow rate: 1.00 ml/min: enantiomer (*R*): 8.00 min; enantiomer (*S*): 34.0 min.

¹H-NMR: (400 MHz, CDCl₃): δ = 8.32 (d, 1H, ³*J*_{HH} = 8.00 Hz), 8.23 (d, 1H, ³*J*_{HH} = 7.60 Hz), 8.20-8.13 (m, 3H), 8.02 (t, 1H, ³*J*_{HH} = 7.60 Hz), 7.95-7.87 (m, 4H), 7.56 (d, 1H, ³*J*_{HH} = 8.40 Hz), 7.48 (d, 1H, ³*J*_{HH} = 9.2 Hz), 7.41 (t, 1H, ³*J*_{HH} = 8.00 Hz), 7.19 (t, 1H, ³*J*_{HH} = 6.80 Hz), 7.09 (d, 1H, ³*J*_{HH} = 8.4 Hz), 2.13 (s, 3H).

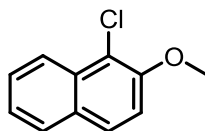


8f

Synthesis of the naphthalene halide substrates:

2-Methoxy-chloronaphthalene (6d): A suspension of 2-methoxy-bromonaphthalene (190 mg, 0.8 mmol, 1.00 eq.) and CuCl (87.1 mg, 0.88 mmol, 1.10 eq.) in DMF (15 ml) was refluxed overnight. After cooling to room temperature, the mixture was filtered and the solvent evaporated. The residue was then purified by column chromatography using a hexane/ethyl acetate gradient to obtain the product as white crystals (**6d**) (186 mg, **quant. yield**, Lit.^[12]: 93%).

¹H-NMR: (400 MHz, CDCl₃): δ = 8.23 (d, 1H, ³J_{HH} = 8.80 Hz), 7.79 (d, 2H, ³J_{HH} = 8.40 Hz), 7.59-7.55 (m, 1H), 7.43-7.39 (m, 1H), 7.31 (d, 1H, ³J_{HH} = 9.2 Hz), 4.04 (s, 3H).



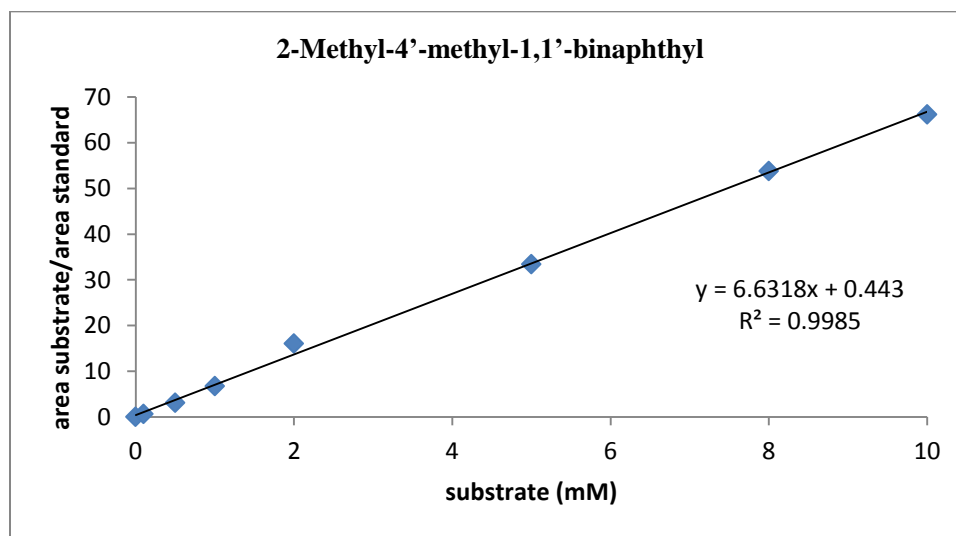
6d

Calibration curves to determine HPLC yield:

The calibration curve was prepared using 1,2,4-Trimethylbenzene in TBME as an internal standard and the measurement was carried out on an analytical Chiracel OJ-H column (5 μ m, 250 x 4.6 mm) using a hexane / isopropanol mixture as eluent. The calibration curves (Table 1; Fig. 3-8) are shown below.

Table 6: Sample preparation for the calibration curve

	1	2	3	4	5	6	7	8
substrate [mM]	0	0.100	0.500	1.00	2.00	5.00	8.00	10.0
internal standard [mM]	10.0	10.0	10.0	10.0	10.0	10.0	10.0	10.0
TBME [μ L]	900	895	875	850	800	650	500	400

Fig. 5: Calibration curve of 2-Methyl-4'-methyl-1,1'-binaphthyl **8d**

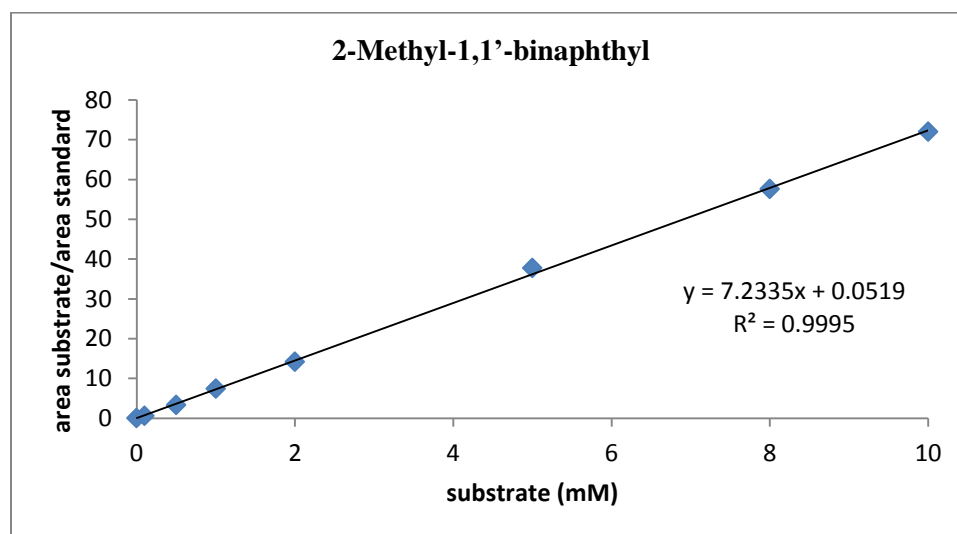


Fig. 6: Calibration curve of 2-Methyl-1,1'-binaphthyl **8a**

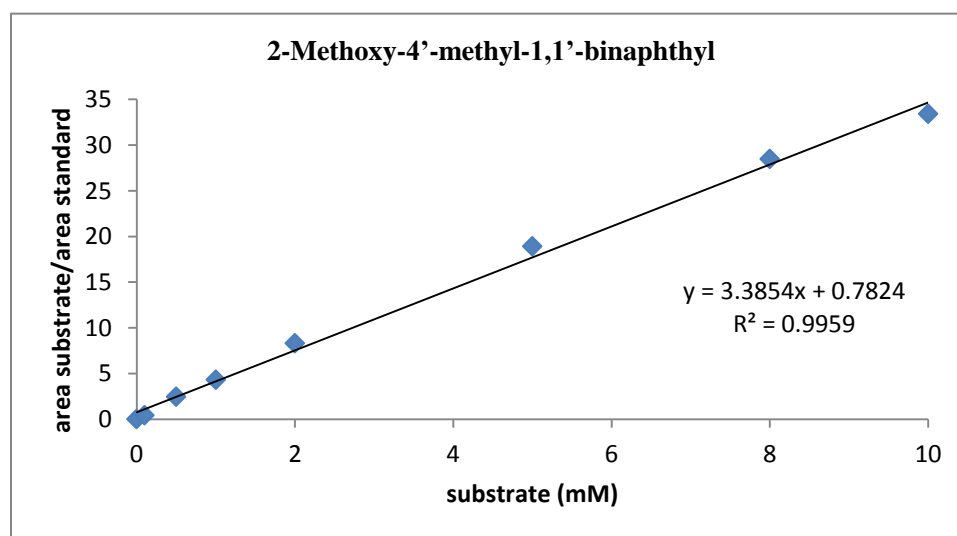


Fig. 7: Calibration curve of 2-Methoxy-4'-methyl-1,1'-binaphthyl **8e**

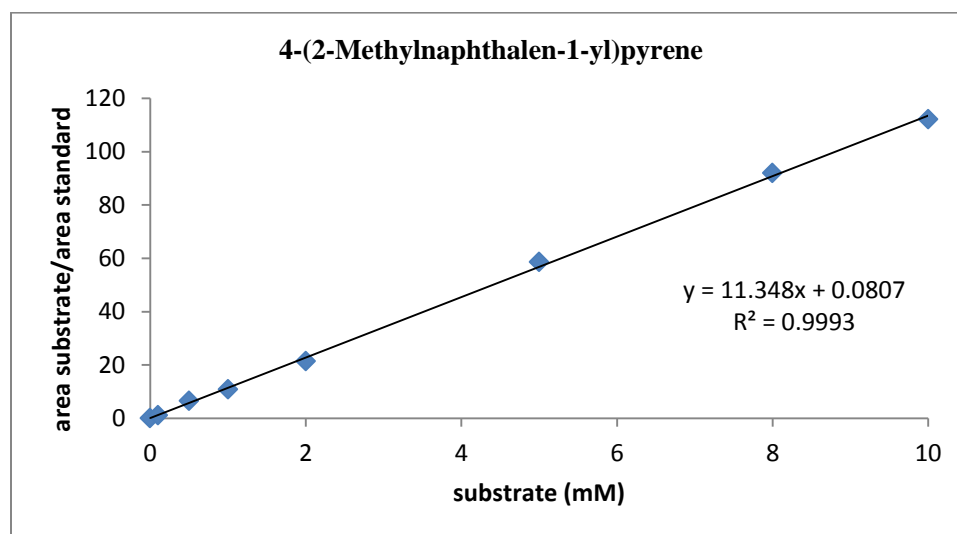


Fig. 8: Calibration curve of 4-(2-Methylnaphthalen-1-yl)pyrene **8f**

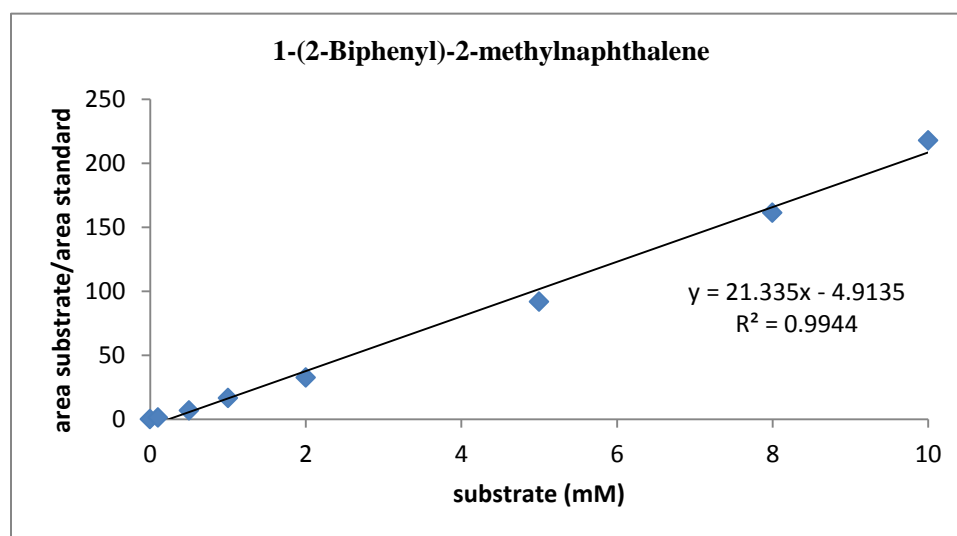
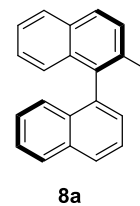
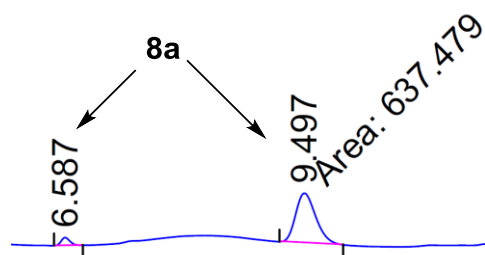
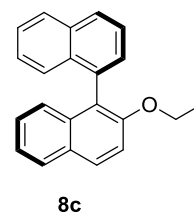
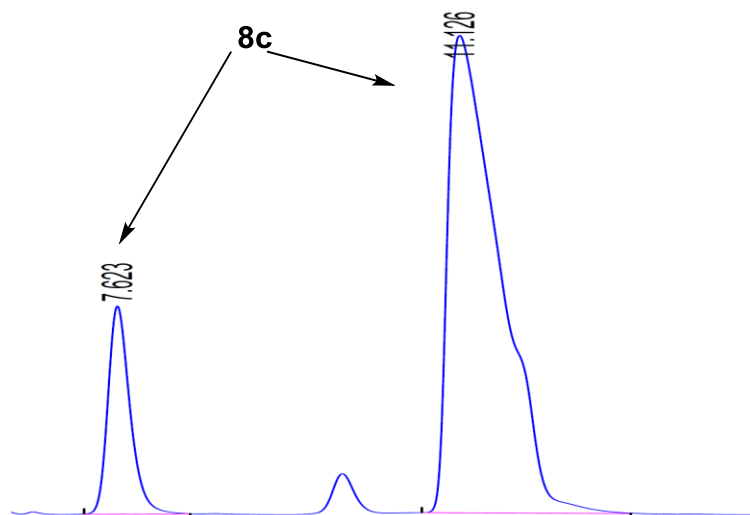


Fig. 9: Calibration curve of 1-(2-Biphenyl)-2-methylnaphthalene **8h**

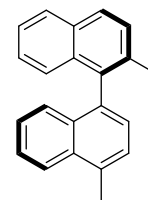
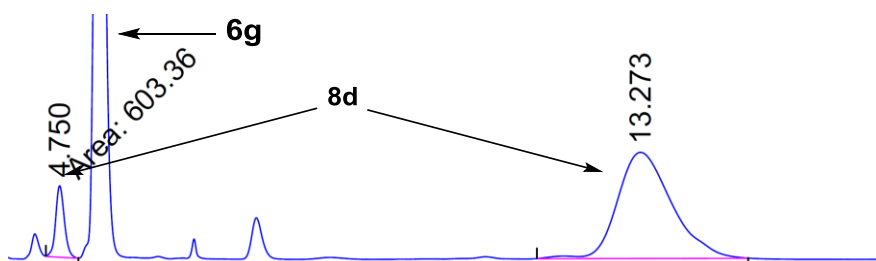
HPLC Traces:



Peak #	RetTime [min]	Type	Width [min]	Area [mAU*s]	Height [mAU]	Area %
1	6.587	BB	0.1138	44.10846	5.99840	6.4714
2	9.497	MM	0.2832	637.47858	37.52067	93.5286

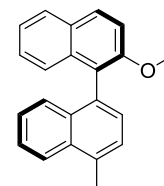
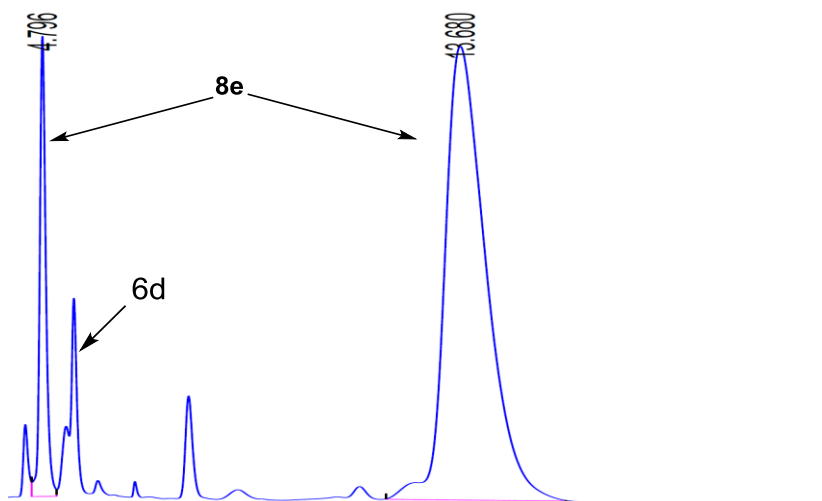


Peak #	RetTime [min]	Type	Width [min]	Area [mAU*s]	Height [mAU]	Area %
1	7.623	BB	0.2391	3172.33325	202.10664	15.7944
2	11.126	BB	0.5356	1.69129e4	463.60785	84.2056



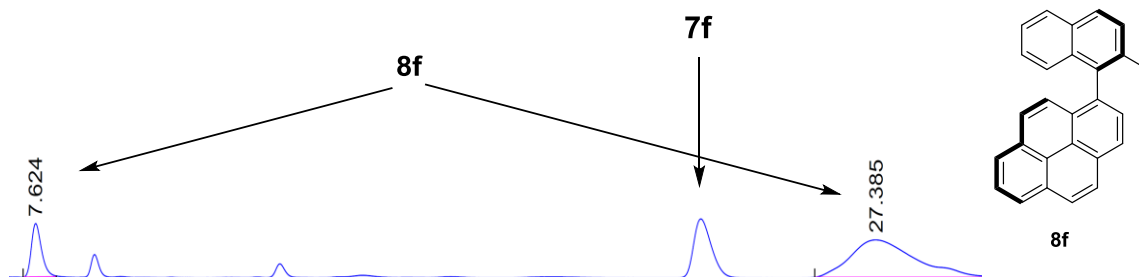
8d

Peak #	RetTime [min]	Type	Width [min]	Area [mAU*s]	Height [mAU]	Area %
1	4.750	MM	0.1493	603.35974	67.35346	9.8032
2	13.273	BB	0.8488	5551.34424	99.82427	90.1968

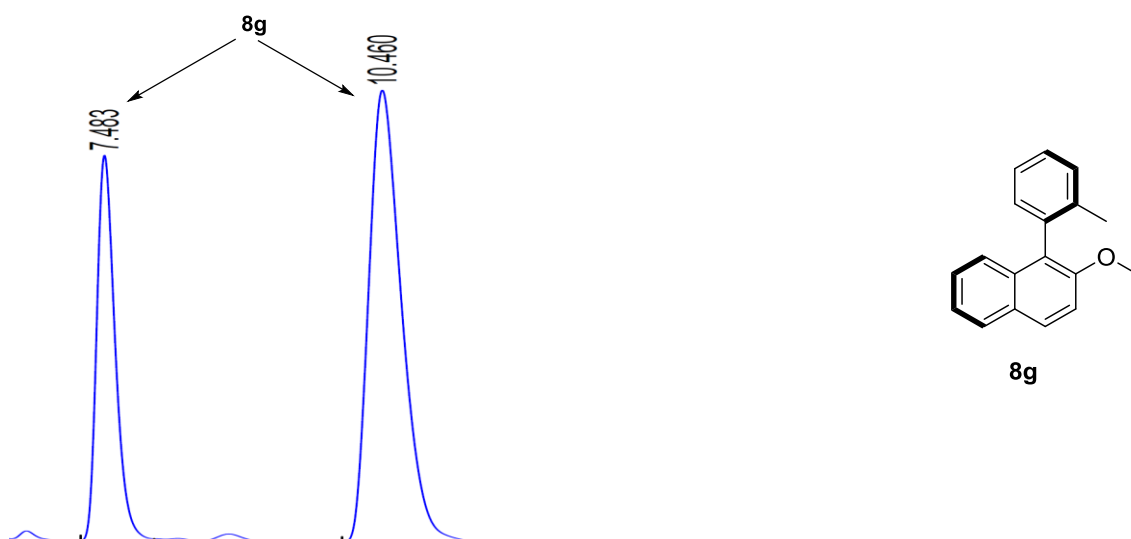


8e

Peak #	RetTime [min]	Type	Width [min]	Area [mAU*s]	Height [mAU]	Area %
1	4.796	VV	0.1377	2434.32202	268.72095	13.1397
2	13.680	BB	0.9431	1.60921e4	264.74277	86.8603

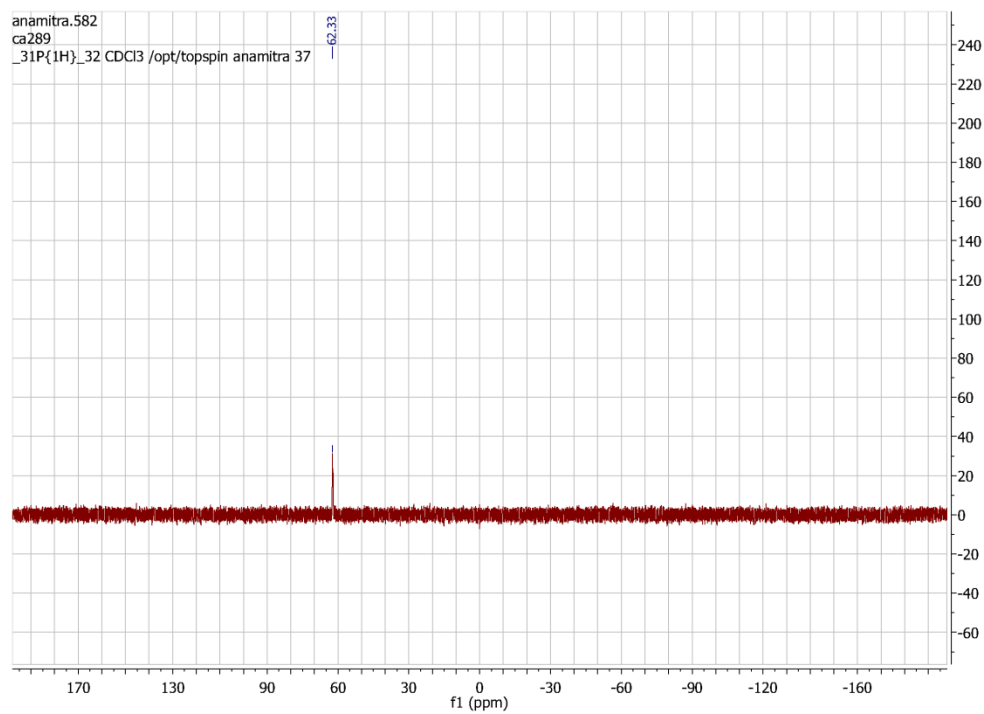
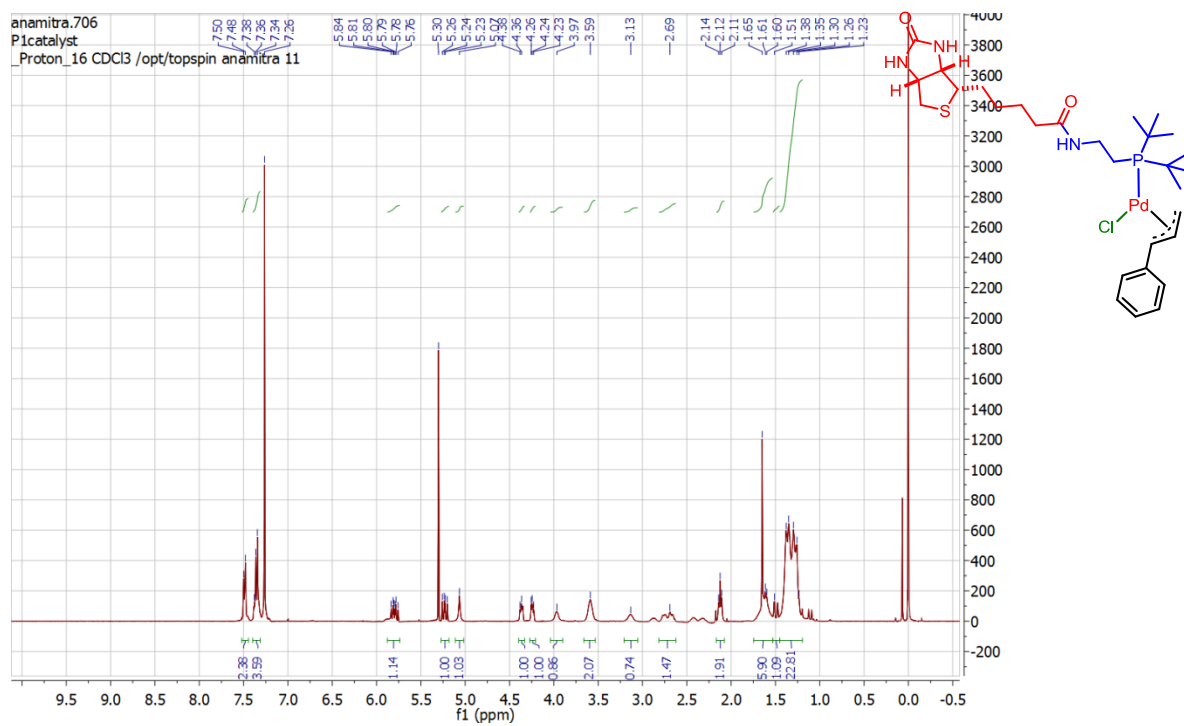


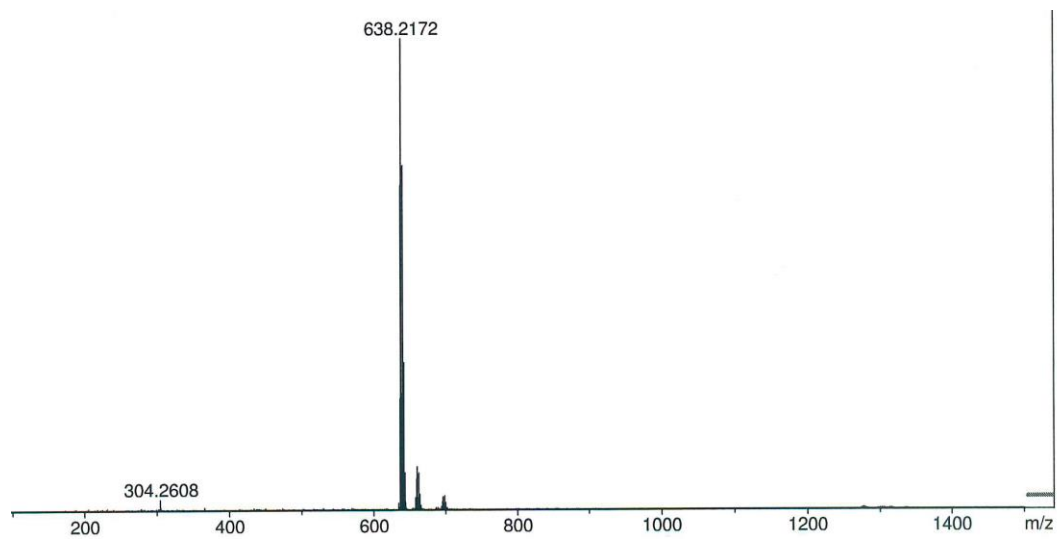
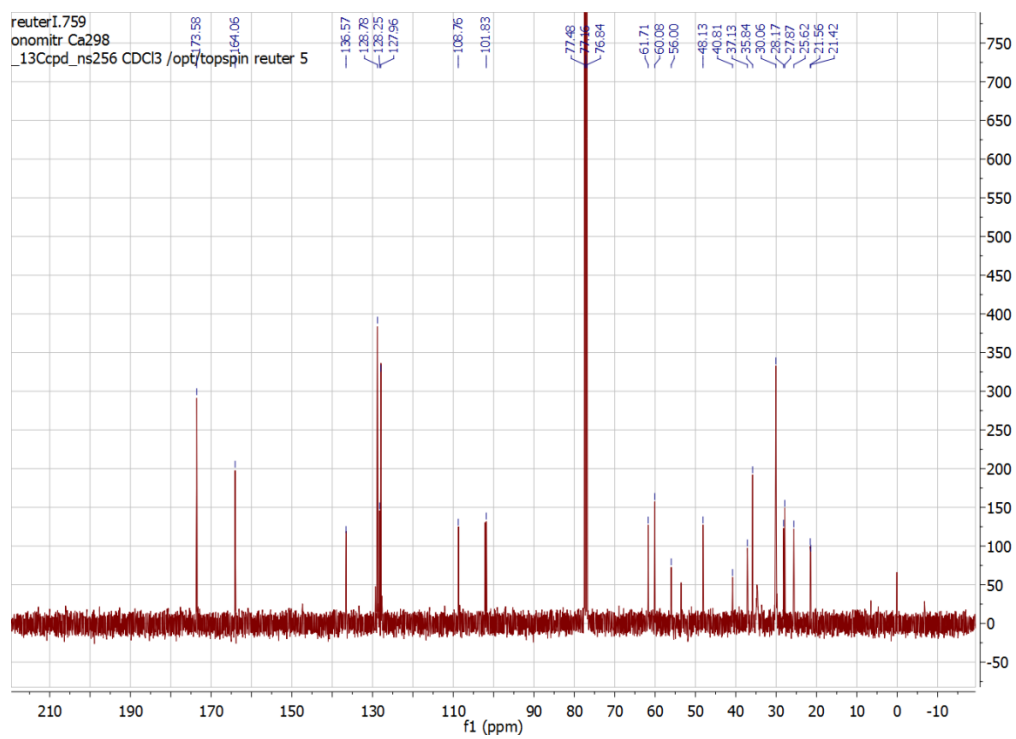
Peak #	RetTime [min]	Type	Width [min]	Area [mAU*s]	Height [mAU]	Area %
1	7.624	BB	0.2545	380.14203	22.80054	18.1378
2	27.385	BBA	1.2633	1715.71448	16.02250	81.8622



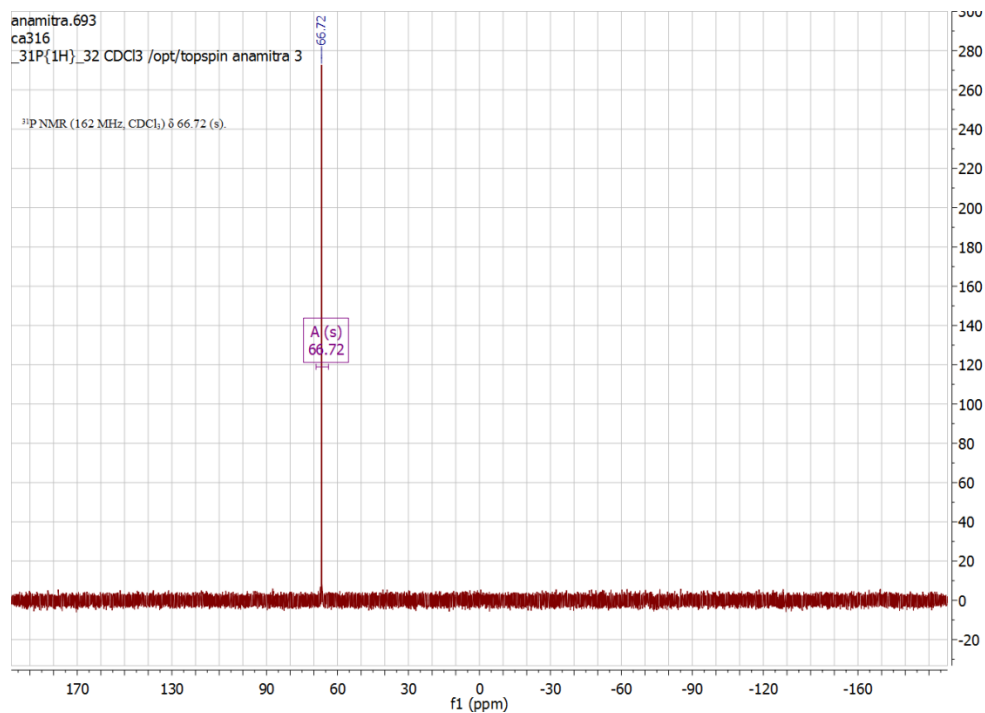
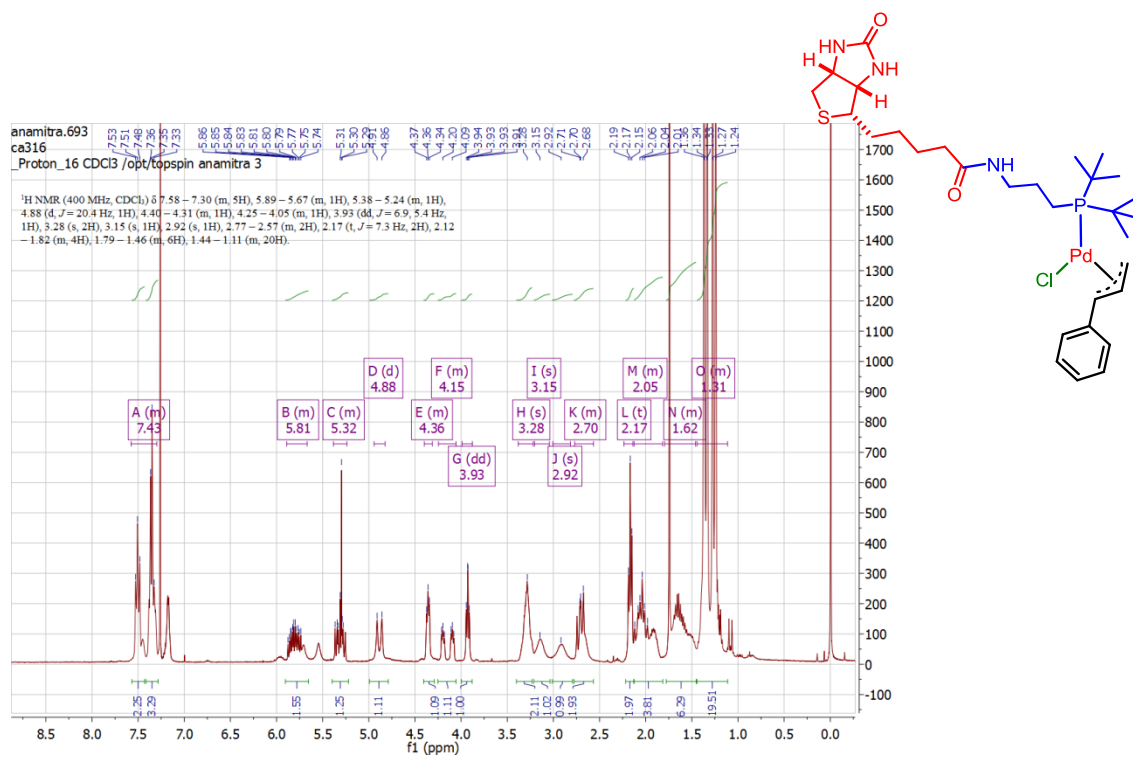
Peak #	RetTime [min]	Type	Width [min]	Area [mAU*s]	Height [mAU]	Area %
1	7.483	BB	0.2111	3083.98999	223.29436	32.6223
2	10.460	BB	0.3731	6369.64307	260.67050	67.3777

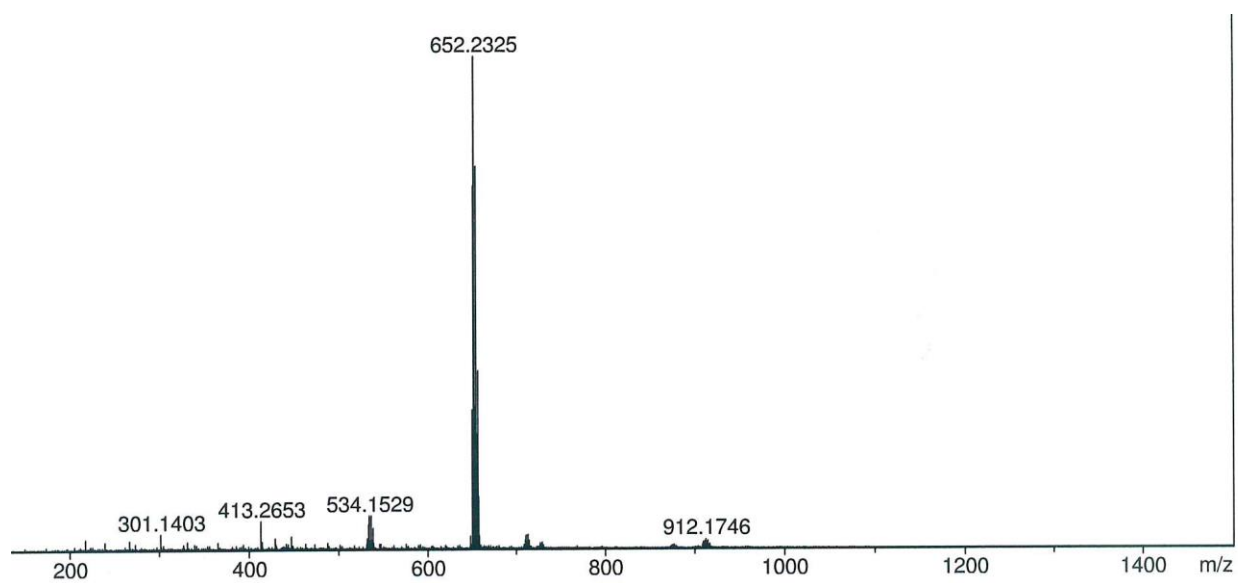
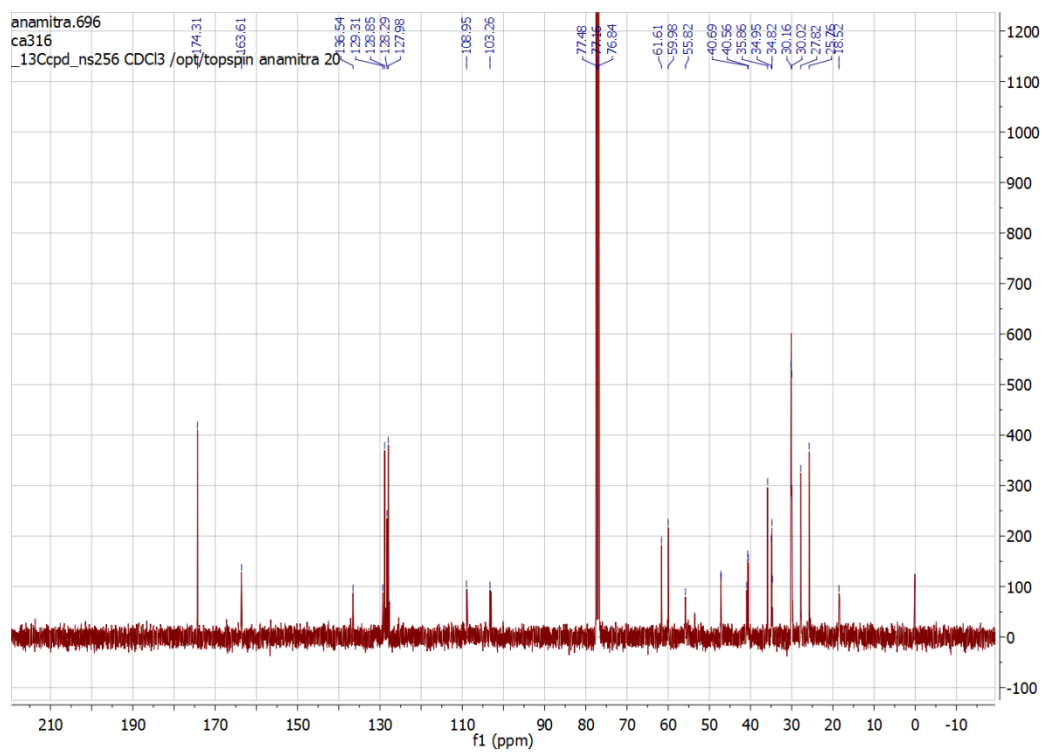
Spectra for complex 1:



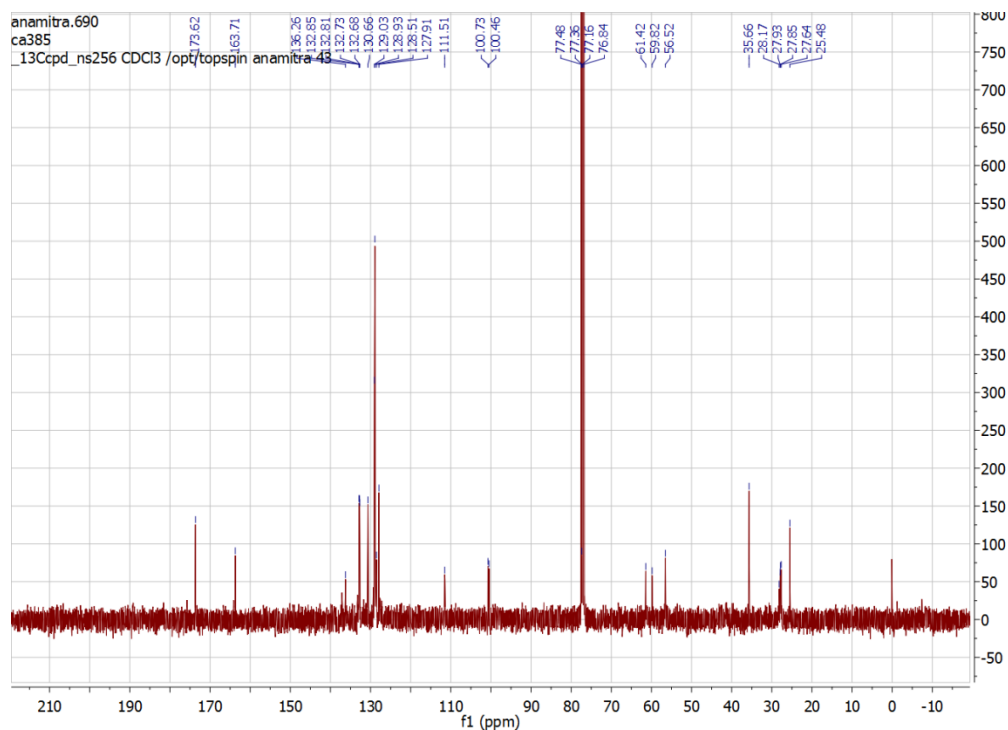
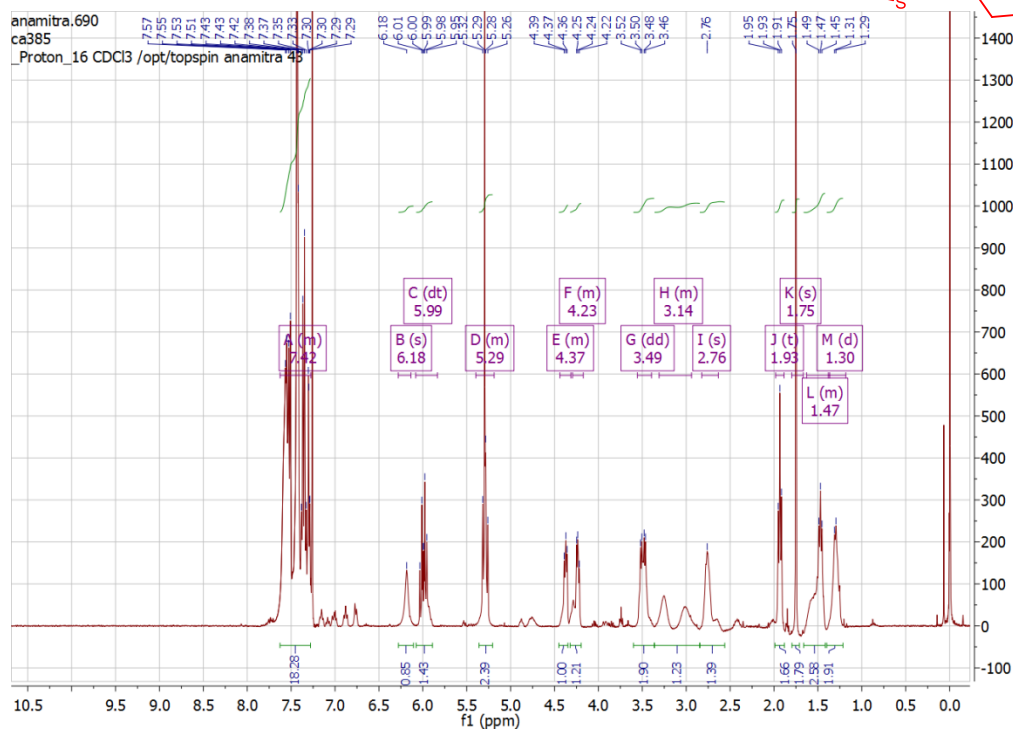
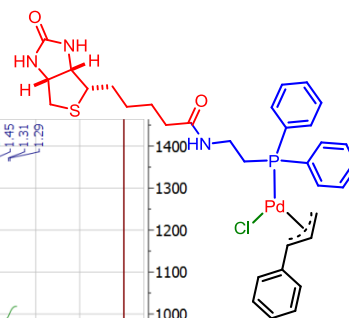


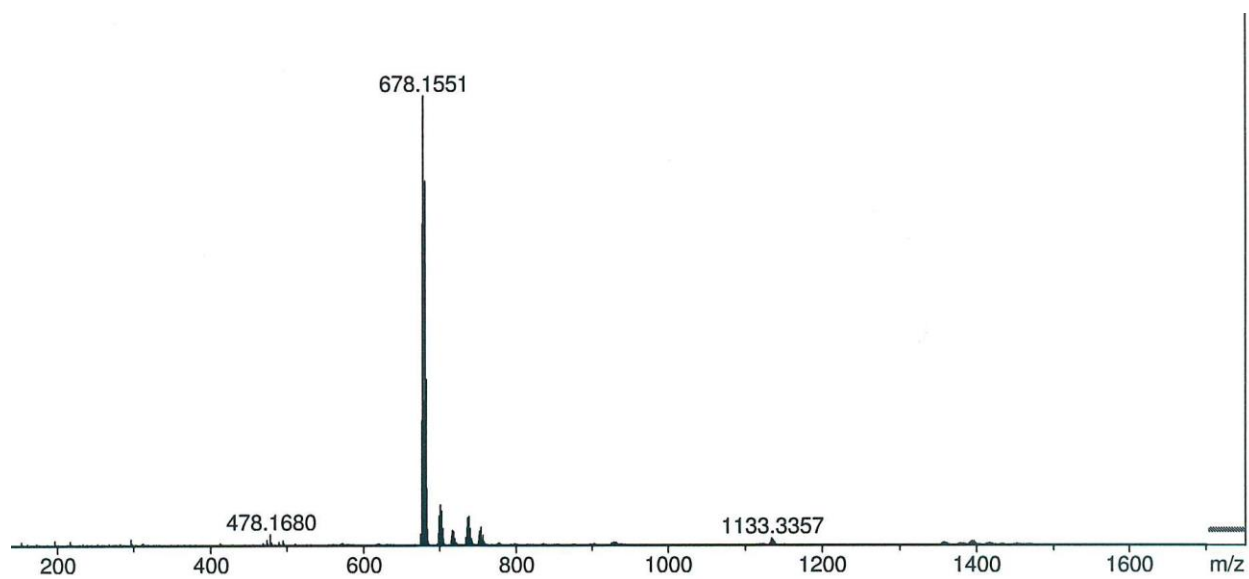
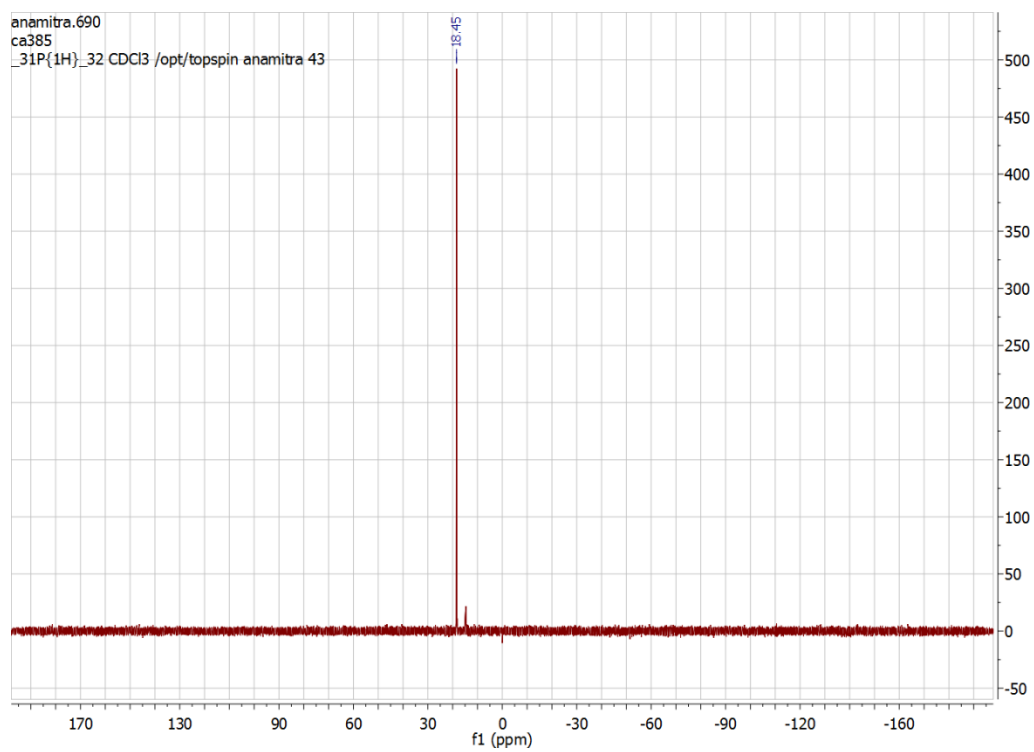
Spectra for complex 2:



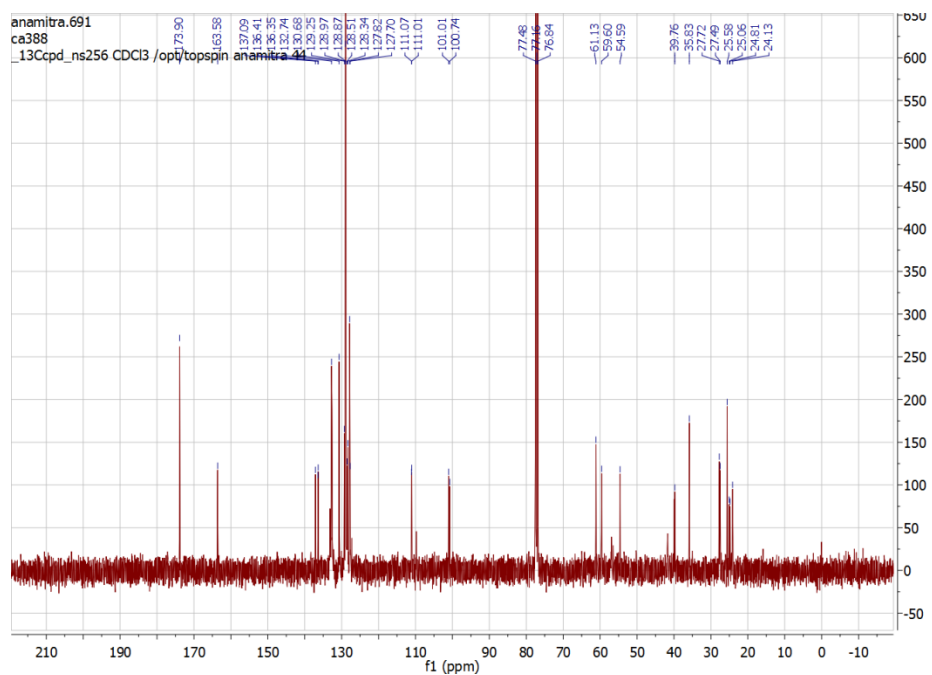
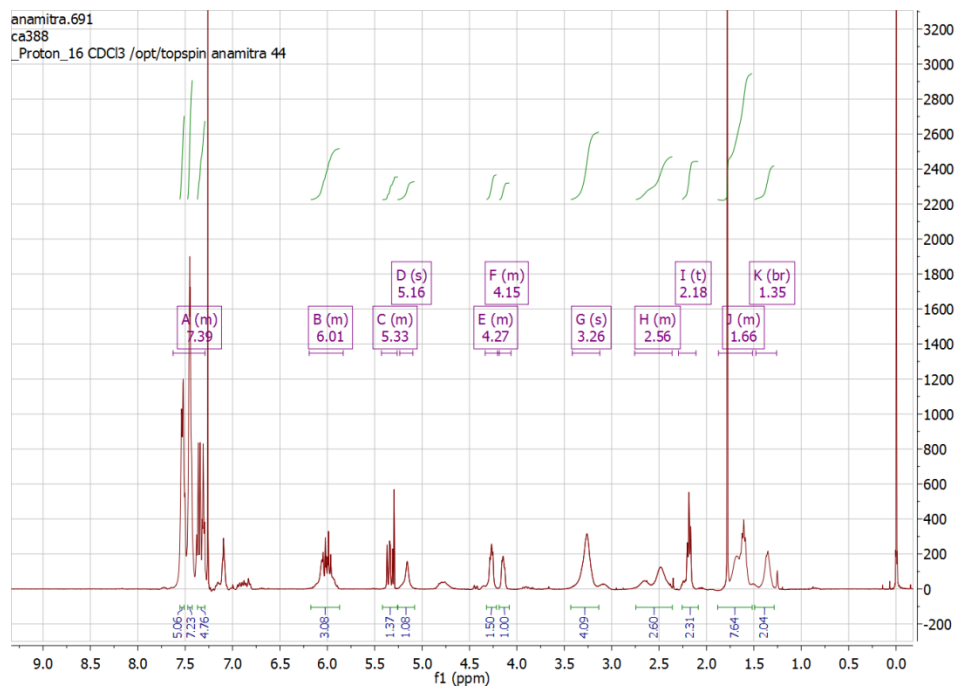
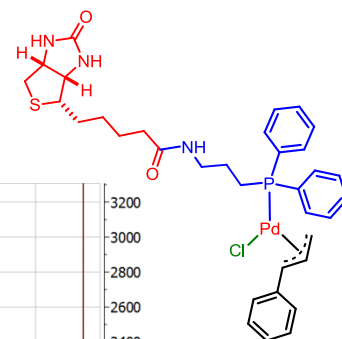


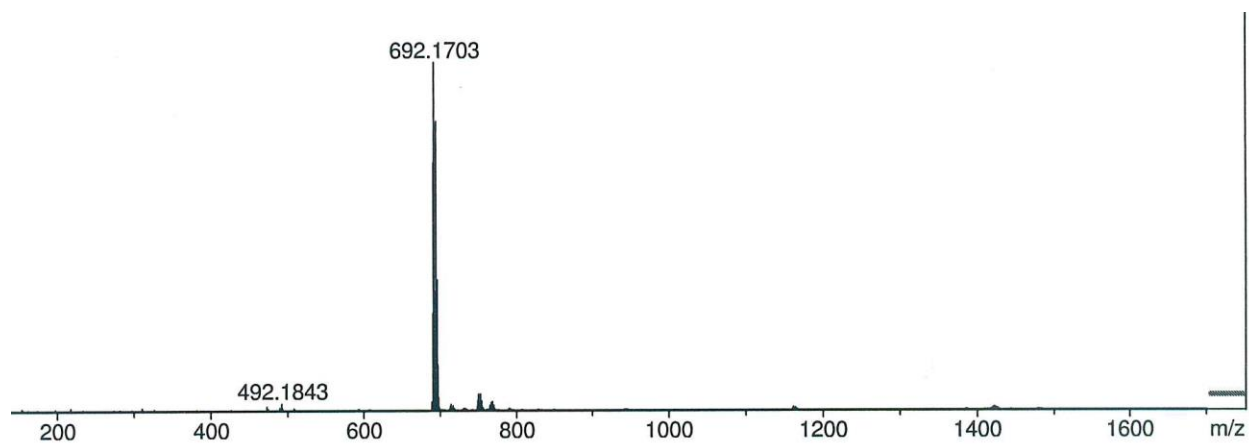
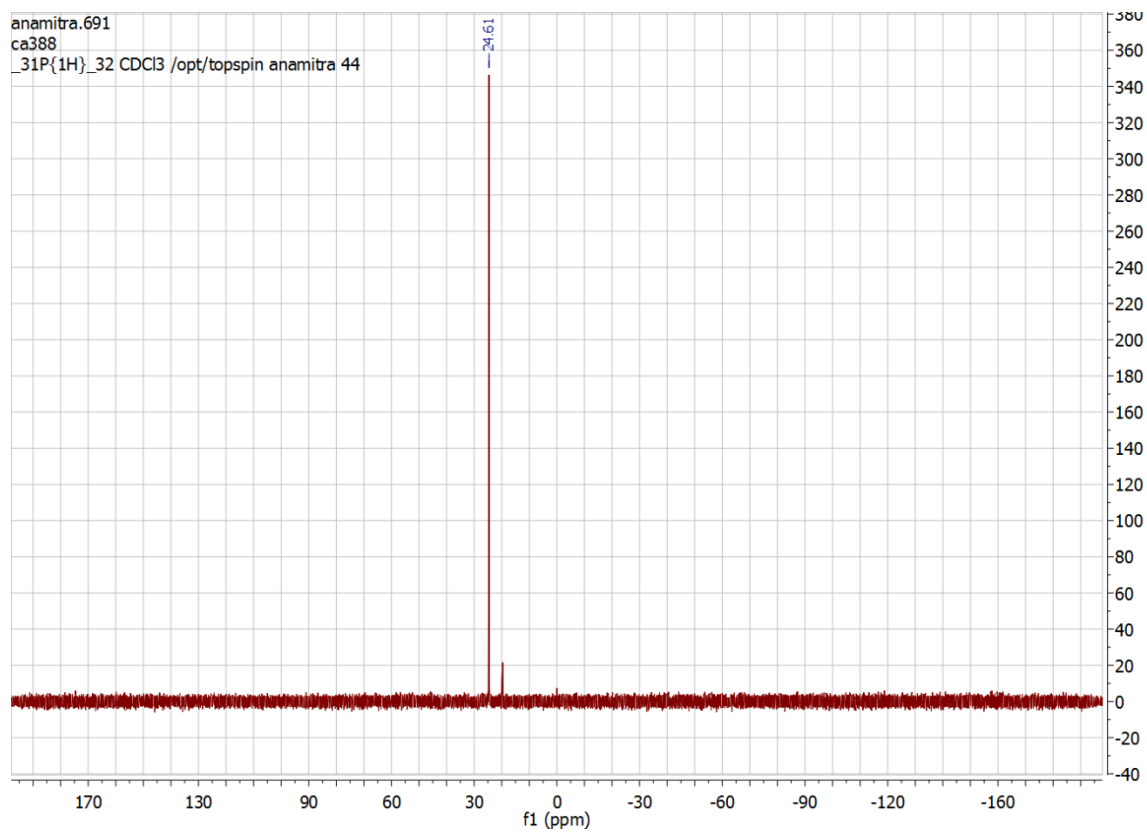
Spectra for complex 3:



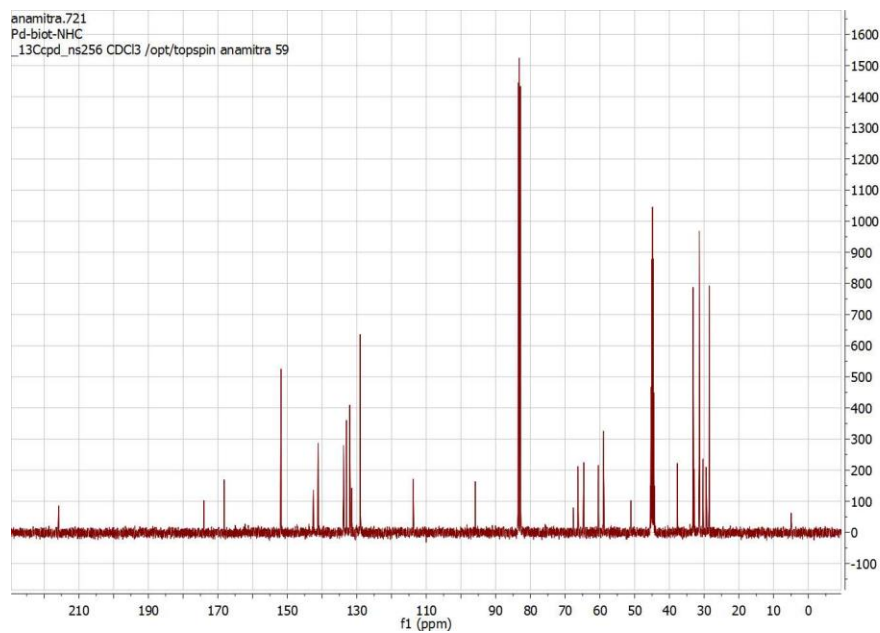
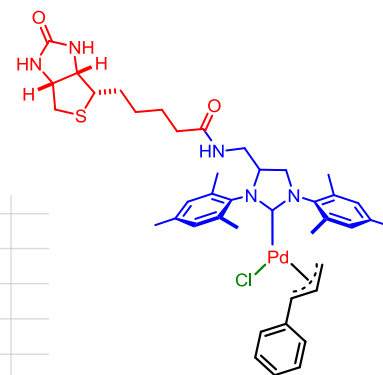
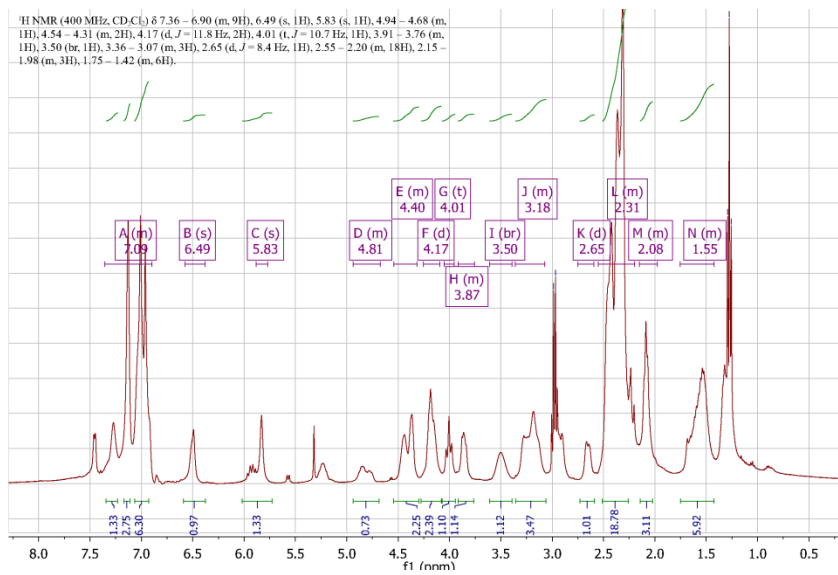


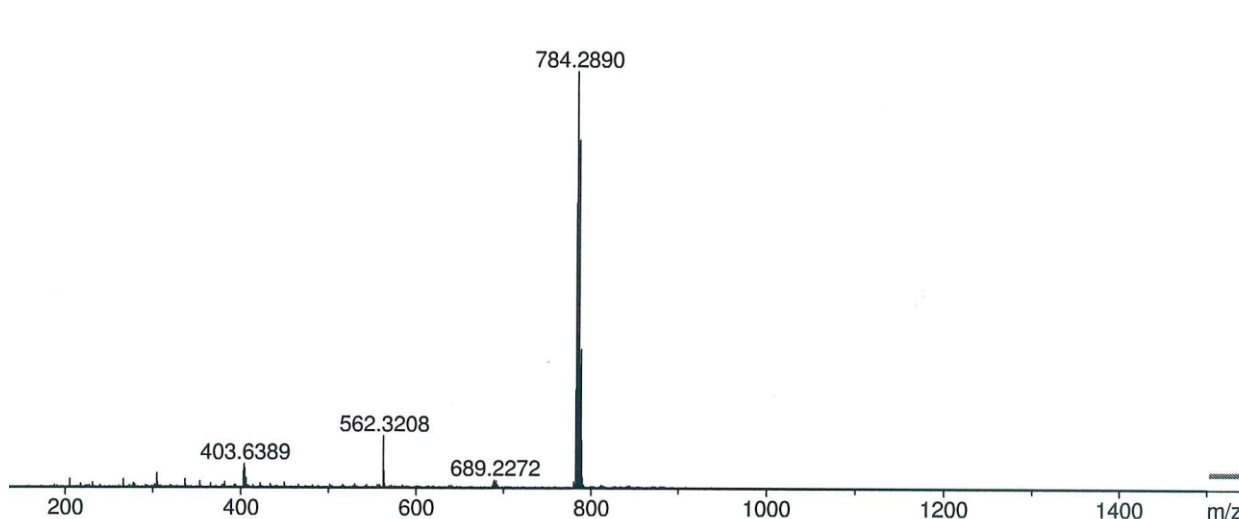
Spectra for complex 4:





Spectra for complex 5:





Literature Cited:

- [1] G. Klein, N. Humbert, J. Gradinaru, A. Ivanova, F. Gilardoni, U. E. Rusbandi, T. R. Ward, *Angew. Chem. Int. Ed.* **2005**, *44*, 7764; *Angew. Chem.* **2005**, *117*, 7942–7945
- [2] Reizelman, A.; Wigchert, S. C. M.; Bianco, C.; Zwanenburg, B. *Org. Biomol. Chem.* **2003**, *1*, 950–959.
- [3] Jordan, J. P.; Grubbs, R. H. *Angew. Chem. Int. Ed.* **2007**, *46*, 5152; *Angew. Chem.* **2007**, *119*, 5244–5247
- [4] E. A. Bayer, S. Ehrlich-Rogozinski, M. Wilchek, *Electrophoresis* **1996**, *17*, 1319.
- [5] N. Humbert, A. Zocchi, T. R. Ward, *Electrophoresis* **2005**, *26*, 47.
- [6] Newman, J. *Acta Cryst.* **2004**, *D60*, 610–612.
- [7] Stura, E. A.; Wilson, I. A. *J. Cryst. Growth.* **1991**, *110*, 270–282.
- [8] Vera, L.; Stura, E. A. *Cryst. Growth Des.* **2013**, *13*, 1878–1888.
- [9] Kabsch, W. *Acta Cryst.* **2010**, *D66*, 125.

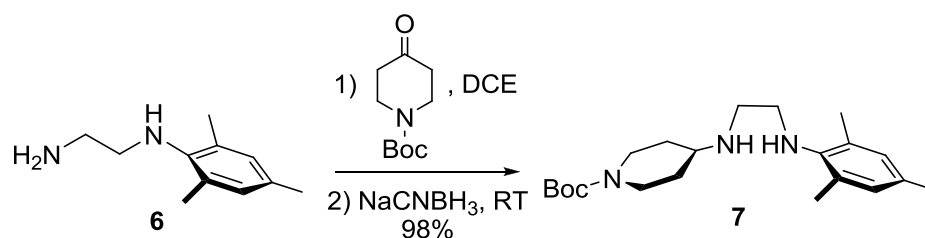
- [10] Adams, P. D.; Afonine, P. V.; Bunkoczi, G.; Chen, V. B.; Davis, I. W.; Echols, N.; Headd, J. J.; Hung, L. W.; Kapral, G. J.; Grosse-Kunstleve, R. W.; McCoy, A. J.; Moriarty, N. W.; Oeffner, R.; Read, R. J.; Richardson, D. C.; Richardson, J. S.; Terwilliger, T. C.; Zwart, P. C. *Acta Cryst.* **2010**, *D66*, 213.
- [11] Moriarty, N. W.; Grosse-Kunstleve, R. W.; Adams, P. D. *Acta Cryst.* **2009**, *D65*, 1074.
- [12] Chartoire, A.; Lesieur, M.; Slawin, A. M. Z.; Nolan, S. P.; Cazin, C. S. J. *Organometallics* **2005**, *30*, 4432.
- [13] Hanwell, M. D.; Curtis, D. C.; Lonie, D. C.; Vandermeersch, T.; Zurek, E.; Hutchison, G. R. *J. Cheminformatics* **2012**, *4*, 17.

APENDIX 2

Biotinylated Metathesis Catalysts: Synthesis and Performance in Ring Closing Metathesis

Experimental Section

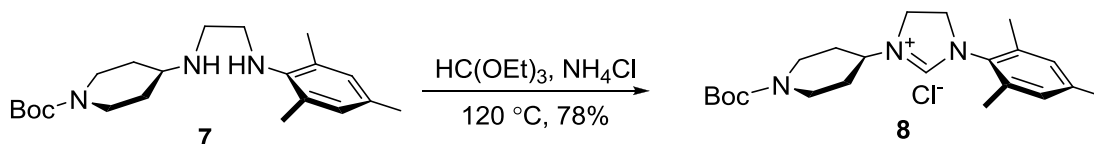
General: ^1H and ^{13}C spectra were recorded on a Bruker 400 MHz and 500 MHz. Chemical shifts are reported in ppm (parts per million). Signals are quoted as s (singlet), d (doublet), t (triplet), brs (broad) and m (multiplet). Electron Spray Ionization Mass Spectra (ESI-MS) were recorded on a Bruker FTMS 4.7T bioAPEX II. Analysis of the catalytic runs was performed on an Agilent 1100 reverse phase HPLC. All solvents were degassed prior to use.



tert-butyl 4-((2-(mesitylamino)ethyl)amino)piperidine-1-carboxylate **7**:¹

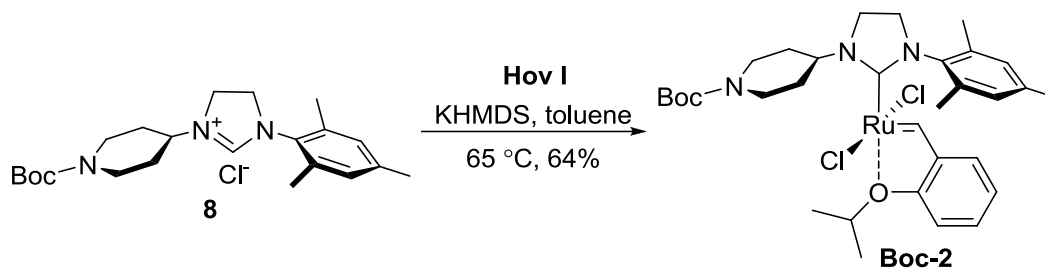
N-Mesitylethane-1,2-diamine **6** (1.09 g, 6.11 mmol, 1.00 eq.), *N*-*tert*-butoxy-carbonyl-4-piperidone (1.24 g, 6.11 mmol, 1.00 eq.) and acetic acid (0.350 ml, 6.11 mmol, 1.00 eq.) were suspended in DCE (15 mL) and the reaction mixture was heated at 40 °C for 10 min. resulting in the formation of an orange suspension. After cooling to room temperature and stirring for an additional hour, NaBH_3CN (576 mg, 9.16 mmol, 1.50 eq.) was added portionwise resulting in the dissolution of the solid. The reaction was stirred overnight. Then concentrated HCl was added dropwise. The solution was stirred until gas evolution ceased. The solution was evaporated to dryness, and the solid was triturated with water. Then NaOH was added until the whole solution became cloudy. Extraction with diethyl ether and drying under vacuum yielded diamine **7** as an essentially pure yellow oil (2.12 g, 98%). ^1H NMR (400 MHz, CDCl_3): δ = 6.82 (s,

2H), 4.82 (brs, 2H), 3.81- 3.87 (m, 1H), 3.21-3.24 (m, 4H), 2.76 (t, $^3J_{\text{HH}} = 8 \text{ Hz}$, 2H), 2.25 (s, 6H), 2.22 (s, 3H), 2.08-2.11 (m, 2H), 1.62-1.72 (m, 2H), 1.46 (s, 9H). ESI-MS for $\text{C}_{21}\text{H}_{35}\text{N}_3\text{O}_2$: 362.3 $[\text{M}+\text{H}]^+$.

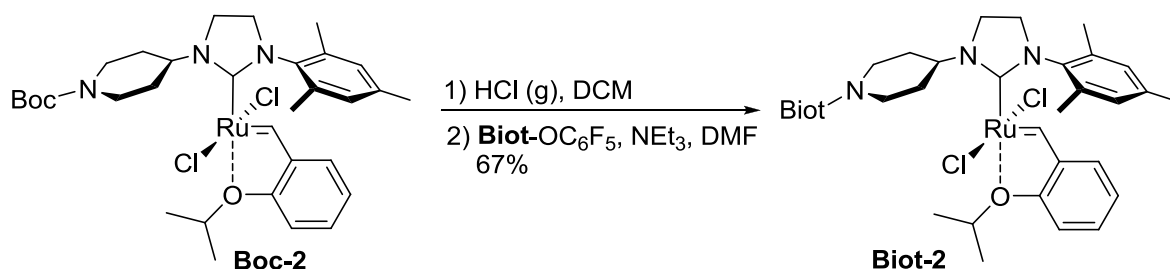


3-(1-(tert-butoxycarbonyl)piperidin-4-yl)-1-mesityl-4,5-dihydro-1H-imidazol-3-ium chloride 8:

An oven-dried round-bottom flask equipped with a magnetic stir-bar was charged with **7** (1.95 g, 5.40mmol, 1.00 eq.), NH_4Cl (289 mg, 5.40mmol, 1.00 eq.), and $\text{HC}(\text{OEt})_3$ (18.4 mL, 108 mmol, 20.0 eq.). The flask was equipped with a condenser and purged with N_2 prior to heating to 120 °C. The reaction was allowed to stir at 120 °C for 16 hours under a positive N_2 pressure. The reaction mixture was allowed to cool to room temperature, and the product precipitated upon adding ether. The grey precipitate was isolated by vacuum filtration and rinsed generously with ether to yield 1.70 g (78 %) of imidazolium salt **8**. ^1H NMR (400 MHz, CDCl_3): $\delta = 9.99$ (s, 1H), 6.93 (s, 2H), 4.86-4.92 (m, 1H), 4.19-4.21 (m, 1H), 4.14-4.17 (m, 4H), 2.82-3.02 (m, 2H), 2.31 (s, 6H), 2.28 (s, 3H), 2.11-2.15 (m, 2H), 1.86 (s, 1H), 1.60-1.70 (m, 2H), 1.46 (s, 9H). ^{13}C NMR (100 MHz, CDCl_3): $\delta = 159.1, 154.3, 140.2, 135.1, 130.6, 129.9, 99.9, 80.0, 55.6, 50.6, 45.5, 30.0, 28.3, 20.9, 17.9$. ESI-MS for $\text{C}_{22}\text{H}_{34}\text{ClN}_3\text{O}_2$: 372.3 $[\text{M}-\text{Cl}]^+$.

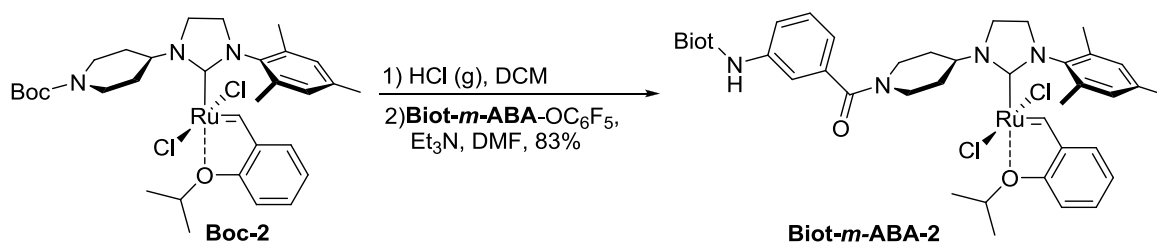
**Boc-2:**

A N_2 -filled schlenk-flask equipped with a magnetic stir-bar was charged with imidazolium salt **8** (94 mg, 0.23 mmol, 1.2 eq.), **KHMDS** (0.40 mg, 0.23 mmol, 1.2 eq.), and dry, degassed toluene (3.3 mL). The suspension was allowed to stir for 1 hour at room temperature. **Hov I** (0.11 mg, 0.19 mmol, 1.0 eq.) was added to the reaction mixture and the reaction was allowed to stir for 10 minutes at 65 °C. Purification was accomplished by flash column chromatography with 50% ethyl acetate in cyclohexane (product loaded with CH_2Cl_2). The green compound **Boc-2** was obtained in 64 % yield (85 mg). 1H NMR (400 MHz, CD_2Cl_2): δ = 16.16 (s, 1H), 7.55-7.59 (m, 1H), 7.09 (s, 2H), 6.95-7.00 (m, 3H), 5.14-5.20 (m, 2H), 4.33 (d, $^3J_{HH}$ = 12 Hz, 2H), 3.84-3.99 (m, 4H), 2.82-3.02 (m, 2H), 2.46 (s, 3H), 2.38-2.41 (m, 2H), 2.19 (s, 6H), 1.75-1.85 (m, 2H), 1.74-1.75 (d, $^3J_{HH}$ = 4 Hz, 6H), 1.49 (s, 9H). ESI-MS for $C_{32}H_{45}Cl_2N_3O_3Ru$: 656.5 $[M-Cl]^+$.



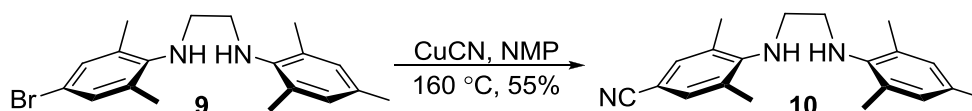
Biot-2:²

Complex **Boc-2** (31 mg, 0.045 mmol, 1.0 eq.) was dissolved in CH₂Cl₂ (2 mL) and HCl gas was purged through the solution for 1 h at room temperature. The gaseous HCl was generated by dropwise addition of concentrated H₂SO₄ to NH₄Cl. The solution was stirred for an additional 2 h at room temperature. Upon completion of the reaction as revealed by TLC (hexane/AcOEt 2:1), the solvent was evaporated under reduced pressure. The green solid was dissolved in DMF (2 mL) and biotin pentafluorophenol (18 mg, 0.045 mmol) and Et₃N (0.13 mL, 0.91 mmol) were added to the solution, followed by stirring at RT for 16 h. The solvent was removed under reduced pressure and the crude product was purified on silica gel using 10% MeOH/CH₂Cl₂ to yield **Biot-2** as a green solid (25 mg, 67%). ¹H NMR (400 MHz, CD₂Cl₂): δ = 16.17 (s, 1H), 7.97 (s, 1H), 7.55-7.60 (m, 1H), 7.09 (s, 2H), 6.95-7.00 (m, 3H), 5.14-5.20 (m, 2H), 4.84-4.96 (m, 2H), 4.53-4.57 (m, 1H), 4.35-4.38 (m, 1H), 4.07-4.11 (brs, 1H), 3.87-3.96 (m, 4H), 3.22 (m, 2H), 2.95 (s, 6H), 2.86 (s, 4H), 2.69-2.77 (m, 2H), 2.52 (m, 2H), 2.46 (s, 3H), 2.18 (s, 6H), 1.90 (m, 1H), 1.74 (d, ³J_{HH} = 4 Hz, 6H). HRMS [ESI(+)]calculated for C₃₇H₅₁ClN₅O₃RuS: 782.2445 [M-Cl]⁺; found 782.2414.

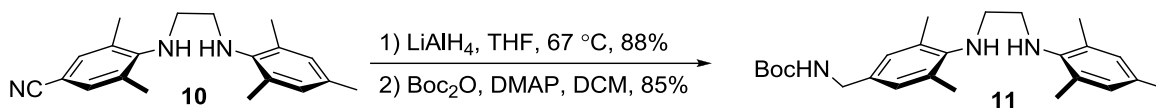


Biot-*m*-ABA-2:²

Complex **Biot-*m*-ABA-2** was synthesized following the same procedure used for the synthesis of **Biot-2**, using **Biot-*m*-ABA-OC₆F₅** (19 mg, 0.036 mmol, 0.80 eq.) and **Boc-2** (31mg, 0.045 mmol, 1.0 eq.). The crude product was purified on silica gel by 10% MeOH/DCM to yield **Biot-*m*-ABA-2** as a green solid (28 mg, 83%). ¹H NMR (400 MHz, CDCl₃): δ = 16.22 (s, 1H), 7.80-7.99 (m, 4H), 7.47-7.50 (m, 2H), 7.03 (s, 2H), 5.28-5.32 (m, 2H), 5.15-5.18 (m, 2H), 4.52 (brs, 3H), 3.91-3.94 (m, 6H), 3.44 (m, 2H), 2.95 (s, 5H), 2.87 (s, 4H), 2.43 (s, 4H), 2.15-2.19 (m, 10H), 1.76-2.01 (m, 9H). HRMS [ESI(+)]calculated for C₄₄H₅₆ClN₆O₄RuS: 901.2818 [M-Cl]⁺; found 901.2825.

**4-((2-(mesitylamino)ethyl)amino)-3,5-dimethylbenzonitrile 10:**³

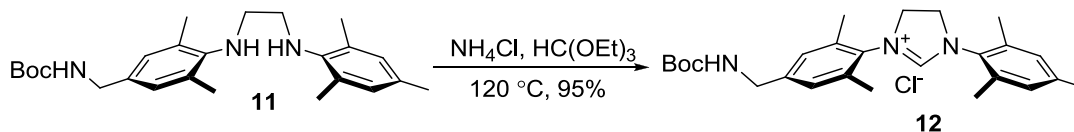
The mixture of **9** (1.50 g, 4.14 mmol, 1.00 eq.) and copper (I) cyanide (749 mg, 8.28 mmol, 1.00 eq.) in NMP (7 mL) was stirred at 160°C overnight. The reaction mixture was cooled to room temperature and water (10 mL) and ammonium hydroxide (10 mL) were added. The product was extracted with ethyl acetate (2×50 mL). The product was purified by flash chromatography (CH₂Cl₂) to give white solid (700 mg, 86%). ¹H NMR (400 MHz, CDCl₃): δ = 7.25 (s, 2H), 6.85 (s, 2H), 3.40 (t, ³J_{HH} = 8 Hz, 2H), 3.13 (t, ³J_{HH} = 8 Hz, 2H), 2.30 (s, 6H), 2.26 (s, 6H), 2.24 (s, 3H). ¹³C NMR (100 MHz, CDCl₃): δ = 150.7, 142.7, 133.0, 132.5, 130.5, 129.7, 127.4, 120.1, 102.7, 48.8, 48.3, 20.7, 19.2, 18.3. ESI-MS for C₂₀H₂₅N₃: 308.2 [M+H]⁺.



***tert*-butyl 4-((2-(mesitylamino)ethyl)amino)-3,5-dimethylbenzyl carbamate **11**:**

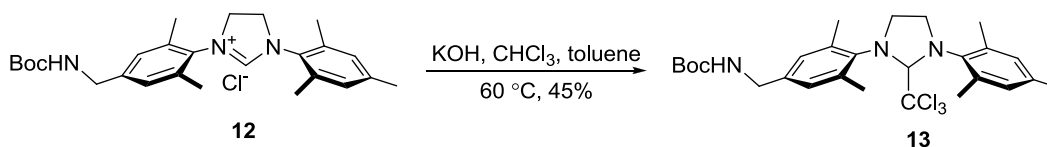
A solution of **10** (2.27 g, 7.41 mmol, 1.00 eq.) in THF (10 mL) was added dropwise to a suspension of LiAlH₄ (0.702 g, 18.5 mmol, 2.50 eq.) in THF (30 mL). The reaction mixture was refluxed for 3 hours and cooled to room temperature. The reaction mixture was quenched with 1.0N NaOH aqueous solution. The precipitate was filtered off and the solvent was evaporated in vacuo to provide the crude product, which can be used without purification. ¹H NMR (400 MHz, CDCl₃): δ = 6.95 (s, 2H), 6.84 (s, 2H), 3.74 (s, 2H), 3.16-3.20 (m, 4H), 2.32 (s, 6H), 2.28 (s, 6H), 2.24 (s, 3H). ¹³C NMR (400 MHz, CDCl₃): δ = 144.8, 143.3, 137.0, 131.6, 129.9, 129.8, 129.6, 127.8, 49.2, 49.1, 46.1, 20.6, 18.7, 18.4. ESI-MS for C₂₀H₂₉N₃: 295.3 [M-NH₂]⁺. A round-bottom flask, equipped with a magnetic stir-bar, was purged with nitrogen and charged with the above crude product, Boc₂O (1.4 g, 6.4 mmol, 1.0 eq.), and degassed CH₂Cl₂ (3 mL). The flask was cooled to 0 °C with an ice/water bath prior to the addition of DMAP (79 mg, 0.64 mmol, 0.10 eq.). The reaction was stirred at 0 °C for an additional 30 minutes prior to warming to room temperature and stirring for 2 hours. The reaction mixture was extracted with water followed by brine. The organic layer was dried over Na₂SO₄, and the CH₂Cl₂ evaporated. Chromatography on silica-gel 60 (15% EtOAc in hexanes) yielded 2.0 g (85%) carbamate **11** as a white powder. ¹H NMR (400 MHz, CDCl₃): δ = 6.91 (s, 2H), 6.83 (s, 2H), 4.73 (brs, 1H), 4.18 (d, ³J_{HH} =

4 Hz, 2H), 3.31 (brs, 1H), 3.12-3.20 (m, 4H), 2.29 (s, 6H), 2.27 (s, 6H), 2.23 (s, 3H), 1.46 (s, 9H). ^{13}C NMR (100 MHz, CDCl_3): δ = 155.9, 145.4, 143.3, 131.7, 130.0, 129.7, 129.6, 128.3, 110.1, 49.2, 49.1, 28.5, 27.0, 20.6, 20.0, 18.7, 18.5. ESI-MS for $\text{C}_{25}\text{H}_{37}\text{N}_3\text{O}_2$: 412.3 $[\text{M}+\text{H}]^+$.



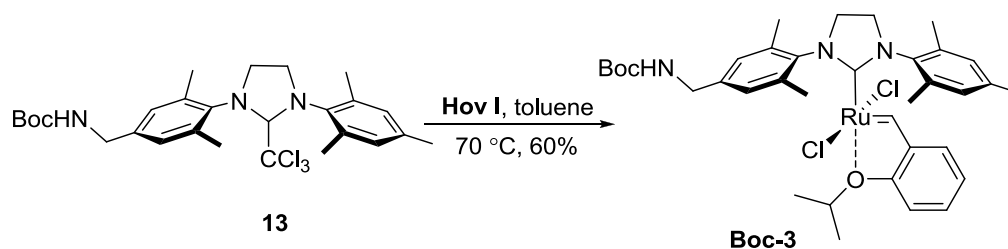
3-(4-(((tert-butoxycarbonyl)amino)methyl)-2,6-dimethylphenyl)-1-mesityl-4,5-dihydro-1H-imidazol-3-ium chloride 12:

An oven-dried round-bottom flask equipped with a magnetic stir-bar was charged with carbamate **11** (2.00 g, 5.05 mmol), NH_4Cl (270 mg, 5.05 mmol, 1.00 eq.), and $\text{HC}(\text{OEt})_3$ (16.6 mL, 101 mmol, 20.0 eq.). The flask was equipped with a condenser and purged with N_2 prior to stirring under an N_2 atmosphere at 120 °C for 16 hours. After cooling to RT, the product precipitated by addition of ether. The solid was isolated by vac-filtration and rinsed with ether to yield 2.20 g (95 %) of product **12** as a grey powder. ^1H NMR (400 MHz, CDCl_3): δ = 9.54 (s, 1H), 7.00 (s, 2H), 6.91 (s, 2H), 5.35 (brs, 1H), 4.51 (s, 4H), 4.15 (d, $^3J_{\text{HH}} = 4$ Hz, 2H), 2.36 (s, 6H), 2.34 (s, 6H), 2.25 (s, 3H), 1.41 (s, 9H). ^{13}C NMR (400 MHz, CDCl_3): δ = 163.9, 160.1, 155.9, 141.4, 140.0, 135.3, 134.7, 131.5, 130.1, 129.7, 127.8, 79.2, 57.3, 51.5, 43.5, 28.1, 20.8, 17.7. ESI-MS for $\text{C}_{26}\text{H}_{36}\text{ClN}_3\text{O}_2$: 422.3 $[\text{M}-\text{Cl}]^+$.



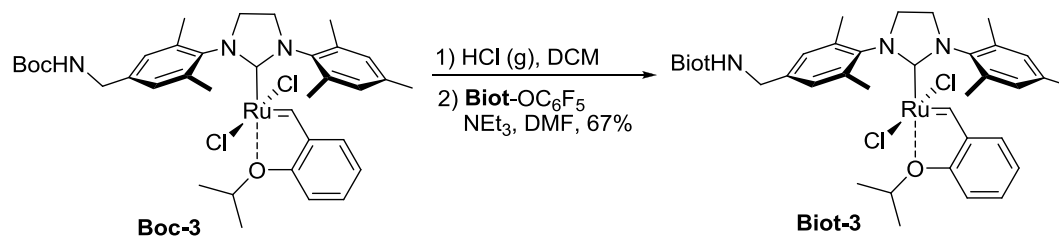
Chloroform adduct 13:⁴

Following the procedure of Grubbs, dry, degassed toluene (15 mL) was added to an oven-dried, 50 mL Schlenk flask equipped with stir bar and a reflux condenser. A large excess of powdered potassium hydroxide (5.37 g, 95.6 mmol, 127 eq.) was added to the flask, and the resulting suspension was stirred. Chloroform (0.405 mL, 5.00mmol, 6.67 eq.) was then added to the suspension. After 10 min at RT, **12** (0.344 g, 0.750mmol, 1.00 eq.) was added and the reaction mixture was heated at 60 °C for 75 min. The mixture was allowed to cool to room temperature and filtered. The filtrate was concentrated under vacuum to give a light brown solid. This crude product was purified by column chromatography (20% ethyl acetate/hexane, $R_f = 0.2$) to yield 0.185 g (45 %) of the desired chloroform adduct **13** as a light yellow solid. ¹H NMR (400 MHz, CDCl₃): $\delta = 6.95$ (s, 1H), 6.92 (s, 1H), 6.87 (s, 1H), 6.83 (s, 1H), 5.58 (s, 1H), 4.76 (brs, 1H), 4.22 (d, $^3J_{\text{HH}} = 4$ Hz, 2H), 3.89-3.92 (m, 2H), 3.25-3.35 (m, 2H), 2.49 (s, 3 H), 2.47 (s, 6H), 2.45 (s, 3H), 2.25 (s, 3H), 1.47 (s, 9H).

**Boc-3:**

An oven-dried, 10 mL Schlenk tube was charged with **Hov I** (36 mg, 60 μ mol, 1.0 eq.), the chloroform adduct **13** (65 mg, 0.12 mmol, 2.0 eq.), and dry, degassed toluene (2 mL). The reaction mixture was heated at 70 °C for 90 min under a nitrogen

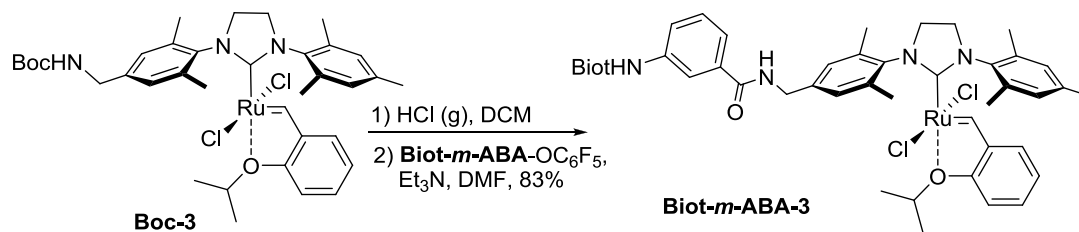
atmosphere. After cooling to room temperature, the solvent was removed under vacuum. The dark-brown solid was passed through a short silica gel column using ethyl acetate/cyclohexane (1:1) as eluent. The green band was collected and concentrated to give a green solid (27 mg, 60%). ^1H NMR (400 MHz, CDCl_3): δ = 16.52 (s, 1H), 7.48 (t, $^3J_{\text{HH}} = 8$ Hz, 1H), 7.16 (s, 2H), 7.07 (s, 2H), 6.92-6.96 (m, 1H), 6.83-6.87 (m, 1H), 6.79 (d, $^3J_{\text{HH}} = 8$ Hz, 1H), 4.84-4.94 (m, 1H), 4.36 (d, $^3J_{\text{HH}} = 4$ Hz, 2H), 4.18 (s, 4H), 2.51 (s, 6H), 2.46 (s, 6H), 2.41 (s, 3H), 1.50 (s, 9H), 1.26 (d, $^3J_{\text{HH}} = 4$ Hz, 6H). ESI-MS for $\text{C}_{36}\text{H}_{48}\text{Cl}_2\text{N}_3\text{O}_3\text{Ru}$: 706.3 $[\text{M}-\text{Cl}]^+$.



Biot-3:

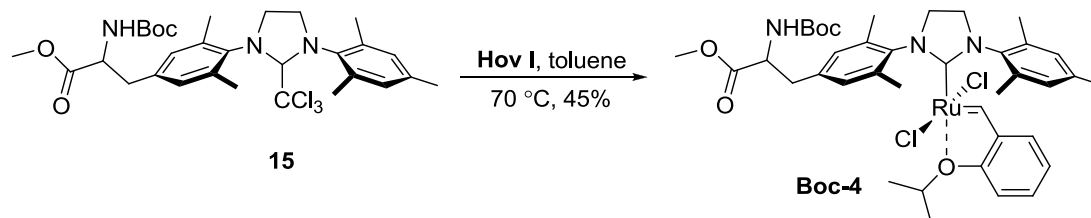
Complex **Biot-3** was synthesized following the same procedure used for the synthesis of **Biot-2**, using **Biot-OC₆F₅** (13 mg, 0.032 mmol, 0.80eq) and **Boc-3**(30 mg, 0.041mmol, 1.0 eq.). The crude product was purified on silica gel by 10% MeOH/ CH_2Cl_2 to yield **Biot-3** as a green solid (19 mg, 67%). ^1H NMR (400 MHz, CDCl_3): δ = 16.52 (s, 1H), 7.50 (t, $^3J_{\text{HH}} = 8$ Hz, 1H), 7.17 (s, 2H), 7.07 (s, 2H), 6.94-6.96 (m, 1H), 6.83-6.89 (m, 1H), 6.80 (d, $^3J_{\text{HH}} = 8$ Hz, 1H), 4.87-4.92 (m, 2H), 4.40-4.49 (m, 3H), 4.17 (s, 4H), 2.82 (s, 1H), 2.49 (brs, 10H), 2.40 (s, 3H), 2.28-2.30 (m, 3H), 2.18-2.23 (m, 1H), 1.42-1.50 (m, 2H), 1.17-1.32 (m, 12H), 0.83-0.94 (m, 3H). HRMS [ESI(+)]calculated for $\text{C}_{41}\text{H}_{53}\text{ClN}_5\text{O}_3\text{RuS}$: 832.2602 $[\text{M}-\text{Cl}]^+$; found 832.2593

EA calculated for $C_{41}H_{53}Cl_2N_5O_3RuS$: C, 56.35, H, 6.33, N 8.54; found: C, 56.74; H, 6.15; N, 8.07.



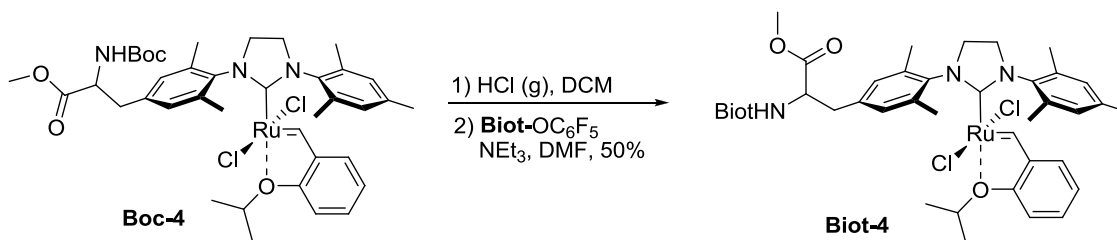
Biot-*m*-ABA-3:

Complex **Biot-*m*-ABA-3** was synthesized following the same procedure used for the synthesis of **Biot-2**, using **Biot-*m*-ABA-OC₆F₅** (6.8 mg, 0.012 mmol, 0.75eq) and **Boc-3** (12 mg, 0.016 mmol, 1.0 eq.). The crude product was purified on silica gel by 10% MeOH/CH₂Cl₂ to yield **Biot-*m*-ABA-3** as a green solid (11 mg, 83%). ¹H NMR (400 MHz, CDCl₃): δ = 16.56 (s, 1H), 8.01 (s, 1H), 7.45 (t, ³J_{HH} = 8 Hz, 1H), 7.05-7.08 (m, 4H), 6.93-6.95 (m, 2H), 6.82-6.86 (m, 2H), 6.78-6.80 (m, 2H), 4.87-4.91 (m, 1H), 4.16 (s, 6H), 3.80 (s, 2H), 3.45 (brs, 2H), 2.50 (brs, 6H), 2.46 (brs, 6H), 2.41 (brs, 3H), 1.90-1.94 (m, 4H), 1.67-1.72 (m, 4H), 1.57-1.61 (m, 2H), 1.27 (d, ³J_{HH} = 4 Hz, 6H). HRMS[ESI(+)]calculated for C₄₈H₅₈ClN₆O₄RuS: 951.2975 [M-Cl]⁺; found 951.2963



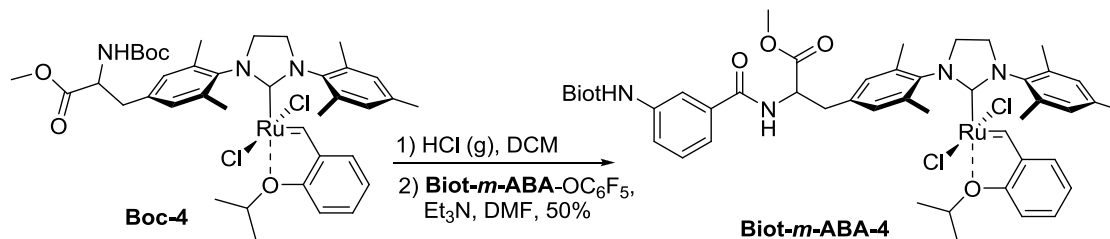
Boc-4:

An oven-dried, 10 mL Schlenk tube was charged with **Hov I** (118 mg, 0.197 mmol, 1.00 eq.), chloroform adduct **15** (242 mg, 0.394 mmol, 2.00 eq.), and dry, degassed toluene (20 mL). The reaction mixture was heated at 70 °C for 90 min under a nitrogen atmosphere. After cooling to RT, the solvent was removed under vacuum. The dark-brown solid was passed through a short silica gel column using ethyl acetate/cyclohexane (1:1) as eluent. The green band was collected and concentrated to give a green solid (0.720 g, 45%). ¹H NMR (400 MHz, CDCl₃): δ = 16.56 (s, 1H), 7.48 (t, ³J_{HH} = 8 Hz, 1H), 7.07 (s, 2H), 7.00-7.03 (m, 1H), 6.97 (s, 2H), 6.84-6.88 (m, 1H), 6.79 (d, ³J_{HH} = 8 Hz, 1H), 5.04 (brs, 1H), 4.87-4.93 (m, 1H), 4.63 (brs, 1H), 4.16 (s, 4H), 3.78 (s, 3H), 3.06-3.22 (m, 2H), 2.48 (brs, 12H), 2.40 (s, 3H), 1.56 (s, 9H), 1.28 (d, ³J_{HH} = 4 Hz, 6H). ESI-MS for C₃₉H₅₁Cl₂N₃O₅Ru : 778.3 [M-Cl]⁺.

**Biot-4**

Complex **Biot-4** was synthesized following the same procedure as for **Biot-2**, using **Biot-OC₆F₅** (8.8 mg, 0.021 mmol, 0.77eq) and **Boc-4** (22 mg, 0.027 mmol, 1.0). The crude product was purified on silica gel by 10% MeOH/CH₂Cl₂ to yield **Biot-4** as a green solid (10 mg, 50%). ¹H NMR (400 MHz, CDCl₃): δ = 16.54 (s, 1H), 7.48 (t, ³J_{HH} = 8 Hz, 1H), 7.07 (s, 2H), 6.94-6.97 (m, 3H), 6.86 (t, ³J_{HH} = 8 Hz, 1H), 6.79 (d, ³J_{HH} =

8 Hz, 1H), 4.85-4.93 (m, 2H), 4.64 (brs, 1H), 4.53 (brs, 1H), 4.32 (brs, 1H), 4.16 (s, 4H), 3.76 (s, 3H), 3.12-3.18 (m, 2H), 2.94-2.96 (m, 1H), 2.68-2.72 (m, 2H), 2.45 (brs, 12H), 2.39 (s, 3H), 1.81-1.85 (m, 2H), 1.57 (brs, 8H), 1.25-1.29 (m, 6H). HRMS [ESI(+)]calculated for $C_{44}H_{57}ClN_5O_5RuS$: 904.2815 $[M-Cl]^+$; found 904.2816.



Biot-*m*-ABA-4

Complex **Biot-*m*-ABA-4** was synthesized following the same procedure used for the synthesis of **Biot-2**, using **Biot-*m*-ABA-OC₆F₅** (11 mg, 0.021 mmol, 0.77 eq.) and **Boc-4** (22 mg, 0.027 mmol, 1.0 eq.). The crude product was purified on silica gel by 10% MeOH/CH₂Cl₂ to yield **Biot-*m*-ABA-4** as a green solid (12 mg, 50%). ¹H NMR (400 MHz, CDCl₃) δ = 16.56 (s, 1H), 8.01 (s, 1H), 7.45 (t, ³*J*_{HH} = 8 Hz, 1H), 7.05-7.08 (m, 6H), 6.82-6.86 (m, 2H), 6.79 (d, ³*J*_{HH} = 8 Hz, 2H), 4.87-4.93 (m, 1H), 4.16 (s, 6H), 3.80 (s, 3H), 3.47 (brs, 2H), 2.50 (brs, 6H), 2.46 (brs, 6H), 2.41 (brs, 3H), 1.90-1.94 (m, 4H), 1.63-1.72 (m, 4H), 1.53-1.61 (m, 2H), 1.27 (d, ³*J*_{HH} = 4 Hz, 6H), 1.06-1.11 (m, 6H). ESI-MS for $C_{51}H_{62}Cl_2N_6O_6RuS$: 1029.8 $[M-Cl]^+$.

General procedure for ring closing metathesis of *N*-tosyldiallylamine in CH₂Cl₂.

A 10mM stock solution of the complex (**Hov II**, **Biot-1** to **Biot-5** and **Biot-*m*-ABA-1** to **Biot-*m*-ABA-4**) was prepared by adding CH₂Cl₂ (60 μ L) to an aliquot of the

complex (0.61 μmol). A 111 mM stock solution of *N*-tosyldiallylamine (65 mg, 0.24 mmol in 2.2 ml CH_2Cl_2) was prepared in a separate vial. In a pyrex tube was added the solution of *N*-tosyldiallylamine (90 μL), followed by the addition of the catalyst's stock solution (10 μL) and the reaction flask was placed in a shaking incubator for 24 h at 37°C and 200 rounds per minute.

Upon completion of the reaction the reaction mixture was transferred to an eppendorf tube and MeOH (800 μL) was added to the tube. The solution was filtered, transferred into an HPLC vial and the sample was subjected to RP-HPLC to determine the conversion.

For experiments performed with ten-fold lower concentration of substrate 5 μL of previously prepared stock solutions of each complex was transferred into separate vials and 45 μL of CH_2Cl_2 was added to each of them. In the other vial 11 mM stock solution of *N*-tosyldiallylamine was prepared by adding CH_2Cl_2 (1800 μL) to 200 μL of previously used stock solution. Reactions were performed according to the same procedure.

General procedure for ring closing metathesis of *N*-tosyl/diallylamine in a mixture DMSO/ H_2O .

A 12.5 mM stock solution of the complex (**Hov II**, **Biot-1** to **Biot-5** and **Biot-*m*-ABA-1** to **Biot-*m*-ABA-4**) was prepared by adding DMSO (46 μL) to an aliquot of the complex (0.57 μmol). A 1.25 M stock solution of *N*-tosyldiallylamine (50.0 mg, 187 μmol in 149 μL DMSO) was prepared in a separate vial. In a pyrex tube was added water (84 μL), followed by the addition of the catalyst's stock solution (8 μL) and the

N-tosyldiallylamine (8 μ L of the stock solution), and the reaction flask was placed in an incubator for 24 h at 37°C.

Upon completion of the reaction the reaction mixture was transferred to an Eppendorf tube and MeOH (800 μ L) was added to the tube. The solution was transferred to an eppendorf tube and centrifuged at 14'000 rpm for 2 minutes. The supernatant (500 μ L) was transferred in an HPLC vial and the sample was subjected to RP-HPLC to determine the conversion.

General procedure for ring closing metathesis of 5-hydroxy-2-vinylphenyl acrylate in CH₂Cl₂.

A 2.5 mM stock solution of the complex (**Hov II**, **Biot-1** to **Biot-5** and **Biot-*m*-ABA-1** to **Biot-*m*-ABA-4**) was prepared by adding CH₂Cl₂ (92 μ L) to an aliquot of the complex (0.230 μ mol). A 27.8 mM stock solution of 5-hydroxy-2-vinylphenyl acrylate(15.0 mg, 78.8 μ mol in 2839 μ L CH₂Cl₂) was prepared in a separate vial. Reactions were performed according to the same procedure as reactions of *N*-tosyldiallylamine in CH₂Cl₂.

General procedure for ring closing metathesis of 5-hydroxy-2-vinylphenyl acrylate in a mixture DMSO/H₂O.

A 3.125 mM stock solution of the complex (**Hov II**, **Biot-1** to **Biot-5** and **Biot-*m*-ABA-1** to **Biot-*m*-ABA-4**) was prepared by adding DMSO (184 μ L) to an aliquot of the complex (0.575 μ mol). A 312.5 mM stock solution of 5-hydroxy-2-vinylphenyl acrylate(12 mg, 63 μ mol in 202 μ L DMSO) was prepared in a separate vial. Reactions

were performed according to the same procedure as reactions of *N*-tosyldiallylamine in DMSO/H₂O.

HPLC analysis. Column: XDB-C18, Eclipse by Agilent: 150 x 4.6 mm; 5 μm with guard column. Method: V_{injected}: 6 μl. Eluent (Solvent A: H₂O), (Solvent B: CH₃CN) 10% B at 0 min, 10% B at 5 min; 90% B at 15 min; 90 % B at 20 min. Detection at 210 nm.

Retention times: Phenylethanol (internal standard): 10.7 min; *N*-tosyl-3-pyrroline **20**: 13.5 min; *N*-tosyldiallylamine **19**: 15.3 min; umbelliferone**25**: 9.4 min; 5-hydroxy-2-vinylphenyl acrylate **24**: 12.9 min.

General Procedure for RCM with pure protein

In a 96 well-plate, 50 μM Sav in acetate buffer and 25μM of biotinylated catalyst in DMSO were added. After that, 10 mM coumarin precursor **24** is added to the reaction mixture at 37 °C in acetate buffer. The reaction mixture was incubated for 19 hours at 37 °C under air and measured by Tecan plate reader between 50 and 250 nm wavelengths. The fluorescence intensity were compared at maximum wavelength (100 nm) to determine relative activity.

References:

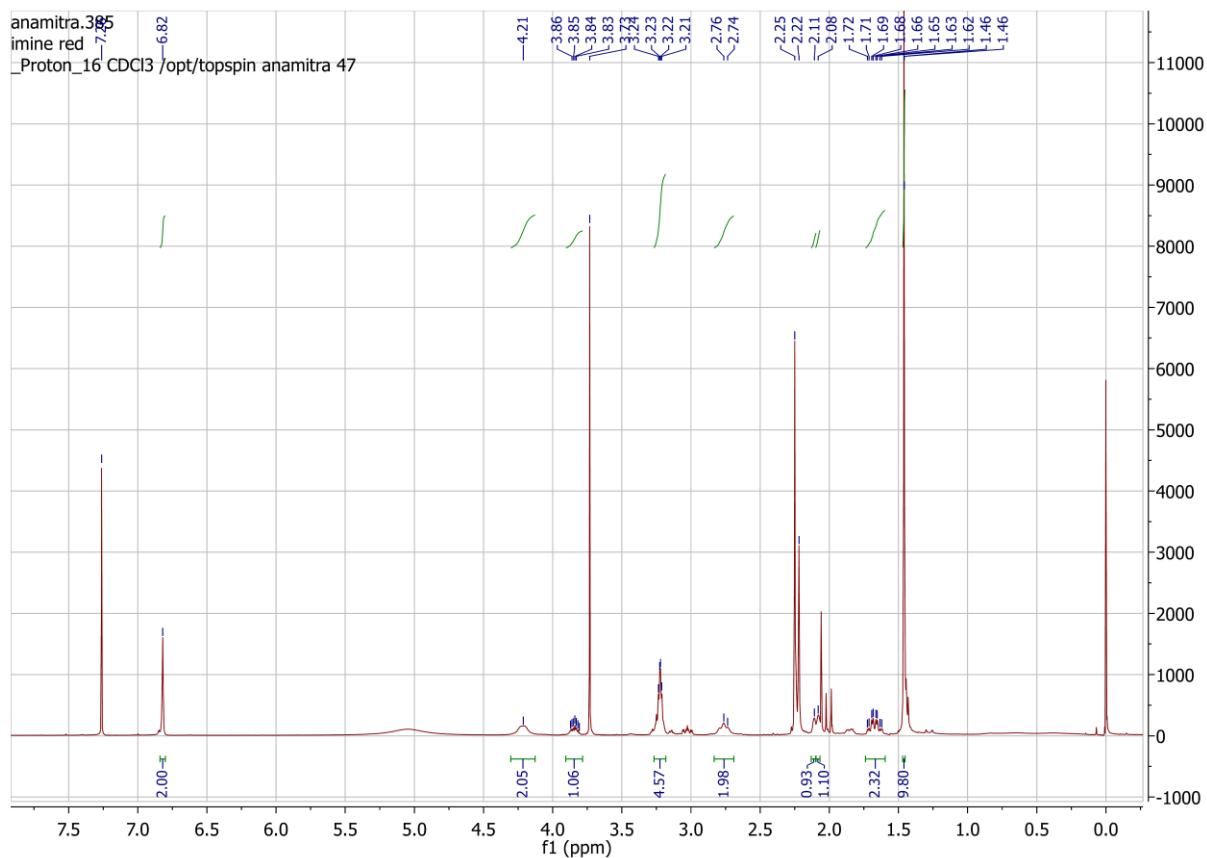
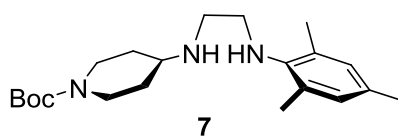
- [1] Roche S.P., Teyssot M., Gautier A. *Tetrahedron Letters* **2010**, 51, 1265.
- [2]Lo C., Ringenberg M., Gnant D., Wilson Y., Ward T.R. *Chem. Commun.* **2011**, 47, 12065.
- [3] a)Xu G., Gilbertson S. *Org. Lett.* **2005**, 7, 4605; b) Dinger M.B., Nieczypor P., Mol J.C. *Organometallics* **2003**, 22, 5291.

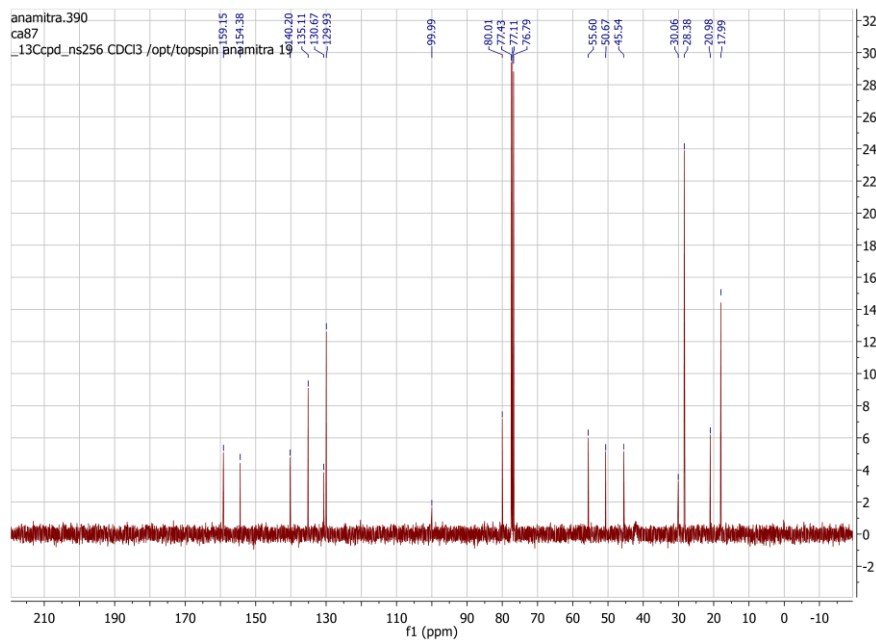
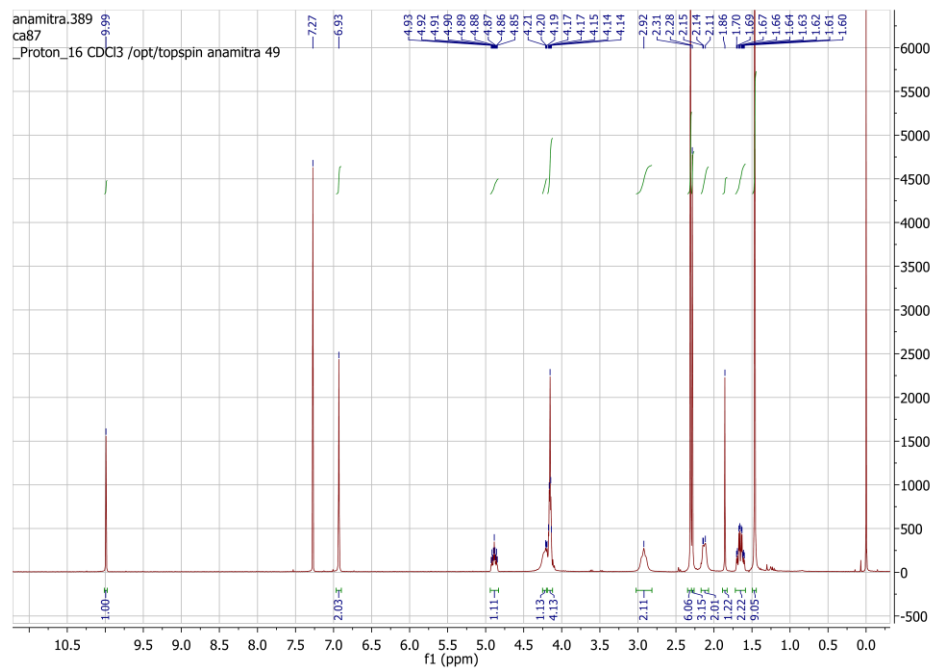
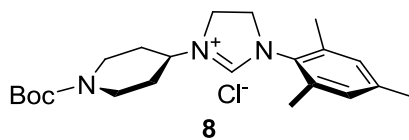
[4]Trnka T.M., Morgan J.P., Sanford M.S., Wilhelm T.E., Scholl M., Choi T.L., Ding S., Day M.W., Grubbs R.H. *J. Am. Chem. Soc.* **2003**,125, 2546.

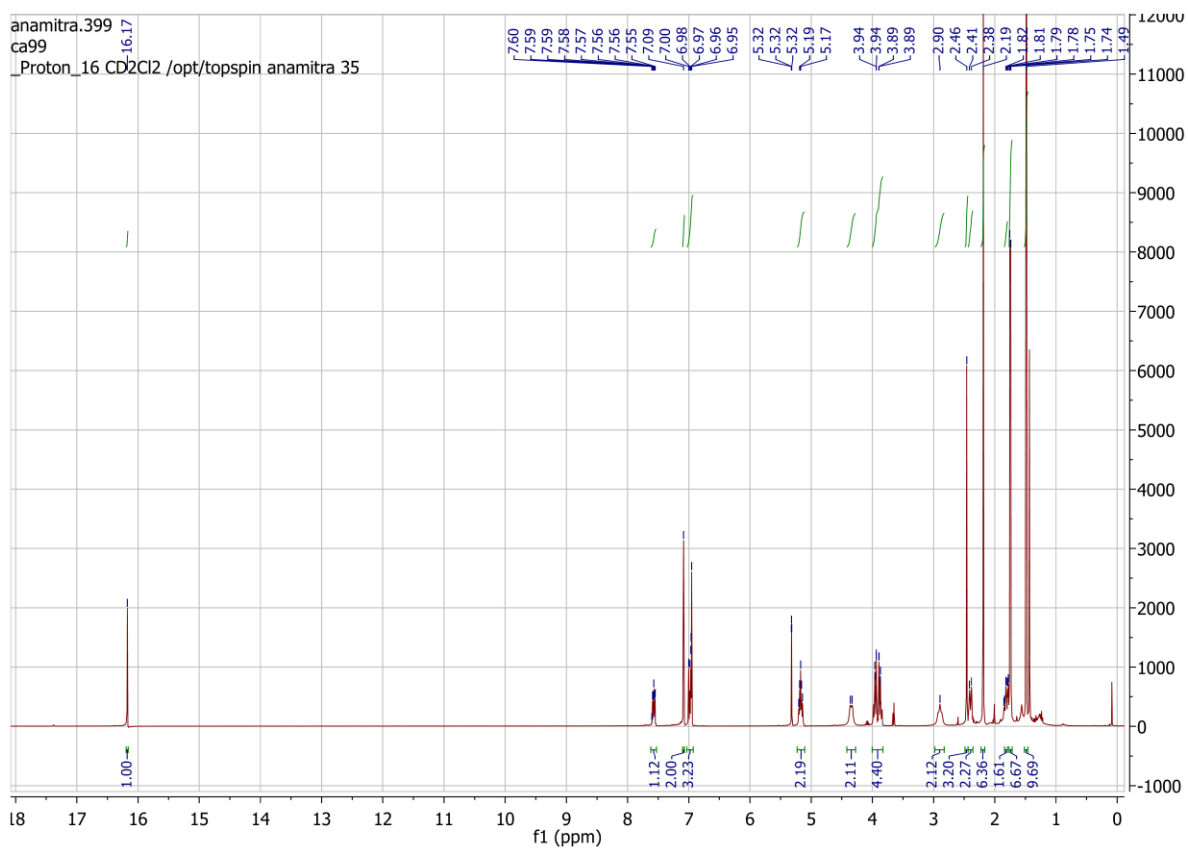
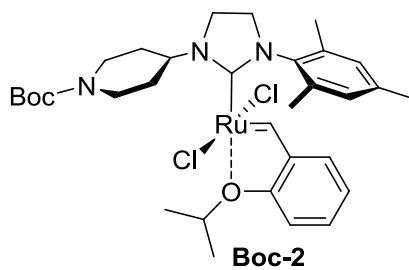
[5]Smith L.H.S., Nguyen T.T., Sneddon H.F., Procter D.J. *Chem. Commun.* **2011**, 47, 10821.

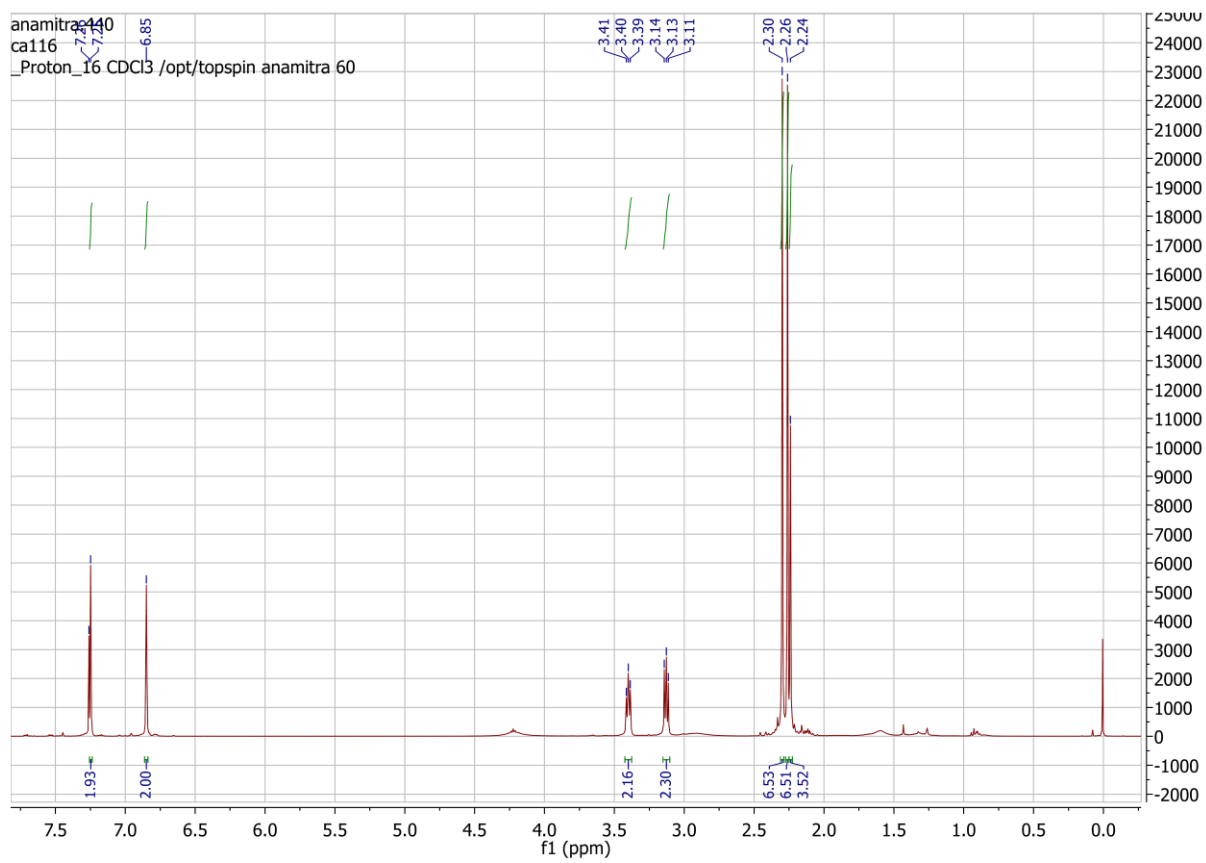
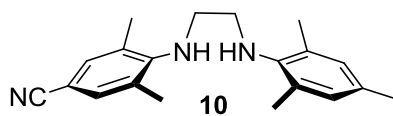
[6]Schmidt B., Krehl S., Kelling A., Schilde U. *J. Org. Chem.* **2012**, 77, 2360.

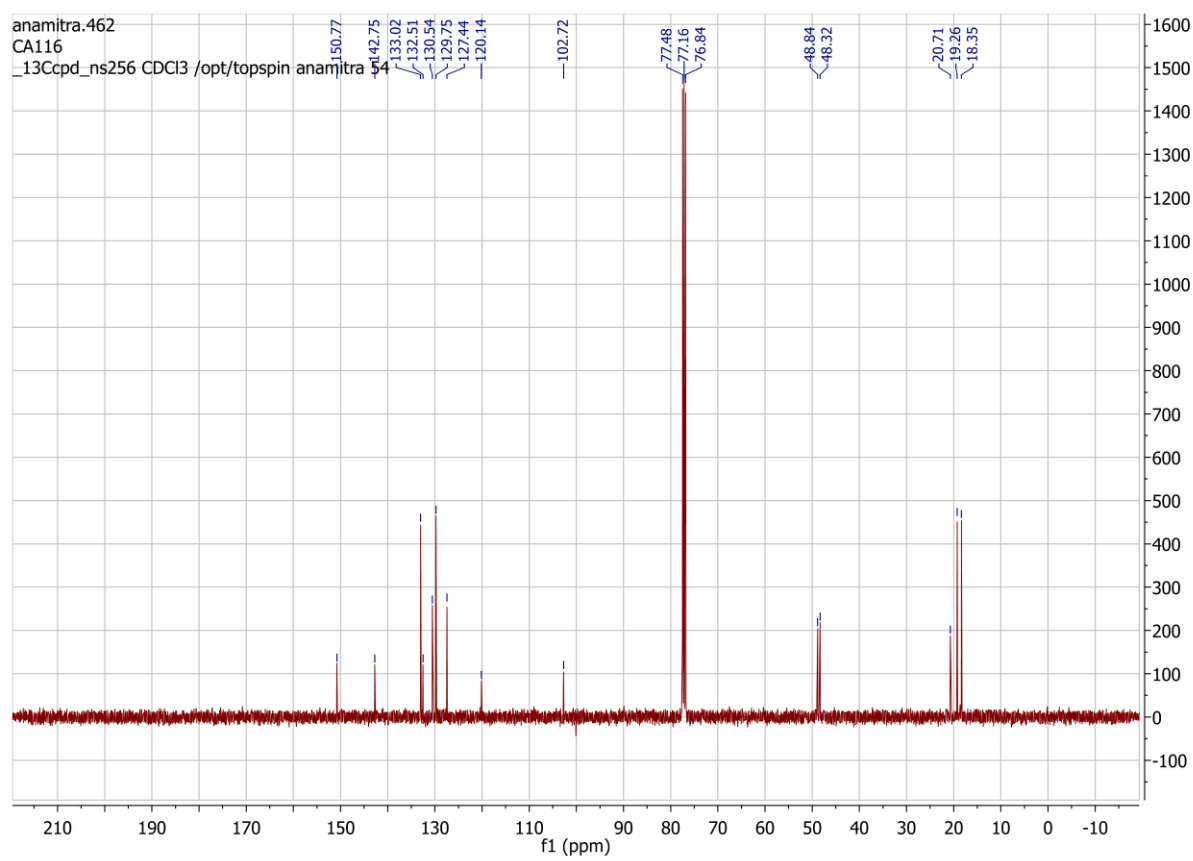
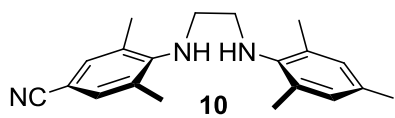
Spectra of the compounds:

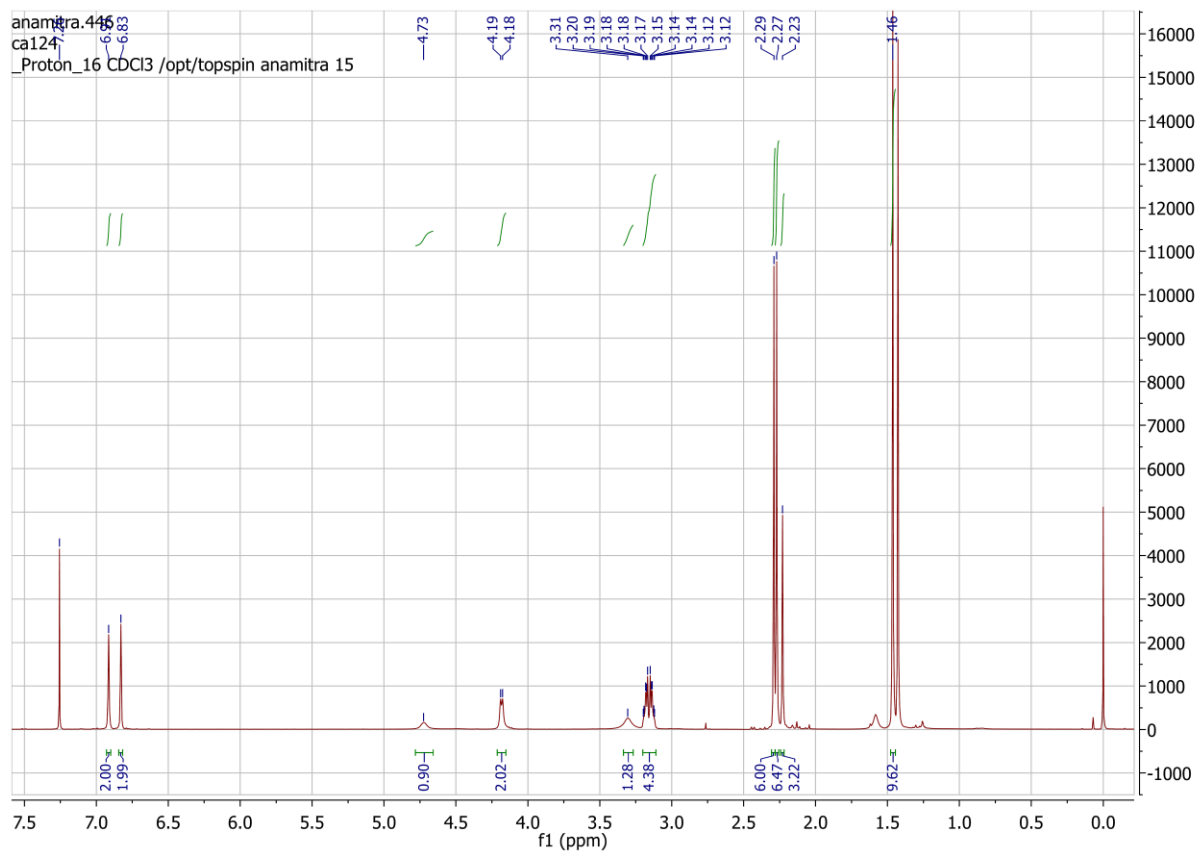
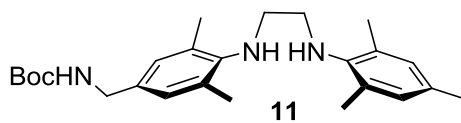


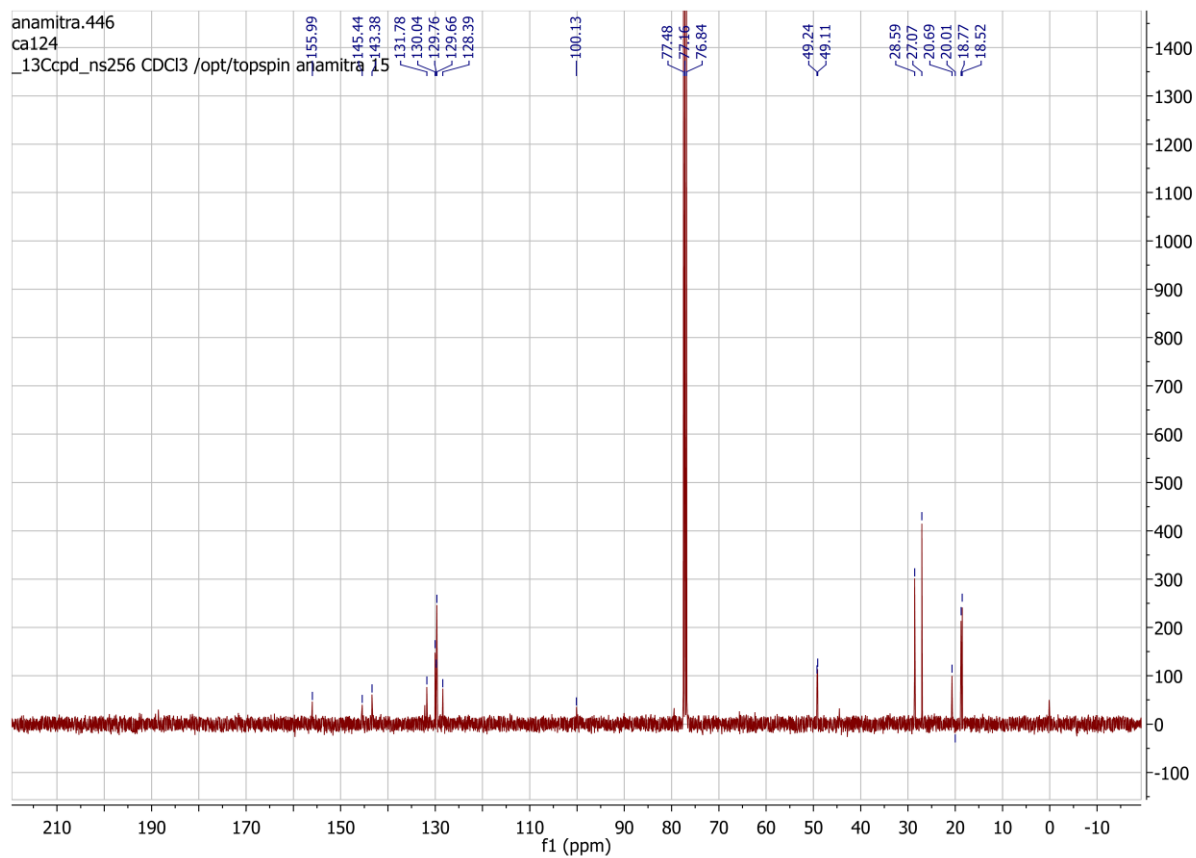
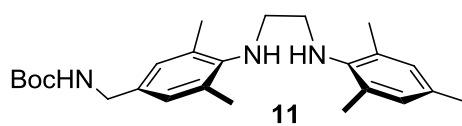


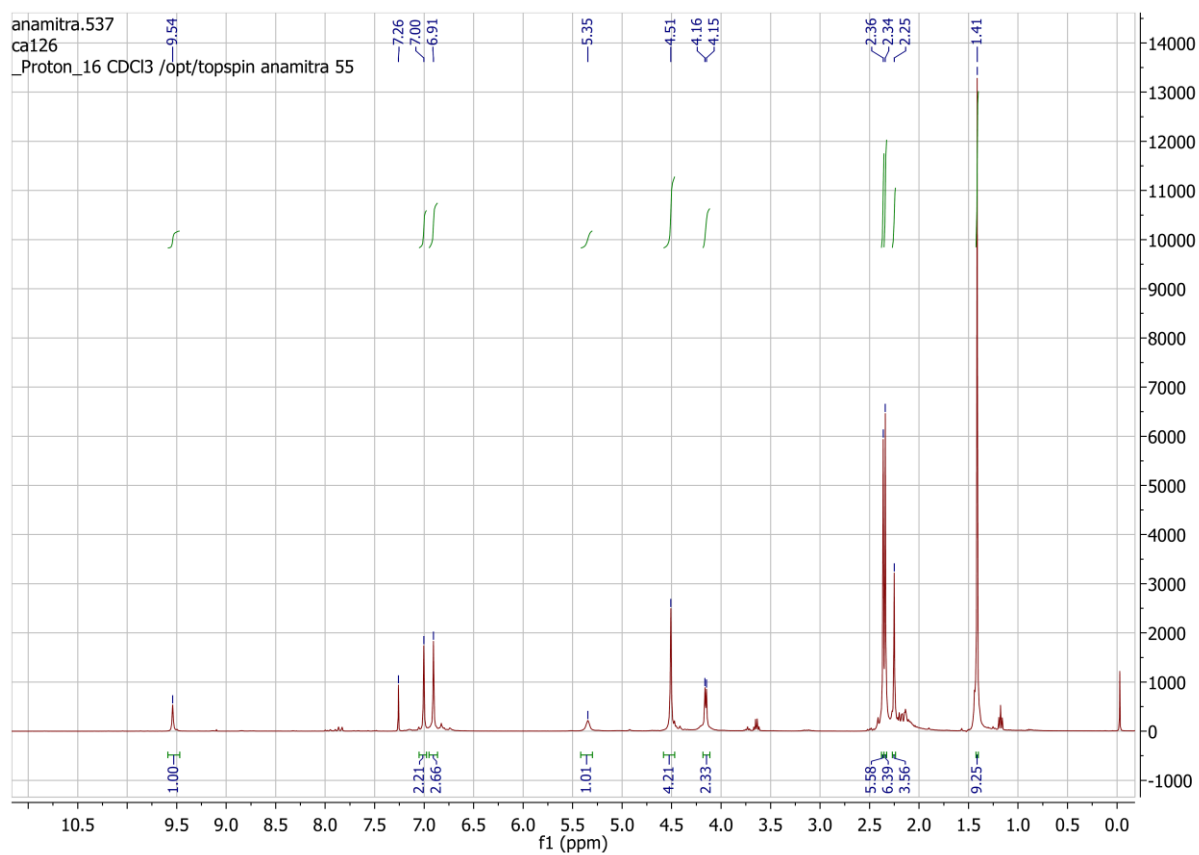
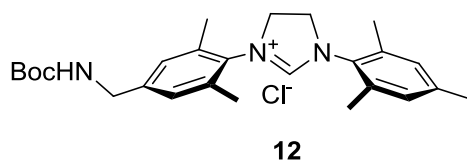


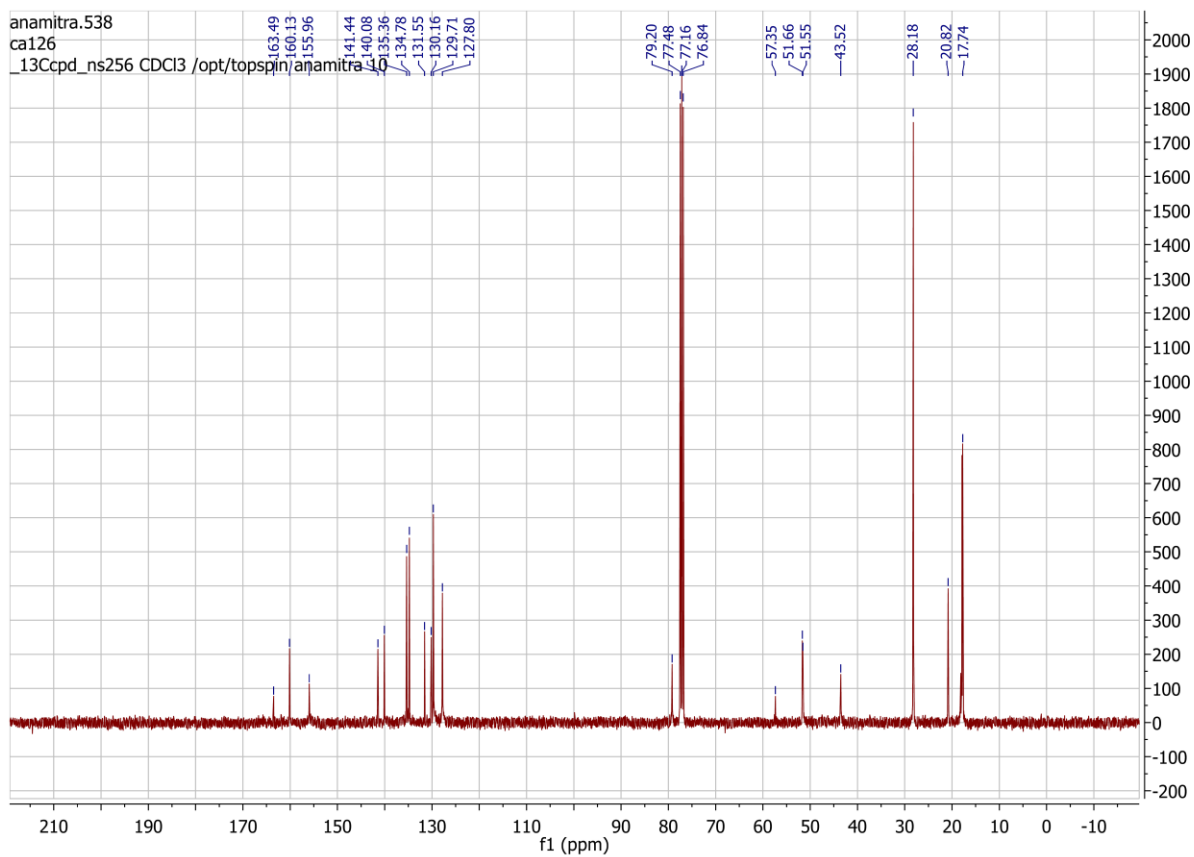
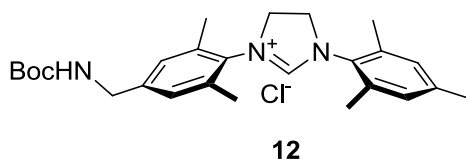


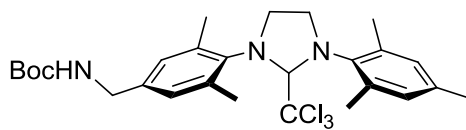




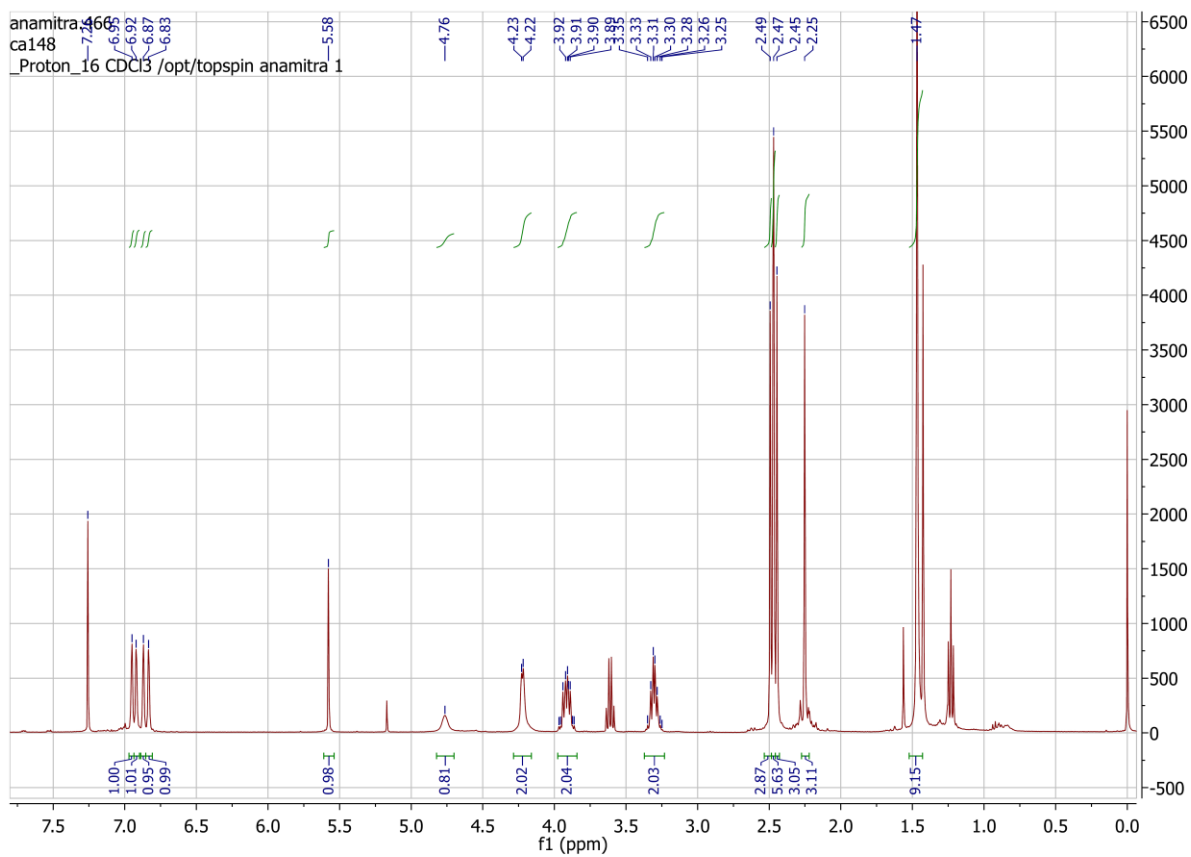


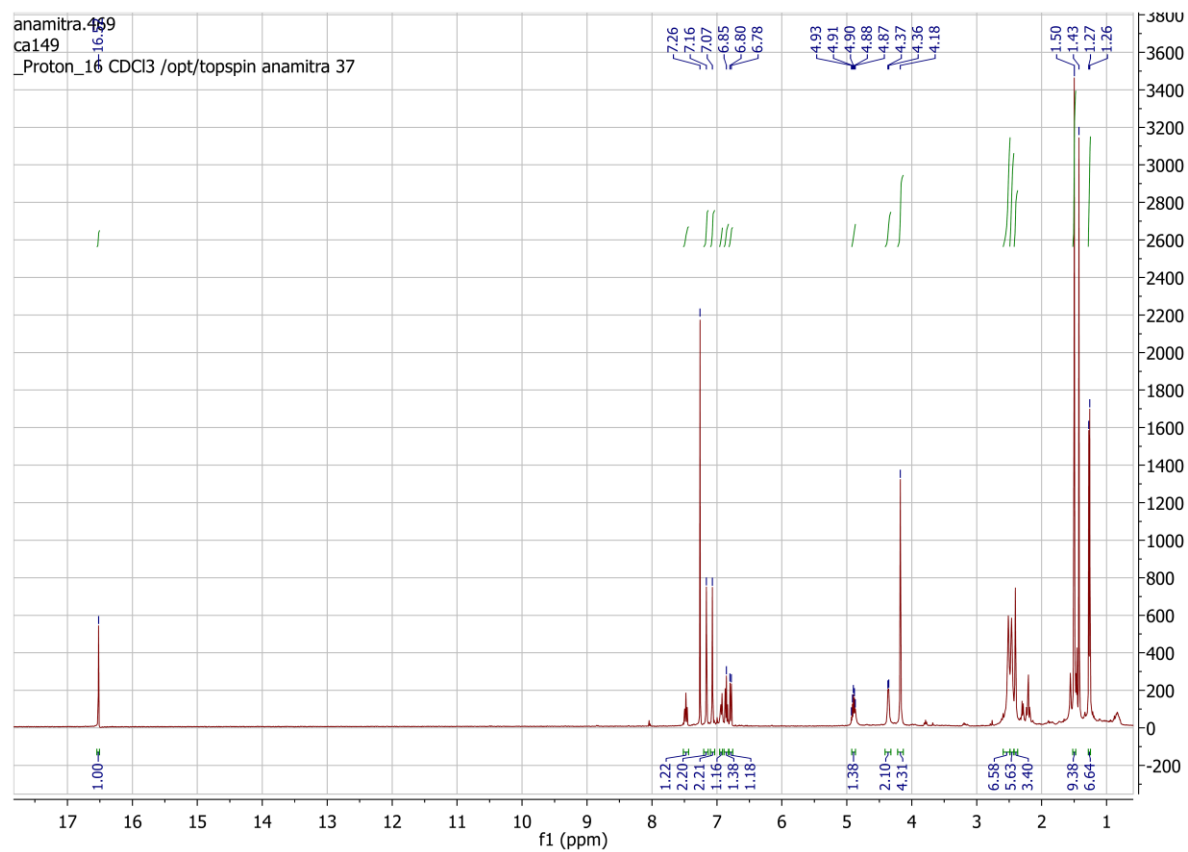
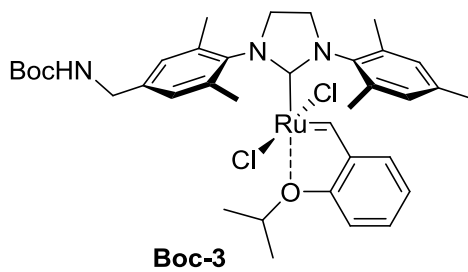


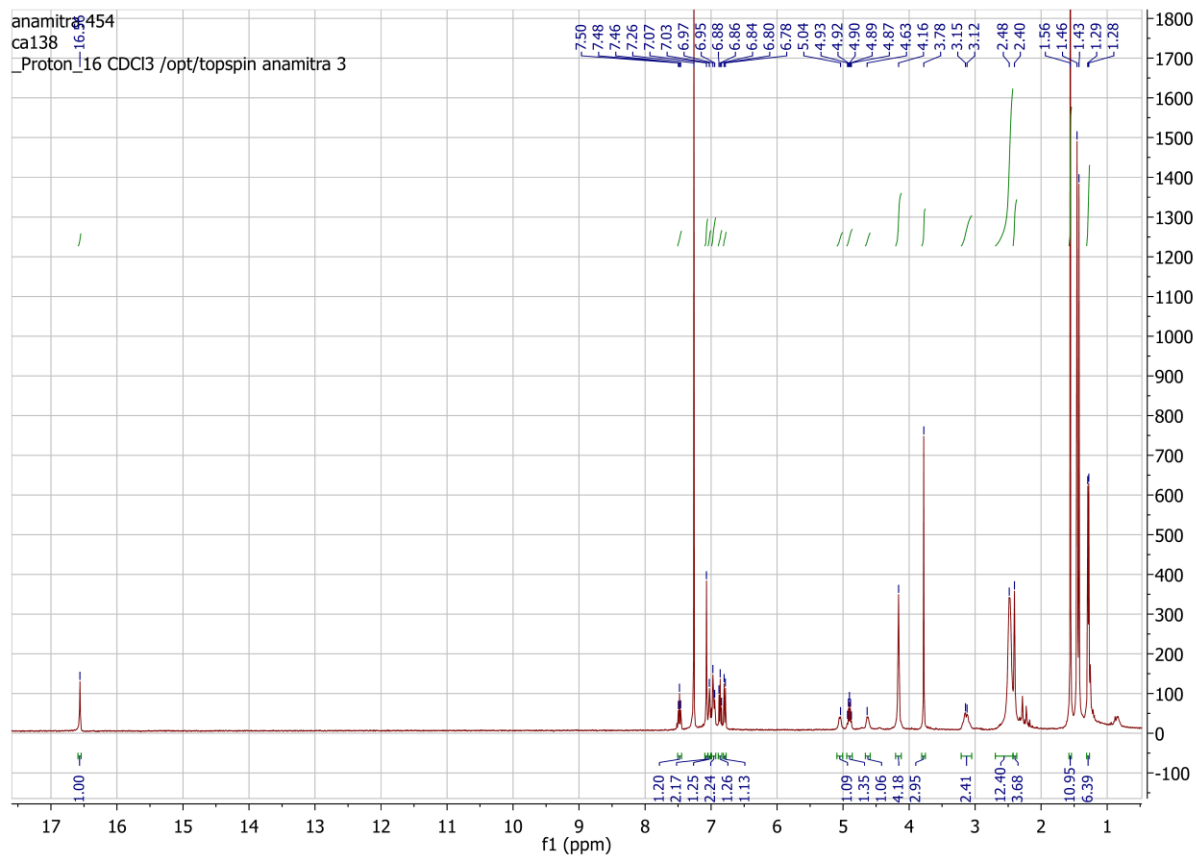
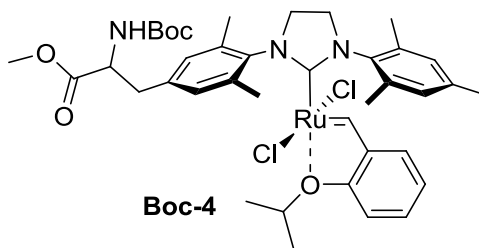


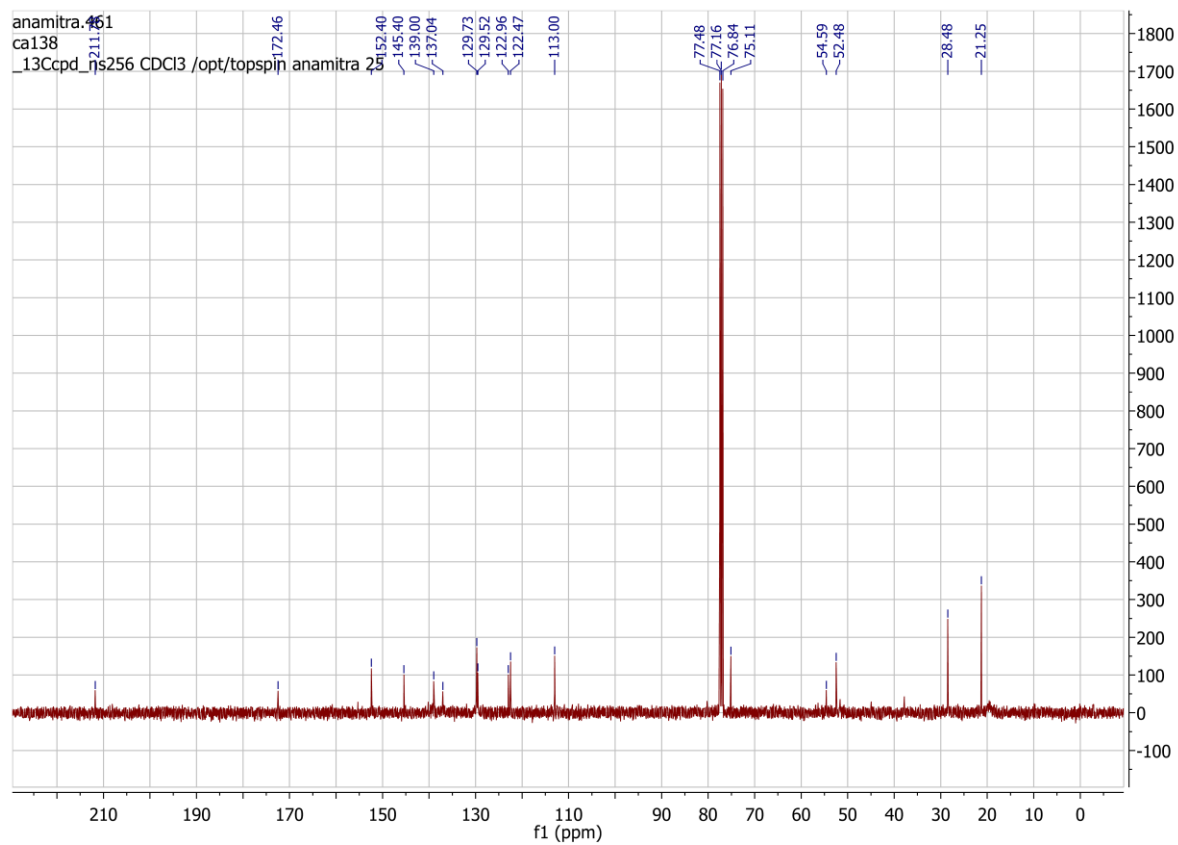
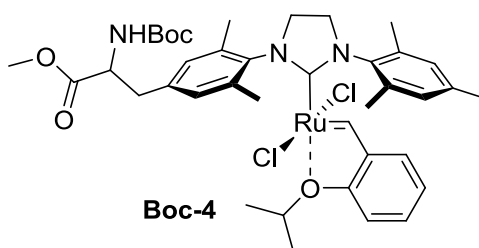


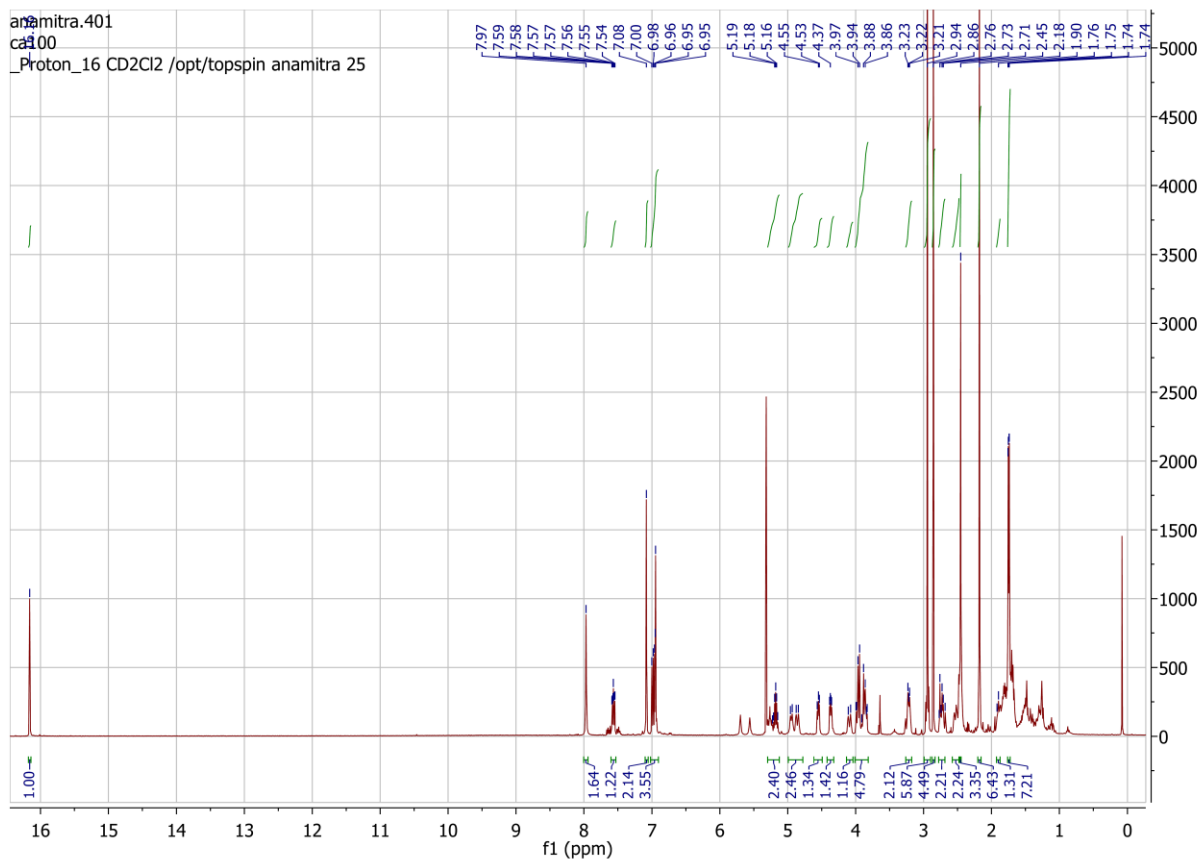
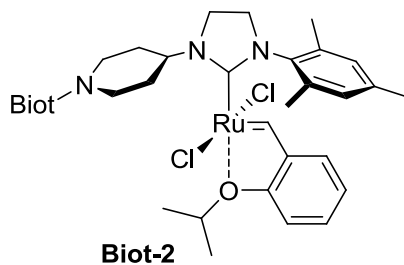
13





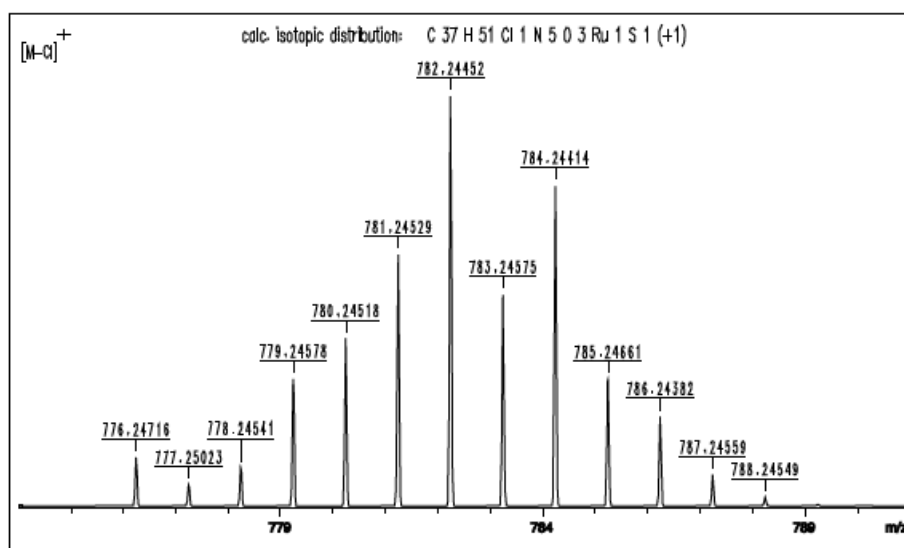
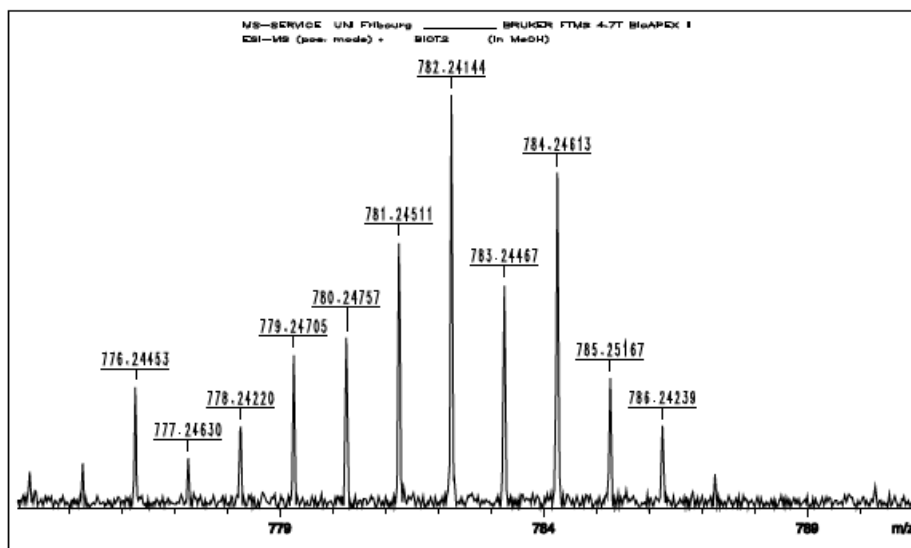


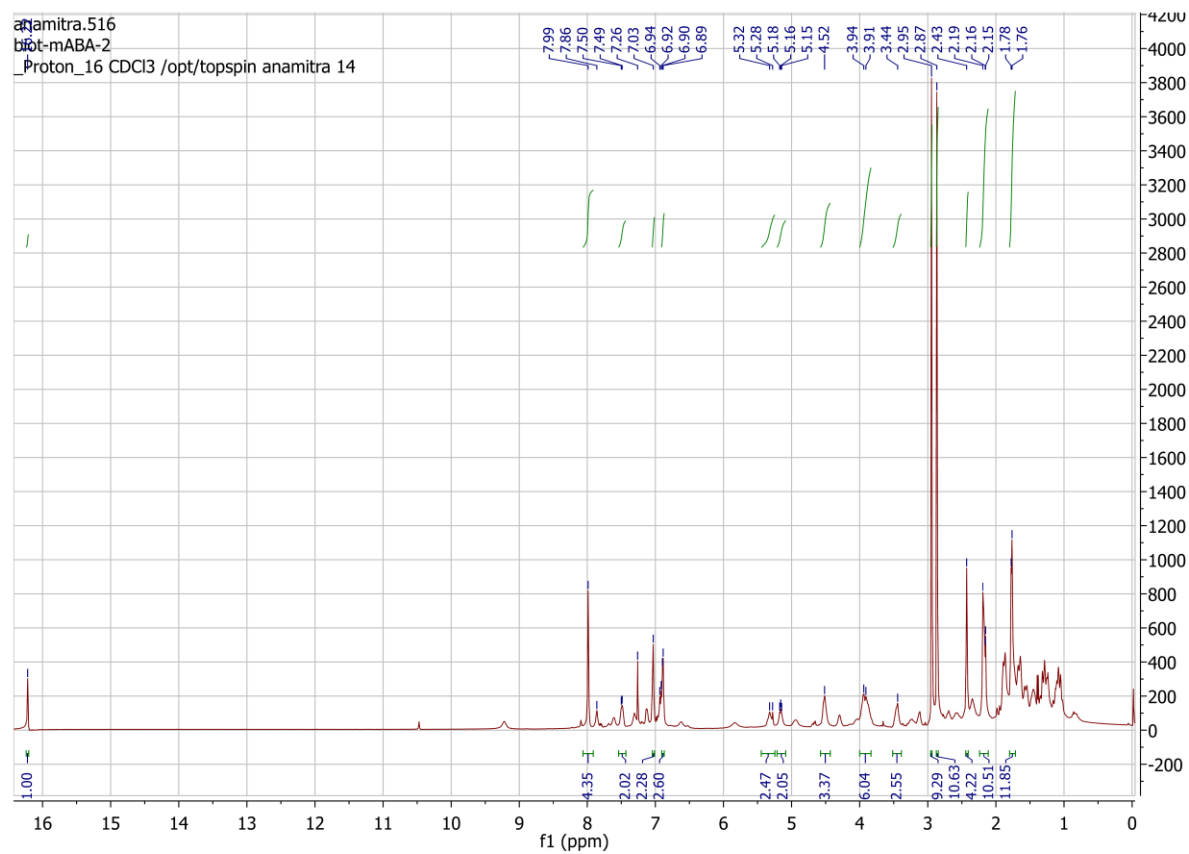
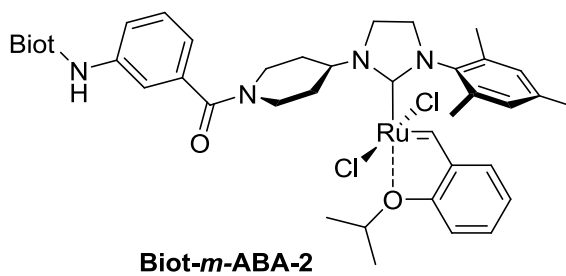






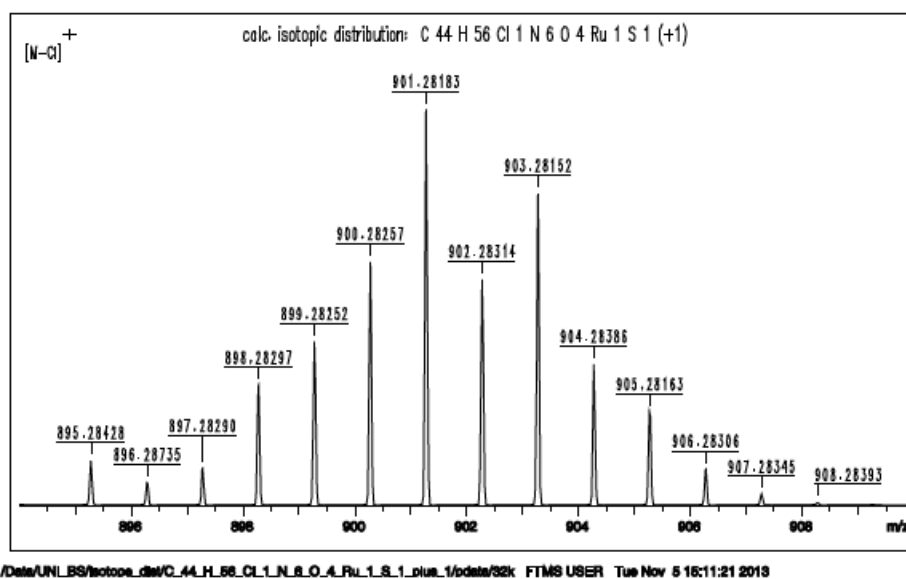
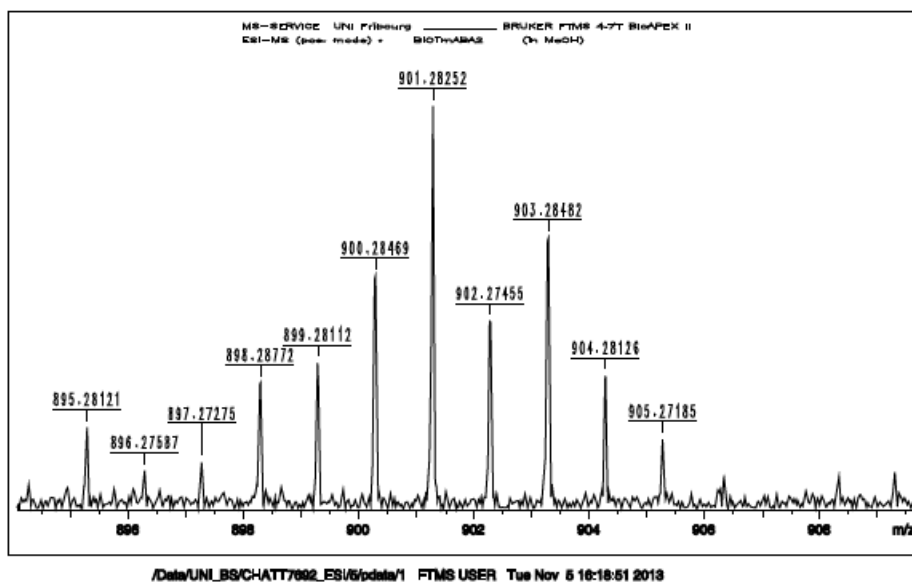
ESI-MS: BIOT2

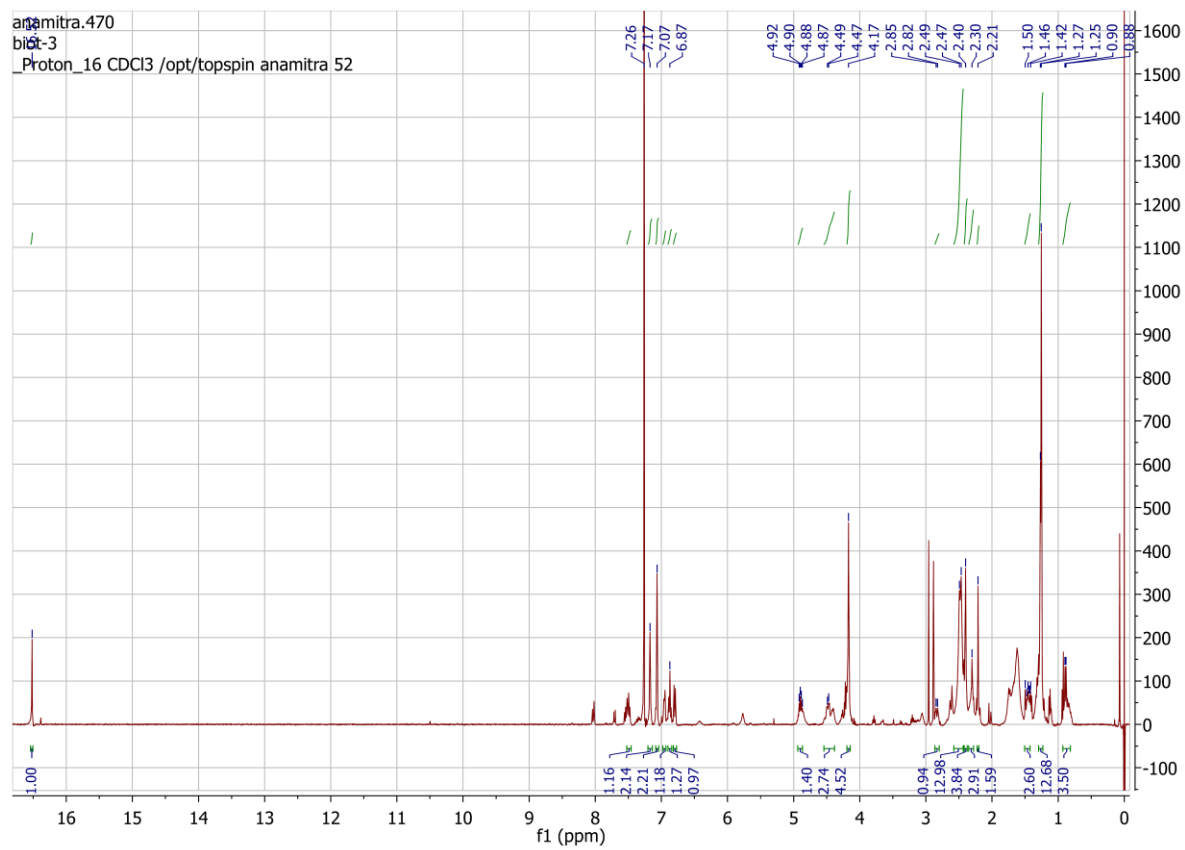
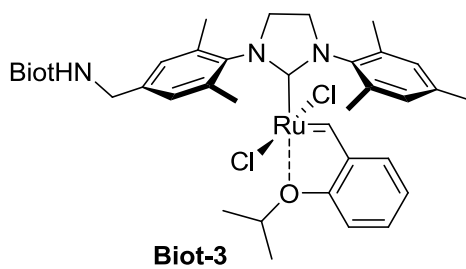


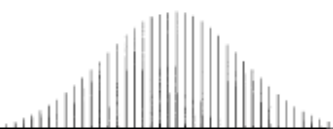




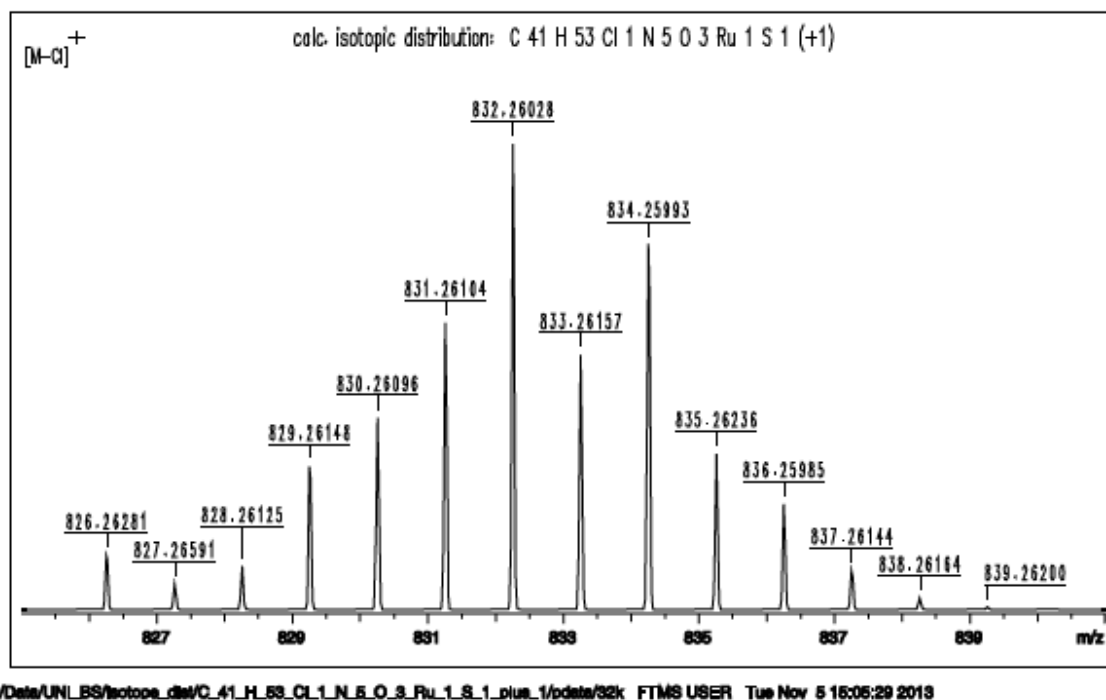
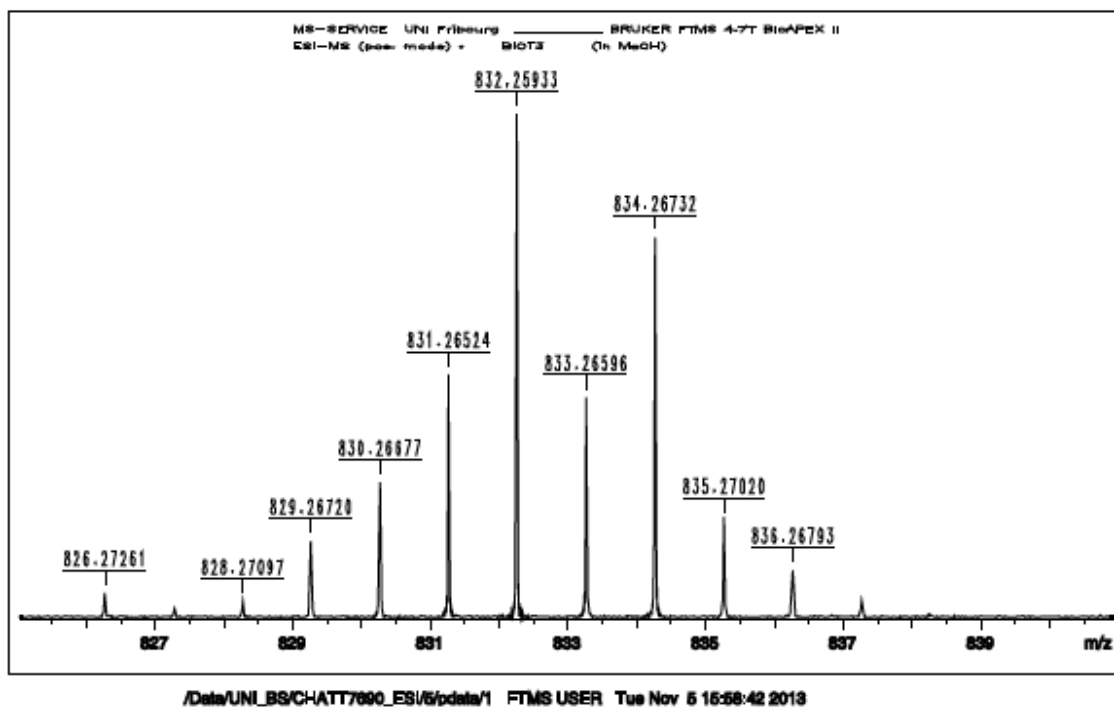
ESI-MS: BIOTmABA2

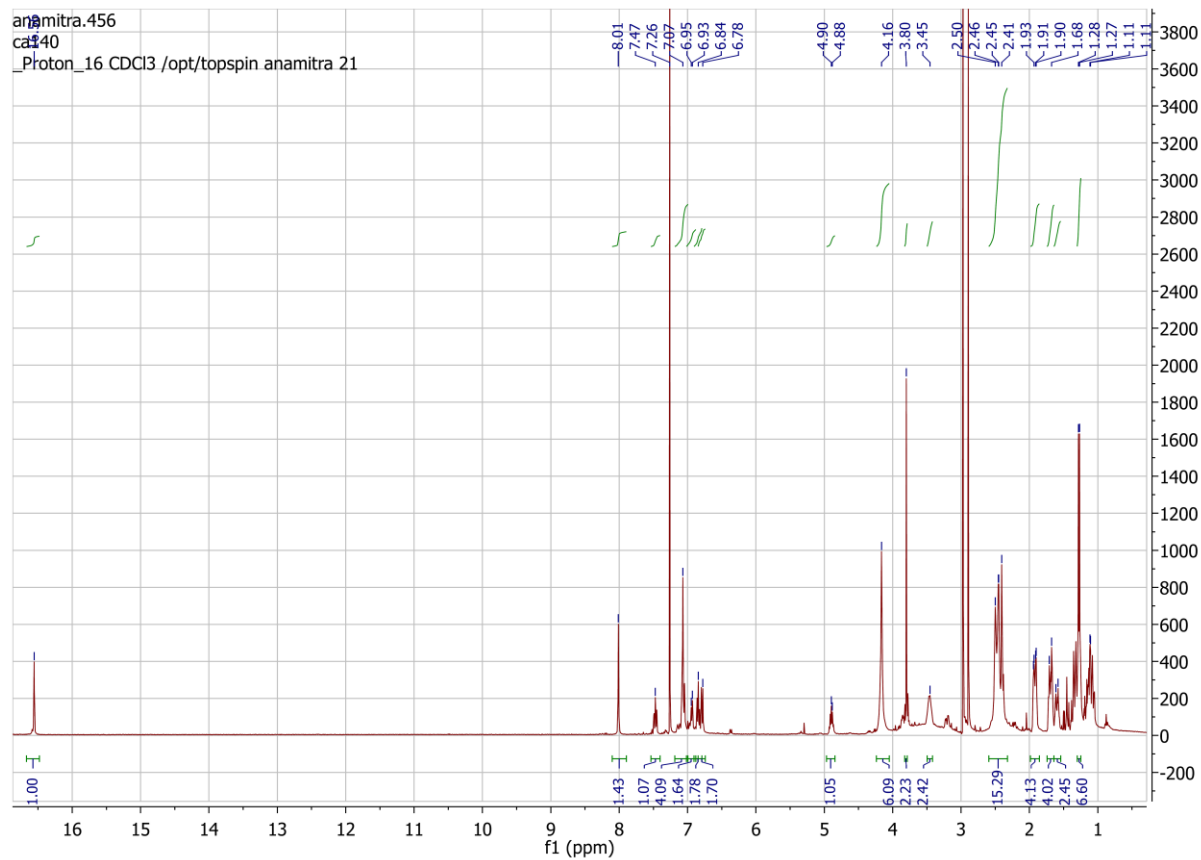
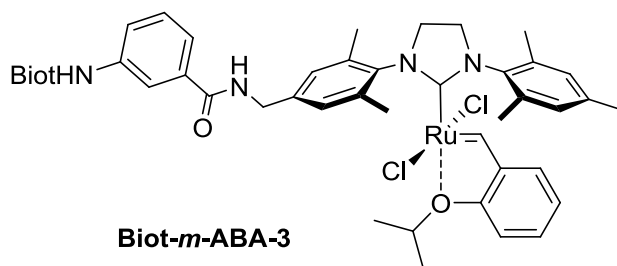






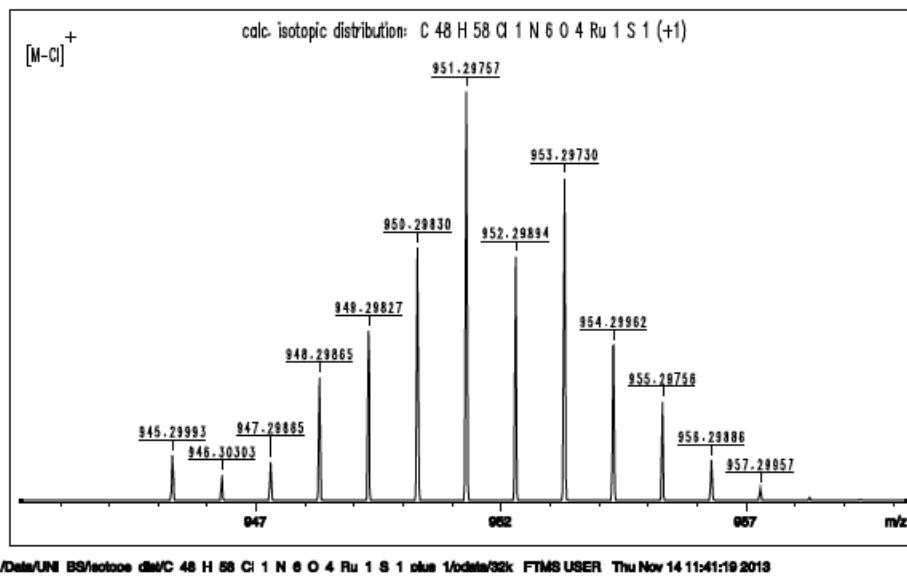
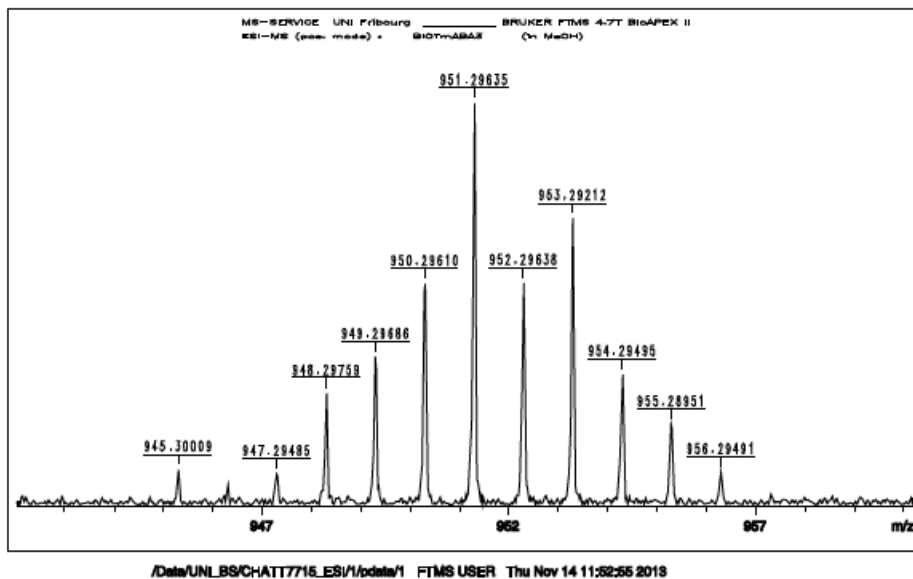
ESI-MS: BIOT3

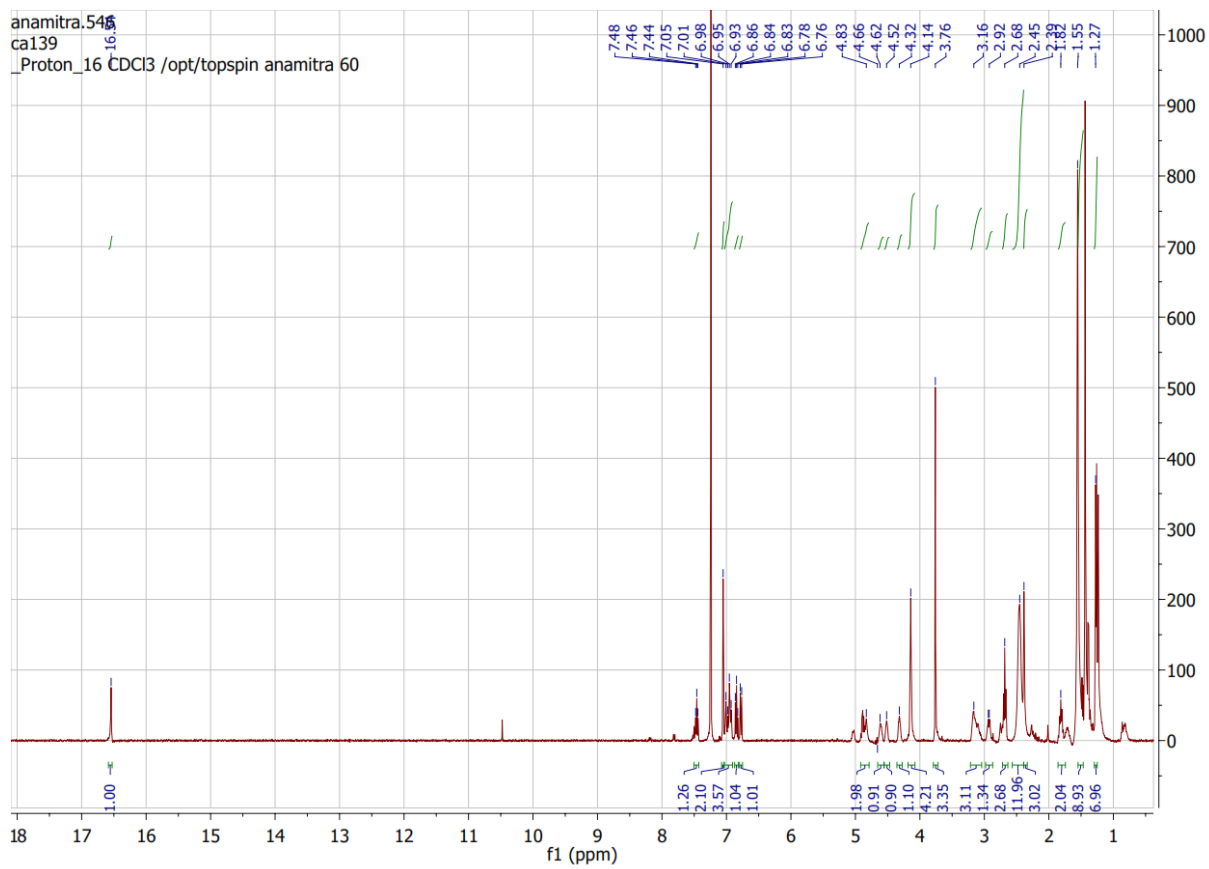
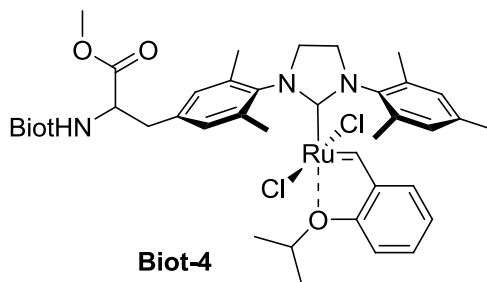


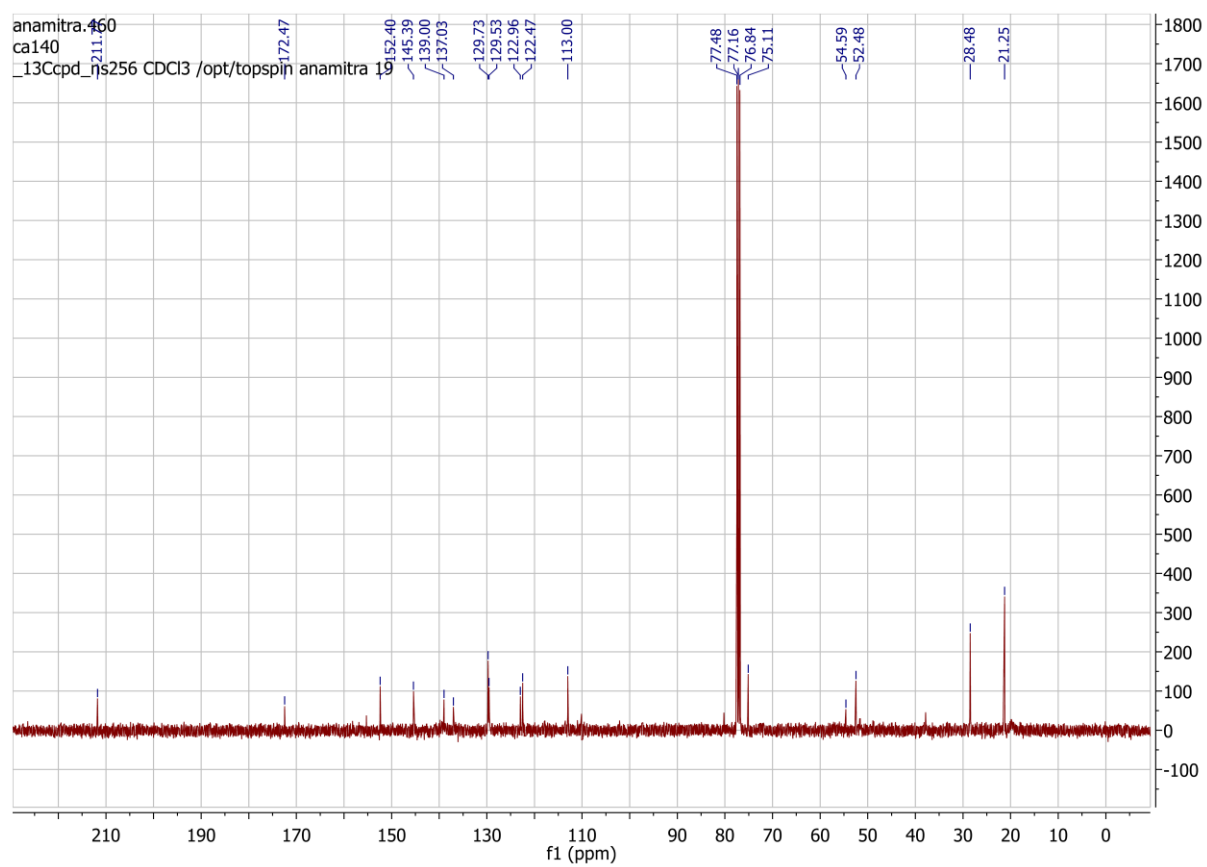
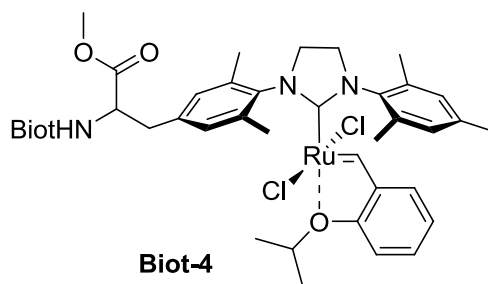




ESI-MS: BIOTmABA3

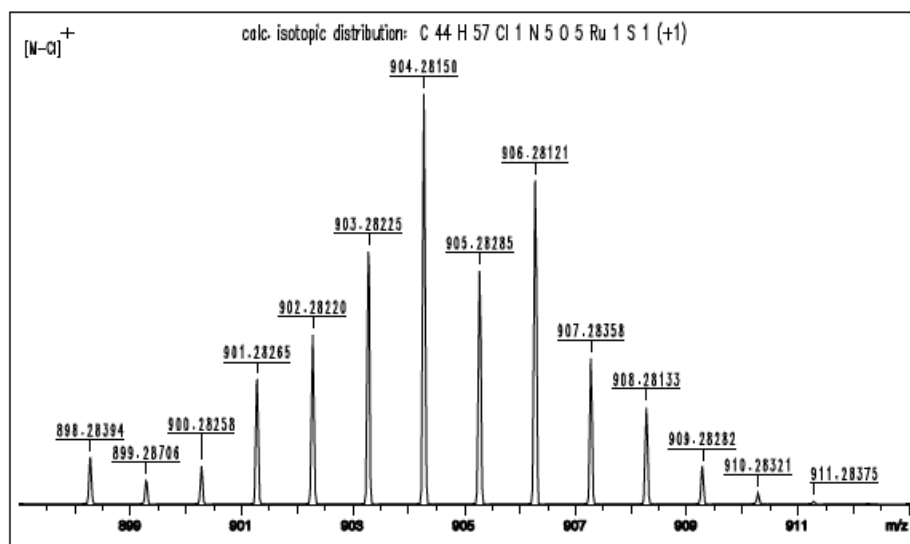
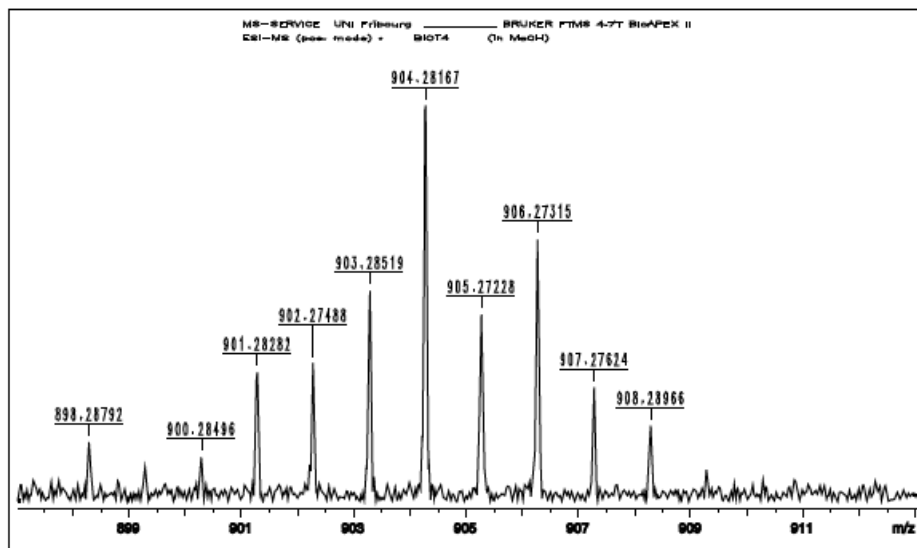


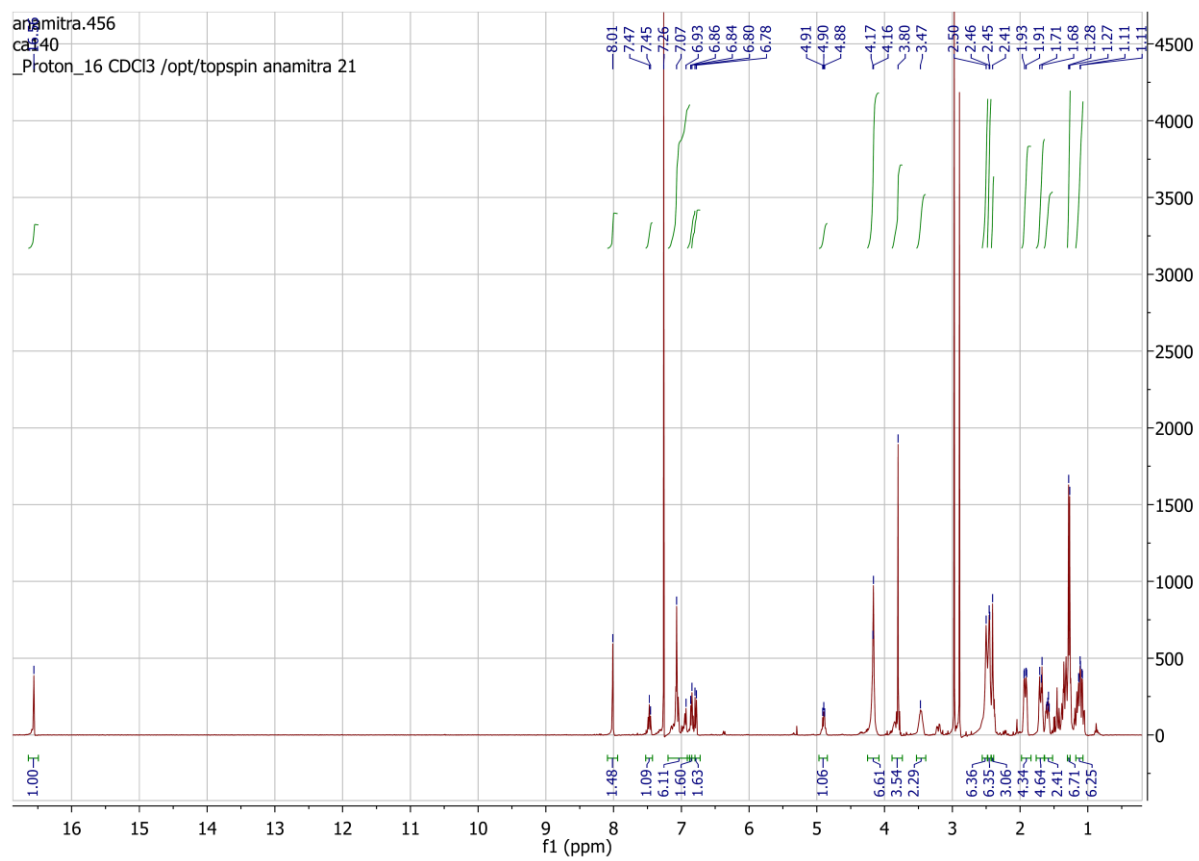
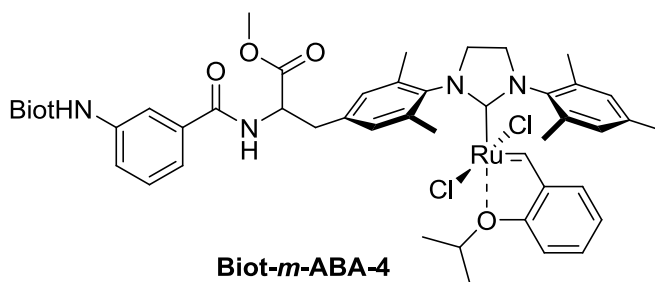






ESI-MS: BIOT4





APENDIX 3

*Asymmetric C–H Activation Reaction Catalyzed
by an Artificial Benzannulase Using Unpurified
Protein Samples*

General Methods

All reactions were carried out in 0.5 dram sealed vials under an atmosphere of air with magnetic stirring without drying or degassing of the vial. Conversions and regioselectivities were determined by GC with a calibrated internal standard (1,3,5-trimethoxybenzene). Enantiomeric ratio was determined by Chiral HPLC.

Site-Directed Mutagenesis

A pET11b plasmid containing the gene encoding for streptavidin fused with a T7-tag was used as a template for PCR. Primers were designed following the method described by Zheng et al. and tested in silico to minimize hairpin formation.¹ Primers were obtained from Microsynth. PCR reactions of 50 μ L total volume contained 5 – 25 ng of template plasmid, forward and reverse primers (300 nM each, Microsynth), dNTPs (0.1 mM each, Stratagene), DMSO (5 %), Pfu buffer (1x, Stratagene), polymerase Pfu turbo (3.75 U, Stratagene). The cycle conditions were: initial denaturation (95 °C, 5 min), followed by 16 cycles of denaturation (1 min at 95 °C), annealing (1 min at 50 – 60 °C, depending on the primers used), elongation (10 min at 68 °C). The final elongation was performed at 68 °C for 1 h. PCR products were analysed by gel electrophoresis (1 % agarose). The initial DNA template was digested by DpnI (1 h at 37 °C, New England Biolabs). 5 μ l of PCR product were used to transform chemically competent XL1-blue *E. coli* cells (produced in-house). Plasmids were purified using a Wizard Plus SV Miniprep DNA purification System (Promega) and were sequenced either by Microsynth.

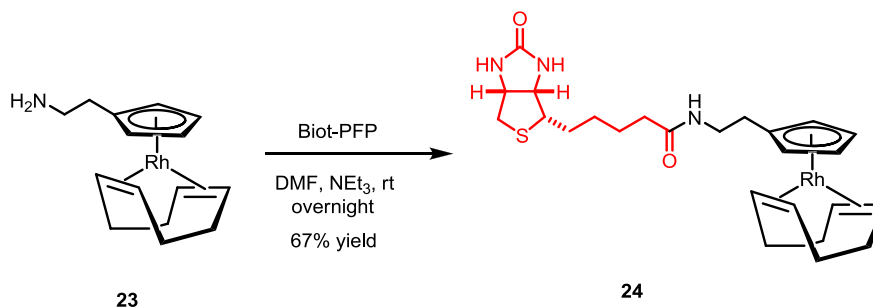
Production of Recombinant Streptavidin

Chemically competent BL21(DE3)pLysS *E. coli* cells (produced in-house) were transformed by the plasmids containing the desired mutations. Transformed cells were plated on LB-Lennox agar plates containing ampicillin (50 µg/mL, AppliChem), chloramphenicol (34 µg/mL, AppliChem) and glucose (2 % w/v), and incubated overnight at 37 °C. The culture medium (300 mL total, 20 g/L bactotryptone (BD), 1.3 g/L Na₂HPO₄, 1 g/L KH₂PO₄, 8 g/L NaCl, 15g/L bacto yeast extract (Merck) containing ampicillin (50 µg/mL), chloramphenicol (34 µg/mL), and glucose (2% w/v) was inoculated with a single colony. This preculture was incubated overnight on an orbital shaker (37 °C, 250 rpm). The fermentation was performed in a 30 L fermenter (NLF22, Bioengineering). The culture medium (20 L) containing ampicillin (50 µg/mL), chloramphenicol (34 µg/mL) and glucose (0.4 % w/v) was inoculated with the whole preculture. To avoid the formation of inclusion bodies, cells were grown at 20 °C, 30 °C or 37 °C, depending on the mutant. When an OD₆₀₀ of 2 – 3 was reached the expression of streptavidin was induced by addition of isopropyl β-D-1- thiogalactopyranoside (final concentration 0.4 mM, AppliChem). The cells were harvested 3 - 4 h after induction (expression at 30 °C and 37 °C) or after overnight expression (20 °C) by centrifugation (3600 x g, 10 min, 4 °C). The supernatant was discarded and the pellet was frozen at -20 °C until it was thawed for purification. Protein expression was confirmed by SDS-PAGE analysis.

Protein Purification

The pellet was thawed and resuspended in Tris-HCl buffer (20 mM, pH 7.4, 500-1000 ml / 150 - 450 g pellet). DNase I (2 - 3 mg, Roche) and phenylmethylsulfonyl fluoride (to a final concentration of 1 mM, AppliChem) were added and the resuspended cells were incubated at RT under vigorous shaking until the mixture became less viscous. The sample was dialyzed against 6 M guanidinium hydrochloride (Acros), pH 1.5 at room temperature for 24 hours. Two further dialysis steps were performed (20 mM Tris-HCl, pH 7.4, 4 °C, followed by 50 mM Na₂CO₃, pH 9.8, 0.5 M NaCl, 4°C) to prepare the proteic extract for affinity chromatography. The proteic extract was centrifuged (18000 x g, 30 min, 4 °C) to remove cell debris. The supernatant was filtered (Whatman paper filter) and applied to a 2-iminobiotin sepharose column (Affiland) equilibrated at pH 9.8 (50 mM Na₂CO₃, 0.5 M NaCl). Pure streptavidin was eluted with 1% acetic acid, immediately dialyzed against Tris- buffer (10 mM Tris-HCl, pH 7.4) for 24 h at 4 °C, followed by distilled water for 24 h and finally two times against mQ-water for 24 h at 4 °C. The purified protein solution was frozen at -80 °C, lyophilized, and the lyophilized protein stored at 4 °C. The molecular weight of the purified protein was assessed by ESI-MS.

Synthesis of Rh(I) Complex :



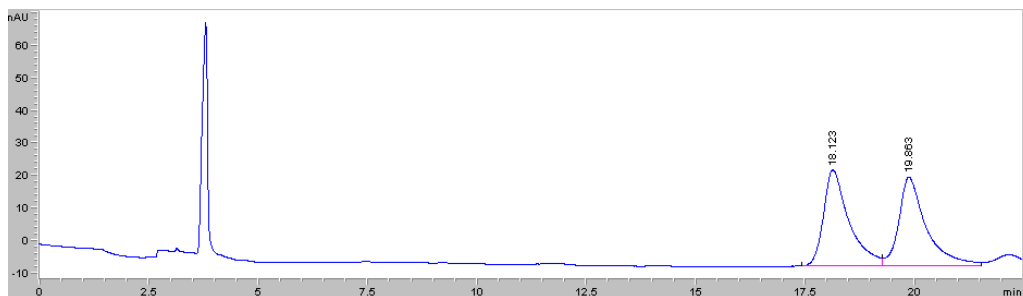
Complex **23** was synthesized according to the literature procedure.¹ The complex **23** was prepared in DMF (2 mL) and biotin pentafluorophenol (18 mg, 0.045 mmol) and Et₃N (0.13 mL, 0.91 mmol) were added to the solution, followed by stirring at RT for 16 h. The solvent was removed under reduced pressure and the crude product was purified on silica gel using 10% MeOH/CH₂Cl₂ to yield **24** as a yellow solid (25 mg, 67%). ¹H NMR (400 MHz, CD₂Cl₂): δ = 6.17 (dd, J = 15.5, 9.7 Hz, 2H), 5.25 – 5.17 (m, 1H), 5.10 (t, J = 1.8 Hz, 2H), 5.02 (t, J = 1.9 Hz, 2H), 4.55 – 4.44 (m, 1H), 4.31 (dd, J = 7.1, 5.2 Hz, 1H), 3.46 – 3.37 (m, 2H), 3.15 (td, J = 7.3, 4.7 Hz, 1H), 2.99 – 2.85 (m, 2H), 2.73 (d, J = 12.8 Hz, 1H), 2.35 (dt, J = 13.9, 4.1 Hz, 2H), 2.27 – 2.12 (m, 6H), 1.96 – 1.86 (m, 4H), 1.79 – 1.58 (m, 6H), 1.52 – 1.39 (m, 2H). ESI-TOF-MS (Positive mode) calculated for C₂₇H₃₆N₃O₂RhS: 567.0, [M+H]⁺; found 568.0.

General Synthesis for Dihydroisoquinolone 10:

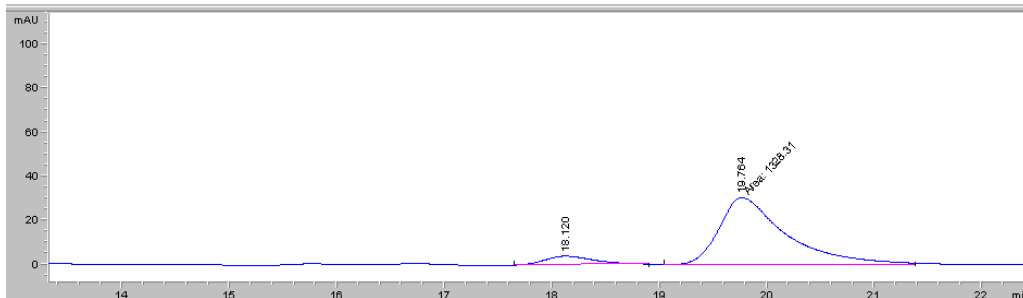
A 0.5 dram flask is charged with an oven dried stir bar and the appropriate tetrameric strept(avidin) mutant (0.66 mol %, 6.6 x 10⁻⁵ mmol, 4.3 mg). The solution was dissolved in deionized water (160 μl) and allowed to stir for 2

minutes. A solution of $[\text{RhCp}^*\text{biotinCl}_2]_2$ (1 μl of a solution in DMSO (0.1 M, 1 mol %, 0.11 mg)) was added to the solution and stirred at 500 rpm. After 5 minutes, a solution of pivaloyl protected hydroxamic acid in MeOH (0.25M solution, 40 μl , 1 equiv., 2.12 mg) was added to the reaction and stirred for 30 seconds. After alkene was added (1 equiv, 0.9 mg) the reaction is sealed and allowed to stir at 23 °C. After 36 hours the reaction is quenched with 400 μl of ethyl acetate and a 50 μl solution of 1,3,5 trimethoxybenzene in ethyl acetate (0.2M). The reaction is allowed to stir for 10 minutes (1000 rpm) before 200 μl of the organic layer was removed. Yield and diastereoselectivity was determined via GC, enantioselectivity was determined by HPLC.

This compound has been previously reported. Absolute configuration determined by HPLC trace of enantiopure sample. Included is the ^1H NMR. ^1H (400 MHz, CDCl_3) δ = 8.08 (dd, J = 7.7, 1.1 Hz, 1H), 7.49 - 7.45 (m, 1H), 7.38 (t, J = 7.5 Hz, 1H), 7.24 (d, J = 7.5 Hz, 1H), 6.50 (s, 1H), 4.41 (ddd, J = 10.0, 5.1, 1.9 Hz, 1H), 3.80 (s, 3H), 3.33 (dd, J = 15.7, 5.1 Hz, 1H), 3.21 (dd, J = 15.7, 10.0 Hz, 1H). *Chiral HPLC*: IA Column; 90:10 Hexane/*i*PrOH.



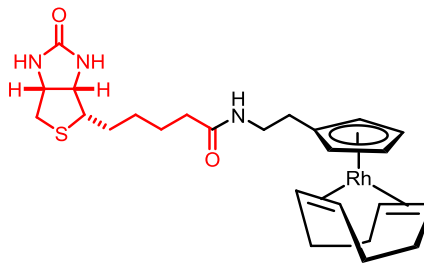
#	Time	Area	Height	Width	Area%	Symmetry
1	18.123	1213	29.7	0.589	50.053	0.537
2	19.863	1210.5	27.4	0.6269	49.947	0.542



#	Time	Area	Height	Width	Area%	Symmetry
1	18.12	127.6	3.9	0.4911	8.764	0.689
2	19.764	1328.3	30.5	0.7267	91.236	0.507

References:

1. Zheng, L; Baumann, U.; Reymond, J.-L. *Nucleic Acids Res.* **2004**, 32, e115.
2. Onoda A., Fukumoto K., Arlt M., Bocola M., Schwaneberg U., Hayash T.
Chem. Commun., **2012**, 48, 9756.



24

